Springer Series
in Biophysics 9

C. Reyes Mateo
Javier Gómez
José Villalaín
José M. González Ros (Eds.)

Protein-Lipid Interactions

New Approaches and Emerging Concepts

Springer

Springer Series in Biophysics 9

C. Reyes Mateo Javier Gómez José Villalaín
José M. González-Ros (Eds.)

Protein-Lipid Interactions

New Approaches and Emerging Concepts

With 54 Figures, 20 in Color and 4 Tables

Professor C. Reyes Mateo
Professor Javier Gómez
Professor José Villalaín
Professor José M. González-Ros

Instituto de Biología Molecular y Celular
Universidad Miguel Hernández
Avda. de la Universidad s/n, edificio Torregaitán
03202 Elche-Alicante
Spain

ISSN 0932-2353
ISBN 10 3-540-28400-1 Springer-Verlag Berlin Heidelberg NewYork
ISBN 13 978-3-540-28400-0 Springer-Verlag Berlin Heidelberg NewYork

Library of Congress Control Number: 2005930633

Springer is a part of Springer Science+Business Media

springeronline.com

Printed in Germany

Editor: Dr. Sabine Schreck, Heidelberg
Desk Editor: Anette Lindqvist, Heidelberg
Production: LE-TEX Jelonek, Schmidt & Vöckler GbR, Leipzig
Typsetting: Satz-Druck-Service, Leimen
Cover Design: Design & Production, Heidelberg

Printed on acid-free paper 39/3150/YL 5 4 3 2 1 0

Preface

Biological membranes have long been identified as key elements in a wide variety of cellular processes, including cell defence, communication, photosynthesis, signal transduction and motility, and thus they emerge as primary targets in both basic and applied research. In order to fully appreciate the role that biological membranes play in these essential biological processes it becomes crucial to get a molecular-level picture of the structure of their main components (i.e. lipids and membrane proteins) as well as the nature of their cross-interactions in order to decipher how these molecular recognition processes determine the modulation of membrane-related functions. In this respect, the high-resolution structure of quite a few membrane proteins determined in recent years, many of them of prokaryotic origin, are at centre stage in modern membrane research as they allow for the rational design and interpretation of experiments, which were unthinkable not too long ago.

This book is an attempt to assemble in a single volume the most recent views of some of the experts in the area of protein–lipid interactions which draw a general picture of the advances that this field has achieved in recent years, from very basic aspects to specialized technological applications. The topics in this book include the application of X-ray and neutron diffraction, infrared and fluorescence spectroscopies, as well as high-resolution NMR methodologies that improve our understanding of the specific interactions established between lipids and proteins within biological membranes, their structural relationships, and the implications to the biological functions they mediate. In addition, the insertion of proteins and peptides into the membrane and the concomitant formation of definite lipid domains within the membrane, are other topics covered in this volume. We hope that the selection of subjects is timely and stimulating both for the dedicated scientist and for the general reader.

Alicante, September 2005

C. Reyes Mateo
Javier Gómez
José Villalaín
José M. González-Ros

Contents

List of Contributors

Rodrigo F.M. de Almeida
Centro de Química e Bioquímica
Faculdade de Ciências de Lisboa
1749-016 Lisbon
Portugal

Jungyuen Choi
The Burnham Institute
10901 North Torrey Pines Road
La Jolla, CA 92037
USA

Antonio Cruz
Dept. Bioquímica
Fac. Biología
Universidad Complutense
28040 Madrid
Spain

José A Encinar
Instituto de Biología Molecular
y Celular
Universidad Miguel Hernández
03206 Elche (Alicante)
Spain

Richard M. Epand
Department of Biochemistry
McMaster University
Hamilton, ON
L8N 3Z5
Canada
E-mail: epand@mcmaster.ca

Asia M. Fernandez
Instituto de Biología Molecular
y Celular
Universidad Miguel Hernández
03206 Elche (Alicante)
Spain

Xiao-min Gong
The Burnham Institute
10901 North Torrey Pines Road
La Jolla, CA 92037
USA

José M. González-Ros
Instituto de Biología Molecular
y Celular
Universidad Miguel Hernández
03206 Elche (Alicante), Spain
E-mail: gonzalez.ros@umh.es

Juan A. Hermoso
Grupo de Cristalografía
Macromolecular y Biología
Estructural
Instituto Química-Física Rocasolano
CSIC
Serrano 119, 28006 Madrid
Spain

Anthony G. Lee
School of Biological Sciences
University of Southampton
Southampton, SO16 7PX
UK
E-mail: agl@soton.ac.uk

Luis M.S. Loura
Centro de Química-Física Molecular
Instituto Superior Técnico
1049-001 Lisbon
Portugal
and
Centro e Departamento de Química
Universidade de Évora, 7000 Évora
Portugal

José M. Mancheño
Grupo de Cristalografía
Macromolecular y Biología
Estructural
Instituto Química-Física Rocasolano
CSIC
Serrano 119, 28006 Madrid
Spain

Francesca M. Marassi
The Burnham Institute
10901 North Torrey Pines Road
La Jolla, CA 92037
USA
E-mail: fmarassi@burnham.org

C. Reyes Mateo
Instituto de Biología Molecular
y Celular
Universidad Miguel Hernandez
Elche 03202
Spain

Andres Morales
División de Fisiología,
Universidad Alicante
03080 Alicante
Spain

Eva Pebay-Peyroula
Laboratoire des Protéines
Membranaires
Institut de Biologie Structurale
J.-P. Ebel CEA-CNRS-UJF. 41
Rue Jules Horowitz
38027 Grenoble Cedex 1
France

Jesús Pérez-Gil
Dept. Bioquímica
Fac. Biología
Universidad Complutense
28040 Madrid
Spain

José A. Poveda
Instituto de Biología Molecular
y Celular
Universidad Miguel Hernández
03206 Elche (Alicante)
Spain

Manuel Prieto
Centro de Química-Física Molecular
Instituto Superior Técnico
1049-001 Lisbon
Portugal
E-mail: prieto@alfa.ist.utl.pt

Jorge Bernardino de la Serna
Dept. Bioquímica
Fac. Biología
Universidad Complutense
28040 Madrid
Spain

Yechiel Shai
Department of Biological Chemistry
Weizmann Institute of Science
Rehovot 76100
Israel
E-mail: Yechiel.Shai@weizmann.ac.il

From Lipid Phases to Membrane Protein Organization: Fluorescence Methodologies in the Study of Lipid–Protein Interactions

C. Reyes Mateo, Rodrigo F.M. de Almeida, Luis M.S. Loura, Manuel Prieto

1.1 General Background

The fluid mosaic model of biological membranes (Singer and Nicolson 1972) emphasizes membrane fluidity and free lateral diffusion of membrane components. This has led to the generalized idea of biomembranes as solutions of proteins embedded in bilayers of randomly distributed phospholipids. The current view is moving towards the probable equal importance of lipids and proteins in the determination of the constitution, structure and dynamics of membrane domains and the hierarchic structure of the membrane, in which small patches revealed by non-random patterns of co-distribution of specific proteins are the building blocks of large aggregates (Vereb et al. 2003).

The use of model systems of membranes prepared with pure lipids and lipid mixtures in the absence or presence of peptide/proteins has proved useful in elucidating the organization, topology, and orientation of membrane proteins. To approach this study the following possibilities have to be considered: (1) diverse phase behaviour of the lipid or the lipid mixture in the absence of peptide/protein (knowledge of the phase diagram); the balance between different molecular interactions will change markedly, e.g. if the lipid is in the gel or in the fluid phase; if there is phase coexistence the protein can partition preferentially to one phase and have different aggregation states in each phase, etc.; (2) the influence of the protein on the phase behaviour (shifts in the phase diagram, creation of new regions/types of phase separation); and (3) the influence of the peptide/protein on the phase separation topology, without changing the lipid phase diagram. In fact, the formation of lipid domains is thought to be a key process in several biological functions (e.g. Simons and Ikonen 1997) and the clarification of the relationship between lipid domains and the binding and functional properties of membrane-associated proteins is an emerging area in membrane research (Hurley and Meyer 2001). The phase behaviour for a ternary lipid mixture (e.g. mimicking raft-containing membranes) can be quite complex, as well as the variation of domain size with lipid composition (de Almeida et al. 2005), and it is necessary to characterize it before studying the effect of the protein. Other kinds of heterogeneities, such as the lipid annulus around a transmembrane protein, which do not correspond to a true phase separation, may also occur. Depending on the proportion of peptide/protein and lipid, or the type of lipid, the protein/peptide system can undergo strong alterations, such as peptide displacement from a position parallel to a perpendicular one, in relation to the membrane axis. Some important prin-

Springer Series in Biophysics
C.R. Mateo et al. (Ed.)
Protein-Lipid Interactions

ciples have been established, namely the prediction of membrane protein topology (Jayasinghe et al. 2001), the hydrophobic mismatch principle (Mouritsen and Bloom 1984), and also more specific aspects like the distinct roles of tryptophan and lysine anchors (de Planque et al. 1999). Approaches based on fluorescence spectroscopic techniques, due to their intrinsic sensitivity, suitable time-scale, non-invasive nature and minimum perturbation, can be useful in studying all these aspects of lipid–protein interaction. Examples of when and how to use this technique will be given in the later sections of this chapter, after a brief review of the most important fluorescence methodologies and parameters, and a survey of the more useful fluorophores in these types of studies. Direct inspection of fluorescence steady-state data allows us to qualitatively assess the physical details of the system. On the other hand, state-of-the-art analysis of time-resolved fluorescence data (e.g. FRET and anisotropy) can give detailed information on the dynamics as well as the topology (e.g. vesicle interaction and phospholipid lateral distribution).

1.2 Fluorescence Methodologies

1.2.1 Fluorescence Resonance Energy Transfer

Fluorescence resonance energy transfer (FRET) is a photophysical phenomenon upon which the excited state of a molecule, the donor, is transferred to another, the acceptor. This latter molecule can be either identical to the donor, or a different species, resulting in homotransfer (energy migration, homo-FRET) or heterotransfer (hetero-FRET). As a result of FRET, the donor fluorescence is quenched, and the acceptor becomes excited (and may fluoresce). The rate constant for FRET, k_T, depends on the inverse of the sixth power of the separation distance between the donor and acceptor, R (Förster 1949). The FRET efficiency, E, can be obtained experimentally from the reduction of fluorescence intensity (I_{DA}) or lifetime (τ_{DA}) in the presence of the acceptor, relative to their values in the absence of the acceptor (I_D and τ_D, respectively):

$$E = 1 - \frac{I_{DA}}{I_D} = 1 - \frac{\tau_{DA}}{\tau_D} \tag{1.1}$$

In the case that the donor decay is described by a sum of exponentials (where α_i are the normalized pre-exponential factors):

$$i(t) = \sum_{i=1}^{n} \alpha_i \exp(-t / \tau_i) \tag{1.2}$$

τ_{DA} and τ_D in Eq. 1.1 should be replaced by the lifetime quantum yields $<\tau>_{DA}$ and $<\tau>_D$, defined by (e.g. Lakowicz 1999)

$$\langle \tau \rangle = \sum_{i=1}^{n} \alpha_i \tau_i \tag{1.3}$$

In membranes, each donor is surrounded by a distribution of acceptors, at varying distances, therefore, FRET kinetics are considerably more complex. For the derivation of the donor decay law in this situation, the starting point is usually the master equation

$$i_{DA}(t) = \exp(-t/\tau_D)\prod_{i=1}^{N_A}\exp\left[-\left(\frac{t}{\tau_D}\right)\left(\frac{R_0}{R_i}\right)^6\right] \tag{1.4}$$

where N_A is the number of acceptors, and Ri is the distance between the donor molecule in question and the ith acceptor molecule. Although this equation concerns a single donor molecule, it can be used for any situation where all donor molecules are equivalent. In this way, expressions for the donor decay for geometries relevant to bilayer systems have been obtained. These include FRET to an ensemble of acceptors in an infinite plane, from donors located either in the same plane (planar geometry or *cis* FRET) or 2D FRET, as in Eq. 1.5 (Tweet et al. 1964), or in another parallel plane (bilayer geometry or *trans* FRET), as in Eq. 1.6 (Davenport et al. 1985).

$$\begin{aligned} i_{DA,\,cis}(t) = {} & \exp\left(-\frac{t}{\tau_D}\right)\exp\left\{-\pi R_0^2 n\gamma\left[\frac{2}{3}\left(\frac{R_0}{R_e}\right)^6\left(\frac{t}{\tau_D}\right)\right]\left(\frac{t}{\tau_D}\right)^{1/3}\right\} \\ & \cdot\exp\left\{\pi R_e^2 n\left(1-\exp\left[-\left(\frac{R_0}{R_e}\right)^6\left(\frac{t}{\tau_D}\right)\right]\right)\right\} \end{aligned} \tag{1.5}$$

$$i_{DA,\,trans}(t) = \exp\left(-\frac{t}{\tau_D}\right)\exp\left\{-2n\pi l^2\int_0^{\frac{1}{\sqrt{l^2+R_e^2}}}\frac{1-\exp(-tb^3\alpha^6)}{\alpha^6}\,d\alpha\right\} \tag{1.6}$$

In these equations, n is the number of acceptors per unit area, γ is the incomplete gamma function (see Lakowicz 1999, page 426), R_e is the distance of closest approach between donor and acceptor molecules, l is the distance between the planes of donors and acceptors and $b = (R_o/l)^2\tau_D^{-1/3}$. In the case that $R_e << R_o$ (in practice, if $R_e < R_o/4$), the incomplete gamma term in Eq. 1.5 can be replaced by $\Gamma(2/3)$ (where Γ is now the complete gamma function) and the last exponential term in that equation can be omitted, whereas the upper limit in the integral in Eq. 1.6 becomes 1.

In the above cases, a uniform distribution of acceptors was always assumed (for the kinetics of FRET in the case of separation of two infinite phases with a uniform acceptor distribution within each phase see, e.g. Loura et al. 2001). A relevant situation in the context of lipid–protein interaction for which this clearly does not hold is when the composition of the annular lipid region surrounding the protein is different from that of the bulk. In a recent study (Fernandes et al. 2004), FRET from a protein-located donor (in the centre of the bilayer) to a labelled-phospholipid acceptor, with fluorophores located on both lipid/water interfaces, was modelled assuming a single layer of annular lipid. The model assumes two populations of energy transfer acceptors, one located in the single annular lipid

shell around the protein and the other outside the shell. The donor fluorescence decay curve has FRET contributions from both populations:

$$i_{DA}(t) = i_D(t)\,\rho_{annular}(t)\,\rho_{random}(t) \tag{1.7}$$

Here i_D and i_{DA} are the donor fluorescence decay in the absence and presence of acceptors, respectively, and $\varrho_{annular}$ and ϱ_{random} are the FRET contributions arising from energy transfer to annular labelled lipids and to uniformly distributed labelled lipids outside the annular shell, respectively. Considering a hexagonal-type geometry for the protein–lipid arrangement, each donor protein will be surrounded by 12 annular lipids. In bilayers composed by both labelled and unlabelled phospholipids, these 12 sites will be available for both of them. The probability μ of one of these sites being occupied by a labelled phospholipid is given by

$$\mu = K_S \cdot n_{acceptor} / (n_{acceptor} + n_{lipid}) \tag{1.8}$$

Here, $n_{acceptor}$ is the concentration of labelled lipid, and n_{lipid} is the concentration of unlabelled lipid. K_S is the relative association constant, which reports the relative affinity of the labelled and unlabelled phospholipids. Using a binomial distribution, the probability of each occupation number (0–12 sites occupied simultaneously by labelled lipid), and finally the FRET contribution arising from energy transfer to annular lipids is computed

$$\rho_{annular}(t) = \sum_{n=0}^{12} \exp(-nk_T t)\binom{12}{n}\mu^n(1-\mu)^{12-n} \tag{1.9}$$

The FRET contribution from acceptors uniformly distributed outside the annular region in two different planes at the same distance to the donor plane (from the centre of the bilayer to both leaflets) is given by the latter term of Eq. 1.6, in which n must be corrected for the presence of labelled lipid molecules in the annular region, which therefore are not part of the uniformly distributed acceptor pool.

In all situations, the theoretical energy transfer efficiency E is readily calculated by numerical integration,

$$E = 1 - \frac{\int_0^\infty i_{DA}(t)\,dt}{\int_0^\infty i_D(t)\,dt} \tag{1.10}$$

and can be compared with the experimental observable obtained from Eq. 1.1.

Despite having the obvious advantage of only requiring a single fluorophore, the use of homotransfer is more restricted than that of heterotransfer. One reason for this is that homotransfer does not lead to a reduction in donor fluorescence intensity or lifetime, because the donor excited state population is not dimin-

ished during the act of transfer. In practice, the sole observable which reflects the phenomenon is a reduction in fluorescence anisotropy (see Sect. 1.2.2), the measurement of which requires polarizers and, because these lead to a considerable reduction in the detected emission, often a larger amount of fluorophore (relative to that which would be used in an intensity measurement) is needed for a given precision. In the case that instrumentation is not a problem, the decrease in anisotropy is quite clear.

More importantly, the theory of depolarization due to homotransfer is more complicated than that of heterotransfer, because (1) there is the possibility of back-transfer to the directly excited donor, or transfer to any donor, eventually involving a large number of transfer steps, and (2) since fluorescence anisotropy is the relevant observable, in addition to FRET, another source of depolarization is fluorophore rotation. If rotation and FRET occur in the same time-scale, the two phenomena are coupled. This is why most theories for homotransfer assume static dipoles (see Kawski 1983 and Van der Meer at al. 1994 for reviews and discussion of the theory), even the user-friendly numerical simulations of Snyder and Freire (1982). Some authors assume that the experimental anisotropy decay is the product of a rotational depolarization term by a FRET depolarization term obtained from a static-dipole theory (e.g. Medhage et al. 1992), and therefore the FRET term can be recovered, e.g. from the faster component in the anisotropy decay (Sharma et al. 2004). It must be understood that this independence of rotation and transfer constitutes an approximation (unless the time-scales for the two phenomena are very distinct), whose severity is not easy to ascertain. The coupling of rotation and FRET in the measured anisotropy is therefore the main obstacle to quantitative data analysis of homotransfer. However, this has not completely stopped the use of the latter in the context of lipid–protein interaction, and examples will be given in Sect. 1.4.

1.2.2 Anisotropy

Molecular electronic transitions are characterized by absorption and emission dipoles (and their associated transition moments) fixed with respect to the molecular frame. When an assembly of randomly oriented molecules is illuminated with polarized light of suitable frequency the probability of absorption is proportional to $\cos^2\gamma$, where γ represents the angle between the absorption transition moment and the exciting electric vector. This anisotropy in the photoabsorption process causes preferential excitation (photoselection) of those molecules oriented forming angles γ close to zero. The orientational anisotropy is a maximum at the instant of excitation ($t = 0$) and will decrease as a function of time due, among other things, to the Brownian motion experienced by the excited molecules. Since these random motions depend on the shape and size of the molecules and on the viscosity and temperature of the solvent, the decrease of the orientational anisotropy will be related to these parameters. Therefore, any method able to detect the initial orientation of the photoselected population and monitor its temporal evolution will give important information about the dynamic properties of the

molecule. When the photoselected molecules are fluorescent the disorientation caused by the Brownian motion may be determined by recording the polarized fluorescence components $I_{||}$ and $I_{\perp}$ which represent, respectively, the intensities of emission parallel and perpendicular to the exciting vector. Then, the emission anisotropy, r, is defined by:

$$r = \frac{I_{||} - I_{\perp}}{I_{||} + 2I_{\perp}} \tag{1.11}$$

The maximum value of r (the intrinsic anisotropy r_o) depends on the relative orientation of the excitation and emission transition moments of the molecule and corresponds to the emission anisotropy observed in the absence of other depolarizing process taking place during the lifetime of the excited state (τ). In most cases, decreasing this initial value depends only on the ratio between τ and the speed of the rotational diffusion by an expression originally formulated by Perrin (1926) and later applied and extended by Weber (1953) and Jabłoński (1960):

$$r = \frac{r_0}{1 + \tau/\varphi} \tag{1.12}$$

where φ is the rotational correlation time, which is related to the rotational diffusion coefficient, D ($\varphi = 1/6D$), and, therefore, to the molecular dimensions and to the viscosity and temperature of the solvent. Many fluorescent molecules in water solution have correlation times much shorter than the lifetime ($\varphi << \tau$). Then, the measured anisotropy (r) is zero (the random orientation of the excited molecules is recovered before fluorescence emission). However, for large molecules such as proteins, the rotational motions occur in the same time-scale as the fluorescence lifetime and, consequently, the fluorescence light that they emit will be partially polarized ($r \neq 0$).

Equation 1.12 was deduced assuming spherical rotors in isotropic media and from experiments under continuous illumination, that is, under steady-state conditions. Its use in the determination of any one of the parameters involved in the equation requires the explicit knowledge of all the others parameters and it is limited to fluorophores in isotropic solvents having specific symmetry, with a single fluorescence lifetime. Steady-state anisotropy can also be used to monitor lipid–peptide interactions, as long as the peptides contain an extrinsic or intrinsic fluorophore. The interaction of the peptide with the membrane slows down and partially prevents the rotation of the macromolecule-bounded fluorophore, causing an increasing of the anisotropy value. In addition, steady-state anisotropy measurements have been extensively used to detect alterations induced by peptide and proteins in membrane systems through incorporation of extrinsic probes into the lipid vesicles (e.g. Ahn et al. 2002; Zhao et al. 2001). The anisotropy values obtained under these conditions contain structural and dynamic information about the peptide and the lipid membrane which cannot be separated from a simple steady-state experiment (Jähnig 1979). This and much more information is available if one measures directly the anisotropy decay, that is, the values of $r(t)$ after pulse excitation. In the case of spherical fluorophores dissolved

in isotropic solvents and in the absence of other depolarization processes $r(t)$ is a single exponential:

$$r(t) = r_0 \exp(-t/\varphi) \tag{1.13}$$

For more complex structures (non-spherical fluorophores, fluorophores located in an anisotropic environment such as a lipid membrane, macromolecule-bound fluorophores having internal flexibility, etc.), $r(t)$ can be described as a multi-exponential decay plus a constant term (Dale 1977; Heyn 1989):

$$r(t) = (r_0 - r_\infty)\left[\sum_{i=1}^{n} \beta_i \exp(-t/\varphi_i)\right] + r_\infty$$
$$\sum_{i=1}^{n} \beta_i = 1 \tag{1.14}$$

where r_∞ is the residual anisotropy obtained for $t \to \infty$ when the rotational motion of the fluorophore is restricted and, consequently, depolarization is not complete (which is the usual case for fluorophores inserted in lipid membranes). The anisotropy decay parameters (φ_i, β_i, and r_∞) contain information about the shape, size, flexibility and location of the fluorophore or of the bound macromolecule, and/or about the rigidity of the molecular environment where the fluorophore resides (e.g. a lipid membrane). To extract this information it is necessary to propose a rotational model for the fluorophore and compare the exponential terms corresponding to this model with those obtained from the fit of the experimental anisotropy decay to Eq. 1.14. Some of these rotation models and their associated anisotropy decay laws have been extensively revised by Lakowicz (1999).

Although Brownian motion is the main source of fluorescence depolarization, additional processes such as energy transfer, fluorescence reabsorption or light scattering can indirectly modify the orientation of the emission dipoles affecting the anisotropy value. The extent to which the anisotropy is decreased due to these mechanisms can be minimized if one works with dilute samples and suitable excitation and emission wavelengths.

1.2.3 Quenching

Together with FRET, quenching is the most common methodology in the area of biological applications of fluorescence. In the case that fluorescence quenching is a dynamic process, i.e. diffusion dependent (static mechanisms will be addressed later), this implies the resolution of Fick's diffusion equation. In homogeneous solution the resulting complex formalisms, such as the so-called "radiation boundary condition" can be experimentally verified.

However, in biological systems, specifically the problem of both fluorophore and quencher diffusing in a membrane, "transient effects" due to diffusion cannot be studied in detail due to the following: (1) diffusion is no longer isotropic; (2) the decay of most samples in the absence of a quencher is not a single exponential but is intrinsically complex, which among other reasons can be due to

populations in different microenvironments in the membrane, such as different transversal locations (in addition, for the more relevant fluorescent amino acids, tryptophan and tyrosine, this complexity is also due, among other reasons, to the emission of different ground-state rotamers – see Sect. 1.3.2.1); (3) in most experimental situations there is strong scattering due to the vesicles, and in this way the very beginning of the decay is biased due to this artefact. Although this can be taken into account in the time-resolved analysis, it is always a critical problem.

In this way the well-known Stern–Volmer equation is in most situations the starting point, and from time-resolved data a linear relationship (Eq. 1.15) should be obtained:

$$\frac{\tau_0}{\tau} = 1 + k_q \cdot \tau_0 \cdot [Q] \tag{1.15}$$

where τ_o and τ are the fluorescence lifetimes in the absence and presence of the quencher, k_q is the bimolecular rate constant, and $[Q]$ is the effective quencher concentration in the membrane which is obtained from knowledge of its partition coefficient (see Sect. 1.4.1) . For this rate constant, and related to the "transient effects" described above, the approximation of Umberger and Lamer (1945) can be considered,

$$k_q = 4\pi N_A(2R_c)(2D)[1 + 2R_c/(2\tau_0 D)^{1/2}] \tag{1.16}$$

where R_c is the collisional radius (taken as the sum of the fluorophore and quencher radius), and in this way the diffusion coefficient D can be obtained. In the case that the quenching is not diffusion controlled, the above definition for k_q is multiplied by an efficiency factor γ. This approximation takes into account the fact that only a fraction of the collisions is effective in the excited state deactivation.

As mentioned above, only exceptionally is the intrinsic decay of the fluorophore not complex, and is usually empirically described by a sum of exponentials (Eq. 1.2). Generally, the quenching of each component cannot be detailed, and the use of mean or average lifetimes, which is not uncommon to find described in the wrong way in the literature, is the usual approach.

In Eq. 1.15 above, the lifetime quantum yields (see Eq. 1.3) (integration of the area under the decay) should be used on the left-hand side of the equation, while the mean lifetime should be used on the right-hand side,

$$\bar{\tau} = \frac{\sum_i \alpha_i \tau_i^2}{\sum \alpha_i \tau_i} \tag{1.17}$$

which in fact is the one that describes the mean lifetime that the molecule spends in the excited state, so is the relevant one to consider in the diffusion process. The mean lifetime can be even more refined, such as described by Sillen and Engelborghs (1998).

Regarding the static components that can be present in the steady state, the first step is to consider a sphere of action, which accounts for the statistical pairs

existing at the moment of excitation. So, from the time-resolved linear Stern–Volmer plot (Eq. 1.15), and the fitting of Eq. 1.18 to the steady-state data I_o/I, the volume of the sphere V is obtained,

$$\frac{I_0}{I} = \left(\frac{\tau_0}{\tau}\right) \cdot \exp\left(-V \cdot N_a \cdot [Q]\right) \tag{1.18}$$

In the case that the recovered sphere radius is greater than the sum of the collisional radii of fluorophore and quencher (~ 10 Å for typical molecular pairs), a model considering the formation of a molecular complex should be invoked. The general formalism for the case where the equilibrium constant K_a is not very high, or the quencher concentration is low, is given in Castanho and Prieto (1998).

A specific application of quenching in membranes is related to the determination of the transversal position of molecules, i.e. the in-depth location in a membrane. The most well-known approach of this type of differential quenching is the so-called "parallax method", which will be briefly addressed in Sect. 1.4.5.

Much less used to obtain structural information in membranes is the self-quenching mechanism. However, this is a very common interaction in membrane studies, since the compartmentalization effect of this heterogeneous medium leads to high effective concentrations of molecules in a membrane.

Self-quenching can happen in cases that a protein or a peptide (1) was derivatized with a fluorophore that undergoes self-quenching (BODIPY is an example, Fernandes et al. 2003), or (2) it can also happen in the case of a non-derivatized peptide, since tryptophan can be quenched in an intermolecular way, by another peptide segment, which has in its structure a residue that is a suitable quencher of tryptophan, such as a cysteine or a lysine (e.g. de Almeida et al. 2004).

When studying self-quenching, the Stern–Volmer relationship (Eq. 1.15) for dynamic quenching still holds, where now the quencher concentration $[Q]$, is replaced by the fluorophore concentration $[F]$, and the value of τ_o is the limiting value for a diluted solution, the situation where there is no self-quenching. However, the same formalism is not valid for the steady state, since the total intensity increases due to the increase in fluorophore, but there is a concomitant decrease due to the self-quenching interaction. This leads to the following hyperbolic-type relationship,

$$I_F = \frac{C\,[F]}{\frac{1}{\tau_0} + k_q\,[F]} \exp\left(-VN_A[F]\right) \tag{1.19}$$

where I_F is the fluorescence intensity and C is a constant, and in the case that the effective concentration is high enough, the static contribution can be taken in the framework of the sphere of action model.

The above formalisms assumed that diffusion in the membrane happens in a three-dimensional medium. The solution for a bidimensional system (Razi-Naqvi 1974), when applied to a membrane, is relevant in the case that the fluorescence lifetime was on the order of hundreds of nanoseconds, which is not the case for most probes or fluorescent amino acids.

1.3 Fluorophores in Lipid Protein Studies

1.3.1 Membrane Probes

The kinds of molecules capable of undergoing electronic transitions that finally result in fluorescence are known as fluorophores. Application of fluorescence spectroscopy to study lipid–protein interactions requires the presence of, at least, one of these molecules in the system under study. In many cases, the fluorophore is an inherent component of the protein or peptide – fluorescent amino acids as tryptophan (Trp) and tyrosine (Tyr) – or an extrinsic probe bonded to the macromolecule, and the changes detected in their photophysical properties are related to alterations induced on the macromolecule upon interaction with the membrane macromolecule (see Sect. 1.3.2). Lipid–protein interactions can also be investigated from the alterations induced on the lipid bilayer by the protein or peptide. However, most lipids do not display intrinsic fluorescence, thus application of fluorescence spectroscopy to this kind of study requires the labelling of the bilayer with an extrinsic fluorophore, namely a membrane probe. Membrane probes include fluorescent molecules similar to natural lipids, such as diphenylhexatriene (DPH) and their derivatives or *trans*-parinaric acid (*t*-PnA), as well as small organic dyes having little structural resemblance to natural biomolecules (BODIPY, Laurdan, Pyrene, NBD, etc.). Fluorescent analogues of lipids are commonly used in anisotropy experiments to determine membrane phase-transition temperatures and physical properties of membranes such as order parameter and "microviscosity", as well as for detecting alterations of these parameters induced upon interaction of the membrane with peptides, proteins and other biomolecules. These kinds of experiments are based on the assumption that the probe into the membrane will adopt an orientational distribution which mimics that of membrane components. This information is contained in r_∞ (see Eq. 1.14), the residual anisotropy of the probe. In addition, the correlation times of the anisotropy decay will contain information about the friction that hinders the angular motions of the probe, which is related to the membrane microviscosity. The task of obtaining the membrane molecular properties from a macroscopic observable such as anisotropy decay is only possible if numerous properties of the probe are known, such as its location within the bilayer, size, shape and flexibility, the orientation of its transition moments as well as its orientational diffusion mechanism. DPH and derivatives having the same chromophore, such as TMA-DPH and CE-DPH, are the membrane probes most commonly used in membrane research. DPH is a rigid hydrophobic molecule with rod-like symmetry and transition moments collinear and practically parallel to the longer molecular axis (Mateo et al. 1993). The probe inserts spontaneously into the bilayer and is oriented, on average, parallel to the lipid acyl chains. The simplest treatment that accounts for the orientational diffusion of rod-shaped molecules in a lipid membrane considers the probe as undergoing free rotation in a cone-shaped volume symmetrically distributed about an axis normal to the membrane bilayer plane (Kinosita et al. 1984). In this model, $r(t)$ in Eq. 1.14 is approximated by a monoexponential function plus

the constant term r_∞, where $r_\infty = r_0\, S^2$ and S is the order parameter of the probe (Jähnig,1979), which can be taken as reflective of the membrane acyl chain order parameter. The exponential factor of $r(t)$ is viewed as an average correlation time related to the wobbling diffusion coefficient of the probe and, therefore, to the microviscosity of the membrane (Kinosita et al. 1984; Mateo et al. 1996). Numerous studies have been published in the last few decades, which use this methodology to report the effect of the presence of proteins and peptides on the structural and dynamics properties of membranes and/or on the membrane phase transition (Muller et al. 1996; Voss et al. 1991; Mateo et al. 1991a; Kremer et al. 2001; Shobini and Mishra 2001; Sanders et al. 1992). Most of them conclude that incorporation of peptides and proteins to membranes raises the lipid bilayer order parameter as well as the membrane microviscosity and that, at low concentration, does not affect or slightly shift the phase transition temperature. Similar information about the membrane properties can be extracted using fluorescent fatty acids such as *t*-PnA and *t*-COPA (Wolber et al. 1982; Mateo et al. 1996). *t*-PnA shows two very interesting properties since it dissolves preferentially in lipid environments with gel-like properties and its fluorescence lifetime is very sensitive to the local density (Sklar et al. 1977). Because of these properties the probe has been used to determine membrane heterogeneity induced by the presence of proteins, peptides or other lipids such as cholesterol (Poveda et al. 2002; Mateo et al. 1991b, 1995).

Small organic fluorophores having little structural resemblance to lipids, such as Pyrene, BODIPY or Laurdan, are also extensively used in protein–lipid studies. Incorporated into the lipid bilayer either free or covalently linked to fatty acids, these probes locate at different membrane depths and show numerous applications due to their interesting photophysical properties. Pyrene is commonly used to determine lipid lateral diffusion and to detect lipid domains through formation of excimers (Epand et al. 2003; Vanounou et al. 1993). BODIPY can be used, among other things, to determine the insertion and orientation of peptides in membranes (Epand et al. 1999). Finally, Laurdan shows spectral properties very sensitive to the physical state of the surrounding phospholipids and has been used on numerous occasions to detect lipid domains (Parasassi et al. 1994) and to determine the physical state of lipids surrounding proteins (Antollini et al. 1996).

In addition to the applications reported above for intrinsic and extrinsic fluorophores, these molecules have been extensively used as donors or acceptors in FRET experiments. As was previously described in Sect. 1.2.1, this methodology is extensively used in protein–lipid interaction studies since it yields information about the lipid distribution around proteins, protein–cholesterol interactions, segregation of lipid domains, protein association, location of peptides within the membrane, fusion or aggregation of membranes, etc. Many of these experiments use Trp or Tyr as energy donors and the membrane probes DPH, *t*-PnA or the fluorescent cholesterol analogues cholestatrienol and dehydrocholesterol as acceptors (Poveda et al. 2002; de Almeida et al. 2004; Dergunov and Dobretsov 2000; Nemecz et al. 1991). However, in most cases, donors and acceptors are extrinsic fluorophores having suitable excitation and emission wavelengths and covalently attached to protein and/or phospholipids. Table 1.1 shows some of the donor–acceptor couples of FRET most commonly used in protein–lipid interaction experiments, together with their calculated R_o values.

Table 1.1 Donor–acceptor couples of FRET most commonly used in protein–lipid interaction experiments, together with its calculated R_0 value

Donor	Acceptor	R_0 (Å)	Reference
Tyr	t-PnA	26	Poveda et al. 2002
Trp	Trp	6	Eisinger et al. 1969
	DPH	33	Poveda et al. 2003
	t-PnA	27	Poveda et al. 2003
	Dehydrocholesterol	20	De Almeida et al. 2004
	Pyrene	28	Wu and Brand 1994
	Tyr-NO_2	26	Wu and Brand 1994
	Dansyl	22	Wu and Brand 1994
Dansyl	Rhodamine	49	Yegneswaran et al. 2004
Coumarin	NBD	40	van der Meer et al. 1994
NBD	NBD	28	van der Meer et al. 1994
IAEDANS[a]	BODIPY	49	Fernandes et al. 2003
IAEDANS	FITC[b]	49	Wu and Brand 1994

[a] n-(Iodoacetyl)aminoethyl-1-sulfonaphthylamine.
[b] Fluorescein 5-isothiocyanate.

1.3.2 Protein/Peptide Fluorescence

1.3.2.1 Intrinsic Fluorescence from Aromatic Side-Chains

The photophysical properties of the amino acids containing fluorescent side-chains have been extensively characterized and reviewed (see, e.g. Lakowicz 1999 and references therein, and references in the remainder of this section), though some aspects are not fully understood, as will be described later. In this review the focus will be given on the features more directly relevant to the subject of lipid–protein interaction.

From the three naturally occurring aromatic side-chain amino acids, Phe, Tyr, and Trp, the first has a low molar absorption coefficient and quantum yield, and low maximum absorption and emission wavelengths, and thus is practically use-

less for lipid–protein interaction studies. Tyr and Trp in the zwitterionic form have similar quantum yields (Chen 1967). For proteins that do not contain Trp residues, very elegant studies have been performed based on Tyr fluorescence (some examples will be given later on this chapter). However, if both Tyr and Trp are present, selective excitation of Tyr is not possible, because of the superimposition of its absorption spectrum with Trp, and Tyr emission is usually quenched by Trp by FRET (though this latter effect can be used to obtain structural information, e.g. Moreno and Prieto 1993). When both Tyr and Trp residues are present, selective excitation of Trp can be accomplished by using excitation light of ≥ 295 nm. Both Trp and Tyr are prone to photobleaching, and adequate experimental precautions have to be employed.

Trp contains an indole group whose fluorescence properties are highly sensitive to the local environment. Changes in Trp fluorescent spectra, quantum yield steady-state anisotropy or fluorescence lifetime are often used to investigate the interaction of the macromolecule with lipid membranes and to get information about the location and conformation of the macromolecule upon interaction. One of the most immediate pieces of information about the fluorophore environment comes from its spectral distribution. The emission maximum for Trp undergoes a significant red-shift from a non-polar (~320 nm) to a solvating environment (~350 nm), and this has been used to follow protein denaturation. Analogously, the transfer of the indole moiety from the aqueous (polar) environment to the lipid bilayer (less polar) characteristically causes a blue-shift of emission. However, the membrane interface is a complex anisotropic medium, and from the blue-shift of tryptopthan upon interaction with the membrane, it is not possible to obtain quantitative information about in-depth location. The shape of the emission spectra can be analysed in a more quantitative way, and by fitting a log-normal distribution, from the recovered parameters, information about conformational and penetration heterogeneity can be obtained (see Ladhokin et al. 2000). Trp also shows a red-edge excitation shift (REES), which can be used for obtaining topographical information (Weber and Shinitzky 1970; Chattopadhyay and Raghuraman 2004).

Trp fluorescence emission decay kinetics are usually complex, and in addition to a sum of exponentials, continuous distributions of lifetime populations have also been used to describe the fluorescence decays (e.g. Vincent et al. 2000). In fact, the lifetime of Trp can be influenced by a wide variety of factors that include solvent quenching, quenching by groups in the protein itself and electron transfer to the carbonyl of the peptide bond (Engelborghs 2001). The fluorescence intensity from Trp residues generally exhibits a significant increase upon establishing an interaction with lipid bilayers. This enhancement in quantum yield of the Trp residues upon inclusion in a less polar environment is usually accompanied by a corresponding variation in its mean fluorescence excited state lifetime. However, the reverse situation has also been reported (e.g. Ghosh et al. 1997). In fact, there is no clear correlation between quantum yield and the wavelength of maximum emission in proteins with a single Trp residue (Lakowicz 1999). These effects can be caused by several polar protein groups, which are able to quench Trp fluorescence to some extent (Chen and Barkley 1998).

The intrinsic fluorescence of Tyr has been less exploited than that of Trp. Tyr fluorescence is insensitive to environmental factors like polarity and does not exhibit appreciable solvatochromism in contrast with Trp. Nonetheless, in spite of the apparent disadvantages mentioned above, Tyr shows a high intrinsic anisotropy and a fluorescence lifetime which is equally optimal to characterize nanosecond and subnanosecond motions in peptides and proteins (see Sect. 1.4.4). The multi-exponential behaviour of single Tyr peptides and proteins has been extensively reported, and has been attributed to the existence of ground-state rotamers sensing different chemical environments and interconverting slowly on the nanosecond time-scale (Laws et al. 1986), and thus the fluorescence decay of those peptides and proteins should, in principle, contain some structural information.

The peptide fluorescence, either from Trp or Tyr residue(s), or a covalently labelled probe (see below), can be highly dependent on its aggregation state. Depending on the desired information this can be viewed as an advantage or a disadvantage. If these effects are not aimed at in the study – but they do exist – small variations in concentration (peptide/lipid ratio; labelling efficiency, etc.) can cause significant changes in the experimental observables, leading to incorrect interpretations. Awareness of this fact and a detailed photophysical characterization of the protein are advised. The bright side is that a great deal of relevant information can be obtained from these effects (lipid–protein and protein–protein interactions; see examples in Sect. 1.4.2).

1.3.2.2 Introducing and Changing the Intrinsic Fluorescence of Proteins/Peptides

In many cases, though, the intrinsic fluorescence of the protein/peptide does not exist or does not have suitable properties to help answer the questions under research. The latter problem can be due to the existence of too many fluorescent residues that may hamper the interpretation of the results. It is very common to create single Trp mutants or to attach covalently a fluorescent group to a cysteine residue. With this approach, it is possible to explore the environment around different regions of a protein, by different fluorescent methodologies, obtaining a large amount of information. In any case, it should be stressed that fluorescence usually reports on the local environment of the fluorophores, whereas other techniques, such as infrared, can give global structural information, e.g. about the secondary structure (e.g. Contreras et al. 2001). In the case of extrinsic labelling, though, the fluorescence experiment reveals direct information about the extrinsic fluorophore but informs only indirectly about the particular system where the probe resides. Therefore, a thorough knowledge of the photophysical and chemical properties of the fluorophore is necessary to correctly extract the required information. Numerous fluorophores are available for covalent or non-covalent labelling to proteins and extensive information on a wide range of them is available in the Molecular Probes Catalog (www.probes.com.). For lipid–protein interactions, fluorophores such as dansyl (Plasencia et al. 2001) or NBD are the most frequently used, but also Pyrene (e.g. Barrantes et al. 2000) and others referred to

in the examples of Sect. 1.4. Fluorophores from the Rhodamine family constitute another common group. They are usually FRET acceptors for NBD (e.g. Yano et al. 2002), absorb and emit at high wavelengths, and have high quantum yield and molar absorption coefficient. For fluorescence microscopy, the fluorophores should absorb/emit more in the visible range and have good photostability, e.g. BODIPY (Janosch et al. 2004). Some of these fluorophores were mentioned in Sect. 1.3.1.

NBD, like Trp, is a polarity-sensitive probe, with the advantage, relative to the indole group, of having stronger absorption, large difference in quantum yield between aqueous and lipid environments, and absorption and emission in the visible range. The reversible refolding of the T-domain of difteria toxin was studied by using three single-Cys mutants labelled with NBD (Ladhokin et al. 2004). The mutants were chosen in such way that the label is exposed to the aqueous phase, but in different regions of the protein, in order to detect specific membrane interactions, if they are to occur (if the labels were buried, they would probably be already in a hydrophobic environment, and membrane interactions would be difficult to detect, especially because the study is based on steady-state fluorescence). The interpretation of the fluorescence results in the framework of both transmembane and interfacial hydropathy analysis (see next section) supported the suggestion of a control mechanism for the pH-dependent insertion of the toxin.

Other fluorescent groups, like green fluorescent protein and analogues, or even fluorescently labelled antibodies for a particular protein, commonly used in cell localization and co-localization studies, are generally too large to be useful in biophysical studies of lipid–protein interactions.

1.3.3 Why use Peptides?

In many biophysical studies of lipid–protein interaction, namely, those employing fluorescence techniques, designed peptides or fragments from whole proteins are used instead of the entire macromolecule. Sometimes the choice of using a peptide sequence corresponding to a small part of the protein is due to experimental limitations, but not always, and this type of study has been very important to better understand lipid–protein interaction.

Knowledge about the molecular mechanism of polypeptide interaction with insertion into and final organization within membranes is critical for understanding the activity of many hormones, host-defence peptides and lipopeptides, as well as toxins (White et al. 1998; Epand and Vogel 1999). Additionally, the use of several carefully chosen synthetic or naturally occurring peptide segments from integral membrane proteins or from membrane-binding proteins has helped to clarify the principles that govern molecular recognition between membrane-spanning polypeptides and binding/association at the membrane interface, respectively (Shai 2001).

The study of the interaction of model peptides with a zwitterionic lipid bilayer was fundamental to establish the hydrophilic/hydrophobic energetics of

membrane protein insertion (Wimley and White 1996). The partition of whole proteins into membranes is difficult or impossible to determine, and the problem of membrane protein structure and stability has been addressed by determining separately the different contributions.

The usefulness of model peptides is well demonstrated in the work by Ladokhin and White (2004) and the use of peptides derived from partial protein sequences in the work by Suárez et al. (2000). Further examples will be given in the remainder of this chapter.

A complementary biophysical and cell-biology study of the cholesterol anchor of the Hedgehog protein (Peters et al. 2004) is another illustrative case. In that study, the biophysical data from model peptides in interaction with model membranes was correlated with the effects of functional proteins at the cellular level. The model peptides were labelled with NBD at a Lys side-chain or at the N-terminus and the main fluorescence assay consisted of following the increase in NBD fluorescence when vesicles devoid of the FRET acceptor for that fluorophore (a Rhodamine-labelled lipid) were added to the sample.

1.4 Relevant Problems in Lipid–Protein Interaction and Fluorescence

1.4.1 Partition to the Membrane

The extent of the partition of a peptide between the lipid and water phases is very variable and is usually given by the partition coefficient, K_p. The determination of K_p is usually the first step in the study of the interaction of a peptide with a given membrane system. It is defined by (for an alternative definition and interconversion see Santos et al. 2003)

$$K_p = \frac{n_{S,L} / V_L}{n_{S,W} / V_W} \tag{1.20}$$

where V_i are the volumes of the phases, and $n_{S,i}$ are the moles of solute present in each phase (i = W, aqueous phase; i = L, lipid phase).

Most of the applications of fluorescence spectroscopy to the quantification of the degree of interaction of the peptide with a model membrane rely on the difference in a fluorescence parameter of the partitioning molecule, such as the quantum yield, fluorescence anisotropy or fluorescence lifetime, in the two media. The additivity of the fluorescence emission intensity, I, and steady-state anisotropy, r, lead to the following equations, which are both useful in the calculation of K_p:

$$I = (I_W + I_L K_p \bar{V}_L [L]/(1+K_p \bar{V}_L [L]) \tag{1.21}$$

$$r = \frac{r_W\,((\bar{V}_L[L])^{-1} - 1) + r_L K_p \varepsilon_L \Phi_L/(\varepsilon_W \Phi_W)}{(\bar{V}_L[L])^{-1} - 1 + K_p \varepsilon_L \Phi_L/(\varepsilon_W \Phi_W)} \tag{1.22}$$

where $[L]$ is the lipid concentration, $\bar{V}_L$ is the lipid molar volume, ε_i is the molar absorption coefficient at the excitation wavelength and Φ_i is the fluorescence quantum yield of the peptide in phase i. Equation 1.21 is also valid if lifetime-weighted quantum yields, $<\tau>$ (see Sect. 1.2.1), are used instead of steady-state intensities (in these cases, I, I_W and I_L should be replaced by $<\tau>$, $<\tau>_W$ and $<\tau>_L$, respectively – the latter values are the lifetime-weighted quantum yields in pure water and membrane phases, respectively), because both $<\tau>$ and I are proportional to the fluorescence quantum yield. In fact, the use of data coming from time-resolved experiments is advantageous because they are less prone to artefacts such as light scattering or inner filter effects, and are preferred to the use of steady-state intensities. Anisotropy measurements are also strongly affected by light scattering, which can be critical for the highest lipid concentrations (e.g. Castanho and Prieto 1992).

Measurements are usually carried out by titration, i.e. addition of successive amounts of lipid to the solution keeping the solute concentration constant, apart from the dilution effect. However, this can lead to significant photobleaching, especially if the intrinsic Trp or Tyr fluorescence is being measured. In that case, preparation of aliquots with constant solute concentrations and varying lipid amounts should be considered (see Santos et al. 1998 for an example).

In the case that K_p is not too high, the molar fraction of solute in water, x_W, can be significant. If the peptide fluorophore fluoresces in water (e.g. Trp), the experimental spectrum, $I(\lambda)_{L+W}$, is the sum of the fractions in water, $I(\lambda)_W$, and in the membrane, $I(\lambda)_L$. The latter can be obtained from:

$$I(\lambda)_L = C \cdot \left(I(\lambda)_{L+W} - x_W \frac{1}{1 + \langle\tau\rangle_L / \langle\tau\rangle_W} I(\lambda)_W \right) \tag{1.23}$$

The recovery of the anisotropy decay parameters for the peptide in the lipid phase is more complex. However, in any case, the residual anisotropy of the bound species, (see Sect. 1.2.2), is readily obtained (see Contreras et al. 2001, for an example):

$$r_\infty^L = \left(1 + \frac{x_W \langle\tau\rangle_W}{x_L \langle\tau\rangle_L} \right) \cdot r_\infty \tag{1.24}$$

where r_∞ is the experimentally determined value in the presence of lipid at time $\rightarrow \infty$.

FRET can also be used as evidence of peptide interaction with membranes (e.g. Rosomer et al. 1996). Typically, the increased efficiency of FRET between a Trp residue in the peptide and a membrane-bound acceptor probe reveals the partition of the peptide towards the bilayer. In this way, the extent of the interaction of the HIV fusion inhibitor T1249 with POPC/cholesterol vesicles was recently established, using dehydroergosterol as acceptor, despite the fact that the

fluorescence parameters of the peptide are almost unchanged in the presence of the vesicles (Veiga et al. 2004).

1.4.2 Protein/Peptide Aggregation

There are two main techniques to monitor the peptide/protein aggregation or local enrichment within the membrane: FRET between identical or non-identical protein units and self-quenching of the peptide/protein fluorescence.

The basic formalisms of FRET were described in Sect. 1.2.1, where the strong dependence of this phenomenon on the distance between fluorophores was emphasized. Energy homotransfer between Trp residues is limited to peptide aggregation studies, because of the small value for R_o for the Trp/Trp pair (6–10 Å; Table 1.1 and de Almeida et al. 2004). In any case, it has proved useful, as in a recent study on the organization of the peptide γM4 from the muscle AChR (de Almeida et al. 2004), for which significant aggregation in POPC/cholesterol (3:2) bilayers was excluded, as the decrease in the anisotropy could be explained assuming a uniform distribution of peptide. Energy homotransfer between extrinsic labels has also been used to monitor peptide aggregation within membranes (e.g. Runnels and Scarlata 1995).

Heterotransfer experiments, involving two distinct labelled derivatives of proteins or peptides, were described more than twenty years ago. In a now historical paper, using a simple formalism which neglected intermolecular FRET but took into account different oligomerization schemes (dimmers/trimers/tetramers), Veatch and Stryer (1977) verified that the hypothesis of formation of gramicidin dimers (donor: dansyl-gramicidin C; acceptor: 4-(diethylamino)-phenylazobenzene-4-sulfonyl chloride derivative of gramicidin C) led to better model fits than both trimer and tetramer formation scenarios. Aggregation of proteins of the chromaffin granule membrane, labelled with maleimide iodoaminonaphthyl sulfonate (donor) and fluorescein mercury acetate or fluorescein-5-maleimide (acceptor), was qualitatively verified by Morris et al. (1982) upon addition of calcium ion. Following these studies, FRET has become an important tool in the characterization of protein/peptide aggregation (e.g. Fagan and Dewey 1986; Adair and Engelman 1994; Yano et al. 2002; Sal-Man et al. 2004). However, self-association is not the only possible cause for increased FRET efficiency between proteins/peptides in membranes, as verified in a study of the aggregation state of the M13 major coat protein using an IAEDANS-labelled protein as donor and a BODIPY-labelled protein as acceptor, carried out in vesicles of different lipid mixtures, for which it was concluded that lipid domain formation leads to protein compartmentalization and more efficient FRET, without formation of aggregates (Fernandes et al. 2003; see also below in this section).

In addition to spectroscopic studies in membrane model systems, studies of FRET in cell membranes, carried out under the microscope (including single-pair studies) are becoming common. Kubitscheck et al. (1991) have in this manner ruled out self-association of Fc_ε receptors of type 1 on the surface of mast cells. Homoassociation of erbB2 (a member of the epidermal growth factor receptor-

type tyrosine kinase receptor family) was verified in several types of breast tumour cells (Nagy et al. 1998). Gramicidin dimerization has also been observed in single-pair FRET, and correlated with single-channel current recordings (Borisenko et al. 2003; Harms et al. 2003).

The putative existence of lipid rafts (domains enriched in (glyco)sphingolipids, cholesterol, specific membrane proteins and glycosylphosphatidylinositol (GPI)-anchored proteins) has raised, since its proposal (Simons and Ikonen 1997), considerable interest in the membrane biophysics community, because of their possible implication in a variety of cell processes (see, e.g. Simons and Toomre 2000; Anderson and Jacobson 2002, and Sect. 1.1 of this chapter). The search for lipid rafts in live cells has been carried out using FRET microscopy techniques, where the fluorophores include GPI-anchored fluorescent proteins. In some literature studies, no evidence of protein clustering using hetero-FRET was observed (Kenworthy and Edidin 1998; Kenworthy et al. 2000; Glebov and Nichols 2004). However, homo-FRET microscopy analysis yielded density-independent values of the fluorescent anisotropy of GPI-anchored folate-receptor isoform (at variance with that from transmembrane-anchored folate-receptor isoform), which can only be explained by the clustering of the proteins in domains of < 70-nm size (Varma and Mayor 1998), which are disrupted by the removal of cholesterol. Further experiments by the same group, and attempts to model the resulting complex homo- and hetero-FRET data suggest that cell surface GPI-anchored proteins are present mainly as monomers and in a minor fraction (20–40%) as very small ($<$ 5 nm) clusters containing no more than four GPI-anchored protein molecules (which can be of the same or different species) (Sharma et al. 2004). The authors argue that this cluster distribution would not be detected in the other less-sensitive hetero-FRET studies mentioned above.

Self-quenching of peptide intrinsic or extrinsic fluorescence has often been invoked as evidence for aggregation (e.g. Pecheur et al. 1999; Haro et al. 2003). However, to be certain of this, one should carry out both steady-state and time-resolved experiments to be able to distinguish between dynamic self-quenching (which may reflect local enrichment of peptide, but not necessarily formation of aggregates) and static self-quenching (which comes from aggregation; see Sect. 1.2.3). For example, de Almeida et al. (2004) observed an increased dynamic quenching (but no static quenching) of the above-mentioned γM4 peptide fluorescence in POPC/cholesterol mixtures, which (also taking into account the reduced FRET efficiency between the γM4 Trp residue and dehydroergosterol) they interpreted as reflecting the formation of peptide-rich patches, in which the peptide is not necessarily dimeric. Likewise, whereas enhanced dynamic self-quenching is verified for the BODIPY-labelled M13 major coat protein in mixtures of DMoPC/DOPC and DEuPC/DOPC (see Table 1.2 for abbreviations), from the application of Eq. 1.19, a static quenching component characterized by a reasonable active sphere radius (14 Å in both cases, the same as in pure DOPC) is recovered. This provides evidence that there is no specific protein aggregation in these systems, and confirms that the enhanced FRET efficiency for this system is probably due to protein segregation to DOPC (the hydrophobically matching phospholipid in both mixtures)-enriched heterogeneities (Fernandes et al. 2003). On the other hand, an unreasonable active sphere radius (> 20 Å) is obtained in both DEuPC

and DMoPC pure vesicles, showing that the protein aggregates when there is no hydrophobically matching phospholipids in the bilayer composition. These examples show that separation of the static and dynamic quenching components (which requires that both steady-state and time-resolved experiments be carried out) allows the identification and characterization of peptide oligomerization or segregation in the bilayer. In the case that only one of these phenomena is present, this is readily apparent from the model analysis of the data.

Besides self-quenching, a quenching-based methodology was developed (Mall et al. 2001) and applied to the study of oligomerization of peptides type Ac-LysLysGlyLeu(m)XLeu(n)LysLysAla-amide in PC bilayers, where X is Trp or the quencher 3,5-dibromotyrosine. Formation of heterodimers leads to quenching of Trp fluorescence, from which the characterization of the aggregation state is achieved, for different numbers of Leu residues in the peptides, acyl chain lengths and lipid phases.

1.4.3 Lipid Selectivity: the Annular Region

Proteins incorporated in model membranes containing lipids with different electrostatic properties or hydrophobic lengths may show selectivity to one lipid component at the protein–lipid interface or preferential phase partitioning, depending on the lipid miscibility (Dumas et al. 1997, Lehtonen and Kinnunen 1997; Fahsel et al. 2002). Characterization of the degree of selectivity of a protein for different lipids has been traditionally addressed using electron spin resonance spectroscopy (see Marsh and Horváth 1998, for a review). However, essentially identical information can be obtained using fluorescence spectroscopy tools.

Doxyl spin labels were used by Barrantes et al. (2000) to compare selectivity of the whole acetylcholine receptor and some of its transmembrane fragments (in all cases, Pyrene-labelled derivatives) for fatty acid and sterol spin-labelled probes. The determination of relative binding constants of different phospholipids for a given protein has been carried out by Lee and co-workers, using a methodology based on the quenching of Trp by brominated phospholipids, for more than two decades (East and Lee 1982). This method is still being actively used for selectivity studies in many lipid–protein/peptide systems. For example, (di(C14:1)PC) is the monounsaturated PC phospholipid with the strongest binding for the outer membrane porin OmpF from *Escherichia coli*, with smaller binding constants being measured for both longer or shorter fatty acyl chain lengths (O'Keeffe et al. 2000). The authors propose that in the chain-length range from C14 to C20, hydrophobic matching is achieved mostly by distortion of the lipid bilayer around the OmpF, whereas for chains longer than C20, distortion of both the lipid bilayer and of the protein is required. Whereas PC and PE bind with equal affinity to OmpF, the affinity for PG is about half that for PC.

ESR results report the fraction of motionally restricted lipids, whereas fluorescence collisional quenching depends on molecular contact. On the other hand, FRET only depends on donor–acceptor distances and is an alternative technique to quantify lipid selectivity. Several studies where this is exploited in a qualitative

manner have been described (Wang et al. 1988; Narayanaswami and McNamee 1993; Albert et al. 1996). Gutierrez-Merino derived approximate analytical expressions for the average rate of FRET, $<k_T>$, in membranes undergoing phase separation or protein aggregation (Gutierrez-Merino 1981a,b) and extended this formalism to the study of protein–lipid selectivity (Gutierrez-Merino et al. 1987). His approximate model (which considers only transfer to neighbouring acceptor molecules, and calculates the average rate of FRET, $<k_T>$, whose relation to the FRET efficiency is not straightforward) has proved to be useful to the study of the lipid annulus around the oligomeric acetylcholine receptor (Poveda et al. 2002; Antollini et al. 1996).

Another FRET methodology, described in Sect. 1.2.1, was recently proposed and applied to lipid selectivity of the M13 major coat protein (Fernandes et al. 2004). In one experiment, the protein selectivity for the acceptor (DOPE derivatized with NBD at the head group) was measured in bilayers of either DOPC, DEuPC or DMoPC. In a second set of measurements, several probes were used as acceptors, all studies being made in DOPC vesicles. The probes used as acceptors were phospholipids of identical acyl chains (18:1 and 12:0) and different headgroups, derivatized with NBD at the 12:0 chain. The complete set of experiments is described in Table 1.2, where the recovered association constants (K_S, see Sect. 1.2.1) are summarized. Regarding the hydrophobic matching study, the lower value recovered in DOPC relative to those in DMoPC and DEuPC bilayers confirms the larger protein selectivity towards the hydrophobic matching unlabelled phospholipid (DOPC). On the other hand, from the varying acceptor headgroup study, a larger selectivity for the anionic labelled phospholipids is inferred. The latter results confirm those of Peelen et al. (1992), obtained using ESR and aggregated

Table 1.2. Relative association constant, K_S, of labelled phospholipids towards M13 major coat protein. K_S(PC) is the relative association constant of (18:1-(12:0-NBD)-PC)

Labelled phospholipid	Bilayer composition	KS	KS/KS(PC)
$((18:1)_2$-PE-NBD)	DOPC ($(18:1)_2$PC)	1.4	–
$((18:1)_2$-PE-NBD)	DEuPC ($(22:1)_2$PC)	2.1	–
$((18:1)_2$-PE-NBD)	DMoPC ($(14:1)_2$PC)	2.9	–
(18:1-(12:0-NBD)-PE)	DOPC	2.0	1.0
(18:1-(12:0-NBD)-PC)	DOPC	2.0	1.0
(18:1-(12:0-NBD)-PG)	DOPC	2.3	1.1
(18:1-(12:0-NBD)-PS)	DOPC	2.7	1.3
(18:1-(12:0-NBD)-PA)	DOPC	3.0	1.5

protein, and in fact the relative association constants ratios (K_S(PX)/K_S(PC)) obtained in the two works are almost identical.

1.4.4 Protein/Peptide Dynamics

Time-resolved fluorescence anisotropy studies of protein and peptides in solution containing an intrinsic or extrinsic fluorophore have been carried out on numerous occasions to get an insight into the shape and size of the macromolecule. In addition, these experiments are capable of providing direct information on protein structural fluctuations occurring during the lifetime of the fluorophore that are believed to be fundamental for protein biological activity. However, little information is known about the structural fluctuations of protein and peptides inserted in lipid membranes due to the complex interpretation of the experimental results. Most of these works have explored the dynamics of peptides inserted in membranes but not of proteins, mainly because the main motions of proteins occur out of the time-scale of the fluorescence experiment (generally in microseconds or milliseconds). One of the first dynamical studies of peptides inserted in membranes was made by Maliwal et al. (1986), who labelled the peptide melittin with an anthraniloyl probe, analysing its anisotropy decay in solution and upon incorporation in the membrane. They found that melittin monomer is highly flexible in solution, with greater than 90% of its anisotropy being lost by the local motions. These internal motions drastically decrease upon binding to lipids, being very sensitive to the phase state of the lipid complexes. In 1988, Vogel et al. carried out some very interesting work in which the structural fluctuations of five membrane-incorporated 21 amino acid helical synthetic peptides containing a single Trp residue at sequence positions 1, 6, 11, 16 and 21, were analysed. In all cases the experimental anisotropy decay was fitted, according to Eq. 1.14, by a sum of two exponentials with two characteristic rotational correlation times φ_1 and φ_2, and a residual anisotropy r_∞ different from zero, indicative of the fact that the reorientational motion of the Trp side-chain, irrespective of its sequence position, is restricted on the time-scale of the fluorescence experiment. Since φ_1 and φ_2 differ by more than an order of magnitude, they were assumed to reflect two independent molecular motions, one due to fast movements of the peptide segment containing the Trp residue ($r'(t)$) and the other related to the global rotational motion of the whole peptide into the lipid bilayer (Ichiye and Karplus 1983):

$$\begin{aligned} r(t) &= r'(t)[(1-S_2^2)e^{-t/\varphi_{\text{global}}} + S_2^2] \\ r'(t) &= r(0)[(1-S_1^2)e^{-t/\varphi_{\text{segmental}}} + S_1^2] \end{aligned} \tag{1.25}$$

where S_1 and S_2 are the order parameters characterizing the internal and the whole peptide fluctuations. Since $\varphi_2 >> \varphi_1$, the above expression can be simplified to the sum of two exponential functions plus a constant term:

$$r(t) = r(0)[(1-S_1^2)\exp(-t/\varphi_{\text{segmental}}) + (1-S_2^2)S_1^2\exp(-t/\varphi_{\text{global}}) + S_1^2S_2^2] \tag{1.26}$$

and the experimental rotational correlation times, φ_1 and φ_2, can be directly related to $\varphi_{segmental}$ and φ_{global}, respectively. Using this model, Vogel et al. found that the amplitude of the fast fluctuations was modulated by the physical state of the membrane and were greater near the ends of the peptide rather than at the centre. Similar dynamical studies from different synthetic peptides containing a single Trp residue located at different positions have been carried out during the last few years (Clayton et al. 2000; Talbot et al. 2001; de Foresta et al. 2002).

The intrinsic fluorescence of Tyr has been rarely used to determine structural fluctuations of peptides inserted in lipid membranes due to its low extinction coefficient and its short absorption wavelength. However, as mentioned in Sect. 1.3.2, this amino acid shows a high intrinsic anisotropy and a fluorescence lifetime which should be appropriate to characterize nanosecond and subnanosecond motions of transmembrane peptides. Recently, Poveda et al. (2003) have exploited the intrinsic fluorescence of a 20 amino acid synthetic peptide having a single Tyr residue and no Trp in its sequence to characterize the interaction, insertion and dynamical properties of the peptide into anionic membranes. Following the same approach as Vogel et al. (1988) they found that the rotational mobility of Tyr examined from its fluorescence anisotropy decay could be described by two different rotational correlation times and a residual constant value. The short correlation time should correspond to fast rotation reporting on local Tyr mobility while the longest rotational correlation time and the high residual anisotropy indicated that the peptide diffused in a viscous and anisotropic medium compatible with the aliphatic region of a lipid bilayer. These results supported the hypothesis that the peptide was inserted into the membrane as a monomer to configure an intramolecular β-hairpin structure. Assuming that this hairpin structure behaved like a rigid-body they estimated its dimensions and rotational dynamics and a model for the peptide inserted into the bilayer was proposed.

1.4.5 Protein/Peptide Topography

The transverse location of a fluorophore in a membrane can be determined either from energy transfer or quenching methodologies, but the latter methods are by far much more common. For peptides the aim is to determine the position of the fluorophore, and from this information some global geometry for the membrane–peptide system would be inferred, e.g. a transmembrane situation versus a peptide located at the membrane surface.

The quenching methodologies are based on using a lipophilic membrane and inserting molecules in which the quencher moiety is located at selected positions. This can be reached either using derivatized fatty acids or lipids with nitroxide labels, or brominated. In the case that the fluorophore under study is at a similar position, the effective quencher concentration is higher, so a higher Stern–Volmer constant ($K_{SV} = k_q \tau_o$ in Eq. 1.15) is obtained. This approach is also called the "differential quenching methodology", and a study with at least a pair of quenchers, one near the surface and the other at an inner location, is required. In the case that qualitative information is required, direct inspection of the different plots is

enough, and there is no need to obtain time-resolved data. In all cases the effective quencher concentration should be taken into account and a reference for the nitroxide-labelled fatty acid partition constants (Eq. 1.20) is the work of Blatt et al. (1984). Lipid molar volumes can be found on the book by Marsh (1990).

However, from the above-described quenching data, quantitative information on the position of the fluorophore can be obtained using the so-called "parallax" method of Chattopadhyay and London (1987). This method, which became very popular in membrane biophysics, was later refined by the same authors (Abrams and London 1992). It was originally based on a two-dimensional sphere-of-action (the three-dimensional formalism was presented in Sect. 1.2.3), thus ignoring dynamic contributions for quenching. These contributions, in fact, exist, but if a high quencher concentration is used, their effect is not critical. Very good examples of its application to proteins/peptide topography are described in the literature, so these will not be discussed here in detail. The present state-of-the-art of this methodology was advanced by Fernandes et al. (2002), who obtained the quenching profile distribution by Brownian dynamics, making possible the recovery of both the average location and width of the fluorophore position distribution.

It is not unusual in this type of study that a downward curvature is observed in the Stern–Volmer plots. This can be due to the fraction of peptide that remains in the water under the experimental conditions where the quenching study was carried out, since this fraction is not quenched by the above-described lipophilic probes. This fraction is easily known from the peptide membrane/partition study (see Sect. 1.4.1), and in this case a Lehrer-type formalism can be fitted to the data:

$$\frac{I_0}{I} = \frac{1 + K_{SV}\,[Q]_L}{(1+ K_{SV}[Q]_L)(1-f_B) + f_B} \tag{1.27}$$

Both K_{SV} and the non-accessible fraction f_B are obtained, and the latter parameter should be close to the above-described fraction in the water, and be identical for all the quenchers used, irrespective of their location in the membrane. However this is not always verified, and, for example, in the study of inactivating peptides of the Shaker B potassium channel (Poveda et al. 2003), the clear downward curvature could not be rationalized on the basis of the very small fraction of peptide in water (5% at the most), as determined from independent methodologies. In these cases another process implying complex accessibility to the lipophilic quencher should be present (e.g. peptide aggregation), but this does not preclude obtaining the peptide location from the linear part of the plot.

Other quenching methodologies rely on the use of water-soluble quenchers such as acrylamide and iodide. Shielding from the quencher happens in the case of peptide internalization in the membrane, and in this way a smaller quenching efficiency as compared to that in water should be obtained. However, from our experience, this can only show that there is an interaction with the membrane, for which other approaches are more informative (see Sect. 1.4.1), and no real topographical information as compared to the above-described "differential quenching" can be obtained.

Regarding FRET, the approach is similar to differential quenching, but the probes deactivate the peptide's emission via a dipolar and not a molecular contact interaction. Both tryptophan and tyrosine act as energy transfer donors, since they absorb at short wavelengths, so suitable acceptors with known positions in the membrane should be used (see Table 1.1). Since the efficiency of transfer depends on the donor–acceptor interplanar separation, quantitative information can be obtained from Eqs. 1.5 and 1.6, or again it is possible to qualitatively locate the fluorophores (Moreno and Prieto 1993). A series of stearic acids derivatized with the anthroyl chromophore is available, and is characterized in great detail in the literature (see, e.g. Blatt et al. 1984). Since there is almost invariance of the absorption spectra of the different acceptors, the Förster radius is constant for all of them, and for tryptophan as a donor it is close to $R_0 = 25$ Å.

1.4.6 Modulation of Membrane Properties

The properties of a lipid bilayer membrane can be significantly affected by the interaction with proteins or peptides. These can range from local perturbations, up to drastic alterations in the membrane structure.

Although the dividing line related to the type of induced effects is difficult to establish, the traditional classification of transmembrane and non-transmembrane peptidic systems can be useful for this purpose.

For the transmembrane systems, the so-called "annular region" has been the object of studies for a long time (Sect. 1.4.3). The annular region has been assumed to consist of a single ring of lipids around the protein, but eventually it could be a larger region. In this case the process would be lipid-mediated, and it could be considered that there was a longer-range perturbation induced by the peptide. An interaction of this type was reported for the interaction of the nicotinic acetylcholine receptor, which would generate a cholesterol-rich region in its vicinity (Poveda et al. 2002).

For the case of non-transmembrane peptidic systems bound to the membrane interface, clear phase separation in the case of anionic lipid has been reported. Examples are the interaction of Pep-1, a protein carrier (e.g. Henriques and Castanho 2004), the sequestering effect on PIP_2 of protein basic domains (Gambhir et al. 2004), or strong alterations of the thermotropic behaviour of binary membrane model systems induced by a peptide hormone (Contreras et al. 2001). Cholera toxin subunit B was found to increase the size of the lo domains (rafts) for certain membrane lipid compositions (de Almeida et al. 2005). However, much stronger alterations than lipid lateral redistribution are also verified. Alterations of the hydrocarbon region of the membrane were reported (Giudici et al. 2003). The imbalance due to peptide interaction with the outer leaflet of a vesicle can induce an increase in the membrane curvature (Pokorny and Almeida 2004). This induced strain is concomitant with peptide aggregation and is followed by translocation of the aggregate. During this process the membrane undergoes very strong local perturbations. The same happens for the so-called "cell penetrating peptides", used to induce protein insertion into cells. For these systems vesicle aggregation,

lipid fusion and asymmetric lipid flip-flop are reported (Henriques and Castanho 2004).

References

Abrams FS, London E (1992) Calibration of the parallax fluorescence quenching method for the determination of membrane penetration depth: refinement and comparison of quenching by spin-labelled probes. Biochemistry 31:5312–5322

Adair BD, Engelman DM (1994) Glycophorin A helical transmembrane domains dimerize in phospholipids bilayers: a resonance energy transfer study. Biochemistry 33:5539–5544

Ahn T, Oh DB, Kim H, Park C (2002) The phase property of membrane phospholipids is affected by the functionality of signal peptides from the Escherichia coli ribose-binding protein. J Biol Chem 277: 26157–26162

Albert AD, Young JE, Yeagle PL (1996) Rhodopsin–cholesterol interactions in bovine rod outer segment disk membranes. Biochim Biophys Acta 1285:47–55

Antollini SS, Soto MA, Bonini de Romanelli I, Gutierrez-Merino C, Sotomayor P, Barrantes FJ. (1996) Physical state of bulk and protein-associated lipid in nicotinic acetylcholine receptor-rich membrane studied by laurdan generalized polarization and fluorescence energy transfer. Biophys J 70:1275–1284

Barrantes FJ, Antollini SS, Blanton MP, Prieto M. (2000) Topography of nicotinic acetylcholine receptor membrane-embedded domains. J Biol Chem 275:37333–37339

Blatt E, Chatelier RC, Sawyer WH (1984) The transverse location of fluorophores in lipid bilayers and micelles as dertermined by fluorescence techniques. Phothochem Photobiol 39:477–483

Bonini IC, Antollini SS, Gutierrez-Merino C, Barrantes FJ (2002) Sphingomyelin composition and physical asymmetries in native acetylcholine receptor-rich membranes. Eur Biophys J 31:417–427

Borisenko V, Lougheed T, Hesse J, Fureder-Kitzmuller E, Fertig N, Behrends JC, Woolley GA, Schutz GJ (2003) Simultaneous optical and electrical recording of single gramicidin channels. Biophys J 84:612–622

Castanho MARB, Prieto M (1998) Fluorescence quenching data interpretation in biological systems. The use of microscopic models for data analysis and interpretation of complex systems. Biochim Biophys Acta 1373:1–16

Chattopadhyay A, London E (1987) Parallax method for direct measurement of membrane penetration depth utilizing fluorescence quenching by spin-labelled phospholipids. Biochemistry 26:39–45

Chattopadhyay A, Raghuraman H (2004) Application of fluorescence spectroscopy to membrane protein structure and dynamcs. Curr Sci 87:175–180

Chen, RF (1967) Fluorescence quantum yields of tryptophan and tyrosine. Anal Lett 1:35–42

Chen Y, Barkley MD (1998) Toward understanding tryptophan fluorescence in proteins. Biochemistry 37:9976–9982

Cheng SF, Kantchev AB, Chang DK (2003) Fluorescence evidence for a loose self-assembly of the fusion peptide of influenza virus HA2 in the lipid bilayer. Mol Membr Biol 20:345–351

Clayton AH, Sawyer WH (2000) Site-specific tryptophan dynamics in class A amphipathic helical peptides at a phospholipid bilayer interface. Biophys J 79:1066–1073

Contreras LM, de Almeida RFM, Fedorov A, Villalaín J, Prieto M (2001) Interaction of the peptide hormone α-MSH with binary phospholipid bilayers. Structural changes and relevance of phase behavior. Biophys J 80:2273–2283

Dale RE, Chen LA, Brand L (1977) Rotational relaxation of the "microviscosity" probe diphenylhexatriene in paraffin oil and egg lecithin vesicles. J Biol Chem 252:2163–2169.

Davenport L, Dale RE, Bisby RH, Cundall, RB (1985) Transverse location of the fluorescent probe 1,6-diphenyl-1,3,5-hexatriene in model lipid bilayer membrane systems by resonance energy transfer. Biochemistry 24:4097–4108

de Almeida RFM, Loura LM, Prieto M, Watts A, Fedorov A, Barrantes FJ (2004) Cholesterol modulates the organization of the gammaM4 transmembrane domain of the muscle nicotinic acetylcholine receptor. Biophys J 86:2261–2272

de Almeida RFM, Loura LMS, Fedorov A, Prieto M (2005) Lipid rafts have different sizes depending on membrane composition: a time-resolved fluorescence resonance energy transfer study. J Mol Biol 346:1109–1120

de Foresta B, Tortech L, Vincent M, Gallay J (2002) Location and dynamics of tryptophan in transmembrane alpha-helix peptides: a fluorescence and circular dichroism study. Eur Biophys J 31:185–197

Dergunov AD, Dobretsov GE (2000) Apolipoprotein A-I localization and dipalmitoylphosphatidylcholine dynamics in reconstituted high density lipoproteins. Chem Phys Lipids 104:161–173

de Planque MR, Kruijtzer JA, Liskamp RM, Marsh D, Greathouse DV, Koeppe RE 2nd, de Kruijff B, Killian JA (1999) Different membrane anchoring positions of tryptophan and lysine in synthetic transmembrane alpha-helical peptides. J Biol Chem 274:20839–20846

Dumas F, Sperotto MM, Lebrun M-C, Tocanne J-F, Mouritsen OG (1997) Molecular sorting of lipids by bacteriorhodopsin in dilauroylphosphatidylcholine/distearoylphosphatidylcholine lipid bilayers. Biophys J 73:1940–1953

East JM, Lee AG (1982) Lipid selectivity of the calcium and magnesium ion dependent adenosinetriphosphatase, studied with fluorescence quenching by a brominated phospholipid. Biochemistry 21:4144–4451

Eisinger J, Feuer B, Lamola AA (1969) Intramolecular singlet excitation transfer. Applications to polypeptides. Biochemistry 8:3908–3915

Engelborghs Y (2001) The analysis of time resolved protein fluorescence in multi-tryptophan proteins. Spectrochim Acta A 57:2255–2270

Epand RM, Vogel HJ (1999) Diversity of antimicrobial peptides and their mechanisms of action. Biochim Biophys Acta 1462:11–28

Epand RF, Epand RM, Monaco V, Stoia S, Formaggio F, Crisma M, Toniolo C (1999) The antimicrobial peptide trichogin and its interaction with phospholipid membranes. Eur J Biochem 266:1021–1028

Epand RM, Epand RF, Sayer BG, Datta G, Chaddha M, Anantharamaiah GM (2004) Two homologous apolipoprotein AI mimetic peptides. Relationship between membrane interactions and biological activity. J Biol Chem 279:51404–51414

Epand RF, Martinou JC, Montessuit S, Epand RM (2003) Transbilayer lipid diffusion promoted by Bax: implications for apoptosis. Biochemistry 42:14576–14582

Fagan MH, Dewey TG (1986) Resonance energy transfer study of membrane-bound aggregates of the sarcoplasmatic reticulum calcium ATPase. J Biol Chem 261:3654–3660

Fahsel S, Pospiech EM, Zein M, Hazlet TL, Gratton E, Winter R (2002) Modulation of concentration fluctuations in phaseseparated lipid membranes by polypeptide insertion. Biophys J 83:334–344

Fernandes F, Loura LM, Prieto M, Koehorst R, Spruijt RB, Hemminga MA (2003) Dependence of M13 major coat protein oligomerization and lateral segregation on bilayer composition. Biophys J 85:2430–2441

Fernandes F, Loura LMS, Koehorst R, Spruijt RB, Hemminga MA, Fedorov A, Prieto M (2004) Quantification of protein–lipid selectivity using FRET: Application to the M13 major coat protein. Biophys J 87:344–352

Fernandes MX, García de la Torre J, Castanho MARB (2002) Joint determination by Brownian dynamics and fluorescence quenching of the in-depth location profile of biomolecules in membranes. Anal Biochem 307:1–12

Förster Th (1949) Experimentelle und theoretische Untersuchung des Zwischenenmolekularen übergangs von Elektronenanregungserenergie. Z Naturforsch 4a:321–327

Gambhir A, Hangyás-Mihályné G, Zaitseva I, Cafiso DS, Wang J, Murria D, Pentyala SN, Smith SO, McLaughlin S (2004) Electrostatic sequestration of PIP2 on phospholipid membranes by basic/aromatic regions of proteins. Biophys J 86:2188–2207

Glebov OO, Nichols BJ (2004) Distribution of lipid raft markers in live cells. Biochem Soc Trans 32:673–675

Ghosh AG, Rukmini R, Chattopadhyay A (1997) Modulation of tryptophan environment in membrane-bound melittin by negatively charged phospholipids: implications in membrane organization and function. Biochemistry 36:14291–14305

Giudici M, Pascual R, de la Canal L, Pfuller K, Pfuller U, Villalain J (2003) Interaction of viscotoxins A3 and B with membrane model systems: implications to their mechanism of action. Biophys J 85:971–981

Gutierrez-Merino C (1981a) Quantitation of the Förster energy transfer for two-dimensional systems. I. Lateral phase separation in unilamellar vesicles formed by binary phospholipids mixtures. Biophys Chem 14:247–257

Gutierrez-Merino C (1981b) Quantitation of the Förster energy transfer for two-dimensional systems. II. Protein distribution and aggregation state in biological membranes. Biophys Chem 14:259–266

Gutierrez-Merino C, Munkonge F, Mata AM, East JM, Levinson BL, Napier RM, Lee AG (1987) The position of the ATP binding site on the (Ca2+ + Mg2+)-ATPase. Biochim Biophys Acta 897:207–216

Harms GS, Orr G, Montal M, Thrall BD, Colson SD, Lu HP (2003) Probing conformational changes of gramicidin ion channels by single-molecule patch-clamp fluorescence microscopy. Biophys J 85:1826–1838

Haro A, Velez M, Goormaghtigh E, Lago S, Vazquez J, Andreu D, Gasset M (2003) Reconstitution of holin activity with a synthetic peptide containing the 1–32 sequence region of EJh, the EJ-1 phage holin. J Biol Chem 278:3929–3936

Henriques ST, Castanho MARB (2004) Consequences of nonlytic membrane perturbation to the translocation of the cell penetrating peptide Pep-1 in lipid vesicles. Biochemistry 43:9716–9724

Heyn MP (1989) Order and viscosity of membranes: analysis by time-resolved fluorescence depolarization. Methods Enzymol 172:462–471

Hurley JH, Meyer T (2001) Subcellular targeting by membrane lipids. Curr Opin Cell Biol 13:146–152

Ichiye T, Karplus M (1983) Fluorescence depolarization of tryptophan residues in proteins: a molecular dynamics study. Biochemistry 22:2884–2893

Jablonski A (1960) On the notion of emission anisotropy. Bull Acad Pol Sci, Série des Sci Math et Phys 8:259–264

Janosch S, Nicolini C, Ludolph B, Peters C, Volkert M, Hazlet TL, Gratton E, Waldmann H, Winter R (2004) Partitioning of dual-lipidated peptides into membrane microdomains: lipid sorting vs peptide aggregation. J Am Chem Soc 126:7496–503

Jähnig F (1979) Structural order of lipids and proteins in membranes: evaluation of fluorescence anisotropy data. Proc Natl Acad Sci USA 76:6361–6365

Jayasinghe S, Hristova K, White SH (2001) Energetics, stability and prediction of transmembrane helices. J Mol Biol 312:927–934

Kawski A (1983) Excitation energy transfer and its manifestation in isotropic media. Photochem Photobiol 4:487–508

Kenworthy AK, Edidin M (1998) Distribution of a glycosylphosphatidylinositol-anchored protein at the apical surface of MDCK cells examined at a resolution of <100 A using imaging fluorescence resonance energy transfer. J Cell Biol 142:69–84. Erratum in (1998) J Cell Biol 142:881

Kenworthy AK, Petranova N, Edidin M (2000) High-resolution FRET microscopy of cholera toxin B-subunit and GPI-anchored proteins in cell plasma membranes. Mol Biol Cell 11:1645–1655

Kinosita, K Jr, Kawato S, Ikegami A (1984) Dynamic structure of biological and model membranes: analysis by optical anisotropy decay measurement. Adv Biophys 17:147–203

Kremer JJ, Sklansky DJ, Murphy RM (2001) Profile of changes in lipid bilayer structure caused by beta-amyloid peptide. Biochemistry 40:8563–8571

Kubitscheck U, Kircheis M, Schweitzer-Stenner R, Dreybrodt W, Jovin TM, Pecht I (1991) Fluorescence resonance energy transfer on single living cells. Application of binding of monovalent haptens to cell-bound immunoglobulin E. Biophys J 60:307–318

Ladokhin AS (1997) Dustribution analysis of depth-dependent fluorescence quenching in membranes. Methods Enzymol 278:462–473

Ladokhin AS, White SH (2004) Interfacial folding and membrane insertion of a designed helical peptide. Biochemistry 43:5782–5791

Ladokhin AS, Legmann R, Collier RJ, White SH (2004) Reversible refolding of the diphtheria toxin T-domain on lipid membranes. Biochemistry 43:7451–7458

Lakowicz JR (1999) Principles of fluorescence spectroscopy. 2nd edn. Kluwer Academic, New York

Laws WR, Ross JBA, Wyssbrod HR, Beechem JM, Brand L, Sutherland JC (1986) Time-resolved fluorescence and 1H-NMR studies of tyrosine and tyrosine analogues: correlation of NMR-determined rotamer populations and fluorescence kinetics. Biochemistry 25:599–607

Lehtonen JYA, Kinnunen PKJ (1997) Evidence for phospholipids microdomain formation in liquid crystalline liposomes reconstituted with Escherichia coli lactose permease. Biophys J 72:1247–1257

Loura LMS, de Almeida RFM, Prieto M (2001) Detection and characterization of membrane microheterogeneity by resonance energy transfer. J Fluorescence 11:197–209

Loura LMS, de Almeida RFM, Coutinho A, Prieto M (2003) Interaction of peptides with binary phospholipid membranes: application of fluorescence methodologies. Chem Phys Lipids 122:77–96

MacPhee CE, Howlett GJ, Sawyer WH, Clayton AH (1999) Helix–helix association of a lipid-bound amphipathic alpha-helix derived from apolipoprotein C-II. Biochemistry 38:10878–10884

Maliwal BP, Hermetter A, Lakowicz JR (1986) A study of protein dynamics from anisotropy decays obtained by variable frequency phase-modulation fluorometry: internal motions of N-methylanthraniloyl melittin. Biochim Biophys Acta 873:173–181

Mall S, Broadbridge R, Sharma RP, East JM, Lee AG (2001) Self-association of model transmembrane alpha-helices is modulated by lipid structure. Biochemistry 40:12379–12386

Marsh D (1990) Handbook of lipid bilayers. CRC Press, Boca Raton

Marsh D, Horváth LI (1998) Structure, dynamics and composition of the lipid–protein interface. Perspectives from spin-labelling. Biochim Biophys Acta 1376:267–296

Mateo CR, Acuña AU, Brochon JC (1995) Liquid-crystalline phases of cholesterol/lipid bilayers as revealed by the fluorescence of trans-parinaric acid. Biophys J 68:978–987

Mateo CR, Lillo MP, Brochon JC, Martínez-Ripoll M, Sanz-Aparicio J, Acuña AU (1993) Rotational dynamics of 1,6-diphenyl-1,3,5-hexatriene and derivatives from fluorescence depolarisation. J Phys Chem 97:3486–3491

Mateo CR, Lillo MP, Gonzalez-Rodriguez J, Acuña AU (1991a) Molecular order and fluidity of the plasma membrane of human platelets from time-resolved fluorescence depolarization. Eur Biophys J 20:41–52

Mateo CR, Lillo MP, Gonzalez-Rodriguez J, Acuña AU (1991b) Lateral heterogeneity in human platelet plasma membrane and lipids from the time-resolved fluorescence of trans-parinaric acid. Eur Biophys J 20:53–59

Mateo CR, Souto AA, Amat-Guerri F, Acuna AU (1996) New fluorescent octadecapentaenoic acids as probes of lipid membranes and protein–lipid interactions. Biophys J 71:2177–2191

Medhage B, Mukhtar E, Kalman B, Johansson LB-Å, Molotkovsky JG (1992) Electronic energy transfer in anisotropic systems. Part 5. Rhodamine–lipid derivatives in model membranes. J Chem Soc Faraday Trans 88:2845–2851

Moreno MJ, Prieto M (1993) Interaction of the peptide hormone adrenocorticotropin, ACTH(1-24), with a membrane model system: a fluorescence study. Photochem Photobiol 57:431–437

Morris SJ, Sudhof TC, Haynes DH (1982) Calcium-promoted resonance energy transfer between fluorescently labeled proteins during aggregation of chromaffin granule membranes. Biochim Biophys Acta 693:425–436

Mouritsen OG, Bloom, M (1984) Mattress model of lipid–protein interactions in membranes. Biophys J 46:141–153

Muller JM, van Ginkel G, van Faassen EE (1996) Effect of lipid molecular structure and gramicidin A on the core of lipid vesicle bilayers. A time-resolved fluorescence depolarization study. Biochemistry 35: 488–497

Nemecz G, Jefferson JR, Schroeder F (1991) Polyene fatty acid interactions with recombinant intestinal and liver fatty acid-binding proteins. Spectroscopic studies. J Biol Chem 266:17112–17123

Nagy P, Bene L, Balazs M, Hyun WC, Lockett SJ, Chiang NY, Waldman F, Feuerstein BG, Damjanovich S, Szollosi J (1998) EGF-induced redistribution of erbB2 on breast tumor cells: flow and image cytometric energy transfer measurements. Cytometry 32:120–131

Narayanaswami V, McNamee MG (1993) Protein–lipid interactions and Torpedo californica nicotinic acetylcholine receptor function. 2. Membrane fluidity and ligand-mediated al-

teration in the accessibility of γ subunit cysteine residues to cholesterol. Biochemistry 32:12420–12427

O'Keeffe AH, East JM, Lee AG (2000) Selectivity in lipid binding to the bacterial outer membrane protein OmpF. Biophys J 79:2066–2074

Parasassi T, Di Stefano M, Loiero M, Ravagnan G, Gratton E (1994) Influence of cholesterol on phospholipid bilayers phase domains as detected by Laurdan fluorescence. Biophys J 66:120–132

Pecheur EI, Sainte-Marie J, Bienvenue A, Hoekstra D (1999) Lipid headgroup spacing and peptide penetration, but not peptide oligomerization, modulate peptide-induced fusion. Biochemistry 38:364–373

Peelen, SJCJ, Sanders JC, Hemminga MA, Marsh D (1992) Stoichiometry, selectivity and exchange dynamics of lipidprotein interaction with bacteriophage M13 coat protein studied by spin label electron spin resonance. Effects of protein secondary structure. Biochemistry 31:2670–2677

Perrin F (1926) Polarisation de la lumière de fluorescence. Vie moyenne des molécules dans l'état excité. J Physique 7:390–401

Peters C, Wolf A, Wagner M, Kuhlmann J, Waldmann H (2004) The cholesterol membrane anchor of the Hedgehog protein confers stable membrane association to lipid-modified proteins. Proc Natl Acad Sci USA 101:8531–8536

Plasencia I, Cruz A, Casals C, Perez-Gil J (2001) Superficial disposition of the N-terminal region of the surfactant protein SP-C and the absence of specific SP-B-SP-C interactions in phospholipid bilayers. Biochem J 359:651–659

Pokorny A, Almeida PFF (2004) Kinetics of dye efflux and lipid flip-flop induced by delta-lysin in phosphatidylcholine vesicles and the mechanism of graded release by amphipathic, alpha-helical peptides. Biochemistry 43:8846–8857

Poveda JA, Encinar JA, Fernandez AM, Mateo CR, Ferragut JA, Gonzalez-Ros JM (2002) Segregation of phosphatidic acid-rich domains in reconstituted acetylcholine receptor membranes. Biochemistry 41:12253–12262

Poveda JA, Prieto M, Encinar JA, Gonzalez-Ros JM, Mateo CR (2003) Intrinsic tyrosine fluorescence as a tool to study the interaction of the shaker B "ball" peptide with anionic membranes. Biochemistry 42:7124–7132

Razi-Naqvi K (1974) Diffusion-controlled reactions in two-dimensional fluids: discussion of measurements of lateral diffusion of lipids in biological membranes. Chem Phys Lett 28:280–284

Ren J, Lew S, Wang J, London E (1999) Control of the transmembrane orientation and interhelical interactions within membranes by hydrophobic helix length. Biochemistry 38:5905–5912

Romoser V, Ball R, Smrcka AV (1996) Phospholipase C β2 association with phospholipid interfaces assessed by fluorescence resonance energy transfer. G protein βγ subunit-mediated translocation is not required for enzyme activation. J Biol Chem 271:25071–25078

Runnels LW, Scarlata SF (1995) Theory and application of fluorescence homotransfer to melittin oligomerization. Biophys J 69:1569–1583

Sal-Man N, Gerber D, Shai Y (2004) Hetero-assembly between all-L- and all-D-amino acid transmembrane domains: forces involved and implication for inactivation of membrane proteins. J Mol Biol 344:855–864

Sanders JC, Ottaviani MF, van Hoek A, Visser AJ, Hemminga MA (1992). A small protein in model membranes: a time-resolved fluorescence and ESR study on the interaction of M13 coat protein with lipid bilayers. Eur Biophys J 21:305–311

Santos NC, Prieto M, Castanho, MARB (1998) Interaction of the major epitope region of HIV protein gp41 with membrane model systems. A fluorescence spectroscopy study. Biochemistry 37:8674–8682

Santos NC, Prieto M, Castanho, MARB (2003) Quantifying molecular partition into model systems of biomembranes: an emphasis on optical spectroscopic methods. Biochim Biophys Acta 1612:123–135

Sharma P, Varma R, Sarasij RC, Ira, Gousset K, Krishnamoorthy G, Rao M, Mayor S (2004) Nanoscale organization of multiple GPI-anchored proteins in living cell membranes. Cell 116:577–589

Shai Y (2001) Molecular recognition within the membrane milieu: implications for the structure and function of membrane proteins. J Membr Biol 182:91–104

Shobini J, Mishra AK (2001) Effect of a decapeptide (VPDLLADLLK) on the phase transition of dimyristoylphosphatidylcholine lipid bilayer. J Colloid Interface Sci 240:24–29

Sillen A, Engelborghs Y (1998) The correct use of "average" fluorescence parameters. Photochem Photobiol 67:475–486

Simons K, Ikonen I (1997) Functional rafts in cell membranes. Nature 387:569–572

Sklar LA, Hudson BS, Simoni RD (1977) Conjugated polyene fatty acids as fluorescent probes: synthetic phospholipid membrane studies. Biochemistry 16:819–828

Snyder B, Freire E (1982) Fluorescence energy transfer in two dimensions. A numeric solution for random and non-random distributions. Biophys J 40:137–148

Suárez T, Gallaher WR, Agirre A, Goñi FM, Nieva JL (2000) Membrane interface-interacting sequences within the ectodomain of the human immunodeficiency virus type 1 envelope glycoprotein: putative role during viral fusion. J Virol 74:8038–8047

Talbot JC, Thiaudiere E, Vincent M, Gallay J, Siffert O, Dufourcq J (2001) Dynamics and orientation of amphipathic peptides in solution and bound to membranes: a steady-state and time-resolved fluorescence study of staphylococcal delta-toxin and its synthetic analogues. Eur Biophys J 30:147–161

Tweet AG, Bellamy WD, Gaines GL Jr (1964) Fluorescence quenching and energy transfer in monomolecular films containing chlorophyll. J Chem Phys 41:2068–2077

Umberger JQ, Lamer VK (1945) The kinetics of diffusion controlled molecular and ionic reactions in solution as determined by measurements of the quenching of fluorescence. J Am Chem Soc 67:1099–1109

Van der Meer BW, Coker III G, Chen S-YS (1994) Resonance energy transfer: theory and data. VCH Publishers, New York

Vanounou S, Parola AH, Fishov I (2003) Phosphatidylethanolamine and phosphatidylglycerol are segregated into different domains in bacterial membrane. A study with pyrene-labelled phospholipids. Mol Microbiol 49:1067–1079

Varma R, Mayor S (1998) GPI-anchored proteins are organized in submicron domains at the cell surface. Nature 394:798–801

Veatch W, Stryer L (1977) The dimeric nature of the gramicidin A transmembrane channel: conductance and fluorescence energy transfer studies of hybrid channels. J Mol Biol 113:89–102

Vereb G, Szöllösi J, Matkó J, Nagy P, Farkas T, Vígh L, Mátyus L, Waldmann TA, Damjanovich S (2003) Dynamic, yet structured: the cell membrane three decades after the Singer–Nicholson model. Proc Natl Acad Sci USA 100:8053–8058

Veiga AS, Santos NC, Loura LMS, Fedorov A, Castanho MARB (2004) HIV fusion inhibitor peptide T-1249 is able to insert or adsorb to lipidic bilayers. Putative correlation with improved efficiency. J Am Chem Soc 126:14758–14763

Vincent M, Gilles A-M, de la Sierra IML, Briozzo P, Bârzu O, Gallay J (2000) Nanosecond fluorescence dynamic stokes shift of tryptophan in a protein matrix. J Phys Chem B 104:11286–11295

Vogel H, Nilsson L, Rigler R, Voges KP, Jung G (1988) Structural fluctuations of a helical polypeptide traversing a lipid bilayer. Proc Natl Acad Sci USA 85:5067–5071

Voss J, Birmachu W, Hussey DM, Thomas DD (1991) Effects of melittin on molecular dynamics and Ca-ATPase activity in sarcoplasmic reticulum membranes: time-resolved optical anisotropy. Biochemistry 30: 7498–7506

Wang S, Martin E, Cimino J, Omann G, Glaser M (1988) Distribution of phospholipids around gramicidin and D- -hydroxybutyrate dehydrogenase as measured by resonance energy transfer. Biochemistry 27:2033–2039

Weber G (1953) Rotational Brownian motion and polarization of the fluorescence of solutions. Adv Protein Chem 8: 415–449

Weber G, Shinitzky M (1970) Failure of energy transfer between identical aromatic molecules on excitation at the long wave edge of the absorption spectrum. Proc Natl Acad Sci USA 65:823–830

White SH, Wimley WC, Ladokhin AS, Hristova K (1998) Protein folding in membranes: determining energetics of peptide–bilayer interaction. Meth Enzymol 295:62–87

Wimley WC, White SH (1996) Experimentally determined hydrophobicity scale for proteins at membrane interfaces. Nat Struct Biol 3:842–848

Wolber PK, Hudson BS (1982) Bilayer acyl chain dynamics and lipid–protein interaction: the effect of the M13 bacteriophage coat protein on the decay of the fluorescence anisotropy of parinaric acid. Biophys J 37:253–262

Wu P, Brand L (1994) Resonance energy transfer: methods and applications. Anal Biochem 218:1–13

Yano Y, Takemoto T, Kobayashi S, Yasui H, Sakurai H, Ohashi W, Niwa M, Futaki S, Sugiura Y, Matsuzaki K (2002) Topological stability and self-association of a completely hydrophobic model membrane helix in lipid bilayers. Biochemistry 41:3073–3080

Yegneswaran S, Deguchi H, Griffin JH, Yegneswaran S, Deguchi H, Griffin JH (2003) Glucosylceramide, a neutral glycosphingolipid anticoagulant cofactor, enhances the interaction of human- and bovine-activated protein C with negatively charged phospholipid vesicles. J Biol Chem 278:14614–14621

Zhao H, Mattila JP, Holopainen JM, Kinnunen PK (2001) Comparison of the membrane association of two antimicrobial peptides, magainin 2 and indolicidin. Biophys J 81:2979–2991

NMR of Membrane Proteins in Lipid Environments: the Bcl-2 Family of Apoptosis Regulators

Xiao-Min Gong, Jungyuen Choi, and Francesca M. Marassi

2.1 Introduction

Many fundamental cellular functions are regulated by proteins that are integral to membranes, or that associate peripherally with their surfaces. Understanding the structures of these molecules is a major goal of structural biology; however, despite their importance, only a few structures of membrane proteins have been deposited in the Protein Data Bank (PDB), compared to the thousands of coordinates deposited for globular proteins (www.rcsb.org/pdb/). This deficit reflects the lipophilic character of membrane proteins, which makes them difficult to over-express and purify, complicates crystallization for X-ray analysis, and results in highly overlapped and broadened solution NMR spectral lines. NMR spectroscopy offers two complementary approaches to membrane protein structure determination: solution NMR with samples of membrane proteins dissolved in lipid micelles, and solid-state NMR with samples of proteins incorporated in lipid bilayers, a method that is particularly attractive because it enables structures to be determined in an environment that closely mimics the biological membrane.

High-quality solution NMR spectra can be obtained for some large, helical, membrane proteins in micelles, but it is very difficult to measure and assign a sufficient number of long-range nuclear Overhauser effects (NOEs) for structure determination (Klein-Seetharaman et al. 2002; Oxenoid et al. 2004). This limitation can be overcome by preparing weakly aligned micelle samples for the measurement of residual dipolar couplings (RDCs) and residual chemical shift anisotropies (RCSAs) (Bax et al. 2001; Prestegard and Kishore 2001), as demonstrated for the structure of the bacterial mercury detoxification membrane protein MerF (Howell et al. 2005).

High-resolution solid-state NMR spectra can be obtained for membrane proteins that are expressed, isotopically labeled, and reconstituted in uniaxially oriented planar lipid bilayers. The spectra have characteristic resonance patterns that directly reflect protein structure and topology, and this direct relationship between spectrum and structure provides the basis for methods that enable the simultaneous sequential assignment of resonances and the measurement of orientation restraints for protein structure determination (Marassi and Opella 2000; Wang et al. 2000; Marassi 2001). Recent developments in sample preparation, recombinant bacterial expression systems for the preparation of isotopically labeled membrane proteins, pulse sequences for high-resolution spectroscopy, and

Springer Series in Biophysics
C.R. Mateo et al. (Ed.)
Protein-Lipid Interactions

structural indices that guide the structure assembly process, have greatly extended the capabilities of the technique. The structures of a variety of membrane peptides and proteins have been examined using this approach, and several atomic-resolution structures have been determined and deposited in the PDB (Ketchem et al. 1993; Opella et al. 1999; Valentine et al. 2001; Wang et al. 2001; Marassi and Opella 2003; Park et al. 2003).

In this chapter, the methods are illustrated with examples from the Bcl-2 family proteins, which regulate a major mechanism for commitment to programmed cell death (apoptosis), and play critical roles in tissue development, differentiation, and homeostasis.

2.2 The Bcl-2 Family Proteins and Programmed Cell Death

Programmed cell death is initiated when death signals activate the caspases, a family of otherwise dormant cysteine proteases. External stress stimuli trigger the ligation of cell surface death receptors, thereby activating the upstream initiator caspases, which in turn process and activate the downstream cell death executioner caspases (Denault and Salvesen 2002). In addition, caspases can be activated when stress or developmental cues within the cell induce the release of cytotoxic proteins from mitochondria. This intrinsic mitochondrial pathway for cell death is regulated by the relative ratios of the pro- and anti-apoptotic members of the Bcl-2 protein family.

Several Bcl-2 family members have been identified in humans, including both anti-apoptotic (cytoprotective) and pro-apoptotic (death-promoting) proteins (Green and Reed 1998; Kroemer and Reed 2000; Cory and Adams 2002; Danial and Korsmeyer 2004). The relative ratios of the pro- and anti-apoptotic proteins determine the ultimate sensitivity and resistance of cells to diverse death-inducing stimuli, including chemotherapeutic drugs, radiation, growth factor deprivation, loss of cell attachment to extracellular matrix, hypoxia, infection, and lysis by cytolytic T cells. Imbalances in their relative expression levels and activities are associated with major human diseases, characterized by either insufficient (cancer, autoimmunity) or excessive (AIDS, Alzheimer‘s disease) cell death.

The Bcl-2 proteins span approximately 200 amino acids, and share sequence homology in four evolutionarily conserved domains (BH1–BH4), of which the BH3 domain is highly conserved and essential for both cell killing and oligomerization among Bcl-2 family members (Fig. 2.1). The anti-apoptotic family members have all four domains, while all of the pro-apoptotic members lack BH4, and some others only have BH3. These BH3-only proteins are activated by upstream death signals, which trigger their transcriptional induction or post-translational modification, providing a key link between the extrinsic death receptor and intrinsic mitochondrial pathways to cell death. Most family members also have a hydrophobic C-terminus (C) which is sufficiently long to span the membrane, and is essential for membrane targeting.

The apoptosis regulatory activities of the Bcl-2 family proteins are exerted through binding with other Bcl-2 family members, binding with other non-ho-

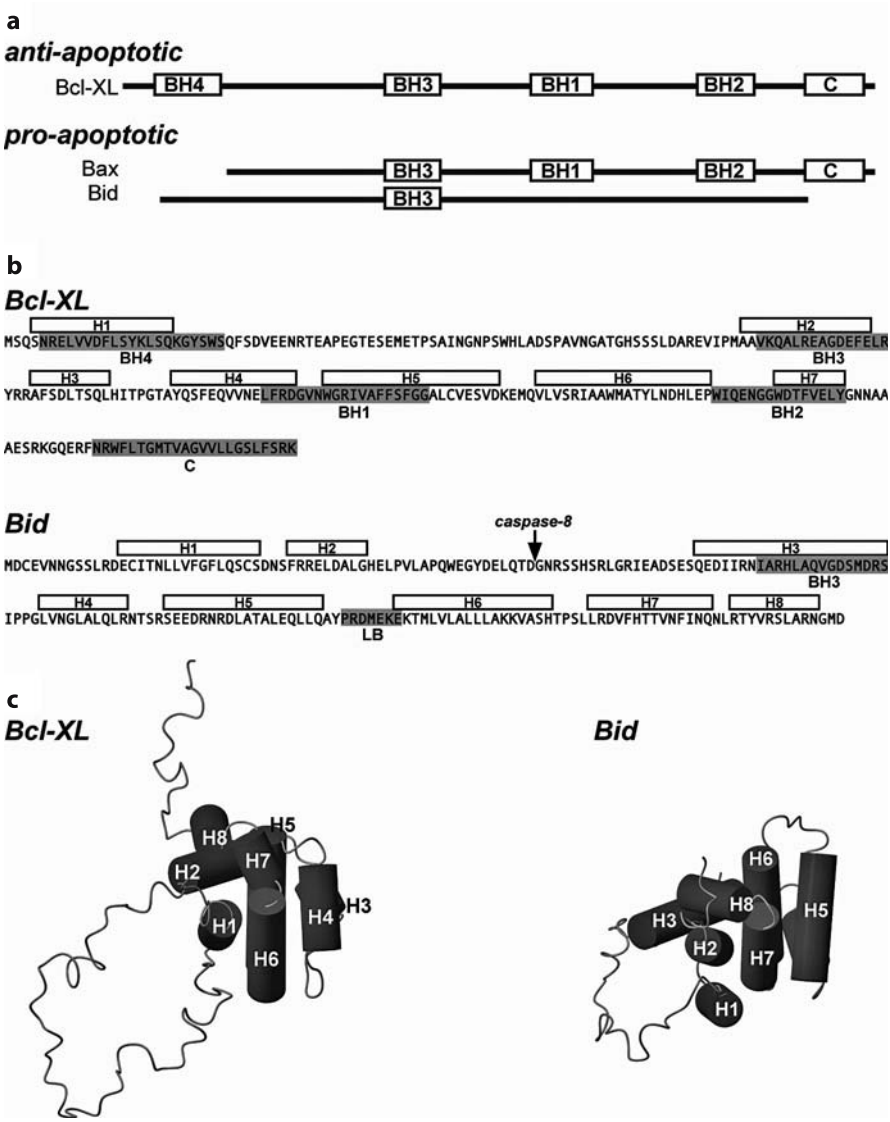

Fig. 2.1. Domain organization (**a**) and amino acid sequences (**b**) of human Bcl-XL and Bid. The helices (H1 to H8) are those identified in the solution NMR structures of Bcl-XL (Muchmore et al. 1996; Aritomi et al. 1997) and Bid (Chou et al. 1999; McDonnell et al. 1999) shown in (**c**). The central core helices are H5 and H6 in Bcl-XL and H6 and H7 in Bid. The C-terminal hydrophobic segment of Bcl-XL is denoted as C. The putative lipid binding motif of Bid is denoted as LB. The sequence of tBid starts at Gly61, and the *arrow* marks the caspase-8 cleavage site at Asp60

mologous proteins, and through the modulation of ion-conducting pores that are thought to influence cell fate by regulating mitochondrial physiology. Their functions are also regulated by subcellular location, as the proteins cycle between soluble and membrane-bound forms. For example, some family members, like anti-apoptotic Bcl-XL, localize to mitochondrial, endoplasmic reticulum, or nuclear membranes, while others, like pro-apoptotic Bid, are found in the cytosol, but are stimulated by death signals to target the mitochondrial outer membrane, where they participate in cytochrome-c release and apoptosis.

The structures of Bcl-XL and Bid, in solution, are very similar. They consist of seven (Bcl-XL) or eight (Bid) α-helices arranged with two central somewhat more hydrophobic helices which form the core of the molecule (Fig. 2.1). In Bcl-XL, the third helix spans the BH3 domain, and is connected to the first helix by a long flexible loop, while helices 5 and 6 form the central hydrophobic hairpin (Muchmore et al. 1996; Aritomi et al. 1997). The structure was determined for a truncated form of the protein lacking the hydrophobic C-terminus. In Bid, the third helix contains the BH3 domain and is connected to the first two helices by a long flexible loop, which includes Asp60, the caspase-8 cleavage site. The hydrophobic hairpin is formed by helices 6 and 7 (Chou et al. 1999; McDonnell et al. 1999). Despite the lack of sequence homology, the structures of Bcl-XL and Bid are strikingly similar to each other, and those of other pro- and anti-apoptotic Bcl-2 family proteins (Suzuki et al. 2000; Petros et al. 2001; Huang et al. 2002; Denisov et al. 2003; Hinds et al. 2003; Huang et al. 2003; Day et al. 2004; Day et al. 2005). Interestingly, they are also similar to the structure of the pore-forming domains of bacterial toxins, and, like the toxins and other Bcl-2 family members, they also form ion-conducting pores in lipid bilayers (Cramer et al. 1995; Schendel et al. 1998; Schendel et al. 1999).

The structural basis for Bcl-2 pore formation is not known, since the structures that have been determined are for the soluble forms of the proteins, and pore formation by the Bcl-2 family proteins has not been established in vivo. Nevertheless, by analogy to the bacterial toxins, the Bcl-2 pores are thought to form by a rearrangement of their compactly folded helices upon contact with the mitochondrial membrane. One model proposes membrane insertion of the core helical hairpin with the other helices folding up to rest on the membrane surface, while an alternative model envisions the helices rearranging to bind the membrane surface without insertion. A third possible mechanism for the regulation of mitochondrial physiology by the Bcl-2 proteins is through their interaction with other mitochondrial channels.

2.3 Protein Expression and Purification

NMR structural studies require milligram quantities of isotopically labeled proteins, and the most versatile and widely used method for obtaining recombinant proteins is by expression in *E. coli*, since this enables a wide variety of isotopic labeling schemes to be incorporated in the NMR experimental strategy. Smaller peptides can be prepared by solid phase peptide synthesis; however, this

is impractical for larger proteins and for the preparation of uniformly labeled samples, where efficient expression systems are essential. The ability to produce milligram quantities of pure proteins also facilitates functional studies that, together with structure determination, can provide important structure–activity correlations.

Some polypeptides, however, are toxic to the bacterial hosts that express them. For example, some membrane proteins and peptides, including some of bacterial origin, congest the cell membranes when they are over-expressed, and act as toxic, antibacterial agents, regardless of their actual biological functions. For these difficult polypeptides, solid-phase synthesis is not a practical alternative, because it is typically limited to sequences shorter than 50 amino acids, and while this size limit can be extended through the use of chemical ligation methods (Dawson et al. 1994; Kochendoerfer 2001) that can also be applied to membrane proteins (Kochendoerfer et al. 1999; Kochendoerfer et al. 2004), NMR studies still require bacterial expression of the polypeptide precursors for the practical introduction of various isotopic labels.

Several *E. coli* cell strains and expression strategies have been developed to address this problem (Miroux and Walker 1996; Rogl et al. 1998; Jones et al. 2000; Majerle et al. 2000; Opella et al. 2001; Sharon et al. 2002; Bannwarth and Schulz 2003; Booth 2003; Kiefer 2003; Lindhout et al. 2003; Smith and Walker 2003; Wiener 2004), and more recently, cell-free expression has been used to obtain milligram quantities of isotopically labeled membrane proteins (Klammt et al. 2004). Many strategies rely on the use of fusion protein tags to improve expression and facilitate purification, and many involve protein expression in inclusion bodies, to keep the hydrophobic polypeptide away from the bacterial membranes, and thus increase the level of expression. The formation of inclusion bodies also limits proteolytic degradation, and simplifies protein purification, which can be further assisted by the incorporation of an engineered His tag for metal affinity chromatography.

The TLE (a portion of the Trp ΔLE 1413 polypeptide) (Miozzari and Yanofsky 1978; Kleid et al. 1981; Staley and Kim 1994), and KSI (ketosteroid isomerase) (Kuliopulos et al. 1994) fusion partners promote the accumulation of expressed proteins as inclusion bodies, and have been used to express several membrane peptides and proteins ranging in size from 20 to 200 amino acids (Opella et al. 2001; Opella and Marassi 2004).

Recently, we developed a fusion protein expression vector, pBCL, that directs the expression of a target polypeptide fused to the C-terminus of a mutant form of the Bcl-2 family protein Bcl-XL, where the hydrophobic C-terminus has been deleted, and Methionine residues have been mutated to Leucine, to facilitate CNBr cleavage after a single Methionine inserted at the beginning of the target polypeptide sequence (Thai et al. 2005). As shown in Fig. 2.2, this fusion partner yields the high-level expression of membrane proteins belonging to the FXYD family of Na,K-ATPase regulators, including some that had resisted expression with TLE and KSI.

The pTLE and pBCL vectors may be generally useful for the high-level expression of other membrane-associated proteins that are difficult to express because of their toxic properties. The use of chemical cleavage eliminates the difficulties,

poor specificity and enzyme inactivation, often encountered with protease treatment of insoluble proteins. However, in cases where Met mutation is not feasible, protein cleavage from the fusion partner can be obtained enzymatically, by engineering specific protease cleavage sites for the commonly used enzymes thrombin, Fxa, enterokinase, and tobacco etch virus (TEV) protease. Thrombin and TEV retain activity in the presence of detergents, including low mM concentrations of SDS.

The pro-apoptotic Bcl-2 family protein, Bid, is activated upon cleavage by caspase-8, to release the 15 kD C-terminal fragment tBid, which translocates from the cytosol to the outer mitochondrial membrane inducing massive cytochrome-c release and cell death (Scorrano and Korsmeyer 2003). Full-length Bid can be expressed at high levels, in *E. coli*, as a soluble protein, however tBid is toxic for bacterial cells. To produce milligram quantities of ^{15}N-labeled tBid for NMR studies we used the TLE fusion protein vector (Fig. 2.2). tBid was separated from the fusion partner by means of CNBr cleavage at the engineered N-terminal Met residue, and this method yields approximately 10 mg of purified ^{15}N-labeled tBid from 1 L of culture. To avoid cleavage within the tBid segment, the four Met residues in the tBid amino acid sequence were mutated to Leu, and therefore, it was important to demonstrate that the recombinant protein retained its biological activity. Recombinant tBid, isolated from inclusion bodies, was fully active in its ability to induce cytochrome-c and SMAC release from isolated mitochondria, and retained its capacity to bind anti-apoptotic Bcl-X_L through its BH3 domain despite the M97L mutation in its sequence (Gong et al. 2004).

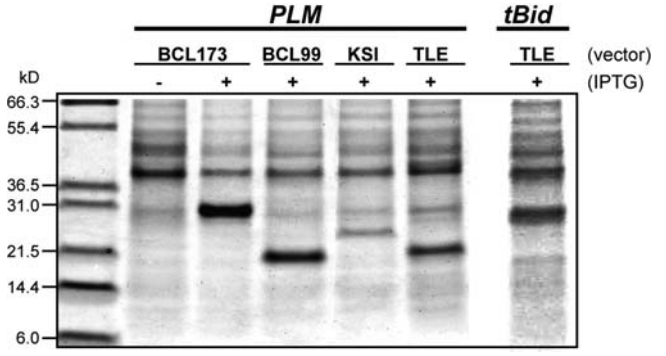

Fig. 2.2. Expression of the membrane protein phospholemman (PLM) and of tBid with four different fusion protein plasmid vectors: pBCL173, pBCL99, pKSI, and pTLE. The gel shows total lysates from cells, transformed with each plasmid, and harvested before (–) or after (+) induction with IPTG. Fusion protein over-expression is marked by the appearance of a distinct band at the molecular weight of the corresponding fusion protein: BCL173-PLM (29.8 kD), BCL99-PLM (21.2 kD), KSI-PLM (23.4 kD), TLE-PLM (22.1 kD), and TLE-tBid (30.0 kD) (Gong et al. 2004; Thai et al. 2005)

2.4 NMR in Micelles

Solution NMR methods rely on rapid molecular reorientation for line narrowing, and can be successfully applied to membrane proteins in micelles (Henry and Sykes 1994; Williams et al. 1996; Almeida and Opella 1997; Gesell et al. 1997; MacKenzie et al. 1997; Arora et al. 2001; Fernandez et al. 2001; Hwang et al. 2002; Ma et al. 2002; Mascioni et al. 2002; Oxenoid et al. 2002; Sorgen et al. 2002; Crowell et al. 2003; Krueger-Koplin et al. 2004; Howell et al. 2005). The size limitation is substantially more severe than for globular proteins, because the many lipid molecules associated with each polypeptide slow its overall reorientation rate. Micelles afford rapid and effectively isotropic reorientation of the protein, and their amphipathic nature simulates that of membranes, offering a realistic alternative to organic solvents for studying membrane proteins. Moreover, for the proteins examined by both solution and solid-state NMR, similar structural features have been found in micelle and bilayer samples (Lee et al. 2003; Mesleh et al. 2003).

The first step in solution NMR studies of proteins is the preparation of folded, homogeneous, and well-behaved samples, and several lipids are available for membrane protein solubilization (Krueger-Koplin et al. 2004). For membrane-bound proteins, small micelles containing approximately 60 lipids and one protein provide a generally effective model membrane environment, without the damaging effects of organic solvents. The primary goal in micelle preparation is to reduce the effective rotational correlation time of the protein so that resonances will have the narrowest possible linewidths. Careful handling of the protein throughout the purification is essential, since subtle changes in the protocol can have a significant impact on the quality of the resulting spectra. It is essential to optimize the protein concentration, lipid nature and concentration, counter ions, pH and temperature, in order to obtain well-resolved NMR spectra, with narrow ^{1}H and ^{15}N resonance linewidths.

Although high-quality solution NMR spectra can be obtained even for some large helical membrane proteins in micelles (Krueger-Koplin et al. 2004; Oxenoid et al. 2004; Howell et al. 2005), there are only very few cases where it has been possible to measure and assign sufficiently long-range NOEs for structure determination. This limitation can be overcome by preparing weakly aligned micelle samples for the measurement of RDCs (Bax et al. 2001; Prestegard and Kishore 2001) from the backbone amide sites, and the analysis of these orientation restraints in terms of dipolar waves (Mesleh et al. 2002; Lee et al. 2003; Mesleh et al. 2003; Mesleh and Opella 2003). Stressed polyacrylamide gels provide an ideal orientable medium for membrane proteins in micelles, because they do not suffer from the drawbacks of bicelles, which bind tightly to membrane proteins, or phage particles, which are destroyed by micelles (Sass et al. 2000; Tycko et al. 2000; Chou et al. 2001; Meier et al. 2002; Howell et al. 2005). Another useful approach to compensate for insufficient NOEs involves the combination of site-directed spin labeling and NMR (Battiste and Wagner 2000), where distances derived from paramagnetic broadening of NMR resonances are used to determine global fold. In addition, spin label probes and metal ions can be incorporated within the micelles in order to probe protein insertion (Papavoine et al. 1994; Van Den Hooven

et al. 1996; Jarvet et al. 1997; Damberg et al. 2001; Sorgen et al. 2002; Kutateladze et al. 2004).

2.4.1 Determining the Structures of Proteins in Micelles

The measurements of as many homonuclear $^1H/^1H$ NOEs as possible among the assigned resonances provide the short-range and long-range distance restraints required for structure determination (Clore and Gronenborn 1989, Wuthrich 1989, Ferentz and Wagner 2000). These are supplemented by other structural restraints, such as spin–spin coupling constants, chemical shift correlations, deuterium exchange data, and RDCs in order to assign resonances and to characterize the secondary structure of the protein. The HSQC (heteronuclear single quantum coherence) spectra of samples in D_2O solutions identify the most stable helical residues, and can provide useful information on the topology of membrane proteins in micelles (Czerski et al. 2000). In addition, hydrogen–deuterium fractionation experiments extend the range of exchange rates that can be monitored to identify more subtle structural features (Veglia et al. 2002).

The two-dimensional HSQC spectra also serve as the basis for the measurement of the ^1H and ^{15}N relaxation parameters of protein backbone amide sites, which are useful for describing protein dynamics. The heteronuclear $^1H–^{15}N$ NOEs of the backbone amide sites provide remarkably direct and sensitive information on local protein dynamics (Gust et al. 1975; Boguski et al. 1987; Bogusky et al. 1988). They can be measured with and without ^1H irradiation to saturate the ^1H magnetization (Farrow et al. 1994).

RDCs are extremely useful both for structure refinement, and for the *de novo* determination of protein folds (Tolman et al. 1995; Clore and Gronenborn 1998; Delaglio et al. 2000; Fowler et al. 2000; Hus et al. 2000; Mueller et al. 2000). During refinement, these measurements supplement an already large number of chemical shifts, approximate distance measurements, and dihedral angle restraints. Among the principal advantages of anisotropic spectral parameters in solution NMR spectroscopy is that they can report on the global orientations of separate domains of a protein and of individual bonds relative to a reference frame, which reflects the preferred alignment of the molecule in the magnetic field. This does not preclude their utility in characterizing the local backbone structure of a protein molecule.

The RDCs and RCSAs measured in solution NMR experiments provide direct angular restraints with respect to a molecule-fixed reference frame (Bax et al. 2001; Prestegard and Kishore 2001; Lee et al. 2003). They are analogous to the non-averaged dipolar couplings and chemical shift anisotropies measured in solid-state NMR experiments (Marassi and Opella 2000; Wang et al. 2000; Marassi 2001). These orientation restraints are the principal mechanism for overcoming the limitations resulting from having few reliable long-range NOEs available as distance restraints, often encountered with samples of membrane-bound proteins in micelles.

Dipolar waves are very effective at identifying the helical residues in membrane-bound proteins and the relative orientations of the helical segments, and also serve as indices of the helix regularity in proteins (Mesleh et al. 2002). The magnitudes of the RDCs are plotted as a function of residue number and fitted to a sine wave with a period of 3.6 residues (Mesleh et al. 2002; Mesleh et al. 2003; Mesleh and Opella 2003). The quality of fit is monitored by a scoring function in a four-residue sliding window and the phase of the fit. Dipolar waves from solution NMR data give relative orientations of helices in a common molecular frame. On the other hand, Dipolar waves from solid-state NMR data give absolute measurements of helix orientations because the polypeptides are immobile and the samples have a known alignment in the magnetic field.

2.4.2 tBid in Micelles

The cleavage of Bid by caspase-8 results in a C-terminal product, tBid, which targets mitochondria and induces apoptosis with strikingly enhanced activity. To characterize the conformation of tBid in lipid environments, we obtained its CD (circular dichroism) and solution NMR $^{1}H/^{15}N$ HSQC spectra in the absence or in the presence of lipid micelles (Fig. 2.3) (Gong et al. 2004). The HSQC spectra of proteins are the starting point for additional multidimensional NMR experiments that lead to structure determination. In these spectra, each ^{15}N-labeled protein site gives rise to a single peak, characterized by ^{1}H and ^{15}N chemical shift frequencies that reflect the local environment. In addition, the peak linewidths and lineshapes, and their dispersion in the ^{1}H and ^{15}N frequency dimensions, are sensitive indicators of protein conformational stability and aggregation state.

In the absence of lipids, the CD spectrum of tBid displays minima at 202 nm and 222 nm, characteristic of predominantly helical proteins (Fig. 2.3a, solid line). However, while tBid retains its helical conformation even when it is separated from the 60-residue N-terminal segment, many of the resonances in its HSQC spectrum cannot be detected (Fig. 2.3b), suggesting that the protein aggregates in solution, adopts multiple conformations, or undergoes dynamic conformational exchange on the NMR time-scales. This is consistent with the dramatic changes in the physical properties of the protein that result from caspase-8 cleavage.

When tBid is dissolved in lipid micelles its HSQC spectrum changes dramatically, and single, well-defined $^{1}H/^{15}N$ resonances are observed for each ^{15}N-labeled NH site, indicating that it adopts a unique conformation in this environment (Figs. 2.3c, d). Several lipids are available for protein solubilization, and we tested both SDS and LPPG for their ability to yield high-quality HSQC spectra of tBid for structure determination. Both gave excellent spectra where most of the 130 amide resonances of tBid could be resolved; for example the resonances from the five Gly amide sites are resolved in SDS (Fig. 2.3c), and four out of five are resolved in LPPG (Fig. 2.3d). Both SDS and LPPG are negatively charged but they differ in the lengths of their hydrocarbon chains (C12 for SDS; C16 for LPPG), and their polar headgroups (sulfate for SDS; phosphatidylglycerol for LPPG), thus the differences in the ^{1}H and ^{15}N chemical shifts between the two HSQC spectra most

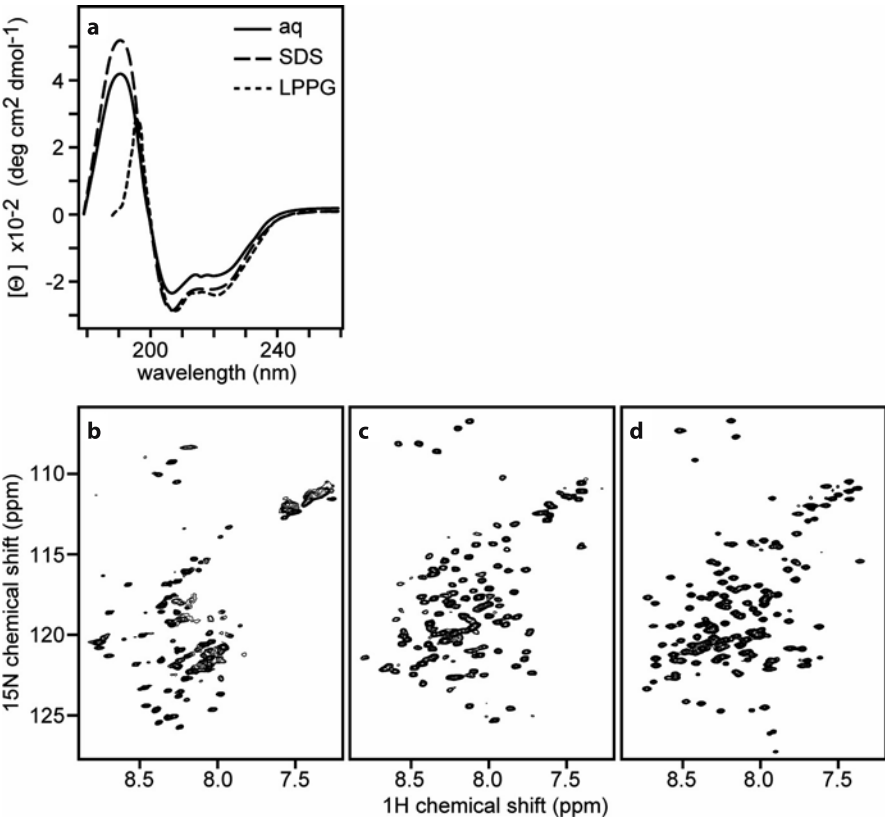

Fig. 2.3. tBid adopt well-defined helical folds in lipid micelles. The CD spectra in (**a**) were obtained at 25 °C for tBid in aqueous solution (*solid line*), SDS micelles (*broken line*), or LPPG micelles (*dotted line*). The $^{1}H/^{15}N$ HSQC NMR spectra in (**b, c, d**) were obtained at 40 °C for uniformly ^{15}N-labeled tBid in (**a**) aqueous solution, (**b**) SDS micelles, or (**c**) LPPG micelles. Aqueous samples were in 20 mM sodium phosphate, pH 5; SDS micelle samples were in 20 mM sodium phosphate, pH 7, 500 mM SDS; and LPPG micelle samples were in 20 mM sodium phosphate, pH 7, 100 mM LPPG

likely reflect the different lipid environments. The spectrum in LPPG has exceptionally well-dispersed resonances with homogeneous intensities and linewidths. LPPG was recently identified as a superior lipid for NMR studies of several membrane proteins (Krueger-Koplin et al. 2004), and is particularly interesting for this study because it is a close analog of cardiolipin and monolysocardiolipin, the major components of mitochondrial membranes that bind tBid. The limited chemical shift dispersion in the two spectra is typical of helical proteins in micelles, and this is confirmed by the corresponding CD spectra, which are dominated by minima at 202 nm and 222 nm, and thus show that tBid retains a predominantly helical fold in both SDS and LPPG (Fig. 2.3a, broken and dashed lines).

2.5 NMR in Bilayer Membranes

When the lipid bilayers are oriented with their surface perpendicular to the magnetic field, the solid-state NMR spectra of the membrane-associated proteins trace out maps of their structure and orientation within the membrane, and thus provide very useful structural information prior to complete structure determination (Marassi and Opella 2000; Wang et al. 2000; Marassi 2001). For example, helices give characteristic solid-state NMR spectra where the resonances from amide sites in the protein trace-out helical wheels that contain information regarding helix tilt and rotation within the membrane. Typically, trans-membrane helices have PISEMA spectra with ^{15}N chemical shifts between 150 and 200 ppm, and ^{1}H–^{15}N dipolar couplings between 2 and 10 kHz, while helices that bind parallel to the membrane surface have spectra with shifts between 70 and 100 ppm and couplings between 0 and 5 kHz. We refer to these as the trans-membrane and in-plane regions of the PISEMA spectrum, respectively.

Glass-supported oriented phospholipid bilayers containing membrane proteins accomplish the principal requirements of immobilizing and orienting the protein for solid-state NMR structure determination. The planar lipid bilayers are supported on glass slides, and are oriented in the NMR probe so that the bilayer normal is parallel to the field of the magnet, as shown in Fig. 2.4a. The choice of lipid can be used to control the lateral spacing between neighboring phospholipid molecules as well as the vertical spacing between bilayers. The use of phospholipids with unsaturated chains leads to more expanded and fluid bilayers, and the addition of negatively charged lipids increases inter-bilayer repulsions leading to larger interstitial water layers between bilayer leaflets.

Samples of membrane proteins in lipid bilayers oriented on glass slides can be prepared by deposition from organic solvents followed by evaporation and lipid hydration, or by fusion of reconstituted unilamellar lipid vesicles with the glass surface (Marassi 2002). The choice of solvents in the first method, and of detergents in the second, is critical for obtaining highly oriented lipid bilayer preparations. In all cases the thinnest available glass slides are utilized to obtain the best filling factor in the coil of the probe. With carefully prepared samples it is possible to obtain ^{15}N resonance linewidths of less than 3 ppm (Marassi et al. 1997). Notably, these linewidths are less than those typically observed in single crystals of peptides, demonstrating that the proteins in the bilayers are very highly oriented, with mosaic spreads of less than about 2°.

2.5.1 Bcl-XL and tBid in Bilayers

To examine the conformations of Bcl-XL and tBid associated with membranes, we obtained one-dimensional ^{15}N chemical shift and two-dimensional ^{1}H/^{15}N PISEMA solid-state NMR spectra of the ^{15}N-labeled proteins reconstituted in lipid bilayers (Franzin et al. 2004; Gong et al. 2004). In these samples, the lipid composition of 60% DOPC and 40% DOPG was chosen to mimic the highly nega-

tive charge of mitochondrial membranes. This lipid composition is identical to that of the liposomes used for the measurement of the ion channel activities of Bcl-XL, Bid, and tBid (Minn et al. 1997; Schendel et al. 1999), which were prepared in the same way as the oriented lipid bilayers used in the NMR study.

The samples of Bcl-XL and tBid in bilayers were prepared by spreading lipid vesicles, reconstituted with ^{15}N-labeled protein, on the surface of the glass slides, allowing bulk water to evaporate, and incubating the sample in a water-saturated atmosphere (Franzin et al. 2004; Gong et al. 2004). Each sample was wrapped in parafilm and then sealed in thin polyethylene film prior to insertion in the NMR probe. The degree of phospholipid bilayer alignment can be assessed with solid-state ^{31}P NMR spectroscopy of the lipid phosphate headgroup. The ^{31}P NMR spectra obtained for lipid bilayers with Bcl-XL are characteristic of a liquid-crystalline bilayer arrangement, in both oriented (Fig. 2.4b) and unoriented samples (Fig. 2.4c). The spectrum from the oriented sample has a single peak near 30 ppm, as expected for highly oriented bilayers.

2.5.1.1 Membrane-Associated Bcl-xL

The spectra in Fig. 2.4 were obtained from samples of uniformly ^{15}N-labeled Bcl-xL in oriented and unoriented lipid bilayers (Franzin et al. 2004). The spectrum obtained from oriented Bcl-xL (Fig. 2.4d) is separated into discernable resonances with distinct intensities near 80 and 170 ppm. These spectral features reflect a structural model where the helices of Bcl-XL associate with the membrane surface with limited transmembrane helix insertion. The spectrum from unoriented bilayers (Fig. 2.4e) provides no resolution among resonances, but it provides an indication of protein dynamics, because of the pronounced effects of motional averaging on such spectra. Most of the backbone sites are structured and immobile on the time-scale of the ^{15}N chemical shift interaction (10 kHz), contributing to the characteristic amide powder pattern between 220 and 60 ppm. Some of the Bcl-XL backbone sites, probably near the termini and loop regions, are mobile, and give rise to the resonance band centered near 120 ppm. Therefore, while certain resonances near 120 ppm, in the spectrum of oriented Bcl-XL, may reflect specific orientations of their corresponding sites, some others arise from mobile backbone sites. The intensity near 35 ppm, also present in the spectrum from the oriented sample, is from the protein amino groups, which have a considerably narrower ^{15}N chemical shift anisotropy. Taken together, the ^{15}N and ^{31}P spectra provide evidence that Bcl-xL, an anti-apoptotic Bcl-2 family protein, associates predominantly with the membrane surface, without disruption of the membrane integrity.

2.5.1.2 Membrane-Associated tBid

The ^{15}N chemical shift spectrum of tBid in spherical lipid bilayer vesicles is a powder pattern (Fig. 2.5a, solid line) that spans the full range (60–220 ppm) of the

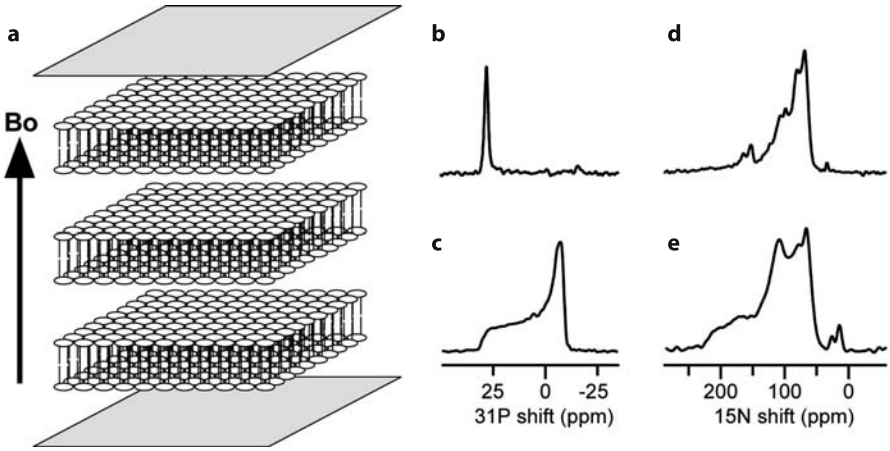

Fig. 2.4. Effect of sample orientation on the solid-state NMR spectra of isotopically labeled proteins. (**A**) The glass-supported phospholipid bilayer samples are oriented in the NMR probe so that the bilayer normal is parallel to the direction of the magnetic field (Bo). (**B**) Oriented phospholipid bilayers give single-line one-dimensional ^{31}P chemical shift NMR spectra, while (**C**) spherical lipid bilayer vesicles give powder patterns. (**D**) The one-dimensional ^{15}N chemical shift NMR spectrum of uniformly ^{15}N-labeled Bcl-XL in oriented lipid bilayers displays multiple resonances, compared to (**E**) the powder pattern that is obtained for the same protein in unoriented lipid bilayer vesicles. The ^{15}N chemical shifts are referenced to 0 ppm for liquid ammonia

amide ^{15}N chemical shift interaction (Fig. 2.5a, dashed line). The absence of additional intensity at the isotropic resonance frequencies (100–130 ppm) demonstrates that the majority of amino acid sites are immobile on the time-scale of the ^{15}N chemical shift interaction, although it is possible that some mobile unstructured residues could not be observed by cross-polarization. The peak at 35 ppm is from the amino groups at the N-terminus and sidechains of the protein. The spectrum of tBid in planar oriented lipid bilayers is very different (Fig. 2.5c). All of the amide resonances are centered at a frequency associated with NH bonds in helices parallel to the membrane surface (80 ppm), while no intensity is observed at frequencies associated with NH bonds in trans-membrane helices (200 ppm). The NMR data show no evidence of conformational exchange on the millisecond to second time-scales of the channel opening and closing events, thus eliminating the possibility of transient insertion of tBid in the membrane. Thus tBid binds strongly to the membrane surface and adopts a unique conformation and orientation in the presence of phospholipids (Gong et al. 2004).

Amide hydrogen exchange rates are useful for identifying residues that are involved in hydrogen bonding, and that are exposed to water. Typically, the amide hydrogens in trans-membrane helices have very slow exchange rates due to their

strong hydrogen bonds in the low dielectric of the lipid bilayer environment, and their ^{15}N chemical shift NMR signals persist for days after exposure to D_2O (Franzin et al. 2004). Trans-membrane helices that are in contact with water because they participate in channel pore formation, and other water-exposed helical region proteins, have faster exchange rates, and their NMR signals disappear on the order of hours (Tian et al. 2003). To examine the amide hydrogen exchange rates for membrane-bound tBid, we obtained solid-state NMR spectra after exposing the oriented lipid bilayer sample to D_2O for 2 h, 5 h, and finally for 7 h. The majority of resonances in the ^{15}N chemical shift spectrum of tBid disappeared within 8 h, indicating that the amide hydrogens exchange and hence are in contact with the bilayer interstitial water.

The tBid amino acid sequence has four Lys residues (Lys144, Lys146, Lys157, and Lys158) all located in or near helix-6, one of the two helices thought to insert in the membrane and form the tBid ion-conducting pore. The spectrum of ^{15}N-Lys labeled tBid in bilayers is notable because its amide resonances all have chemical shifts near 80 ppm, in the in-plane region of the spectrum, and this cannot be reconciled with membrane insertion (Fig. 2.5b). Since tBid maintains a helical fold in lipid micelles and it is reasonable to assume that the helix boundaries are not changed from those of full-length Bid, the solid-state NMR data demonstrate that helix-6 does not insert through the membrane but associates parallel to its surface. This is also supported by a recent EPR study (Oh et al. 2004).

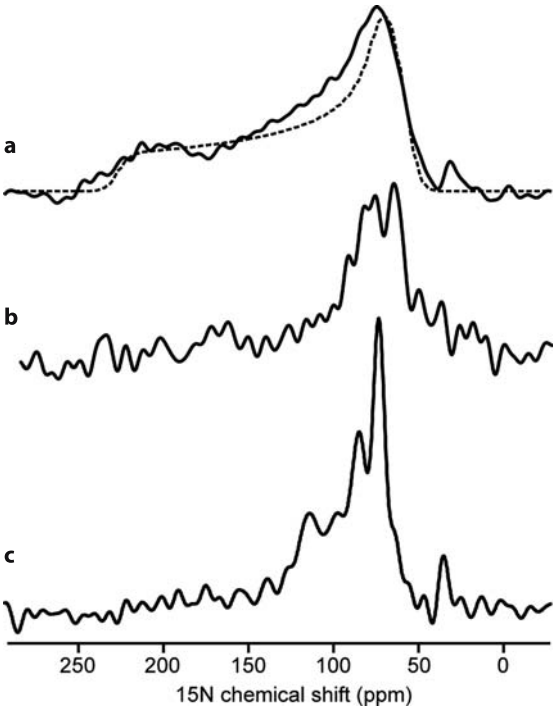

Fig. 2.5. One-dimensional ^{15}N chemical shift spectra of tBid in lipid bilayers. (**a**) Uniformly ^{15}N-labeled tBid in unoriented lipid bilayer vesicles (*solid line*), and powder pattern calculated for a rigid ^{15}N amide site (*dotted line*). (**b**) One-dimensional ^{15}N spectrum of selectively ^{15}N-Lys-labeled tBid in oriented lipid bilayers. (**c**) One-dimensional ^{15}N spectrum of uniformly ^{15}N-labeled tBid in oriented lipid bilayers

2.5.2 Determining the Structures of Proteins in Bilayers

When membrane proteins are incorporated in planar lipid bilayers that are oriented in the field of the NMR magnet, the frequencies measured in their multidimensional solid-state NMR spectra contain orientation-dependent information that can be used for structure determination (Marassi 2002). The PISEMA (polarization inversion with spin exchange at the magic angle) experiment gives high-resolution, two-dimensional, $^{1}H–^{15}N$ dipolar coupling / ^{15}N chemical shift correlation spectra of oriented membrane proteins where the individual resonances contain orientation restraints for structure determination (Wu et al. 1994). PISEMA spectra of membrane proteins in oriented lipid bilayers also provide sensitive indices of protein secondary structure and topology because they exhibit characteristic wheel-like patterns of resonances, called Pisa wheels, that reflect helical wheel projections (Schiffer and Edmunson 1967) of residues in both α-helices and β-sheets (Marassi and Opella 2000; Wang et al. 2000; Marassi 2001). When a Pisa wheel is observed, no assignments are needed to determine the tilt of a helix, and a single resonance assignment is sufficient to determine the helix rotation in the membrane. This information is extremely useful for determining the supramolecular architectures of membrane proteins and their assemblies.

The shape and position of the Pisa wheel in the spectrum depends on the protein secondary structure and its orientation relative to the lipid bilayer surface, as well as the amide N–H bond length and the magnitudes and orientations of the principal elements of the amide ^{15}N chemical shift tensor. This direct relationship between spectrum and structure makes it possible to calculate solid-state NMR spectra for specific structural models of proteins, and provides the basis for a method of backbone structure determination from a limited set of uniformly and selectively ^{15}N-labeled samples (Marassi and Opella 2002; Marassi and Opella 2003).

The Pisa wheels calculated for single helices or strands, oriented at varying degrees in a lipid bilayer, are shown in Fig. 2.6. When the helices or strands cross the membrane with their long axes exactly parallel to the lipid bilayer normal and to the magnetic field direction (0°), all of the amide sites in each structure have an identical orientation relative to the direction of the applied magnetic field, and therefore all of the resonances overlap with the same dipolar coupling and chemical shift frequencies. Tilting the helix or strand away from the membrane normal introduces variations in the orientations of the amide NH bond vectors in the magnetic field, and leads to dispersion of the $^{1}H–^{15}N$ dipolar coupling and ^{15}N chemical shift frequencies, manifest in the appearance of Pisa wheel resonance patterns in the spectra. Since helices and strands yield clearly different resonance patterns, with circular wheels for helices and twisted wheels for strands, these spectra represent signatures of secondary structure (Marassi 2001). The spectra also demonstrate that it is possible to determine the tilt of a helix or strand in lipid bilayers without resonance assignments. Pisa wheels have been observed in the PISEMA spectra of many uniformly ^{15}N labeled α-helical membrane proteins (Opella et al. 1999, Marassi et al. 2000; Wang et al. 2001; Marassi and Opella 2003; Park et al. 2003; Zeri et al. 2003).

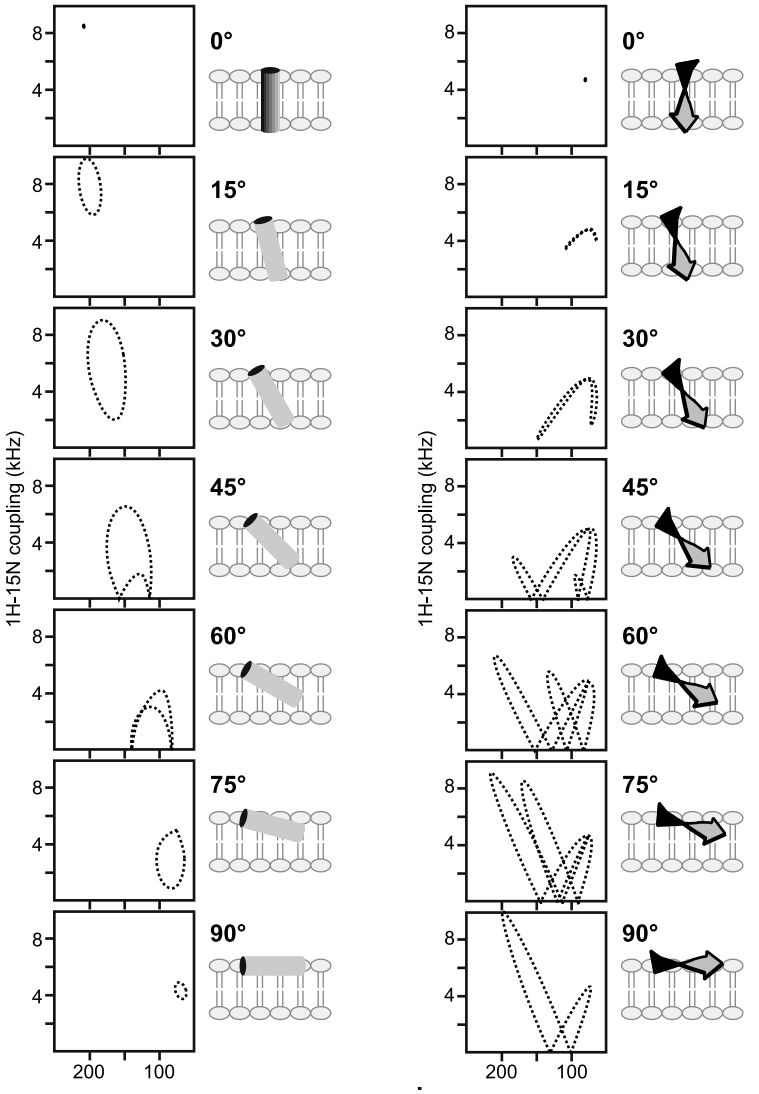

Fig. 2.6. Helices and strands in oriented planar lipid bilayers give characteristic solid-state NMR spectra called Pisa wheels. The ^{1}H–^{15}N dipolar coupling /^{15}N chemical shift PISEMA spectra were calculated for (**a**) an ideal α-helix with uniform dihedral angles (ϕ/ψ = –65/–40°), and (**b**) an ideal β-strand with uniform dihedral angles (ϕ/ψ = –135/140°), at different tilts relative to the magnetic field direction and the membrane normal. The ^{15}N chemical shifts are referenced to 0 ppm for liquid ammonia. Spectra were calculated as described by Marassi 2001

2.5.3 Conformation of tBid in Lipid Bilayers

The two-dimensional $^{1}H/^{15}N$ PISEMA spectrum of tBid in bilayers is shown in Fig. 2.7 (Gong et al. 2004). Each amide site in the protein contributes one correlation peak, characterized by $^{1}H–^{15}N$ dipolar coupling and ^{15}N chemical shift frequencies that reflect the NH bond orientation relative to the membrane. For tBid, the circular wheel-like pattern of resonances in the spectral region bounded by 0–5 kHz and 70–90 ppm, provides definitive evidence that tBid associates with the membrane as surface-bound helices without trans-membrane insertion. The substantial peak overlap reflects a similar orientation of the tBid helices parallel to the membrane, and spectral resolution in this region requires three-dimensional correlation spectroscopy and selective isotopic labeling (Marassi et al. 2000).

As shown in Fig. 2.6, the NMR frequencies directly reflect the angles between individual bonds and the direction of the applied magnetic field, and, therefore, it is possible to calculate solid-state NMR spectra for specific models of proteins in oriented samples. A comparison of the calculated and experimental spectra then provides useful structural information prior to complete structure determination, which requires sequential assignment of the resonances. The spectra calculated for several orientations of an ideal 18-residue helix, with 3.6 residues per turn and identical backbone dihedral angles for all residues (ϕ, ψ = –57°, –47°), are shown in Fig. 2.8. This analysis demonstrates that trans-membrane helices, with orientations between 90° and 45°, have wheel-like spectra in a completely unpopulated region of the tBid spectrum. Based on a comparison of the calculated spectra with the PISEMA spectrum of tBid in lipid bilayers we place the helices of tBid nearly parallel to the lipid bilayer plane (0° orientation), with a tilt of no more than 20° from the membrane surface.

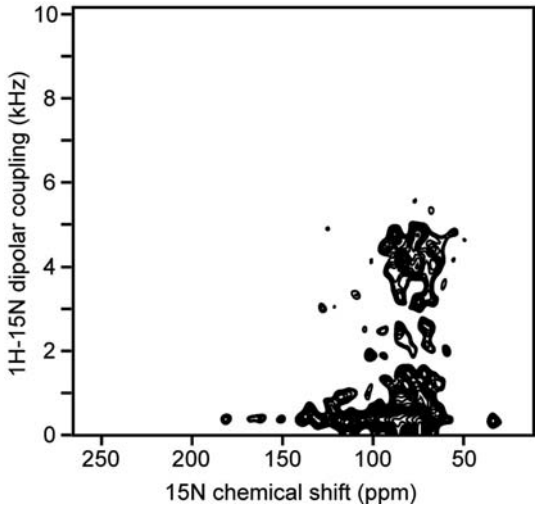

Fig. 2.7. Two-dimensional $^{1}H/^{15}N$ PISEMA spectrum of uniformly ^{15}N-labeled tBid in oriented lipid bilayers

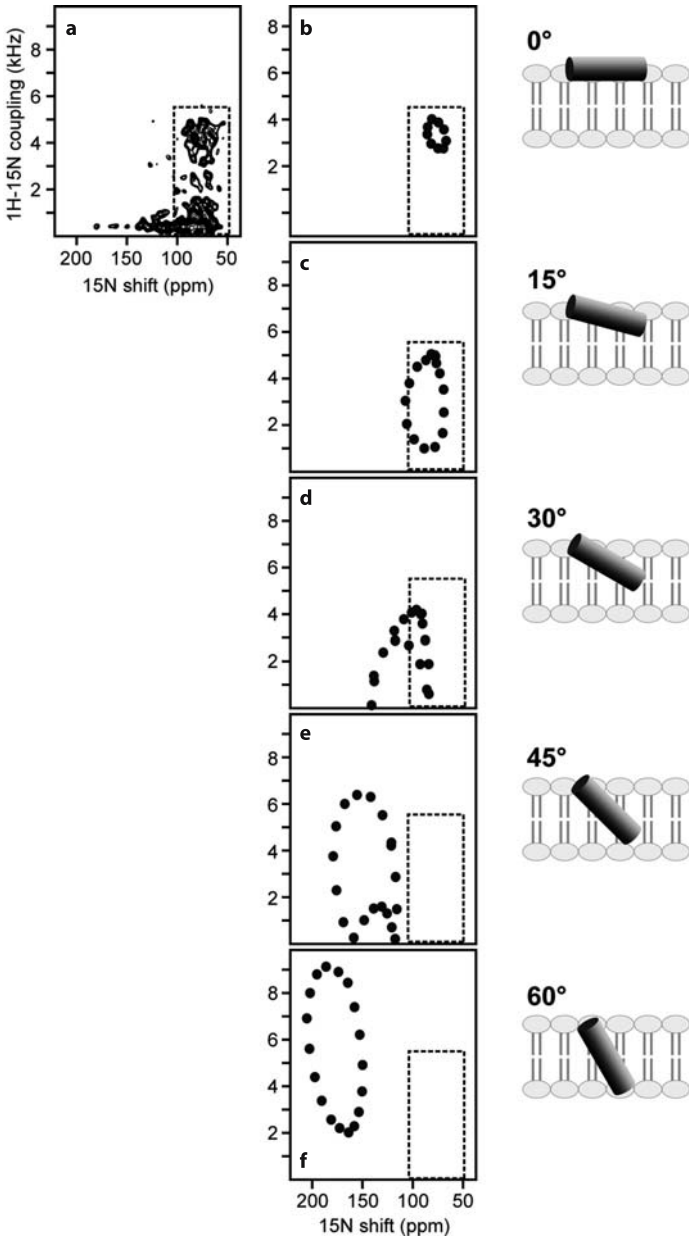

Fig. 2.8. Two-dimensional solid-state NMR $^{1}H/^{15}N$ PISEMA spectrum of uniformly ^{15}N-labeled tBid in oriented lipid bilayers. The experimental spectrum (*inset box*) is compared with the spectra calculated for an 18-residue α-helix, with uniform backbone dihedral angles ($\phi = -57°$; $\psi = -47°$), and different helix tilts (0 to 75°) relative to the membrane, depicted in the cartoon above the spectra. The 0° orientation is for a helix parallel to the membrane surface

Solution and solid-state NMR studies demonstrate that tBid adopts a unique helical fold in lipid environments, and that it binds the membrane without insertion of its helices. Solid-state NMR studies of the anti-apoptotic Bcl-2 family member, Bcl-X_L, also indicate that membrane insertion of the Bcl-X_L helices is only partial (Franzin et al. 2004), and solution NMR studies show that Bcl-X_L adopts an extended helical conformation in lipid micelles (Losonczi et al. 2000). Both tBid and Bcl-X_L form ion-conductive pores that are thought to play a role in apoptosis through their regulation of mitochondrial physiology, and it is important to note that, since the samples in both the solid-state NMR and ion channel activity studies of Bcl-XL and tBid were identical in their lipid composition and the manner of sample preparation, the membrane surface association of Bcl-XL and tBid, observed by solid-state NMR, represents the channel-active conformation of the proteins.

A model for the mode of membrane association by tBid is shown in Fig. 2.9. Cleavage by caspase-8 in the flexible loop of the soluble Bid structure (Fig. 2.9a), generates the C-terminal product tBid (Fig. 2.9b), which undergoes a conformational change and binds the surface of mitochondrial membranes (Fig. 2.9c). It is possible that the structure of tBid, destabilized by dissociation from the N-terminal fragment after caspase-8 cleavage, undergoes a conformational change, whereby it opens about the flexible loops that connect its helical segments, to an extended helical conformation which binds to the membrane surface. This would be similar to the mechanism proposed for the lipoprotein apolipophorin-III, which adopts a marginally stable helix bundle topology that allows for concerted opening of the bundle about hinged loops (Wang et al. 2002). It is notable that the Bid amino acid sequence (P_{141}RDMEKE$_{147}$), at the beginning of helix-6, is similar to the conserved sequence (P_{95}DVEKE$_{100}$) that forms a short lipid recognition helix in apolipophorin-III. In Bid, this sequence forms a short loop that is perpendicular to the axis of helix-6 and solvent-exposed, while in apolipophorin-III it forms a short helix that is perpendicular to the helix bundle and at one solvent-exposed end of the molecule. This short motif is conserved in the Bid sequences from various species, suggesting that it plays a role in the protein biological function, and may constitute a lipid recognition domain for Bid similar to that of apolipophorin-III.

Pore formation by the Bcl-2 family proteins has been thought to involve translocation of the central core helices through the membrane, and the helices of both Bid and Bcl-X_L are sufficiently long to span the lipid bilayer. However, their amphipathic character is also compatible with membrane surface association, in a manner that is reminiscent of the antimicrobial polypeptides where binding of the polypeptide helices to the bacterial membrane surface is thought to transiently destabilize the membrane and change its morphology, inducing leakage of the cell contents, disruption of the electrical potential, and ultimately cell death (Boman 1995; Marassi et al. 1999, Marassi et al. 2000). It is notable that bacterial and mitochondrial membranes have very similar structures and surface charge, and that tBid is both capable of altering bilayer curvature, and of remodeling the mitochondrial membrane, which would be sufficient to cause the release of mitochondrial cytotoxic molecules. Thus, the BH3-independent mechanism of pore-formation and mitochondrial cytochrome-c release by tBid, may be similar to that of the an-

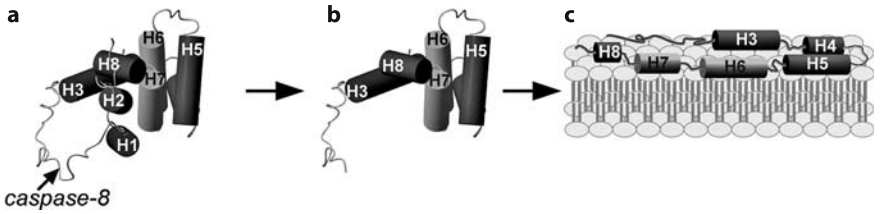

Fig. 2.9. Model for the association of tBid with the membrane surface. (**a**) Cleavage by caspase-8 in the flexible loop of the soluble Bid structure (Chou et al. 1999; McDonnell et al. 1999), generates the C-terminal product tBid (**b**), which undergoes a conformational change and binds the surface of mitochondrial membranes (**c**)

timicrobial polypeptides. In addition, the membrane surface association of tBid may serve to display the BH3 domain on the mitochondrial membrane surface, making it accessible for binding by other Bcl-2 family members. Although tBid does not insert in DOPC/DOPG lipid bilayers, it is possible that trans-membrane insertion may be driven by the presence of natural mitochondrial lipids, such as cardiolipin and monolysocardiolipin. It is also possible that the interactions with other Bcl-2 family proteins such as Bak and Bax, or with other non-homologous proteins such as the mitochondrial voltage-dependent anion channel, may promote insertion of the tBid helices through the mitochondrial membrane.

Acknowledgements. We thank David Cowburn, Stephen Fesik, and Gerhard Wagner, for sharing their solution NMR assignments for Bid and Bcl-XL. This research is supported by grants from the National Institutes of Health (R01GM065374), and the Department of the Army Breast Cancer Research Program (DAMD17-02-1-0313). The NMR studies utilized the Burnham Institute NMR Facility and the Biomedical Technology Resources for Solid-State NMR of Proteins at the University of California San Diego, supported by grants from the National Institutes of Health (P30CA30199; P41EB002031).

References

Almeida FC, Opella SJ (1997) FD coat protein structure in membrane environments: structural dynamics of the loop between the hydrophobic trans-membrane helix and the amphipathic in-plane helix. J Mol Biol 270:481–495

Aritomi M, Kunishima N, Inohara N, Ishibashi Y, Ohta S, Morikawa K (1997) Crystal structure of rat Bcl-xL. Implications for the function of the Bcl-2 protein family. J Biol Chem 272:27886–27892

Arora A, Abildgaard F, Bushweller JH, Tamm LK (2001) Structure of outer membrane protein A transmembrane domain by NMR spectroscopy. Nat Struct Biol 8:334–338

Bannwarth M, Schulz GE (2003) The expression of outer membrane proteins for crystallization. Biochimica et Biophysica Acta (BBA) – Biomembranes 1610:37–45

Battiste JL, Wagner G (2000) Utilization of site-directed spin labeling and high-resolution heteronuclear nuclear magnetic resonance for global fold determination of large proteins with limited nuclear overhauser effect data. Biochemistry 39:5355–5365

Bax A, Kontaxis G, Tjandra N (2001) Dipolar couplings in macromolecular structure determination. Methods Enzymol 339:127–174

Boguski MJ, Schiksnis RA, Leo GC, Opella SJ (1987) Protein backbone dynamics by solid-state and solution 15N NMR spectroscopy. J Magn Reson 72:186–190

Bogusky MJ, Leo GC, Opella SJ (1988) Comparison of the dynamics of the membrane-bound form of fd coat protein in micelles and in bilayers by solution and solid-state nitrogen-15 nuclear magnetic resonance spectroscopy. Proteins 4:123–130

Boman HG (1995) Peptide antibiotics and their role in innate immunity. Annu Rev Immunol 13:61–92

Booth PJ (2003) The trials and tribulations of membrane protein folding in vitro. Biochimica et Biophysica Acta (BBA) – Biomembranes 1610:51–56

Chou JJ, Gaemers S, Howder B, Louis JM, Bax A (2001) A simple apparatus for generating stretched polyacrylamide gels, yielding uniform alignment of proteins and detergent micelles. J Biomol NMR 21:377–382

Chou JJ, Li H, Salvesen GS, Yuan J, Wagner G (1999) Solution structure of BID, an intracellular amplifier of apoptotic signaling. Cell 96:615–624

Clore GM, Gronenborn AM (1989) Determination of three-dimensional structures of proteins and nucleic acids in solution by nuclear magnetic resonance spectroscopy. Crit Rev Biochem Mol Biol 24:479–564

Clore GM, Gronenborn AM (1998) New methods of structure refinement for macromolecular structure determination by NMR. Proc Natl Acad Sci USA 95

Cory S, Adams JM (2002) The Bcl2 family: regulators of the cellular life-or-death switch. Nat Rev Cancer 2:647–656

Cramer WA, Heymann JB, Schendel SL, Deriy BN, Cohen FS, Elkins PA, Stauffacher CV (1995) Structure-function of the channel-forming colicins. Annu Rev Biophys Biomol Struct 24:611–641

Crowell KJ, Franzin CM, Koltay A, Lee S, Lucchese AM, Snyder BC, Marassi FM (2003) Expression and characterization of the FXYD ion transport regulators for NMR structural studies in lipid micelles and lipid bilayers. Biochim Biophys Acta 1645:15–21

Czerski L, Vinogradova O, Sanders CR (2000) NMR-Based amide hydrogen-deuterium exchange measurements for complex membrane proteins: development and critical evaluation. J Magn Reson 142:111–119

Damberg P, Jarvet J, Graslund A (2001) Micellar systems as solvents in peptide and protein structure determination. Methods Enzymol 339:271–285

Danial NN, Korsmeyer SJ (2004) Cell death: critical control points. Cell 116:205–219

Dawson PE, Muir TW, Clark-Lewis I, Kent SB (1994) Synthesis of proteins by native chemical ligation. Science 266:776–779

Day CL, Chen L, Richardson SJ, Harrison PJ, Huang DC, Hinds MG (2004) Solution structure of pro-survival Mcl-1 and characterization of its binding by pro-apoptotic BH3-only ligands. J Biol Chem

Day CL, Chen L, Richardson SJ, Harrison PJ, Huang DC, Hinds MG (2005) Solution structure of prosurvival Mcl-1 and characterization of its binding by proapoptotic BH3-only ligands. J Biol Chem 280:4738–4744

Delaglio F, Kontaxis G, Bax A (2000) Protein Structure Determination Using Molecular Fragment Replacement and NMR Dipolar Couplings. J Am Chem Soc 122:2142–2143

Denault JB, Salvesen GS (2002) Caspases: keys in the ignition of cell death. Chem Rev 102:4489–4500

Denisov AY, Madiraju MS, Chen G, Khadir A, Beauparlant P, Attardo G, Shore GC, Gehring K (2003) Solution structure of human BCL-w: modulation of ligand binding by the C-terminal helix. J Biol Chem 278:21124–21128

Farrow NA, Zhang O, Forman-Kay JD, Kay LE (1994) A heteronuclear correlation experiment for simultaneous determination of 15N longitudinal decay and chemical exchange rates of systems in slow equilibrium. J Biomol NMR 4:727–734

Ferentz AE, Wagner G (2000) NMR spectroscopy: a multifaceted approach to macromolecular structure. Q Rev Biophys 33:29–65

Fernandez C, Adeishvili K, Wuthrich K (2001) Transverse relaxation-optimized NMR spectroscopy with the outer membrane protein OmpX in dihexanoyl phosphatidylcholine micelles. Proc Natl Acad Sci USA 98:2358–2363

Fowler CA, Tian F, Al-Hashimi HM, Prestegard JH (2000) Rapid determination of protein folds using residual dipolar couplings. J Mol Biol 304:447–460

Franzin CM, Choi J, Zhai D, Reed JC, Marassi FM (2004) Structural studies of apoptosis and ion transport regulatory proteins in membranes. Magn Reson Chem 42:172–179

Gesell J, Zasloff M, Opella SJ (1997) Two-dimensional 1H NMR experiments show that the 23-residue magainin antibiotic peptide is an alpha-helix in dodecylphosphocholine micelles, sodium dodecylsulfate micelles, and trifluoroethanol/water solution. J Biomol NMR 9:127–135

Gong XM, Choi J, Franzin CM, Zhai D, Reed JC, Marassi FM (2004) Conformation of membrane-associated proapoptotic tBid. J Biol Chem 279:28954–28960

Green DR, Reed JC (1998) Mitochondria and apoptosis. Science 281:1309–1312

Gust D, Moon RB, Roberts JD (1975) Applications of natural-abundance nitrogen-15 nuclear magnetic resonance to large biochemically important molecules. Proc Natl Acad Sci USA 72:4696–4700

Henry GD, Sykes BD (1994) Methods to study membrane protein structure in solution. Methods Enzymol 239:515–535

Hinds MG, Lackmann M, Skea GL, Harrison PJ, Huang DC, Day CL (2003) The structure of Bcl-w reveals a role for the C-terminal residues in modulating biological activity. Embo J 22:1497–1507

Howell SC, Mesleh MF, Opella SJ (2005) NMR structure determination of a membrane protein with two transmembrane helices in micelles: MerF of the bacterial mercury detoxification system. Biochemistry 44:196:5196–5206

Huang Q, Petros AM, Virgin HW, Fesik SW, Olejniczak ET (2002) Solution structure of a Bcl-2 homolog from Kaposi sarcoma virus. Proc Natl Acad Sci USA 99:3428–3433

Huang Q, Petros AM, Virgin HW, Fesik SW, Olejniczak ET (2003) Solution structure of the BHRF1 protein from Epstein–Barr virus, a homolog of human Bcl-2. J Mol Biol 332:1123–1130

Hus JC, Marion D, Blackledge MJ (2000) De novo determination of protein structure by NMR using orientational and long-range order restraints. J Mol Biol 298:927–936

Hwang PM, Choy WY, Lo EI, Chen L, Forman-Kay JD, Raetz CR, Prive GG, Bishop RE, Kay LE (2002) Solution structure and dynamics of the outer membrane enzyme PagP by NMR. Proc Natl Acad Sci USA 99:13560–13565

Jarvet J, Zdunek J, Damberg P, Graslund A (1997) Three-dimensional structure and position of porcine motilin in sodium dodecyl sulfate micelles determined by 1H NMR. Biochemistry 36:8153–8163

Jones DH, Ball EH, Sharpe S, Barber KR, Grant CW (2000) Expression and membrane assembly of a transmembrane region from Neu. Biochemistry 39:1870–1878

Ketchem RR, Hu W, Cross TA (1993) High-resolution conformation of gramicidin A in a lipid bilayer by solid-state NMR. Science 261:1457–1460

Kiefer H (2003) In vitro folding of alpha-helical membrane proteins. Biochimica et Biophysica Acta (BBA) – Biomembranes 1610:57–62

Klammt C, Lohr F, Schafer B, Haase W, Dotsch V, Ruterjans H, Glaubitz C, Bernhard F (2004) High level cell-free expression and specific labeling of integral membrane proteins. Eur J Biochem 271:568–580

Kleid DG, Yansura D, Small B, Dowbenko D, Moore DM, Grubman MJ, McKercher PD, Morgan DO, Robertson BH, Bachrach HL (1981) Cloned viral protein vaccine for foot-and-mouth disease: responses in cattle and swine. Science 214:1125–1129

Klein-Seetharaman J, Reeves PJ, Loewen MC, Getmanova EV, Chung J, Schwalbe H, Wright PE, Khorana HG (2002) Solution NMR spectroscopy of [alpha-15N]lysine-labeled rhodopsin: The single peak observed in both conventional and TROSY-type HSQC spectra is ascribed to Lys-339 in the carboxyl-terminal peptide sequence. Proc Natl Acad Sci USA 99:3452–3457

Kochendoerfer GG (2001) Chemical protein synthesis methods in drug discovery. Curr Opin Drug Discov Devel 4:205–214

Kochendoerfer GG, Jones DH, Lee S, Oblatt-Montal M, Opella SJ, Montal M (2004) Functional characterization and NMR spectroscopy on full-length Vpu from HIV-1 prepared by total chemical synthesis. J Am Chem Soc 126:2439–2446

Kochendoerfer GG, Salom D, Lear JD, Wilk-Orescan R, Kent SB, DeGrado WF (1999) Total chemical synthesis of the integral membrane protein influenza A virus M2: role of its C-terminal domain in tetramer assembly. Biochemistry 38:11905–11913

Kroemer G, Reed JC (2000) Mitochondrial control of cell death. Nat Med 6:513–519

Krueger-Koplin RD, Sorgen PL, Krueger-Koplin ST, Rivera-Torres IO, Cahill SM, Hicks DB, Grinius L, Krulwich TA, Girvin ME (2004) An evaluation of detergents for NMR structural studies of membrane proteins. J Biomol NMR 28:43–57

Kuliopulos A, Nelson NP, Yamada M, Walsh CT, Furie B, Furie BC, Roth DA (1994) Localization of the affinity peptide-substrate inactivator site on recombinant vitamin K-dependent carboxylase. J Biol Chem 269:21364–21370

Kutateladze TG, Capelluto DG, Ferguson CG, Cheever ML, Kutateladze AG, Prestwich GD, Overduin M (2004) Multivalent mechanism of membrane insertion by the FYVE domain. J Biol Chem 279:3050–3057

Lee S, Mesleh MF, Opella SJ (2003) Structure and dynamics of a membrane protein in micelles from three solution NMR experiments. J Biomol NMR 26:327–334

Lindhout DA, Thiessen A, Schieve D, Sykes BD (2003) High-yield expression of isotopically labeled peptides for use in NMR studies. Protein Sci 12:1786–1791

Losonczi JA, Olejniczak ET, Betz SF, Harlan JE, Mack J, Fesik SW (2000) NMR studies of the anti-apoptotic protein Bcl-xL in micelles. Biochemistry 39:11024–11033

Ma C, Marassi FM, Jones DH, Straus SK, Bour S, Strebel K, Schubert U, Oblatt-Montal M, Montal M, Opella SJ (2002) Expression, purification, and activities of full-length and truncated versions of the integral membrane protein Vpu from HIV-1. Protein Sci 11:546–557

MacKenzie KR, Prestegard JH, Engelman DM (1997) A transmembrane helix dimer: structure and implications. Science 276:131–133

Majerle A, Kidric J, Jerala R (2000) Production of stable isotope enriched antimicrobial peptides in Escherichia coli: an application to the production of a 15N-enriched fragment of lactoferrin. J Biomol NMR 18:145–151

Marassi FM (2001) A simple approach to membrane protein secondary structure and topology based on NMR spectroscopy. Biophys J 80:994–1003

Marassi FM (2002) NMR of peptides and proteins in membranes. Concepts Magn Resonance 14:212–224

Marassi FM, Ma C, Gesell JJ, Opella SJ (2000) Three-dimensional solid-state NMR spectroscopy is essential for resolution of resonances from in-plane residues in uniformly (15)N-labeled helical membrane proteins in oriented lipid bilayers. J Magn Reson 144:156–161

Marassi FM, Opella SJ (2000) A solid-state NMR index of helical membrane protein structure and topology. J Magn Reson 144:150–155

Marassi FM, Opella SJ (2002) Using Pisa pies to resolve ambiguities in angular constraints from PISEMA spectra of aligned proteins. J Biomol NMR 23:239–242

Marassi FM, Opella SJ (2003) Simultaneous assignment and structure determination of a membrane protein from NMR orientational restraints. Protein Sci 12:403–411

Marassi FM, Opella SJ, Juvvadi P, Merrifield RB (1999) Orientation of cecropin A helices in phospholipid bilayers determined by solid-state NMR spectroscopy. Biophys J 77:3152–3155

Marassi FM, Ramamoorthy A, Opella SJ (1997) Complete resolution of the solid-state NMR spectrum of a uniformly 15N-labeled membrane protein in phospholipid bilayers. Proc Natl Acad Sci USA 94:8551–8556

Mascioni A, Karim C, Barany G, Thomas DD, Veglia G (2002) Structure and orientation of sarcolipin in lipid environments. Biochemistry 41:475–482

McDonnell JM, Fushman D, Milliman CL, Korsmeyer SJ, Cowburn D (1999) Solution structure of the proapoptotic molecule BID: a structural basis for apoptotic agonists and antagonists. Cell 96:625–634

Meier S, Haussinger D, Grzesiek S (2002) Charged acrylamide copolymer gels as media for weak alignment. J Biomol NMR 24:351–356

Mesleh MF, Lee S, Veglia G, Thiriot DS, Marassi FM, Opella SJ (2003) Dipolar waves map the structure and topology of helices in membrane proteins. J Am Chem Soc 125:8928–8935

Mesleh MF, Opella SJ (2003) Dipolar waves as NMR maps of helices in proteins. J Magn Reson 163:288–299

Mesleh MF, Veglia G, DeSilva TM, Marassi FM, Opella SJ (2002) Dipolar waves as NMR maps of protein structure. J Am Chem Soc 124:4206–4207

Minn AJ, Velez P, Schendel SL, Liang H, Muchmore SW, Fesik SW, Fill M, Thompson CB (1997) Bcl-x(L) forms an ion channel in synthetic lipid membranes. Nature 385:353–357

Miozzari GF, Yanofsky C (1978) Translation of the leader region of the Escherichia coli tryptophan operon. J Bacteriol 133:1457–1466

Miroux B, Walker JE (1996) Over-production of proteins in Escherichia coli: mutant hosts that allow synthesis of some membrane proteins and globular proteins at high levels. J Mol Biol 260:289–298

Muchmore SW, Sattler M, Liang H, Meadows RP, Harlan JE, Yoon HS, Nettesheim D, Chang BS, Thompson CB, Wong SL, Ng SL, Fesik SW (1996) X-ray and NMR structure of human Bcl-xL, an inhibitor of programmed cell death. Nature 381:335–341

Mueller GA, Choy WY, Yang D, Forman-Kay JD, Venters RA, Kay LE (2000) Global folds of proteins with low densities of NOEs using residual dipolar couplings: application to the 370-residue maltodextrin-binding protein. J Mol Biol 300:197–212

Oh KJ, Barbuto S, Meyer N, Kim RS, Collier RJ, Korsmeyer SJ (2004) Conformational changes in BID, a pro-apoptotic BCL-2 family member, upon membrane-binding: A site-directed spin labeling study. J Biol Chem 280:753–767

Opella SJ, Ma C, Marassi FM (2001) Nuclear magnetic resonance of membrane-associated peptides and proteins. Methods Enzymol 339:285–313

Opella SJ, Marassi FM (2004) Structure determination of membrane proteins by NMR spectroscopy. Chem Rev 104:3587–3606

Opella SJ, Marassi FM, Gesell JJ, Valente AP, Kim Y, Oblatt-Montal M, Montal M (1999) Structures of the M2 channel-lining segments from nicotinic acetylcholine and NMDA receptors by NMR spectroscopy. Nat Struct Biol 6:374–379

Oxenoid K, Kim HJ, Jacob J, Sonnichsen FD, Sanders CR (2004) NMR assignments for a helical 40 kDa membrane protein. J Am Chem Soc 126:5048–5049

Oxenoid K, Sonnichsen FD, Sanders CR (2002) Topology and secondary structure of the N-terminal domain of diacylglycerol kinase. Biochemistry 41:12876–12882

Papavoine CH, Konings RN, Hilbers CW, van de Ven FJ (1994) Location of M13 coat protein in sodium dodecyl sulfate micelles as determined by NMR. Biochemistry 33:12990–12997

Park SH, Mrse AA, Nevzorov AA, Mesleh MF, Oblatt-Montal M, Montal M, Opella SJ (2003) Three-dimensional structure of the channel-forming trans-membrane domain of virus protein "u" (Vpu) from HIV-1. J Mol Biol 333:409–424

Petros AM, Medek A, Nettesheim DG, Kim DH, Yoon HS, Swift K, Matayoshi ED, Oltersdorf T, Fesik SW (2001) Solution structure of the antiapoptotic protein bcl-2. Proc Natl Acad Sci USA 98:3012–3017

Prestegard JH, Kishore AI (2001) Partial alignment of biomolecules: an aid to NMR characterization. Curr Opin Chem Biol 5:584–590

Rogl H, Kosemund K, Kuhlbrandt W, Collinson I (1998) Refolding of Escherichia coli produced membrane protein inclusion bodies immobilised by nickel chelating chromatography. FEBS Lett 432:21–26

Sass HJ, Musco G, Stahl SJ, Wingfield PT, Grzesiek S (2000) Solution NMR of proteins within polyacrylamide gels: diffusional properties and residual alignment by mechanical stress or embedding of oriented purple membranes. J Biomol NMR 18:303–309

Schendel SL, Azimov R, Pawlowski K, Godzik A, Kagan BL, Reed JC (1999) Ion channel activity of the BH3 only Bcl-2 family member, BID. J Biol Chem 274:21932–21936

Schendel SL, Montal M, Reed JC (1998) Bcl-2 family proteins as ion-channels. Cell Death Differ 5:372–380

Schiffer M, Edmunson AB (1967) Use of helical wheels to represent the structures of proteins and to identify segments with helical potential. Biophys J 7:121–135

Scorrano L, Korsmeyer SJ (2003) Mechanisms of cytochrome c release by proapoptotic BCL-2 family members. Biochem Biophys Res Commun 304:437–444

Sharon M, Gorlach M, Levy R, Hayek Y, Anglister J (2002) Expression, purification, and isotope labeling of a gp120 V3 peptide and production of a Fab from a HIV-1 neutralizing antibody for NMR studies. Protein Expr Purif 24:374–383

Smith VR, Walker JE (2003) Purification and folding of recombinant bovine oxoglutarate/malate carrier by immobilized metal-ion affinity chromatography. Protein Expression and Purification 29:209–216

Sorgen PL, Cahill SM, Krueger-Koplin RD, Krueger-Koplin ST, Schenck CC, Girvin ME (2002) Structure of the Rhodobacter sphaeroides light-harvesting 1 beta subunit in detergent micelles. Biochemistry 41:31–41

Staley JP, Kim PS (1994) Formation of a native-like subdomain in a partially folded intermediate of bovine pancreatic trypsin inhibitor. Protein Sci 3:1822–1832

Suzuki M, Youle RJ, Tjandra N (2000) Structure of Bax: coregulation of dimer formation and intracellular localization. Cell 103:645–654

Thai K, Choi J, Franzin CM, Marassi FM (2005) Bcl-XL as a fusion protein for the high-level expression of membrane-associated proteins. Protein Sci 14:948–955

Tian C, Gao PF, Pinto LH, Lamb RA, Cross TA (2003) Initial structural and dynamic characterization of the M2 protein transmembrane and amphipathic helices in lipid bilayers. Protein Sci 12:2597–2605

Tolman JR, Flanagan JM, Kennedy MA, Prestegard JH (1995) Nuclear magnetic dipole interactions in field-oriented proteins: information for structure determination in solution. Proc Natl Acad Sci USA 92:9279–9283

Tycko R, Blanco FJ, Ishii Y (2000) Alignment of biopolymers in strained gels: a new way to create detectable dipole–dipole couplings in high-resolution biomolecular NMR. J Am Chem Soc 122:9340–9341

Valentine KG, Liu SF, Marassi FM, Veglia G, Opella SJ, Ding FX, Wang SH, Arshava B, Becker JM, Naider F (2001) Structure and topology of a peptide segment of the 6th transmembrane domain of the Saccharomyces cerevisae alpha-factor receptor in phospholipid bilayers. Biopolymers 59:243–256

Van Den Hooven HW, Doeland CC, Van De Kamp M, Konings RN, Hilbers CW, Van De Ven FJ (1996) Three-dimensional structure of the lantibiotic nisin in the presence of membrane-mimetic micelles of dodecylphosphocholine and of sodium dodecylsulphate. Eur J Biochem 235:382–393

Veglia G, Zeri AC, Ma C, Opella SJ (2002) Deuterium/hydrogen exchange factors measured by solution nuclear magnetic resonance spectroscopy as indicators of the structure and topology of membrane proteins. Biophys J 82:2176–2183

Wang J, Denny J, Tian C, Kim S, Mo Y, Kovacs F, Song Z, Nishimura K, Gan Z, Fu R, Quine JR, Cross TA (2000) Imaging membrane protein helical wheels. J Magn Reson 144:162–167

Wang J, Kim S, Kovacs F, Cross TA (2001) Structure of the transmembrane region of the M2 protein H(+) channel. Protein Sci 10:2241–2250

Wang J, Sykes BD, Ryan RO (2002) Structural basis for the conformational adaptability of apolipophorin III, a helix-bundle exchangeable apolipoprotein. Proc Natl Acad Sci USA 99:1188–1193

Wiener MC (2004) A pedestrian guide to membrane protein crystallization. Methods 34:364–372

Williams KA, Farrow NA, Deber CM, Kay LE (1996) Structure and dynamics of bacteriophage IKe major coat protein in MPG micelles by solution NMR. Biochemistry 35:5145–5157

Wu CH, Ramamoorthy A, Opella SJ (1994) High-resolution heteronuclear dipolar solid-state NMR spectroscopy. J Magn Reson A 109:270–272

Wuthrich K (1989) Determination of three-dimensional protein structures in solution by nuclear magnetic resonance: an overview. Methods Enzymol 177:125–131

Zeri AC, Mesleh MF, Nevzorov AA, Opella SJ (2003) Structure of the coat protein in fd filamentous bacteriophage particles determined by solid-state NMR spectroscopy. Proc Natl Acad Sci USA 100:6458–6463

X-ray and Neutron Diffraction Approaches to the Structural Analysis of Protein–Lipid Interactions

Juan A. Hermoso, José M. Mancheño and Eva Pebay-Peyroula

3.1 Structure Determination by Protein Crystallography: a General Overview

Biological membranes fulfil vital functions as interfaces to the outside world, as interfaces between cells, and as boundaries of intracellular compartments. Membrane proteins share a common property: part of their structure is embedded in a lipid bilayer. Therefore, being located at an interface, it is almost inevitable that they mediate communication between both sides of the membrane; receptors, pores and channels are all signal transducers. Membrane proteins are abundant; they are estimated to constitute a third of the complement of proteomes. An analysis of the genomes of eubacterial, Archaean and eukaryotic organisms predicted that 20–30% of the open reading frames encode integral membrane proteins (Wallin and von Heijne 1998). The number of lipid-interacting proteins should be increased if we consider the proteins presenting two conformational states, one of them stable in solution and the other one attached to a membrane or a lipid interface. This is the case for the great family of pore-forming toxins, for lipases and also for lipid-carriers. Therefore their scientific importance cannot be overstated, as they are involved in almost every process in the cell. Besides, membrane proteins represent over 50% of the targets of all prescription drugs. This reflects the physiological importance of these proteins, which play key roles in such physiological functions as controlling the homeostasy of the cells and organs, ensuring communication within and across tissues, detoxification, control of cell growth, etc. Describing their structure and function at the molecular level is a determinant asset in understanding their interactions with ligands and devising new and better drugs.

3.1.1 Crystal Structure Determination

Crystallography up till now has been the most powerful technique for determining the atomic structure of proteins. However, of the 31,000 proteins that have been deposited in the Protein Data Bank (PDB) only 25 X-ray structures of unrelated polytopic membrane proteins from the inner membranes of bacteria and mitochondria, as well as from eukaryotic membranes, are available (for a regularly updated list, see http://www.mpibp-frankfurt.mpg.de/michel/pub-

Springer Series in Biophysics
C.R. Mateo et al. (Ed.)
Protein-Lipid Interactions

lic/memprotstruct.html). To understand the reasons for this limited number of membrane protein structures, the fundamentals of crystal structure determination by X-ray crystallography must be mentioned.

The first prerequisite for solving the three-dimensional structure of a protein by X-ray crystallography is a well-ordered crystal that will diffract X-rays strongly. Crystallization is usually quite difficult and obtaining such crystals is the rate-limiting step to structure determination. A pure and homogeneous protein sample is crucial for successful crystallization, and recombinant DNA techniques have been a major breakthrough in this regard. Besides, the past three years have seen some of the greatest achievements in the field of protein crystallization by way of automating and miniaturizing crystallization trials. The ability to dispense trials consisting of nanolitre volumes in a high-throughput mode has reduced the time needed to set up a series of experiments from weeks to minutes, and the subsequent phase of image capture and analysis of crystallization drops is also progressing at high speed (Luft et al. 2003). However, the crystallization problem has not been solved, and it has been estimated than only 4% of the cloned proteins in major structural genomics projects produced diffracting crystals (Chayen 2004).

X-ray waves passing through a crystal generate a diffraction pattern that depends on the reciprocal lattice. However, diffraction patterns register only the amplitude of the waves; and to get the molecular structure, one also needs to know the "phase" (the relative phase of the waves corresponding to each reflection). This information is lost in the diffraction data, and has to be inferred. This is the so-called phase problem. To overcome this problem, different phasing methods are now available; in most of them the aim is to preserve isomorphism, such that the only structural change upon heavy-atom substitution is local and there are no changes in unit-cell parameters or orientation of the protein in the crystal cell. However, single- or multiwavelength anomalous diffraction (SAD/MAD) phasing methods avoid this problem by using a single crystal. These last methods are based on the fact that for certain X-ray wavelengths, the interaction between the X-rays and the electrons of an atom causes the electron to absorb the energy of the X-ray. This produces a small change in the X-ray scattering of the atom that can be used to solve the phase problem. The introduction of more accurate detectors, as well as the use of crystal cryoprotection techniques, has now made it possible to collect diffraction intensities very accurately. Precise control of the wavelength of synchrotron radiation and routine incorporation of seleniomethionine into proteins has contributed to the popularity of the SAD/MAD method of phasing. Once the phase problem is overcame the three-dimensional model of the protein can be, more or less, easily obtained.

3.1.2 Protein Expression, Solubilization and Purification in Membrane Proteins

Concerning the membrane protein structures, the main reason for their scarcity is the difficulty to overproduce membrane proteins, which is compounded by their frequent instability outside their natural environment, and the difficulties

inherent to growing X-ray-quality crystals. Therefore, the problem of crystallizing membrane proteins cannot be reduced to the issue of which screening method or crystallization set-up is to be used. Rather, thorough biochemical work and intensive protein characterization, in combination with comprehensive screening for the most suited detergent, may be the most efficient strategy to cope with the difficulties of membrane protein crystallization (Ostermeier and Michel 1997).

Membrane proteins can often not be purified from natural sources in the amounts required for structural analyses (typically 1–10 mg/batch). This is especially true for proteins that are normally expressed at very low levels or for proteins of human origin. The use of efficient heterologous expression systems as a source of abundant protein is therefore essential. Currently, four major expression systems can be distinguished: those using bacteria, or the eukaryotic systems such as yeast, insect cells, or mammalian cells for expression. It should be obvious that any recombinant protein can be best expressed in the expression system that most closely resembles the natural environment of the protein. It is well known, for example, that the use of prokaryotic or lower eukaryotic expression systems for mammalian proteins can lead to misfolding or loss of functionality of the protein expressed (Tate 2001). However, from a production point of view, higher eukaryotic expression systems are much more expensive, more complex in their handling and often yield less protein per litre of cell culture than their simpler counterparts (Werten et al. 2002). It makes sense, therefore, to check expression of a new recombinant protein in all systems available at least until the stage where functionality and yield can be assessed, and only then decide which system is best suited for large-scale production. For this purpose, a well-designed and flexible cloning procedure, allowing easy cloning of the cDNA of interest into the various systems, is a requirement. Most efforts at developing efficient expression systems tend to concentrate on *E. coli*, *Lactobacillus lactis*, yeast, *Pichia pastoris*, Sf 9 insect cells and various mammalian cell lines. Although efficient production has proved to be successful for some membrane proteins, none of these systems, however, can be considered either as universal or as totally under control, their efficiency varying wildly, often for unknown reasons, from one protein to the next, so that it is now uncertain which proportion of the structures of interest will ever be established, thanks to these particular overexpression systems. For this reason, alternative expression systems like *Drosophila* photoreceptor cells and algal chloroplast thylakoids are now been developed.

A novel expression system for G-protein-coupled receptor (GPCRs) exploiting the membrane stacks naturally present in the photoreceptor cells (PRCs) in the eye of *Drosophila melanogaster* is being developed (Eroglu et al. 2002, 2003). PRCs contain extensive stacks of specialized membranes and a dedicated machinery for the expression, folding and targeting of high levels of rhodopsin. Expression in PRCs provides a number of advantages as compared to conventional expression systems like in these membranes: GPCRs are shielded from proteases and also the internal membranes are reduced to a minimum, about 90% of the membranes being plasma membrane. These two features minimize the problem of proteolysis and of mistargeted or incompletely matured protein.The PRCs have a unique architecture, and they represent an attractive site for the expression of protein membranes. Besides, the expression in tobacco plastids of human soma-

totropin (Staub et al. 2000) has been a milestone in demonstrating the potential of the chloroplast for the heterologous expression of proteins (Gewold 2002). It establishes that the plastid genetic machinery is capable of correctly expressing and folding mammalian proteins and opens a new scenario in the expression of novel membrane proteins.

To obtain well-ordered three-dimensional crystals, membrane proteins must be solubilized with the help of detergents – amphiphilic molecules that form micelles above their micellar concentration – and purified as protein–detergent complexes. Otherwise, extraction of membrane proteins from their native environment generally results in a loss of stability that can be dramatic. The detergent micelle covers the hydrophobic surface of the membrane protein in a belt-like manner (Garavito and Ferguson-Miller 2001). Protein–detergent complexes form three-dimensional crystals of the so-called type II, in which contacts between adjacent protein molecules are made by the polar surfaces of the protein protruding from the detergent micelle (Michel 1983). However, membrane protein–detergent interaction is a complex issue; strong experimental evidence links many cases of inactivation to the dissociating character of detergents, which, by definition, are surfactants selected for their ability to disperse fatty molecules. This dissociating character causes the loss of stabilizing cofactors such as lipids or other amphipathic molecules, the dissociation of protein subunits, and direct interference with the interactions – such as those between transmembrane helices – that stabilize the protein's transmembrane structure. Structuralists therefore have to navigate a narrow strait between the unwanted aggregation and the catastrophic disaggregation (for recent discussions, see Bowie 2001; Gohon 2003). This has prompted the search for milder surfactants, some of which are detergents and some are not (for a review, see Gohon 2003).

3.1.3 Structural Analysis of Protein–Lipid Interactions by X-Ray Crystallography: Some General Remarks

The elucidation of high-resolution structures of membrane-spanning proteins has, over the past few years, yielded fascinating insights into the molecular mechanisms of diverse transmembrane processes, although the number of structures solved to atomic resolution is still small. Therefore, it is clear that to gain an understanding of the function of membrane proteins at a molecular level one must consider their contacts with lipids. However, while a high-resolution snapshot of the 3D structure can be determined for proteins, once a suitable diffracting crystal is obtained, that is not usually the case for the accompanying lipids. X-ray diffraction methods detect only those molecules that are highly ordered in the crystal and that is not usual for lipid molecules due to their inherent flexibility and the lack of specificity in the interaction between the protein molecule and some parts of the lipid moiety. Besides, although lipid molecules can, in some cases, be determined by X-ray crystallography, it is not clear that their structures reflect those of the lipids that are present in the native membrane. It has been observed, for example, that varying lipid stoichiometry affects crystal packing in porin for which

some different crystal forms were obtained (Cowan et al. 1992), which yielded the high-resolution structures of porin (Pebay-Peyroula et al. 1992; Penel et al. 1998), but showing packing arrangements that are distinctly different from the arrangement in the native membrane and thus failing to give information on lipid binding. Furthermore, the precise mode of lipid–protein association in vitro appears to be different from that in vivo (Pebay-Peyroula and Rosenbusch 2001). In this sense, it must be stressed that while the polar interactions between the membrane proteins and the surrounding lipids are clear, the interactions with highly ordered acyl chains may merely mean that flexible chains were sequestered in the crystals to fill the empty space.

When the lipidic/detergent component of the crystal is disordered, the only available technique for studying the structure of this disordered detergent in membrane proteins is neutron diffraction, whereby the individual components (proteins and amphiphiles) may be visualized by contrast variation (substitution of D_2O for H_2O), a technique commonly used in small-angle scattering (see below). The combined use of the high-resolution information gained from X-ray diffraction (usually relative to the protein moieties) with the low-resolution structural information obtained from neutron diffraction experiments for the amphiphilic moiety can reveal relevant insights into protein–lipid interactions; specifically showing the residues interacting with the head groups or the hydrophobic tails of the amphiphiles.

Despite these cautionary remarks, the potential of the diffraction methods in providing the structural information necessary to understand the mechanism of membrane proteins at a molecular level is evident, and from a general point of view in establishing the different protein folds capable of interacting with lipids and the structural basis of the protein–lipid interaction at a molecular level.

3.2 Membrane Protein Crystallization

3.2.1 The "Classical" Approach

Integral membrane proteins are embedded in a lipidic membrane. In order to be crystallized in three dimensions, they have to be solubilized and purified from their native environment. Amphiphilic molecules such as detergent form a belt around the membrane proteins, in which the tails of the detergent protect the hydrophobic protein surface whereas the headgroups protrude toward the solvent. The crystallization was described in several reviews or book chapters (Hunte and Michel 2003; Reiss-Husson and Picot 1999). Neutron diffraction experiments revealed that three-dimensional crystals are built up of such mixed micelles and that crystal contacts leading to high-resolution diffracting crystals implicate protein–protein interactions (Roth et al. 1989). In a very crude approximation, it could be considered that the mixed micelle solution is similar to a solution of a soluble protein. Crystallization can therefore be obtained by adding the adequate precipitants and adjusting their concentrations in order to cross the

solubility curve and to reach the metastable zone where crystallization occurs. In reality, the presence of detergent makes the process more complex as detergents have their own phase behaviour (Zulauf 1991). At low concentration they are solubilized in water as monomers. Above the critical micellar concentration (cmc) they aggregate in micelles in which hydrophilic (polar or charged) moieties are exposed to the solvent; these micelles coexist in solution with monomers. The phase diagram as a function of detergent concentration and temperature shows that at higher detergent concentrations two phases coexist; one is poor, the other is rich in detergent (Fig. 3.1).

The phase diagrams are influenced by the precipitant, its concentration and all other chemical components. Approaching the consolution boundary, from the micellar phase to the phase separation, enhances the micelle–micelle interactions and the probability of inducing protein–protein interactions. In addition, crossing the consolution boundary will concentrate the protein in the phase which is

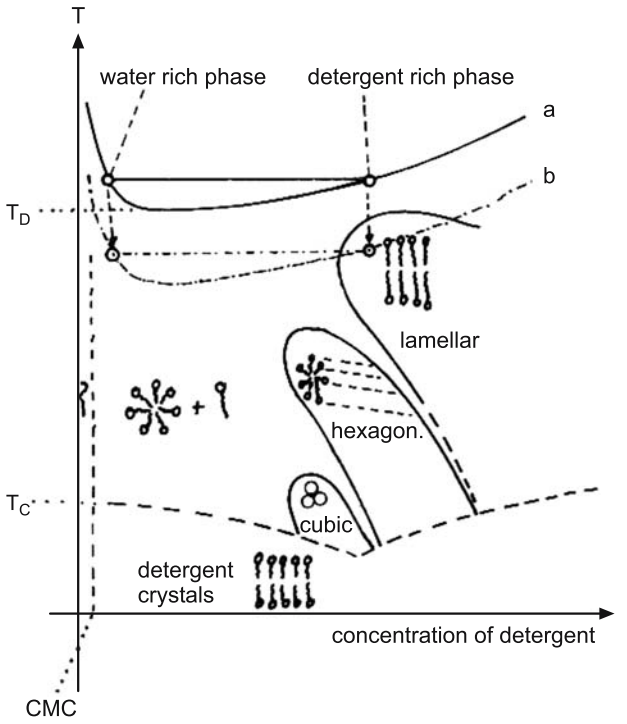

Fig. 3.1. Schematic phase diagram for non-ionic detergent water system. The abscissa and ordinate are without scale. Liquid crystalline phases are typically found at detergent concentrations greater than about 30%. Inserted in the liquid crystalline areas are schemes of the liquid crystalline aggregates. The phase separation boundary for the system without PEG is labelled **a**. The phase separation boundary downshifted by PEG with its detergent-rich phase in the lamellar crystalline area is labelled **b** (Welte and Wacker 1991)

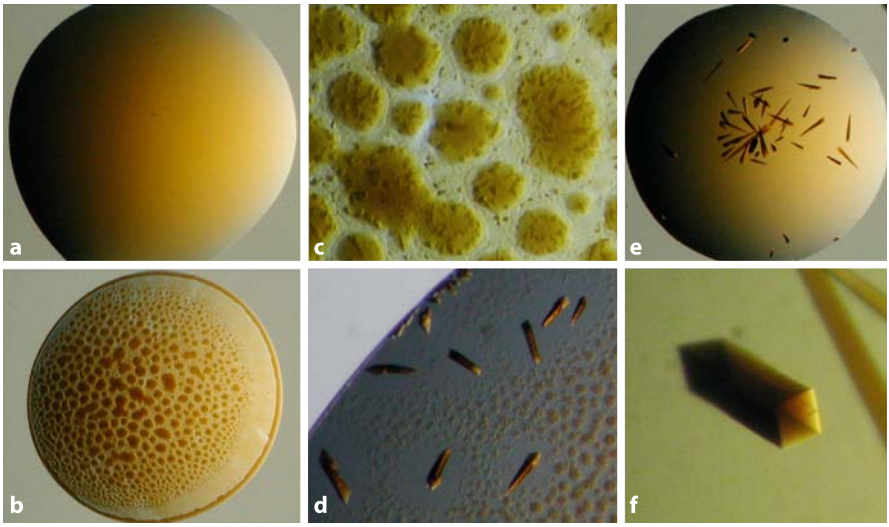

Fig. 3.2. Illustration of the phase separation above the consolution boundary. A photosynthetic complex from a purple bacteria solubilized with dodecyl-maltoside is crystallized in the presence of PEG3350 (from C. Jungas, CEA-DEVM-Cadarache and E. Pebay-Peyroula). (**a**) Below solubility curve and consolution boundary. (**b**) Above consolution boundary. (**c**) Crystal nucleation within the droplets that are highly concentrated in protein and detergent. (**d**) The crystal growth depletes the protein droplets around the crystals. (**e**) and (**f**) The best crystals are obtained in the vicinity of the consolution boundary

rich in detergent and also enhance the probability of protein–protein interactions to occur.

Figure 3.2 illustrates this process with a coloured protein, a bacterial reaction centre. The best crystals are often obtained just below the consolution boundary as illustrated in Fig. 3.2(f). The choice of the detergent is crucial not only for the solubilization of the protein but also for crystal formation. This choice was extensively discussed in several reviews (Reiss-Husson and Picot 1999); the favourite molecules can be deduced from crystallization conditions successful for membrane proteins (see statistics in http://www.mpibp-frankfurt.mpg.de/michel/public/memprotstruct.html). Neutron diffraction also showed that although crystal contacts imply proteins, the size of the detergent belt is an important parameter; it should not prevent protein–protein interactions from taking place and micelles have to fit well in empty spaces within the crystal packing. Additives such as heptane-triol influence the micelle radius and in some cases might favour better crystal contacts (Deisenhofer et al. 1985). The crystal contacts can also be favoured by enlarging the hydrophilic protein surface with an antibody fragment (Hunte and Michel 2003).

3.2.2 Alternative Methods

However, the limited number of membrane protein structures available in the protein data bank also reflects the difficulties in obtaining well-ordered crystalline arrangements. Indeed, the lack of homogeneity in the starting solution is very often the major drawback for several reasons. First the detergent has to provide a homogeneous solubilization without denaturing the protein. The difference in dynamical behaviour of solvent and lipidic membranes certainly influences the dynamical properties of the protein. Extracting the protein from its native environment releases the lateral constraint applied by the membrane and might induce partial denaturing. This should be particularly critical for proteins that undergo large conformational changes for their functions, such as transporters. As a result, the protein solubilized in detergent micelles might be present with a large variety of conformations, including non-functional ones, a very unfavourable situation for crystallization. Individual endogenous lipids can interact strongly with the protein and help in stabilizing native conformations. The difficulty of controlling a constant (and appropriate) amount of well-defined lipids in the protein solutions also contributes to heterogeneity (Lemieux et al. 2003). More recent approaches tend to exploit the lipid phases and to reincorporate the proteins in a lipidic environment in order to get rid of the detergent. The idea was already exploited in the last decade with attempts at stacking two-dimensional crystals of bacteriorhodopsin (naturally present in the purple membrane) but no order in the third dimension could be obtained. More recently, in order to overcome the limitations due to two-dimensional space and to explore the three dimensions, lipidic cubic phases were introduced by Landau and Rosenbusch (1996). They demonstrated the feasibility of the method and obtained for the first time highly diffracting crystals of bacteriorhodopsin leading to the structure (Pebay-Peyroual et al. 1997; Belrahli et al. 1999; Luecke et al. 1999). Other bacterial rhodopsins and reaction centres were further crystallized with this method (Chiu et al. 2000; Kolbe et al. 2000; Gordelyi et al. 2002; Katona et al. 2003; Royant et al. 2001; Vogeley et al. 2004). Interestingly, all these crystals consist of stacked layers of proteins forming type I crystals. The crystallization mechanism proposed by Nollert et al. (2001) is based on the lateral diffusion of the protein within the curved bilayer that constitutes the cubic phase. Increasing the curvature (by adding a precipitant) destabilizes the proteins by creating a hydrophobic mismatch and favours lateral protein–protein interactions. Locally, around the nucleation centre, lipids undergo a phase transition from cubic to lamellar. These various steps are illustrated in Fig. 3.3. The cubic phase can therefore by considered as a milieu that controls the relative orientations of the proteins during their diffusion in three-dimensional space.

The lipidic cubic phase approach is attractive because it can be generalized to other proteins in a rational way. There are still developments to take place either for a deeper mechanistic understanding, or for automating and miniaturizing the process (Qutub et al. 2004; Cherezov et al. 2004). In parallel, other individual cases of inducing membrane protein crystallization in a lipidic environment were also reported. The sarcoplasmic Ca-ATPase was crystallized by dialyz-

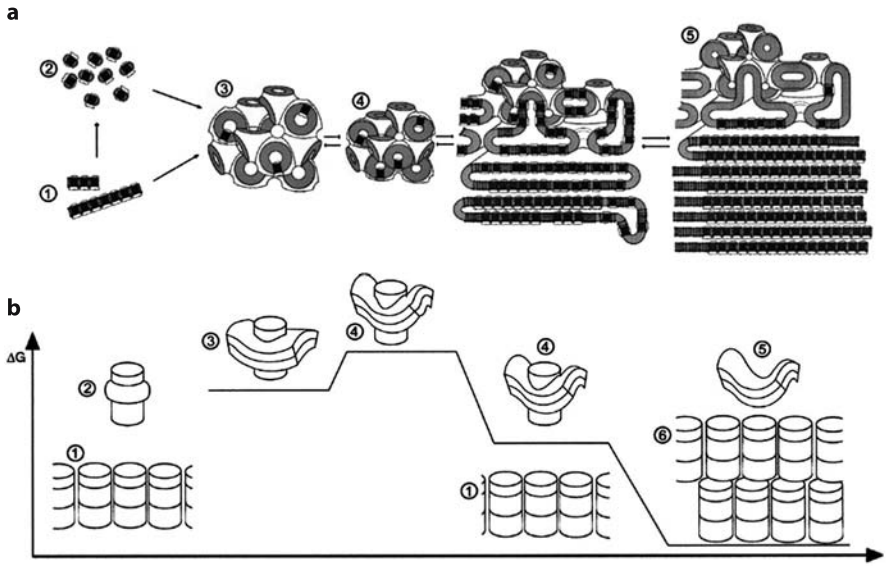

Fig. 3.3. Proposed crystallization mechanism in lipidic cubic phases. (**a**) Proteins solubilized in detergent micelles (2) or in lipid patches (1) are incorporated in the lipidic cubic phase (3). A modification of the cubic cell parameter (4) induces the stress that results in local protein reorganization possibly leading to 3D crystals (5). (**b**) Schematic representation of the various protein-membrane interactions encountered during the crystallization process (Nollert et al. 2001)

ing the detergent away in the presence of lipids leading to well-ordered stacks of 2D crystals. This technique was adapted from a two-dimensional crystallization protocol (Toyoshima et al. 2000). Similarly, the mitochondrial ADP/ATP carrier was crystallized from a protein–detergent solution in which excess detergent was adsorbed on polystyrene beads (Dahout-Gonzalez et al. 2003). The crystal is of type I; moreover each layer in the crystal packing contains only proteins, lipids and possibly monomeric detergent molecules tightly associated to the protein (Pebay-Peyroula et al. 2003). The success of this crystallization was due to the high amount of endogenous lipids still present after solubilization and purification. Adsorbing the detergent, probably forced the protein in lipid patches, which might nucleate the crystallization process. This example and others demonstrate the need for well-characterized systems prior to crystallization. In particular proteins that are overexpressed in heterologous systems might need the addition of a few lipids present in their native membrane and relevant for structural and/or functional reasons.

In conclusion, a new membrane protein after purification and solubilization in detergent should be characterized as far as possible in term of homogeneity, protein/detergent/lipid composition, importance of endogenous lipids, and ligands that stabilize a conformation; all of them are tools that will pave the way

to crystallization. For some proteins a rapid analysis by negative stain electron microscopy could reveal the presence of several oligomeric states. Crystallization should be approached in parallel by several methods. The classical vapour diffusion method can now be efficiently explored with robots that use very small amounts of proteins (100 nL per drop compared to 1 μL manually). A ten-fold reduction in the total amount of protein is noticeable for membrane proteins, which are so difficult to produce in large amounts. The number of parameters to explore can also be reduced by restricting the precipitants to polyethyleneglycols of various molecular weights and alcohols that have proven to be favourable precipitants. Alternative methods such as the lipidic cubic phases should also be exploited.

3.3 Diffraction Studies

3.3.1 X-Ray versus Neutron Diffraction

Nowadays, the development of synchrotron radiation facilities, associated with progress in detectors and computing, makes it possible to solve very complex structures with a large number of atoms, at atomic or near-atomic resolution, even with small crystals. Thus, X-ray diffraction covers the full range of analysis from structure determination to the understanding of biological function. By contrast neutron diffraction techniques are mostly used to analyse particular aspects of the molecular structure. The main reason for this is the scarcity of neutron sources and their low flux, but also that the most common tools for structure determination, such as heavy-atom and anomalous scattering techniques, are strongly limited due to the nature of the scattering factors. It must be stressed that X-rays interact with electrons and therefore have stronger interactions with heavy atoms (the X-ray scattering from an atom is proportional to the number of electrons) whereas neutrons interact with the nuclei and this interaction is similar for most nuclei. Moreover, the scattering of X-rays, being from an extended cloud of electrons, has an angular dependence, while this is not the case for neutrons which are scattered from the much smaller nuclei. Therefore, the applications of neutron diffraction techniques in biology are thus complementary to X-ray analysis.

As previously mentioned, high-resolution X-ray diffraction experiments lead to structural information on the highly ordered parts only. Low-resolution information is obtained from the diffraction at very small Bragg angles. These reflections are usually difficult to record, especially when working with strong X-ray sources where it is important to protect the detector against the main beam. To overcome this technical problem one may increase the wavelength and therefore increase the Bragg angle. Long-wavelength X-rays induce strong absorption and thus damage the crystals rapidly. On the contrary, neutrons do not present these absorption effects and hence do not induce radiation damage even during exposures of several weeks. Therefore neutron diffraction using long wavelengths is

a powerful technique for obtaining low-resolution structural information and is complementary to the high-resolution information gained from X-ray diffraction. In addition to the advantages of the long wavelengths, one can take advantage of the difference in the scattering lengths for hydrogen and deuterium to perform contrast variation experiments in the crystals. The neutron scattering densities for materials containing hydrogen or deuterium are therefore very different. The fact that H_2O and D_2O are chemically almost identical makes it possible to exchange the solvent in the crystals for a deuterated solvent without affecting the crystalline arrangement. As we will see, this technique is a powerful tool for understanding protein–lipid interaction in the crystal.

3.3.2 Neutron Diffraction with Contrast Variation

A three-dimensional crystal diffracting to high resolution does not contain only highly ordered atoms. In many structural models refined from X-ray diffraction data, a few amino-acid side-chains, and N-terminal or C-terminal residues are missing. Also small molecules, ligands, cofactors, individual detergent molecules or lipids are not always easy to locate in electron density maps even if they interact strongly with the protein. In fact, above a certain value of mean-square atomic displacement the atom will not contribute to high-resolution diffraction data. In the case of membrane protein crystals, where a large amount of detergent molecules are often present, the crystal packing seen in the electron density maps shows large empty holes and only a few single detergent molecules interacting directly with the protein. The bulk part of the micelle cannot be detected from the X-ray diffraction, first because it is a rather dynamic structure even within the crystal so that it does not contribute to the high-resolution diffraction. Moreover, at medium or low resolution the contrast between the solvent and the detergent is too low. In other words, the mean electron density is similar for water and detergent. The situation is very different for neutron diffraction where by exchanging hydrogenated water with deuterated water the scattering from the solvent can be notably modified and the contrast therefore changed.

Figure 3.4 shows the mean scattering length density, which is the relevant quantity for neutron scattering (equivalent to mean electron density for X-ray scattering) as a function of D_2O. The contrast, i.e. the difference in scattering length density for one component and solvent, varies as a function of D_2O concentration. The figure also shows that in some cases the contrast can even by cancelled; for example, at 40% D_2O the protein will be matched out. Proteins, lipids, detergents and nucleic acids have different scattering length density curves and thus different contrasts. Neutron scattering at low resolution is therefore of particular interest when the crystal contains at least two different types of molecules, for example protein and detergent, as is the case for many membrane protein crystals. In that case, neutron density maps obtained with a solvent containing 40% D_2O will show only the detergent structure, whereas with 20% D_2O only the protein will be seen. The experimental procedure and following calculations were detailed in several reviews (Timmins et al. 1994; Pebay-Peyroula and Myles 2000).

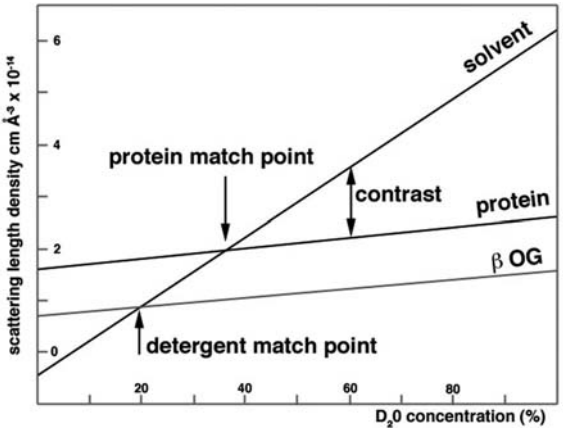

Fig. 3.4. Contrast variation as a function of D_2O concentration in the solvent. The scattering length density varies linearly as a function of the D_2O concentration in the solvent. The diffraction experiment is sensitive to the difference in scattering length density between the molecule in the crystal and the solvent. At null contrast, the match point, the molecule becomes "invisible". The scattering length densities for some chemical components encountered in membrane protein crystals such as protein and a typical detergent are represented

The first low-resolution neutron diffraction experiments were performed on photosynthetic reaction centre crystals from *R. viridis* (Roth et al. 1989), crystals from which the first membrane protein structure has been solved (Deisenhofer et al. 1985). These experiments showed that the crystal is formed by mixed micelles, which pack through protein–protein interactions and highlighted the importance of the micelle size for the packing. Indeed, heptanetriol, known to shrink the micelle size, was an important additive for getting good diffracting crystals. Other neutron diffraction experiments on various porin crystal forms illustrated the dynamic behaviour of the detergent phase that can reorganize during crystallization. Tetragonal porin crystals are of type II. Although micelles pack through protein–protein interactions, it was noted that the crystal consists of two intertwined molecular networks that only interact through detergent contacts (Pebay-Peyroula et al. 1995) (Fig. 3.5A).

In the trigonal form, the detergent phase reorganizes during the crystallization and forms almost inverted micelles around the protein (Penel et al. 1998). For a third porin crystal of type I, neutron diffraction showed that the detergent within each layer of the crystal is not organized as a bilayer but as adjacent micelles (Timmins, personal communication). Indeed, type I crystals can be subdivided into two categories: in the first, each layer contains mixed micelles packed in two dimensions, and in the second, each layer is a lipidic bilayer in which proteins are arranged in two dimensions. More recently, neutron scattering experiments with contrast variation were performed on other membrane protein crystals. De-

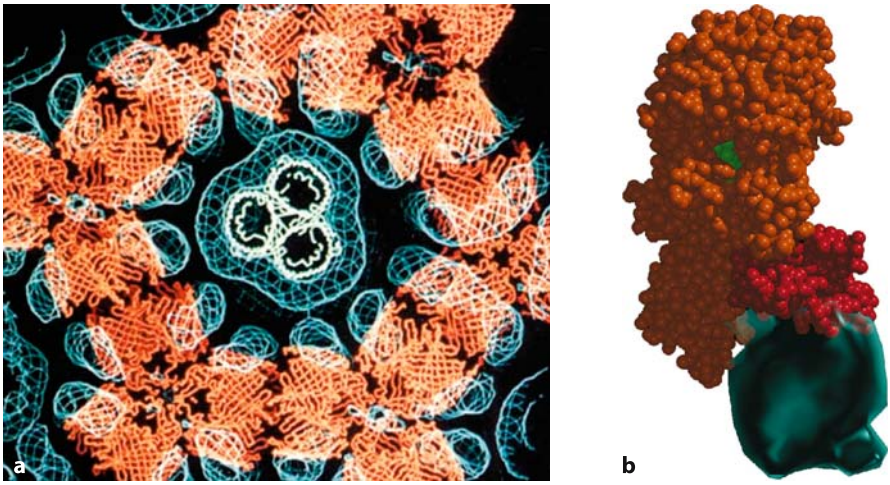

Fig.3.5. (**a**) Crystal packing in tetragonal porin crystals (Pebay-Peyroula et al. 1995). In the centre of the figure the backbone of a porin trimer is represented in green. Proteins surrounding this trimer are shown in orange. The blue density represents the detergent (mainly the hydrophobic chains) as detected from neutron diffraction experiments. It shows that the detergent organizes itself as a belt around the protein, hiding the hydrophobic surfaces from the solvent. The green and the orange proteins form two separated networks in the crystal that interact only through detergent contacts. (**b**) The pancreatic lipase-colipase-micelle complex. The neutron negative scattering-length solvent-flattened map was calculated at the protein match point (41% D_2O). Pancreatic lipase (gold) and Colipase (red) are depicted as CPK models. The catalytic Ser residue of the lipase is coloured in green

tergent organization in crystals of monomeric outer membrane phospholipase A showed a continuous detergent network and sheds light on the detergent coalescence that has to take place during the crystallization process (Snijder et al. 2003). In contrast, the detergent in the crystals of the light-harvesting complex LH2 from *R. acidophila* forms belts around the toroidal shaped protein, which do not interact with each other (Prince et al. 2003). In addition, detergent was also localized in the tore centre; neutron density maps showed that this density could account for a mixture of detergent and benzamidine used as an additive during the crystallization. Again, this result demonstrates the interest of neutron studies for the comprehension of the crystallization process of membrane proteins in the presence of detergent.

Neutron diffraction with contrast variation is not only interesting for membrane proteins but also for proteins that interact with membranes. The catalytic activity of lipases depends on the aggregation state of their substrates. The activated lipase–colipase complex was crystallized in the presence of detergent at a concentration above the cmc. The neutron density revealed the presence of a disc-shaped detergent micelle, which interacts with the colipase and the lipase (Hermoso et al. 1997) (Fig. 3.5b).

These examples illustrate the complementarity of neutron diffraction versus X-ray crystallography. However, the limited flux provided by the neutron sources compared to the photons flux produced by synchrotron radiation restricts the neutron studies to larger crystals (a few hundredths of a micron in each direction).

3.4 Protein–Lipid Interactions in 3D Structures

A large number of molecular processes involve protein–lipid interactions occurring in different biological environments. Thus, they are essential in the folding mechanism of membrane proteins (Marsh 1993; Bogdanov and Dowhan 1999), as well as in their activity (Gouaux and White 2003), which includes an astounding range of biological functions: respiration, signal transduction and cellular recognition, molecular transport, etc. However, and despite the critical importance of membrane proteins, nowadays only 86 unique structures have been solved, which is mainly due to technical difficulties in the production of three-dimensional crystals suitable for X-ray analyses (Pebay-Peyroula and Rosenbusch 2001).

Conversely, many intracellular processes involve the specific and transient association of peripheral proteins with different cell membranes in response to specific cell stimuli (Teruel and Meller 2000). Remarkably, the membrane targeting of diverse peripheral proteins is mediated by a reduced number of membrane-interacting domains, including protein kinase C (PKC) conserved 1 (C1), PKC conserved 2 (C2), FYVE domains (Misra and Hurley 1999), and pleckstrin homology domains (Hurley and Misra 2000; Cho 2001). On the other hand, a wide variety of proteins produced by diverse organisms is also known to facilitate the transfer of lipids, fatty acids, steroids, retinoids, prostaglandins, acyl-CoA, which are broadly classified as lipid-transfer proteins.

In addition, protein–lipid interactions are also present in other biological contexts. Thus, they are also essential for the understanding of the molecular mechanisms of enzymes such as lipases or esterases (Lowe 2002), the cytotoxic character of peptides and proteins which are initially hydrosoluble but in the presence of a target membrane become membrane-bound species (Heuck et al. 2001; Tweten et al. 2001; Zasloff, 2002), or processes of chemical modification of signaling proteins with lipid molecules (Mann and Beachy 2004). The underlying structural features of the above-mentioned groups of proteins will be briefly described herein, with the purpose of providing a general overview of the wide variety of proteins for which the interaction with lipids or hydrophobic ligands is essential for a detailed knowledge of their molecular mechanism of action.

3.4.1 Integral Membrane Proteins

3.4.1.1 General Features of Membrane Protein Structures

Presently, about 160 coordinate files of membrane protein structures are accessible in the PDB. Among them, roughly 80 are unique proteins (see http://blanco.biomol.uci.edu/Membrane_Proteins_xtal.html). Despite a significant increase in the last couple of years, the growth rate since 1986 is still not comparable to the early days of soluble protein structure determination (White 2004). The large majority of membrane proteins in the PDB span over both sides of the membrane, with a few exceptions (prostaglandin synthase, cyclooxigenase and squalene-hopene cyclase) which are monotopic. A third of the proteins are β-barrel proteins found in bacterial outer membranes. The first to be structurally characterized were porins, which are very stable and were very useful in the early development of membrane protein crystallization. Most of them are involved in transport processes and their structures contributed to the understanding of the mechanisms. However, there are still open questions. The transport of ferrichrome through FhuA (or FepA or FecA) still remains unclear; although a putative plug was identified in the structure, the access control through the plug mechanism needs additional evidence (Buchanan et al. 1999; Ferguson et al. 1998; Locher et al. 1998). TolC is a trimer that forms a single barrel, each monomer contributing with four strands. It is part of a complex machinery that drives the transport of small molecules between the cytosol and the exterior; the ensemble is still to be deciphered. Except in bacterial outer membranes, all other proteins are constituted by transmembrane helices. Proteins that are anchored in the membrane through a single transmembrane helix are clearly underrepresented in the PDB (except for monoamide oxidase and fatty acid amide hydrolase). Because the catalytic site is located in a large extramembrane domain, structural studies are undertaken after cleaving the transmembrane helix. However, this helix is often implicated in dimerization and therefore plays a crucial role in signaling. Solid state NMR is probably the best experimental approach to understand the dimerization process of such helices. The number of transmembrane helices in all the other integral membrane proteins present in the PDB is at least six or seven in the quartenary structures.

Figure 3.6 represents a sample of structures from the PDB, highlighting a variety of topologies. Some proteins consist as several subunits (11 subunits for the bovine heart cytochrome bc1 complex, Fig. 3.6a). Others, such as ion channels, function as oligomers and the structures were determined in the oligomeric form (Figs. 3.6b, c and e). Whereas for a few of them the crystal structure is monomeric, they were shown to function in an oligomeric state in vivo (mitochondrial ADP/ATP carrier, PDB code 1okc). It is also interesting to note the existence of pseudo-symmetries either present in the structure (lactose permease, Fig. 3.6d) or resulting from multiple gene duplication (ADP/ATP carrier). Figure 3.6 also shows that transmembrane helices are more or less tilted with respect to the membrane, and that they can be straight or kinked. In some cases, helices can even span only over

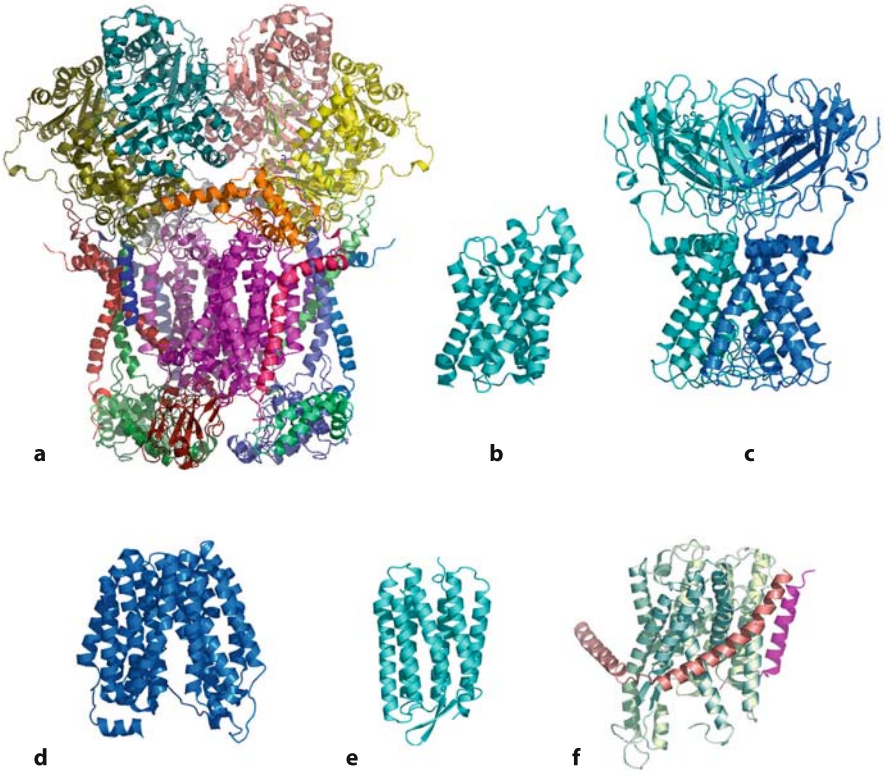

Fig. 3.6. Examples of membrane protein structures. The transmembrane helices of all the proteins are aligned. It highlights the different tilt angles that these helices can adopt. Each colour represents a different subunit. The figure illustrates several membrane protein topologies (differences in size, in the number of transmembrane helices, in the number of subunits and in the size of the extramembrane domains). (**a**) Bovine bc1 complex (11 subunits), PDB code: 1bgy. (**b**) One monomer of the glycerol facilitator (tetrameric structure), PDB code: 1fx8. (**c**) Inward rectifier potassium channel, PDB code: 1p7b. (**d**) Lactose permease, PDB code: 1pv7. (**e**) Monomer of bacteriorhodopsin (trimeric structure), PDB code: 1qhj. (**f**) Preprotein translocase SecY, PDB code: 1rhz. The figure was prepared with the program PyMOL

half the membrane (aquaporins, Fig. 3.6b). As a result the global topology is more compact (bacterial rhodopsins, Fig. 3.6e), or forms large cavities (ADP/ATP carrier, Fig. 3.7).

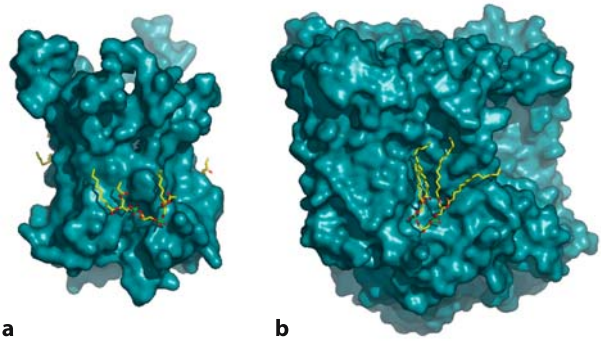

Fig. 3.7. Examples of cardiolipins in membrane protein structures. The surfaces of the proteins are depicted in blue and the cardiolipins as ball and sticks. (**a**) ADP/ATP carrier, PDB code: 1okc. (**b**) The photosynthetic reaction centre from *R. sphaeroides*, PDB code: 1qov. The figure was drawn with the program PyMOL

3.4.1.2 Lipids Identified in the Structures

The most frequent molecules associated with membrane proteins observed in the structures are pigments and chromophores for which the protein is often a scaffold. In order to ensure highly efficient energy or electron transfer, the pigments have to be precisely located with respect to each other. Therefore, their location is well defined in the structure and easy to obtain from the diffraction data. Locating and identifying lipids from electron density maps is less obvious and encounters several difficulties. As described in Sect. 3.3.2, X-ray diffraction mainly detects well-ordered ligands in a protein crystal. This is possible for highly diffracting crystals. Except for membrane protein crystals grown from lipidic cubic phases for which the resolution ranges from 1.5 to 2 Å, diffraction from most of the crystals is more limited and stays in the range 2.5–3.5 Å. Moreover, lipids are not necessarily perfectly ordered molecules in the crystals; more floppy lipids have a very low contrast compared to the solvent (or detergent) background. As a result, only well-ordered lipids in crystals diffracting to high resolution can be seen in electron density maps. This is a severe limitation of membrane protein X-ray crystallography. In addition, the refinement of these lipids is not very efficient, again because of the limitation in resolution (and thus in experimental data) but also because of the lack of stereochemical constraints. With a few exceptions, one should not expect a complete description of lipids surrounding a membrane protein from X-ray crystallography experiments. In addition, the purification already biased the problem by disrupting lipids from the protein that are important for the function and/or the structure. These limitations were reviewed by Pebay-Peyroula and Rosenbusch (2001).

Despite the limitations, the PDB files of several membrane proteins for which the 3D structure was solved contain a few lipid molecules. Very often, the residual electron density obtained after construction and refinement of the protein shows

elongated densities representative of hydrophobic moieties of either detergents or lipids. In some cases, the densities are clearly interpretable as lipids. In bacteriorhodopsin crystals, they could be identified as phytanyl chains well characterized with their branched methyl groups (Belrhali et al. 1999; Luecke et al. 1999). These lipids are known to be the endogenous lipids of the purple membrane, copurified with the protein. The chains interact through numerous van der Waals contacts with hydrophobic side-chains. The lipids participate in the bacteriorhodopsin trimer formation and also connect the trimers together within the purple membrane. However, the head groups, despite the presence of sulfur or phosphor atoms, could not be located in the electron density maps. Additional experiments ascertained the chemical nature of these molecules. Mass spectrometry on the crystals and on the purple membrane demonstrated that the same lipids (and no additional amphiphiles) are present in both samples. Neutron scattering on purple membranes in which the lipid head groups could be deuterated, located the head groups with respect to the protein (Weik et al. 1998). Bacteriorhodopsin is a unique case because the protein already exists as a 2D crystal in the native membrane from which the first structure at 3.5 Å was solved by electron microscopy (Grigorief et al. 1996). The 3D crystallization in the lipidic cubic phases reconstitutes the purple membrane in the 3D crystal, and thus reveals the complete high-resolution structure of the purple membrane.

The function of several membrane proteins was shown to be influenced by specific lipids, in particular cardiolipins. The ADP/ATP carrier, responsible for the import of ADP into the mitochondria and the export of ATP toward the cytosol after being resynthetized, is located in the inner mitochondrial membrane. Its function is influenced by cardiolipins and lipids, which are abundant in inner mitochondrial membranes. The electron density maps of ADP/ATP carrier crystals exhibited characteristic densities with four acyl chains. Figure 3.7(a) indicates the location of one of the three cardiolipins identified from the crystallographic data. The lipids might control the conformational changes during the nucleotide transport process. It was suggested that modifying the kink of three sharply kinked helices occurs during the transport (Pebay-Peyroula and Brandolin 2004). Cardiolipins interact with these kinked lipids and could maintain the hydrophobic environment of the helices during these movements. Cardiolipins could also participate in forming the dimeric state of the carrier. Although a putative dimer is not obvious from the crystal (Pebay-peyroula et al. 2003), another crystal form shows that the dimerization could implicate the cardiolipins (Pebay-Peyroula, personal communication). Cardiolipins were also identified in several bacterial proteins. They were shown to be able to stick to the protein with the four chains like an octopus and also to glue proteins together. In the case of succinate dehydrogenase the chains even interpenetrate the bundle of transmembrane helices (Yankovskaya et al. 2003). In the *E. coli* formate dehydrogenase (Jormakka et al. 2002), a cardiolipin is located within two molecules of the trimer. The photoreaction centre of *R. sphaeroides* was crystallized by two different approaches. In the structure solved from crystals grown by the "classical" approach, where protein–detergent micelles are formed (McAuley et al. 1999) a complete cardiolipin was identified sticking to the surface of the protein (Fig. 3.7b). More recently, the reaction centre crystallized from a lipidic cubic phase (Katona et al. 2003)

revealed the same protein structure with a cardiolipin bound to the same location. However, the crystal packing in the two crystals is very different: the first crystal is of type II and the protein is monomeric, whereas the second is of type I and a dimeric organization mediated by the cardiolipin is observed. Katona et al. discuss the possibility of the biological relevance of the cardiolipin in the dimer formation. If this hypothesis is correct, it reinforces the interest for crystallization in a lipidic environment.

3.4.2 Structural Features of Peripheral Proteins Involved in Signaling and Subcellular Targeting

Recent structural and biochemical studies of a wide variety of eukaryotic peripheral proteins participating in signal transduction and membrane-trafficking have shown that their molecular activity involves the reversible binding to specific lipid ligands in cell membranes (Hurley and Misra 2000). Importantly, the membrane-binding ability of these proteins is conferred by a reduced number of protein domains, the best known being PKC C1 (Hurley et al. 1997), PKC C2 (Rizo and Sudhof 1998), FYVE domains (Misra and Hurley 1999), and pleckstrin homology domains (Rebecchi and Scarlata 1998). It must be remarked that the mechanism of membrane association of the different peripheral proteins involves a combination between both specific and non-specific interactions. Thus, in addition to specific binding pockets for signal molecules, basic and aromatic residues play important roles in providing a non-specific driving force for membrane association (Cho 2001).

Figure 3.8 shows 3D structures for different domains showing the main structural features of each family. The C1 domains are known to occur not only in PKCs but also in more than 200 non-redundant proteins (Hurley and Misra 2000). This domain was first identified as the binding site for diacylglycerol (DAG) and phorbol ester in PKCs (Nishizuka 1988), although many of the known C1 domains do not bind such molecules. Proteins bearing C1 domains not competent for DAG or phorbol ester binding are called atypical. C1 domains are compact motifs composed of ~50 residues. They contain five β-strands, arranged into two sheets, a short α-helix and two 3-Cys-1-His-2-Zn^{2+} clusters (Hommel et al. 1994; Zhang et al. 1995). Briefly, the current model explaining the interactions of C1 domains with membranes can be summarized as follows: DAG or phorbol ester bind to a specific binding pocket rich in aliphatic and aromatic residues, which is surrounded by basic residues which in turn are involved in electrostatic interactions with acidic phospholipids (Bittova et al. 2001). Whereas these last residues enhance the association rate with the membrane, the specific interaction with the second messenger decreases the dissociation rate, thus favouring the formation of a tight association of the domain with the membrane. Remarkably, there is a strong synergism between DAG or phorbol ester binding and membrane binding (Mosior and Newton 1996). It is evident that the presence of an exposed hydrophobic surface in C1 domains demands a tightly controlled triggering mechanism of membrane targeting (Cho 2001). In fact, the scenario is more complex as

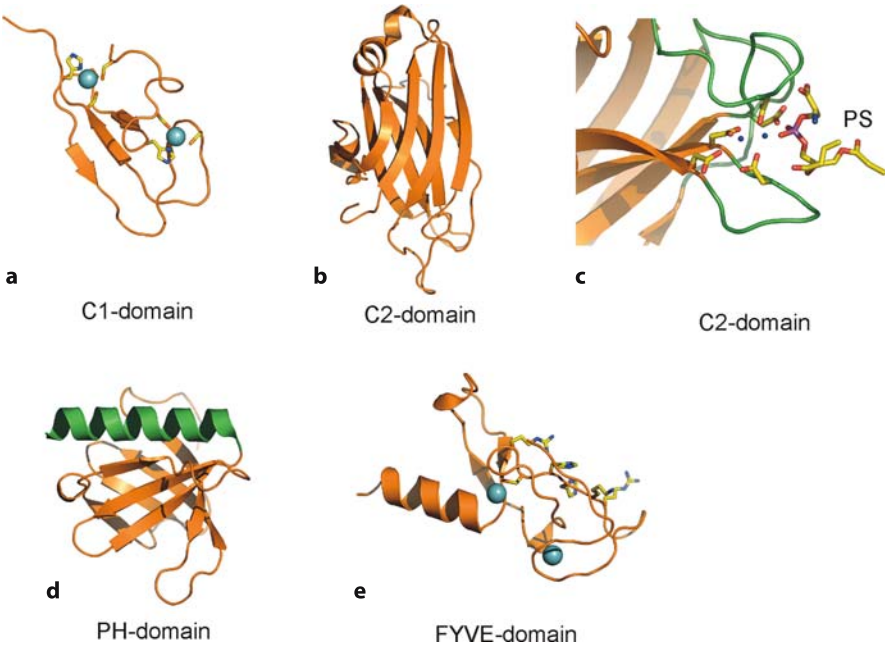

Fig. 3.8. Three-dimensional structures of representative members of peripheral proteins involved in signal transduction and membrane-trafficking showing the main structural details of the membrane-interacting domains. (**a**) *Cyan* spheres in C1-domain correspond to Zn^{2+} ions (PDB code: 1KBE). (**b**) and (**c**) *Green* segments in the C2-domain correspond to those loops directly involved in Ca^{2+}-binding (PDB code: 1DSY). Ca^{2+} ions are indicated as small *blue* spheres; phosphatidylserine molecule is indicated as PS. (**d**) The characteristic C-terminal α-helix above the β-structure core of the pleckstrin-homology domain (PDB code:1FB8) appears in *green*. (**e**) As above, *cyan* spheres in the FYVE-domain (PDB code: 1VFY) correspond to Zn^{2+} ions. Figures were prepared with the program PyMOL

the majority of peripheral proteins have more than one membrane-targeting C1 domain which may interact between them as well as with additional parts of the protein to modulate the interaction with the membrane.

C2 domains were originally discovered as the Ca^{2+} binding site of conventional PKCs (Xu et al. 1997). Proteins with C2 domains (>400 different proteins) are not only involved in signal transduction roles, but also in other cellular processes, which is consistent with the degree of variability of primary structures (Rizo and Sudhof 1998). Thus, many C2 domains bind membranes in a Ca^{2+}-dependent manner, others do not bind Ca^{2+}, and finally others do not bind membranes at all but other proteins both in a calcium-dependent or independent manner (Hurley and Misra 2000). The structure of the C2 domain is composed of an antiparallel β-sandwich made up of two four-stranded β-sheets, with the Ca^{2+}-binding site located at one tip of the structure being formed by three connecting loops (Fig. 3.8c). It has been shown that Ca^{2+} ions may play two fundamental roles: they serve

as a bridge between the C2 domain and anionic phospholipids (Verdaguer et al. 1999), and as inductor of intra- or interdomain conformational changes which may further affect the interaction with the membrane (Cho 2001). A model for membrane interaction of C2 domains has been proposed from the crystal structure of the phospholipase Cδ1 (Grobler et al. 1996); in this case, the loops involved in Ca^{2+}-binding are directed towards the membrane interface, where the acidic lipid headgroups are situated with the concave face of the domain facing the membrane plane.

Although most Ca^{2+}-dependent C2 domains bind acidic phospholipids, others, like cPLA2-C2, seem to be phosphatidylcholine specific (Nalefski et al. 1998). Interestingly, whereas in the first group of domains there is a predominance of basic residues in the surroundings of the Ca^{2+}-binding loops, in the second group hydrophobic residues can be found in equivalent positions. In addition, this lipid specificity correlates with the respective subcellular localization of the corresponding domains: those with preference for phosphatidylserine translocate to plasma membrane, and those with preference for phosphatidylcholine translocate to the PC-rich nuclear envelope and endoplasmic reticulum (Perisic et al. 1999).

FYVE domains constitute a recently described family of membrane-binding domains present in ~60 proteins (Hurley and Misra 2000). They are involved in the endosomal translocation of proteins implicated in membrane-trafficking (Stenmark et al. 1996; Wurmser et al. 1999). FYVE domains specifically bind phosphatidylinositol-3-phosphate (PI3P), i.e. they are lipid-directed targeting domains. The crystal structure of the FYVE domain from Vps27p (Misra and Hurley 1999) reveals that it is formed by two antiparallel β-sheets and an α-helix stabilized by two Zn^{2+} ions, resembling C1 domains (Fig. 3.8e). A basic region located in the surface of the domain, contributed by the sequence RKHHCR, has been shown by mutagenesis analyses to participate in PI3P-binding. In fact, this sequence motif, (R/K)(R/K)HHCR, is a defining feature of the FYVE domain. Analysis of the solvent accessible hydrophobic and basic residues suggests a non-specific mechanism of membrane interaction (Misra and Hurley 1999), in which the tip of the N-terminal loop, containing two contiguous Leu residues, would penetrate into the PI3P-containing bilayer. Yet, experimental evidence points to the specific binding of PI3P as the major driving force for interaction with the membrane, which is consistent with the structural data.

Pleckstrin homology (PH) domains have been found in more than 500 proteins, most of them involved in phosphoinositides (PIs) binding, exhibiting a broad range of specificities (Rebecchi and Scarlata 1998). In addition, similarly to the functional variability observed with C2 domains, there also exist PH domains which do not bind PIs, but are involved in protein–protein interactions (Lemmon et al. 1997; Rebecchi and Scarlata 1998). The consensus structure of the PH domains as derived from the known three-dimensional structures can be described as follows: the domain consists of two nearly orthogonal and antiparallel β-sheets composed of three and four strands, respectively. The core of the β-structure is stabilized by a C-terminal α-helix which packs one of its edges (Fig. 3.8d). A distinct feature of PH domains is the clearly asymmetric distribution of charged residues in the protein surface: whereas basic residues predominate in one side of the domain (the membrane-binding face) and also partially in the

loops, acidic residues are concentrated in the opposite side (Rebecchi and Scarlata 1998). The structures of complexes of PLCδ1-PH with Ins(1,4,5)P_3 (Ferguson et al. 1995) and Btk-PH with Ins(1,3,4,5)P_4 (Baraldi et al. 1999) define four different phosphate-binding subsites that participate in high-affinity specific PI-binding. Finally, membrane binding of PH domains is driven by non-specific electrostatic interactions with acidic phospholipids, together with the specific recognition of phosphoinositides. This agrees with the finding that some mutations increasing the number of basic residues in PH domains result in constitutive activation of the proteins (Baraldi et al. 1999).

3.4.3 Pore-Forming Protein Toxins

Many organisms produce polypeptide chains that can exist either as a water-soluble state or as a membrane-embedded species, usually an oligomeric integral membrane protein (Gouaux 1997; Heuck et al. 2001). The conversion between both protein forms is spontaneous, and it is generally accepted that it proceeds through discrete steps: water-soluble state, membrane-receptor binding, oligomerization, membrane insertion and final formation of the functional pore. The current structural information on these pore-forming proteins (PFPs) demonstrates that the above conversion entails concerted large-scale conformational changes which raises numerous questions, nowadays only partially understood, which connect not only with protein structure but also with protein folding and dynamics.

Despite their structural diversity (Parker and Feil, 2005), PFPs are usually classified into two types on the basis of the putative structure of the transmembrane (TM) domain: α-PFP, which are predicted to insert amphipathic α-helices, and β-PFP, which utilize amphipathic β-hairpins to form a membrane-spanning β-barrel. Regarding PFPs with known three-dimensional structure, the group of α-PFPs includes colicins (Wiener et al. 1997; Stroud et al. 1998), exotoxin A from *Pseudomonas aeruginosa* (Allured et al. 1986), insecticidal crystal proteins Cry3A (Li et al. 1991) and CryIAa (Grochulski et al. 1995) from *Bacillus thuringiensis*, and diphteria toxin from *Corynebacterium diphteriae* (Choe et al. 1992) (Fig. 3.9).

On the other hand, the group of β-PFP, includes aerolysin from *Aeromonas hydrophyla* (Parker et al. 1994), ε-toxin from *Clostridium septicum* (Cole et al. 2004), hemolytic lectin LSL from the mushroom *Laetiporus sulphureus* (Mancheño et al. 2005), crystal protein Cyt2A from *B. thuringiensis* (Li et al. 1996), α-hemolysin from *Staphylococcus aureus* (Song et al. 1996), perfringolysin O from *C. perfringens* (Rossjohn et al. 1997), and the anthrax toxin produced by *Bacillus anthracis* which is composed of anthrax protective antigen (PA) (Petosa et al. 1997), directly involved in the formation of heptameric pores in the target membrane, and the enzymatic domain lethal factor (LF) and edema factor (EF). Remarkably, in this last case, the crystal structure of the complex between PA and its host cell receptor has been recently solved for the first time (Santelli et al. 2004) (Fig. 3.10).

In addition to the above-mentioned α-PFPs and β-PFPs, all coming from prokaryotic sources, the crystal structures of two eukaryotic toxins from sea

anemones have recently been solved, those of equinatoxin II from *Actinia equina* (Athanasiadis et al. 2001) and sticholysin II from *Stichodactyla helianthus* (Mancheño et al. 2003). In this last case, the determination of the low-resolution structure of a tetrameric assembly of sticholysin II by means of electron microscopy analyses of 2D crystals of the toxin formed on lipid monolayers suggested a model for the functional pore, which is consistent with the formation of toroidal membrane pores (Fig. 3.11).

In Figs. 3.9 and 3.10, a gallery of the crystal structures of the above mentioned PFPs can be observed; these reveal the broad diversity of structural protein architectures present in the hitherto poorly understood PFPs realm. In the following, we present a brief overview of the structural basis of the mechanism of the biological activity of a deeply analysed member of each group of PFPs: colicin Ia from the group of α-PFPs, α-hemolysin from the β-PFPs, and also recent results from the eukaryotic actinoporins.

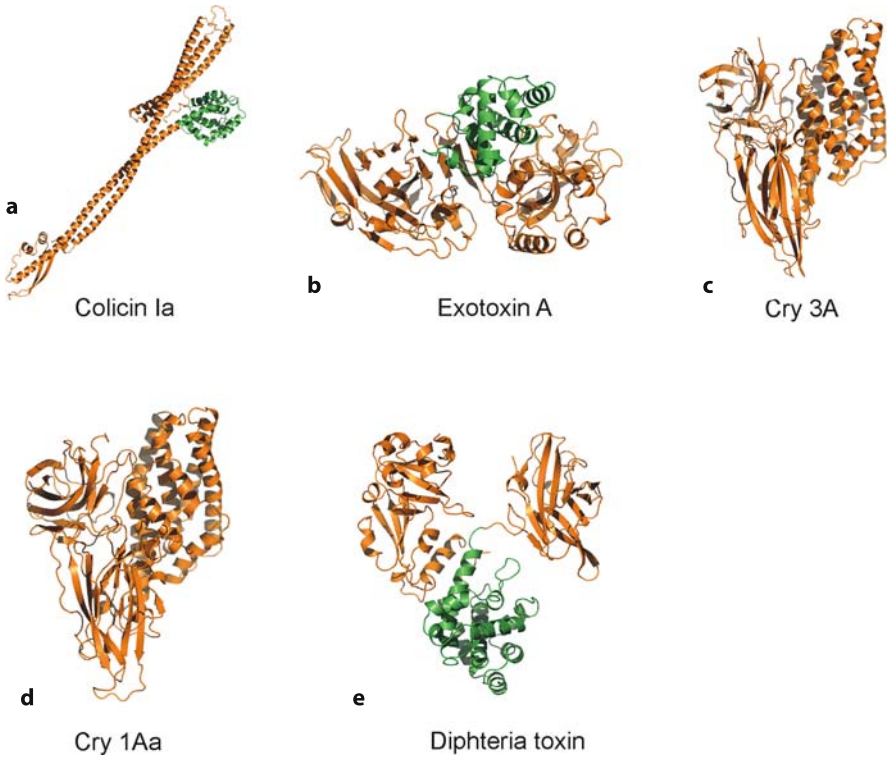

Fig. 3.9. Ribbon representations of α-PFPs. Regions directly involved in pore-formation are indicated in *green*. For clarity, the scales of the different proteins are not comparable. PDB codes are: (**a**) 1CII for colicin Ia from *E. coli*, (**b**) 1IKQ for exotoxin A from *Pseudomonas aeruginosa*, (**c**) 1DLC for Cry3A and (**d**) 1CIY for Cry1Aa, both from *B. thuringiensis*, and (**e**) 1XDT for diphteria toxin from *Corynebacterium diphteriae*. Figures were prepared with the program PyMOL

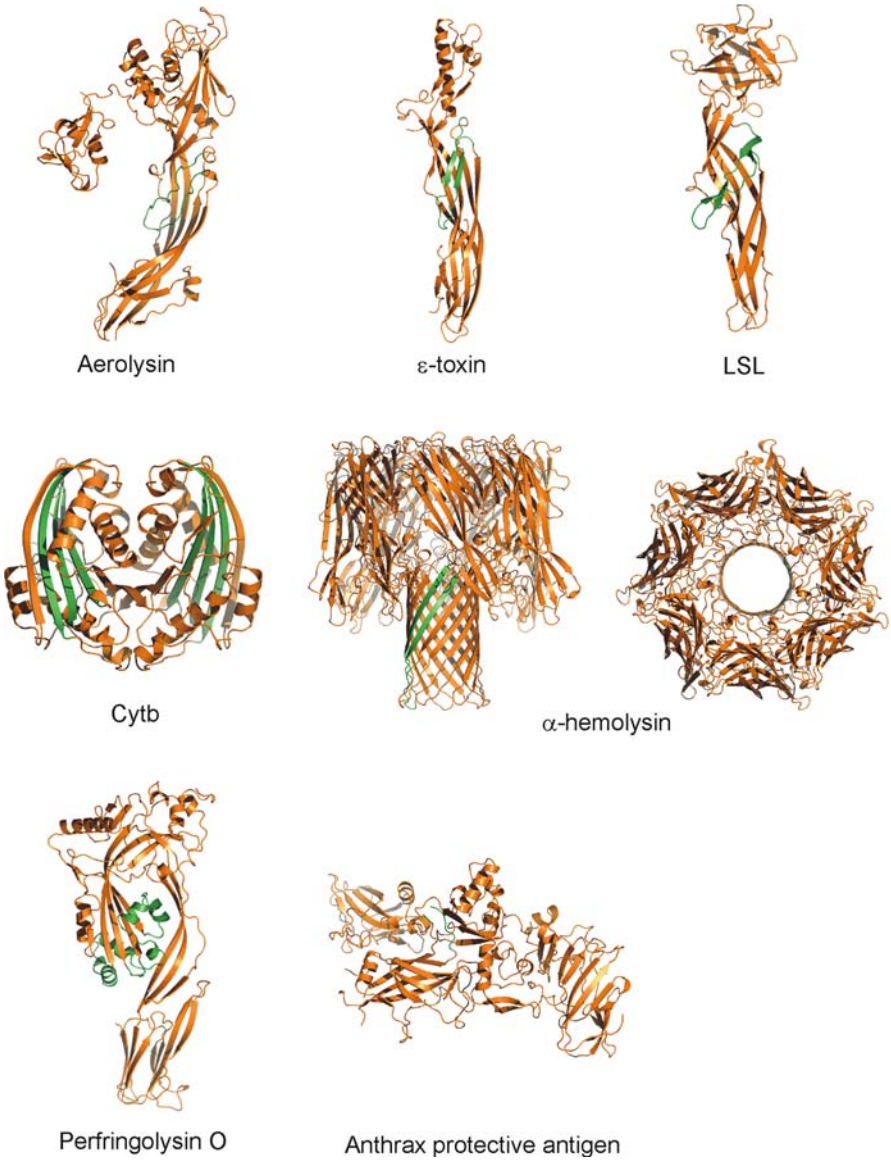

Fig. 3.10. Ribbon representations of β-PFPs. Domains responsible for pore-formation are highlighted in *green*. PDB codes are: 1PRE for aerolysin from *Aeromonas hydrophyla*, 1UYJ for ε-toxin from *Clostridium septicum*, 1W3A for the hemolytic lectin LSL from the mushroom *Laetiporus sulphureus*, 1CBY for Cytb from *B. thuringiensis*, 7AHL for the oligomeric pore of α-hemolysin from *Staphylococcus aureus,* 1PFO for perfringolysin O from *C. perfringens*, and 1ACC for anthrax protective antigen from *Bacillus anthracis*. Figures were prepared with the program PyMOL

Colicins are α-PFPs produced by several strains of *E. coli* which act on closely related bacteria (Stroud et al. 1998). The plasmid responsible for the production of colicins also provides the colicin-producing cells with an immunity system which protects them against their own toxins. Colicins present distinct structural domains arranged along the primary structure, corresponding to specific functional domains (Fig. 3.12): receptor binding (R-domain), translocation across the outer membrane (T-domain), and cytotoxic (membrane pore-formation, DNAse, RNAse, etc.; C-domain). The first step in their biological activity is binding to an outer membrane receptor through the R-domain, which is a porin involved in active transport, usually composed of a 12–14 β-stranded TM barrel. Then, to gain access to the plasma membrane, colicins parasite either the Tol or the Ton pathways of transport through the periplasm. After spanning the periplasm, the C-terminal domain is translocated across the outer membrane and finally reaches the plasma membrane.

Colicin Ia is an extremely elongated molecule (~210 Å), in which two long α-helices (T3 and C1) segregate the R-domain from the T- and C-domains (Fig. 3.12) (Wiener et al. 1997). The R-domain binds to the porin Cir which is involved in the transport of iron-chelated siderophores (Stroud et al. 1998). Once the receptor has been recognized, colicin Ia uses the integral plasma membrane TonB protein to gain access to the plasma membrane. In this sense, colicin Ia has a

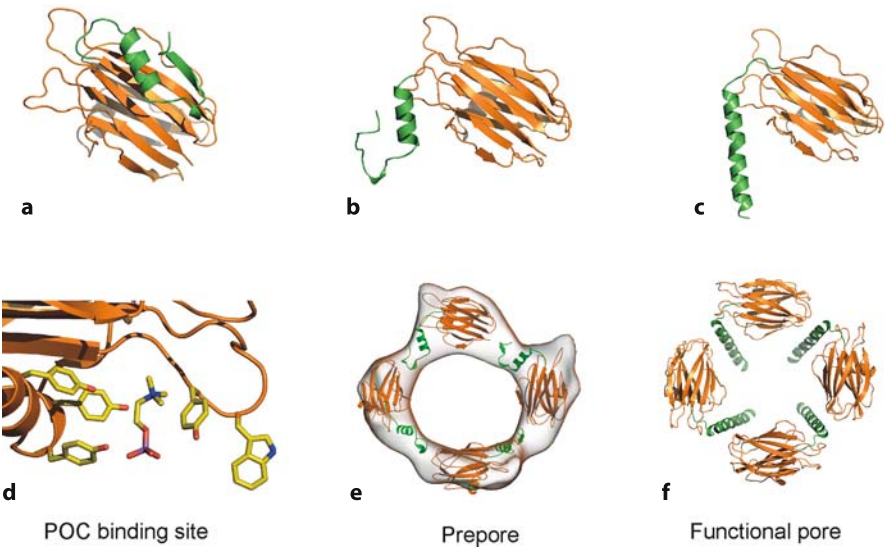

Fig. 3.11. Ribbon model of the colicin Ia molecule (PDB code: 1CII) indicating the different functional domains: R-domain (*violet*), which is involved in receptor binding; T-domain (*violet*), which directly participates in protein translocation across the outer membrane, and C-domain or channel forming domain (*green*). Hydrophobic helices α8 and α9, which are sandwiched by eight amphipathic helices, are indicated. Figures were prepared with the program PyMOL

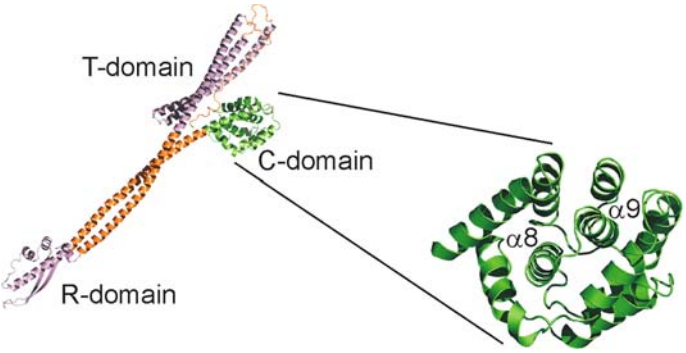

Fig. 3.12. Three-dimensional structures of the Staphylococcus aureus α-hemolysin (**a**) heptameric pore, and that of the (**b**) water-soluble homologue LukF (PDB code: 2LKF), as ribbon models. Comparison of both structures reveals a mechanism of pore-formation involving large-scale conformational changes essentially in two regions: the N-terminal segment latch (*violet*) and the stem (*green*). Figures were prepared with the program PyMOL

hydrophobic stretch near the N-terminal end called the TonB box, which is conserved in TonB-dependent colicins and receptors participating in the TonB pathway, and which is required for the interaction with TonB. The length of α-helices T3 and C1 (~160 Å) permits colicin Ia to span the periplasm (average width 150 Å), while interacting both with the receptor and the inner membrane. Final channel formation in the plasma membrane of the target cell requires the translocation of the C-domain, which is formed by two hydrophobic helices surrounded by eight additional amphipathic α-helices (Fig. 3.12). The C-domain of colicin Ia interacts best with acidic rather than neutral phospholipids, indicating that electrostatic interactions are important in the initial steps of membrane association (Elkins et al. 1997). This electrostatically driven association is followed by insertion into the lipid bilayer which is driven by hydrophobic interactions (Zakharov et al. 1996; Heymann et al. 1996). It must be remarked that despite the very low sequence identity between the C-domains from colicins Ia, A and E1, they share the same C-domain scaffold (Parker et al. 1996; Elkins et al. 1997; Wiener et al. 1997), which suggests this helical domain is an efficient membrane-inserting motif. The current model, explaining membrane penetration by pore-forming colicins, is the umbrella model initially proposed for colicin A (Parker et al. 1990), with minor modifications (Parker and Feil, 2005). This mechanism involves the penetration of the hydrophobic α-helices, after previous opening of the domain. The conformational transition between the different states may be facilitated by the existence of a molten globule intermediate induced at low pH conditions (van der Goot et al. 1991; Muga et al. 1993).

Without doubt, α-hemolysin from *S. aureus* predominates the scenario of the β-PFPs as it represents the first and so far unique β-PFP oligomeric state whose high-resolution three-dimensional structure has been solved (Song et al. 1996). Comparison of this structure with those of the water-soluble states of various α-hemolysin homologues, LukF (Olson et al. 1999), LukF-PV (Pèdelacq et al.

1999), is of special interest for understanding not only the structural basis of the pore-formation mechanism by β-PFPs, but also the folding and structure of integral membrane proteins containing TM barrels (Montoya and Gouaux 2003). This structural information, together with other experimental evidence, points to a complex mechanism of α-hemolysin pore-formation, which may proceed through several discrete conformational states: water-soluble, membrane-bound monomer, heptameric prepore, and final functional inserted heptameric pore. Although the crystal structure of the water-soluble states of the α-hemolysin homologues LukF (Olson et al. 1999) (Fig. 3.13) and LukF-PV (Pèdelacq et al. 1999) exhibit close resemblances with the overall structure of the α-hemolysin protomer, there are two regions that adopt dramatically different conformations when these states are compared; the so-called amino latch and the pre-stem regions suffer large-scale conformational changes upon pore formation (see below) (Fig. 3.13b).

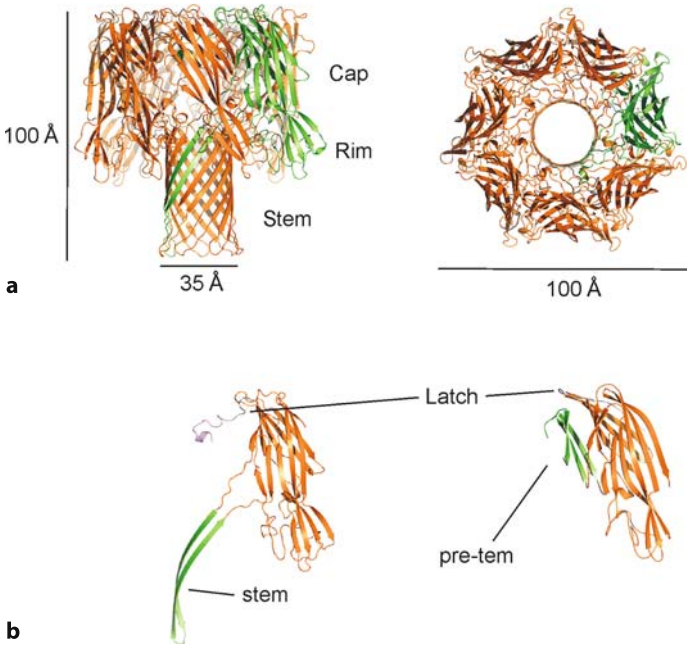

Fig. 3.13. (**a**) Crystal structure of the pore-forming toxin StnII from the anemone *Stichodactyla helianthus* (PDB code: 1GWY), and a (**d**) snapshot of the phosphocholine-binding site (PDB code: 1O72), indicating residues involved in lipid-headgroup. (**b**) and (**e**) The electron microscopy envelope clearly revealed the existence of tetrameric species, and also conformational changes in the N-terminal α-helix of StnII. (**c**) and (**f**) A putative model for the functional pore in which the N-terminal region adopts an extended helical conformation is also shown. Figures were prepared with the programs MOLSCRIPT and PyMOL

The crystal structure of the heptameric α-hemolysin pore (Song et al. 1996), reveals a mushroom-shaped assembly (Fig. 3.13), with three distinct regions: stem, rim and cap. The oligomeric complex measures approximately 100 Å in height and up to 100 Å in diameter, with an inner solvent-filled tunnel parallel to the seven-fold axis, which ranges from ~15 to ~46 Å in diameter. The stem or transmembrane region is composed of a 14-stranded β-barrel which results from the association of seven β-hairpins, each one contributed from a single monomer. This folding may indicate that the β-hairpin constitutes the basic structural unit of TM β-barrels which in fact agrees with current studies on constitutive TM β-barrels (Wimley 2003). Another evident structural feature of the stem region, also typically found in constitutive TM β-barrels (Schulz 2000; Wimley 2003), is that it is formed by an even number of strands with an alternating pattern of hydrophobic and small and polar residues. Whereas hydrophobic residues are oriented toward the hydrophobic core of the membrane, polar residues constitute the walls of the barrel lumen. On the other hand, the rims are the protein regions located in the close vicinity of the membrane outer interface. A characteristic feature of these regions, also in common with porins (Wimley 2003), is the presence of a high concentration of aromatic residues, which are known to exhibit a high affinity for membrane interfaces (Killian and von Heijne 2000), and also the presence of basic residues which would interact with the phospholipid headgroups. Finally, the cap regions constitute large hydrophilic domains protruding from the extracellular membrane surface.

As stated above, the amino latch and the pre-stem regions suffer drastic conformational changes upon formation of the functional pore. The residues comprising the amino latch either in LukF (Olson et al. 1999) or in LukF-PV (Pèdelac et al. 1999) adopt a β-strand conformation which forms part of the inner β-sheet of the sandwich domain. On the contrary, in the α-hemolysin protomer this region is irregular, establishing numerous contacts with one adjacent protomer (Fig. 3.13b). In the case of the pre-stem region, it forms a three-stranded antiparallel β-sheet packed against the β-sandwich, which in the oligomeric state extends away from it forming a definite β-hairpin. Noticeably, the region initially occupied by the pre-stem segment constitutes the binding site for the latch segment of the neighbour protomer.

Recently, the crystal structures of the water-soluble states of the eukaryotic PFPs equinatoxin II (EqtII) from *Actinia equina* (Athanasiadis et al. 2001) and sticholysin II (StnII) from *Stichodactyla helianthus* (Mancheño et al. 2003) (Fig. 3.11) have been reported. They are formed by a ten-stranded antiparallel β-sandwich, which is flanked on each side by a short α-helix. Remarkably, whereas the longest connecting loops concentrate on one tip of the sandwich, the other tip is formed by tight turns. An important structural feature observed is the existence of a solvent-exposed region with a high concentration of aromatic residues, in which is located a phosphocholine-binding site (Fig. 3.11d) which may explain the high affinity these PFPs exhibit towards sphingomyelin (Mancheño et al. 2003). In this regard, recent mutagenesis studies on StnII have shown the critical role of Tyr-111 in pore-formation (Alegre-Cebolleda et al. 2004), which perfectly agrees with the above structural studies. Additionally, electron microscopy (EM) analyses on 2D-crystals of StnII formed on lipid monolayers (Martín-Benito et al.

2000; Mancheño et al. 2004) have shown the existence of tetrameric species with a pore-like topology which may represent a pre-pore state. Docking of the high-resolution atomic model of StnII into the EM envelope indicates the existence of conformational changes affecting the N-terminal helix, which may translocate essentially as a pseudo-rigid body from the β-sandwich to the membrane interface (Fig. 3.11B, e). This is in agreement with molecular biology results which showed that the presence of a disulfide bridge connecting the N-terminal helix and the β-sandwich inhibits pore-formation by EqtII (Hong et al. 2003). Finally, a model for the functional pore has been proposed (Mancheño et al. 2003) based on the structure of the tetrameric species and previous extensive biochemical data (de los Ríos et al. 1998; Anderluh and Macek 2002; Malovrh et al. 2003), in which these eukaryotic PFPs may form tetrameric toroidal pores with the N-terminal region adopting a helical conformation (Fig. 3.11c, f). The oligomeric assembly may interact with the membrane interface, with no protein segments spanning the hydrophobic core of the membrane.

3.4.4 Lipases

The lipolytic enzymes belong to a large family of enzymes that facilitate the degradation of lipids. Lipases and phospholipases are members of this family that have been investigated extensively (Rubin and Dennis 1997). Lipolytic enzymes are water-soluble enzymes that are characterized by their ability to hydrolize aggregated lipids with a much higher velocity than the same lipid in its monomolecular form. This rate enhancement at lipid–water interfaces is the central theme in the study of lipolysis and distinguishes lipases from all other kinds of water-soluble enzymes, which invariably act on monomolecularly dispersed substrates.

Lipases with known three-dimensional structures span a wide range of molecular weights from 19kDa (cutinase) to 60 kDa (*C. rugosa* lipase). All of them, with exception of pancreatic lipases, contain only one domain that contains the α/β-hydrolase fold (Ollis et al. 1992) made by a five-stranded β sheet and two α helices. The residues of the catalytic triad (serine, histidine and acid) are located at definite positions in this fold. A specific feature of lipases, when compared with other classical serine hydrolases, is that the catalytic site is inaccessible to substrate in solution. A structural basis for this inaccessibility was originally proposed for the lipase from *Rhizomucor miehei* (Brady et al. 1990; Brzozowski et al. 1991) (Fig. 3.14a). These studies have shown that in the former structure, the enzyme adopts an inactive closed conformation with a surface loop from the N-terminal domain (the flap) covering the active site, and that in the latter, lipase has an active open conformation resulting from the repositioning of the flap. The inner surface of the lid, which is exposed on opening, is sufficiently hydrophobic to facilitate association of the enzyme with a lipid interface. Thus the exposure of the catalytic residues is accompanied by a marked increase in the non-polarity of the surrounding surface, providing a plausible structural basis for the interaction of the lipase with triglyceride (TG) and diglyceride (DG) substrates.

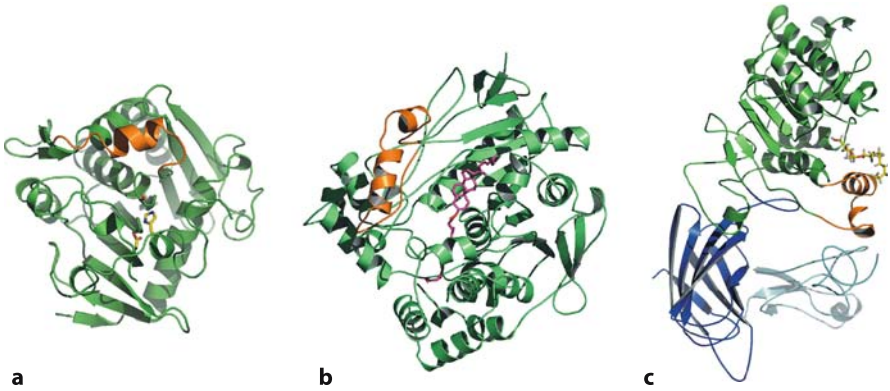

Fig. 3.14. Gallery of ribbon structures of members from the lipase family. (**a**) The crystal structure of *Rhizomucor miehei* lipase (PDB code 3TGL) showing the α/β hydrolase fold and the catalytic residues as sticks. (**b**) The *Candida rugosa* lipase in complex with cholesteryl linoleate (magenta) (PDB code 1CLE). (**c**) Crystal structure of the lipase–colipase complex (PDB code 1ETH) with the α/β hydrolase domain coloured in green, the C-terminal domain coloured in dark blue and the colipase cofactor coloured in cyan. The detergent mimicking the lipid at the active site is represented as sticks. In all cases the flap is coloured in orange. Figures were prepared with PyMOL

C. rugosa lipases show a substrate binding-site formed by an extensive hydrophobic pocket together with a narrow internal tunnel in which the substrate aliphatic chains are stabilized (Ghosh et al. 1995) (Fig. 3.14b). Recent studies (Mancheño et al. 2003) propose that residues situated in the hydrophobic pocket are partly responsible for the differences in substrate specificity observed between the several closely related extracellular lipases produced by the yeast *Candida rugosa*. Structural inspection of their hydrophobic substrate tunnel revealed two definite regions regarding their amino-acid composition, which suggests a correlation between the aromatic/aliphatic balance and the esterase/lipase character of the enzyme (Mancheño et al. 2003). Conversely, the structural variability in narrow regions exhibited in the *C. rugosa* lipases family may provide to this yeast the ability to metabolize a broad spectrum of substrates, justifying the presence of several closely related isoenzymes.

Pancreatic lipases exhibit a more complicated organization related to their physiological function in mammals. Crystal structures of the human pancreatic lipase have shown that the polypeptide chain is divided into two domains bearing specific functions. The N-terminal domain, which follows the α/β-hydrolase fold as other lipases, contains the catalytic triad and is responsible for triglyceride hydrolysis. The C-terminal domain displays a β-sandwich fold and is involved in binding a small protein, the colipase (molecular mass, 10 kDa), which counteract the inhibitory effect of bile salts in the intestine (Fig. 3.14c). Crystal-structure determination of the activated lipase–colipase–micelle complex (Hermoso et al. 1997), as determined using both high-resolution X-ray and low-resolution

neutron diffraction techniques, revealed that the disk-shaped micelle interacts extensively with the concave face of colipase and the distal tip of the C-terminal domain of lipase (Fig. 3.5b). This structure showed that the micelle- and substrate-binding sites concern different regions of the protein complex and revealed the residues involved in micelle interaction. Interestingly, in contrast with what is generally observed with membrane proteins, the protein surfaces involved in micelle binding are amphipathic without forming patches of either hydrophilic or hydrophobic amino-acid side-chains. Considering all these facts, the authors concluded that pancreatic lipase activation is not interfacial, as proposed for other lipases, but occurs in the aqueous phase and is mediated by the colipase and a bile salt micelle.

3.4.5 Hydrophobic Ligand-Binding Proteins

The considerable effort dedicated in recent years to the structural characterization at high resolution of a wide array of diverse proteins (both functionally and at the amino-acid sequence level) endowed with the ability to bind different types of hydrophobic ligands has revealed the existence of an underlying structural simplicity which in turn has permitted the definition of a reduced number of distinct protein families. Due to their biological relevance, we will briefly describe the major structural features of the following protein families, together with the main molecular details of the interactions established with their ligands: lipocalins and the intracellular lipid-binding proteins (iLBPs), which together with avidins form part of the structural superfamily of calycins (Flower 1996); serum albumin and finally, lipid-transfer proteins (LTPs), including non-specific LTPs from plants, and a survey of proteins from mammals that posses the so-called START domain, which are involved in numerous biological processes involving lipids (see below).

3.4.5.1 Lipocalins

The lipocalin protein family is a large group of small extracellular proteins which are characterized by common ligand-binding properties: they all bind small hydrophobic molecules (retinoids, arachidonic acid and steroids), specific cell-surface receptors and form complexes with soluble macromolecules (Flower 1996). The large degree of variation in amino-acid sequences found within the family may be consistent with the functional diversity found for these proteins. Thus, they participate in retinol transport, in invertebrate cryptic coloration, olfaction, and pheromone transport, prostaglandin synthesis, etc. (see Flower 1996, for a review).

Sequence comparison analyses have revealed the existence of three defining sequence motifs according to which two lipocalin subgroups can be identified: kernel and outlier lipocalins. Whereas kernel lipocalins share the three sequence

motifs, the more divergent and in fact minor subgroup of outlier lipocalins matches no more than two. Concerning this, more recently, a classification of lipocalins has been proposed based on the three-dimensional superposition of the β-barrel fold (see below; Skerra 2000). On the other hand, analysis of available crystal structures of lipocalins, among others, plasma retinol-binding protein (RBP) (Newcomer et al. 1984; Cowan et al. 1990), β-lactoglobulin (Papiz et al. 1986; Monaco et al. 1987; Brownlow et al. 1997), insecticyanin (Holden et al. 1987), a_{2u}-globulin (Böcskei et al. 1992; Chaudhuri et al. 1999), epididymal retinoic acid-binding protein (Newcomer 1993), and odorant-binding protein (Tegoni et al. 1996; Bianchet et al. 1996), shows a highly conserved calyx-shaped fold composed of an eight-stranded antiparallel β-barrel with an elliptical cross-section and an internal ligand-binding cavity (Fig. 3.15) (Skerra 2000). In addition to the barrel scaffold, other conserved structural elements are: a single-turn 3_{10} helix located in the N-terminal end, and a four-turn α-helix together with a small β-strand in the C-terminal end. The barrel topology is simple in that each successive strand is adjacent to the previous one, the last strand hydrogen bonding to the first one.

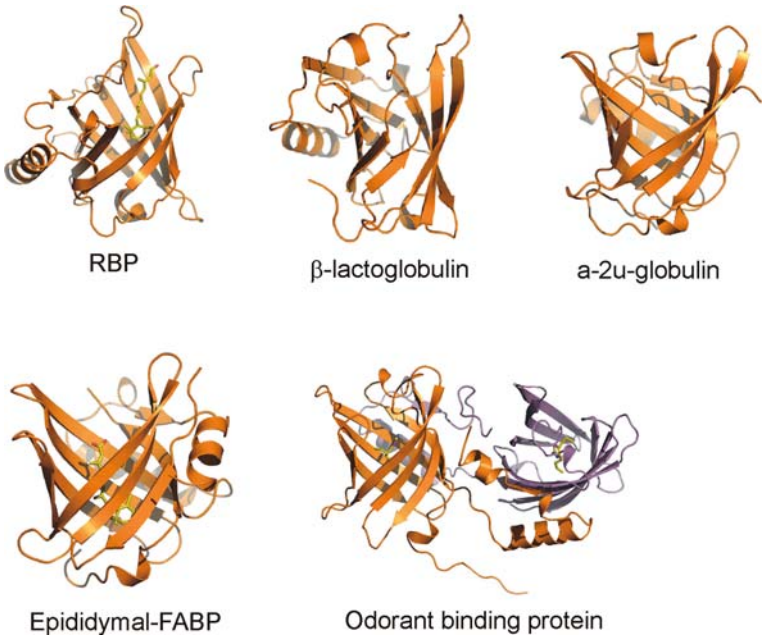

Fig. 3.15. Gallery of ribbon structures of members from the lipocalin family. The conserved calyx-shaped fold is composed of an eight-stranded antiparallel β-barrel with an internal ligand-binding cavity. PDB codes are: 1IIU for the plasma retinol-binding protein (RBP); 1BEB, for β-lactoglobulin; 2A2U, for a_{2u}-globulin; 1EPB, for epididymal fatty acid-binding protein; 1PBO, for the dimer of the odorant-binding protein. The retinol molecule bound to RBP, the retinoic acid bound to epididymal-FABP, and the hydrophobic ligand of the odorant-binding protein, appear as *stick* models. Figures were prepared with the program PyMOL

Whereas one end of the barrel, precisely that defining the base of the calyx, is capped by an amino-terminal sequence stretch and two short connecting loops (those between strands β2/β3 and β6/β7), the other end is open to the solvent, and conforms the entrance to the ligand-binding site. In this region, the unique longest connecting loop (loop between β1 and β2) acts as a lid which partially covers the ligand-binding site.

Lipocalins bind a great diversity of hydrophobic ligands: retinoids, pheromones, FAs, biliverdin, carotenoids, progesterone, prostaglandin H2, etc. (Flower 1996). In all structurally characterized cases, the ligand occupies the internal cavity of the barrel. For example, in the holo-RBP form, the β-ionone ring of the ligand is bound deepest in the barrel, the isoprene chain is fully extended, and the hydroxyl group reaches the protein surface (Zanotti et al. 1994). Comparison of this last structure with that of the apo-RBP reveal the existence of conformational changes mainly affecting the above-mentioned lid segment (Zanotti et al. 1993).

3.4.5.2 Intracellular Lipid-Binding Proteins

Since the description of the first cellular fatty acid-binding protein (FABP) (Ockner et al. 1972), different types of iLBPs have been reported from various organisms and tissues (Hanhoff et al. 2002; Zimmerman and Veerkamp 2002; Haunerland and Spener 2004). Although much effort has been spent in elucidating the specific roles of iLBPs, this issue has thus far not been fully explored. Accordingly, various functions have been proposed for iLBPs, including not only uptake and transport of FAs, but also regulation of gene expression and cell growth (Haunerland and Spener 2004). A remarkable feature of the iLBPs family is that despite the high degree of sequence diversity and ligand binding properties observed, they share a common three-dimensional fold (Fig. 3.16).

All iLBPs consist of a ten-stranded antiparallel β-barrel with an internal ligand-binding cavity lined by both polar and apolar residues together with tightly bound water molecules (Banaszak et al. 1994; Thompson et al. 1997). In addition, a helix-turn-helix motif, which covers the opening of the barrel, together with two connecting loops (those between strands βC and βD, and βE and βF), has been postulated to function as a lid or flap (Hanhoff et al. 2002). Generally, one or two basic residues located within the cavity are directly involved in ligand binding; conversely, the hydrocarbon tail of the ligand is lined on one side by hydrophobic side-chains and the other with ordered water molecules. Four major subfamilies have been considered within the iLBPs based on sequence homology and lipid binding properties (Haunerland and Spener 2004): subfamily I comprises proteins specific for vitamin A derivatives: cellular retinoic acid-binding proteins (CRABP-I and II), and the cellular retinol-binding proteins (CRBP-I, II, III and IV) (Ross 1993); subfamily II is composed of proteins with larger binding sites which can accommodate not only different FAs but also heme, bile acids and certain eicosanoids. Members from this subfamily are liver-FABP (L-FABP), intestinal bile acid-binding protein (I-BABP), and also the basic liver-type (Lb-FABP), which is the only iLBP that is not expressed in mammals; it is found in

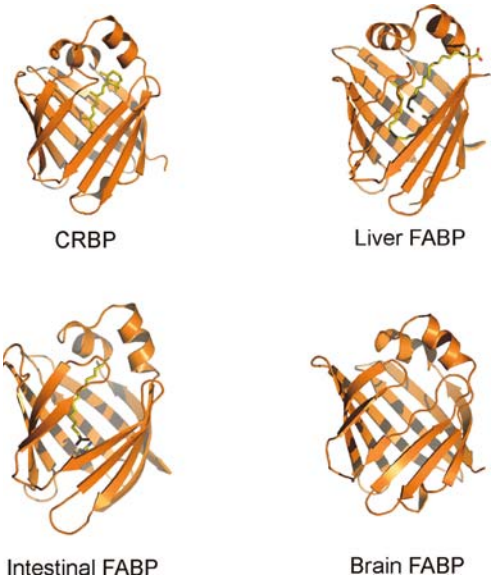

Fig. 3.16. Structures of some members of the intracellular lipid-binding proteins. iLBPs consist of a ten-stranded antiparallel β-barrel with an internal ligand-binding cavity. PDB codes are: 1CRB for the complex between the cellular retinol-binding protein and retinol; 1LFO, for liver FABP complexed with two molecules of oleate; 1ICM, intestinal FABP with bound myristate, and 1FDQ for brain FABP. Bound ligands appear as *stick* models. Figures were prepared with the program PyMOL

the liver of birds, fishes, reptiles and amphibians (Di Pietro et al. 1999). It is remarkable that L-FABP is the only FABP that forms a ternary complex with two fatty acid molecules (Thompson et al. 1997). The only member of the subfamily III is the intestinal type FABP (I-FABP). This protein is rather peculiar in both sequence and ligand binding properties. In this sense, the bound FA adopts a bent conformation, with the carboxylate moiety located deep inside the barrel cavity, interacting with an arginine residue (Sacchettini et al. 1992). Finally, subfamily IV includes among others, FABPs from heart (H-FABP) (Lassen et al. 1995), adipocyte (A-FABP) (Ringom et al. 2004), epidermal (E-FABP) (Hohoff et al. 1999), myelin (M-FABP), testis (T-FABP) and brain (B-FABP) (Balendiran et al. 2000). These last proteins, which have an extra 3_{10}-helical loop in the N-terminal end when compared to the iLBPs, are characterized because the acyl chain of the ligand adopts a U-shape conformation.

3.4.5.3 Serum Albumin

Without doubt, one of the most extensively studied proteins is serum albumin. Recent high-resolution crystallographic studies of human serum albumin (HSA) complexed with different FAs (Curry et al. 1998; Bhattacharya et al. 2000; Petitpas et al. 2001) have permitted the analysis of the molecular details of the interactions involved. The protein is heart-shaped, with a high helical content (67%) and consists of three repeating domains, each one composed of 10 α-helices, which can be further divided into two subdomains (Fig. 3.17).

Despite the capability of tight binding, FA ligands rapidly exchange between aqueous solution and the different and asymmetrically distributed FA-binding sites. The above studies reveal that, although structurally heterogeneous, the seven key FA-binding sites share common structural features: they are hydrophobic cavities that accommodate the methylene tail of the FA molecule, which are invariably capped by two or three solvent-exposed basic (Arg, Lys) or polar (Tyr, Ser) side-chains, which directly interact with the anionic carboxyl group of the FA. Although binding sites are compact they can accommodate either saturated (Curry et al. 1998; Bhattacharya et al. 2000) or unsaturated FAs (Petitpas et al. 2001). In this sense, although stearic (C18:0) and oleic (C18:1) bound to the same sites essentially adopt the same conformation, the presence of multiple *cis* double bonds in arachidonic acid (C20:4) induces dissimilar conformations at some sites, what may account for differences in binding affinities towards polyunsaturated and saturated or monunsaturated FAs (Petitpas et al. 2001).

3.4.5.4 Lipid-Transfer Proteins

Lipid-transfer proteins (LTPs) facilitate the transfer of lipids between membranes. They are widely distributed, being produced by both prokaryotic and eukaryotic organisms: bacteria, yeasts, plants and animals (Rueckert and Schmidt 1990). LTPs cover a wide spectrum of ligand specificities: FAs, phospholipids, glycolipids, steroids, acyl-CoA, etc.; in this regard, it must be remarked that whereas some LTPs are highly specific (Roderick et al. 2002), others are non-specific (Tsujishita and Hurley 2000; Han et al. 2001). Nowadays, numerous LTPs have been characterized at high resolution, both from plants: wheat (Charvolin et al. 1999), maize (Shin et al. 1995; Han et al. 2001) and rice (Lee et al. 1998; Cheng et al. 2004); and from animals: rabbit (Choinowski et al. 2000), mouse (Romanowski et al. 2002), human (Tsujishita and Hurley 2000; Roderick et al. 2002).

Non-specific LTPs (ns-LTPs) from plants are small (~9 kDa), disulfide-rich, basic proteins, which show no sequence homology with mammalian ns-LTP. Both

Serum albumin

Fig. 3.17. Ribbon representation of serum albumin (PDB code: 1GNI). Seven oleic acid molecules are also shown as *stick* models. Figures were prepared with the program PyMOL

high-resolution crystallographic and NMR studies have revealed that plant ns-LTPs are single-domain proteins, composed of four α-helices and four disulfides and a long C-terminal loop (Fig. 3.18).

Interestingly, this fold was first described for a hydrophobic protein from soybean (Baud et al. 1993). A remarkable structural feature is the presence of a hydrophobic tunnel which is large enough to accommodate a long fatty acyl chain. In this regard, the crystal structures of ns-LTP from maize complexed with palmitate (Shin et al. 1995), and wheat ns-LTP complexed with lyso-myristoyl-phosphatidylcholine (Charvolin et al. 1999) (Figs. 3.18B and a) show that the hydrocarbon chain of the ligand is deeply inserted into the protein cavity and the polar head group is exposed on the protein surface. Nevertheless, the scenario of ligand-binding to the hydrophobic cavity is more complex as NMR results indicate that the existence of the same ligand adopting different orientations is possible (Lerche et al. 1998). Moreover, the solution structure of the ns-LTP from wheat in complex with prostaglandin B2 shows that the ligand is fully buried into the protein (Tassin-Moindrot et al. 2000).

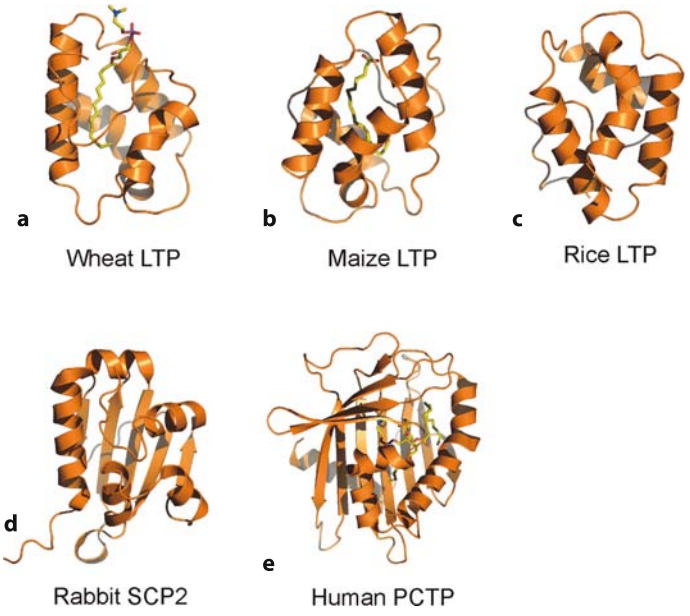

Fig. 3.18. Schematic representation of members of the diverse family of lipid-transfer proteins (LTPs). Non-specific LTPs from plants are composed of four α-helices and four disulfides, and a long C-terminal loop. PDB codes: (**a**) 1BWO for wheat ns-LTP complexed with two phospholipid molecules; (**b**) 1FK4, for ns-LTP from maize with stearate bound; (**c**) 1RZL, for ns-LTP from rice. (**d**) The ribbon representation of the ns-LTP sterol-carrier protein 2 from rabbit (PDB code: 1C44), and (**e**) that of the human phosphatidylcholine (PC) transfer protein complexed with two PC molecules (PDB code: 1LN1) are also shown. Figures were prepared with the program PyMOL

The crystal structure of the intracellular ns-LTP from rabbit sterol carrier protein 2 (SCP2) has been solved at 1.8 Å resolution (Choinowski et al. 2000) (Fig. 3.18d). Despite SCP2 having been shown to participate in diverse in vitro functions, which permit defining SCP2 either as a LTP or as a carrier for FAs, fatty acid-CoAs, or sterols such as cholesterol, neither the actual physiological role(s) nor the mechanism of action of SCP2 is yet known. SCP2 is a small (13 kDa), basic protein, highly conserved in different species. It is remarkable that various intracellular proteins, such as peroxisomal D-hydroxyacyl-CoA dehydrogenase and the *Caenorhabditis elegans* behavioural protein, posses a C-terminal SCP2 domain which would act as a putative lipid-binding domain. SCP2 is composed of a five-stranded β-sheet, which can be divided in two minor antiparallel sheets: strands I–III and IV–V, respectively (Fig. 3.18d). Whereas one side of the sheet is predominantly hydrophobic, the other is highly polar. In addition, this central β-sheet is flanked by five α-helices (Choinowski et al. 2000), the longest one (helix A) being clearly amphipathic with its apolar side packed against the hydrophobic side of the central β-sheet. Functionally, the most remarkable feature of SCP2 is the presence of a hydrophobic tunnel, which may provide a binding site for apolar ligands. Although there is neither sequence homology, nor three-dimensional resemblances between plant nsLTPs (see above) and SCP2, in both cases the hydrophobic tunnel observed has similar dimensions.

A wide diversity of proteins involved in lipid transport and metabolism, signal transduction, and transcriptional regulation possess the so-called START domains (after steroidogenic acute regulatory protein lipid transfer) (Tsujishima and Hurley 2000). In this context, the crystal structure of the START domains from human MLN64 (Tsujishima and Hurley 2000), from mouse cholesterol-regulated protein 4 (Romanowski et al. 2002), and from human phosphatidylcholine transfer protein (PC-TP) (Roderick et al. 2002) have been solved at high resolution. The overall structure of the START domain in all cases is highly conserved: it consists of a curved antiparallel nine-stranded U-shaped β-sheet, flanked by four α-helices (Fig. 3.18e). The N-terminal helix rests against one side of the sheet. As described above for SCP2, the most striking feature is the presence of a hydrophobic tunnel extending nearly the entire length of the protein. The structures of the complexes between PC-TP and dilinoleoyl-PC (DLPC) and PC-TP and palmitoyl-linoleoyl-PC (PLPC) have revealed the molecular details of the embedded ligand, which in turn explains the exquisite specificity of PC-TP for this kind of lipid (Roderick et al. 2002). The acyl chains of both lipids adopt similar C-shaped conformations and establish numerous hydrophobic contacts both with aliphatic and aromatic side-chains. Additionally, the phosphorylcholine headgroup of the ligand interacts with hydrophilic side-chains; in particular the phosphoryl group interacts with Arg 78 which in turn forms a salt bridge with Asp 82, this motif Arg-Asp being conserved in the sequence of many START proteins (Tsujishima and Hurley 2000). Conversely, the quaternary amine of the lipid mainly interacts with aromatic side-chains through cation-π interactions (Burley and Petsko 1985; Gallivan and Dougherty 1999). This type of interaction has been observed in numerous substrate-binding pockets of diverse enzymes (Bellamy et al. 1989; Sussman et al. 1991), as well as in pore-forming toxins (Mancheño et al. 2003).

3.5 Conclusions and Future Prospects

Knowledge of the precise three-dimensional structure of proteins is a requirement for understanding how they work. Nowadays, high-resolution structures of macromolecules can be readily determined by using X-ray crystallography and nuclear magnetic resonance (NMR). However, despite the huge amount of structural information obtained for soluble proteins, only the structures of a few membrane proteins are available. The reasons for their scarcity are mainly derived from their low solubility and stability outside their natural environment. Thus the difficulties to overproduce, to stabilize and to crystallize membrane proteins become bottlenecks that are, in most cases, intractable. Precisely these facts have prompted the development of new imaginative experimental approaches, some of them reviewed herein.

Despite the technical limitations previously mentioned, nowadays general principles governing the mechanisms of protein–lipid interactions can be envisaged from current structural knowledge. In this regard, the high-resolution structures of numerous proteins whose molecular mechanisms involve the interaction with lipids has been reported: integral membrane proteins, peripheral proteins involved in signal transduction, pore-forming toxins, lipases, hydrophobic ligand-binding proteins, lipocalins, intracellular lipid-binding proteins, serum albumin and lipid transfer proteins. The intrinsic low solubility of lipids and their protein-interacting counterpart necessitates the existence of regulation mechanisms to avoid unspecific and undesired processes. Thus, the existence of controlled large-scale conformational changes is observed in the mechanism of pore-forming toxins and lipases, and the design of hydrophobic environments, such as the cavities is present in several families of lipid-interacting proteins like lipocalins and other lipid-binding proteins. The structural diversity observed in the large families of lipid-interacting proteins lead to the conclusion that there is not a unique protein fold related to lipid interaction. The constraints imposed by the above-mentioned general principles are thus fulfilled by a large number of different structural motifs.

Current developments in the production of high-quality crystals and in the synchrotron radiation facilities and also in the biophysical characterization of lipidic systems, will provide us, in the near future, with a more accurate scenario of the lipid–protein interaction, particularly the molecular mechanism occurring in biological membranes.

References

Alegre-Cebolleda J (2004) Phenotypic selection and characterization of randomly produced non-haemolytic mutants of the toxic sea anemone protein sticholysin II. FEBS Lett 575:14–18

Allured VS, Collier RJ, Carroll SF, McKay DB (1986) Structure of exotoxin A of Pseudomonas aeruginosa at 3.0 Å resolution. Proc Natl Acad Sci USA 83:1310–1324

Anderluh G, Macek P (2002) Cytolytic peptide and protein toxins from sea anemones (Anthozoa: Actiniaria). Toxicon 40:111–124

Anthanasiadis A, Anderluh G, Macek P, Turk D (2001) Crystal structure of the soluble form of equinatoxin II, a pore-forming toxin from the sea anemone Actinia equina. Structure 9:341–346

Balendiran GK, Schnutgen F, Scapin G, Borchers T, Xhong N, Lim K, Godbout R, Spener F, Sacchettini JC (2000) Crystal structure and thermodynamic analysis of human brain fatty acid-binding protein. J Biol Chem 275:27045–27054

Banaszak L, Winter N, Xu Z, Bernlohr DA, Cowan S, Jones TA (1994) Lipid-binding proteins: a family of fatty acid and retinoid transport proteins. Adv Prot Chem 45:89–151

Baraldi E, Djinovic Carugo K, Hyvönen M, Lo Surdo P, Riley AM, Potter BV, O'Brien R, Ladbury JE, Saraste M (1999) Structure of the PH domain from Bruton's tyrosine kinase in complex with inositol 1,3,4,5-tetrakisphosphate. Structure 7:449–460

Baud F, Pebay-Peyroula E, Cohen-Addad C, Odani S, Lehmann MS (1993) Crystal structure of hydrophobic protein from soybean; a member of a new cysteine-rich family. J Mol Biol 231:877–887

Bellamy HD, Lim LW, Mathews FS, Dunham WR (1989) Studies of crystalline trimethylamine dehydrogenase in three oxidation states and in the presence of substrate and inhibitor. J Biol Chem 264:11887–11892

Belrhali H, Nollert P, Royant A, Menzel C, Rosenbusch JP, Landau EM, Pebay-Peyroula E (1999) Protein, lipid and water organization in bacteriorhodopsin crystals: a molecular view of the purple membrane at 1.9 Å. Structure 7:909–917

Bhattacharya AA, Grune T, Curry S (2000) Crystallographic analysis reveals common modes of binding of medium and long-chain fatty acids to human serum albumin. J Mol Biol 303:721–732

Bianchet MA, Bains G, Pelosi P, Pevsner J, Snyder SH, Monaco HL, Amzel LM (1996) The three-dimensional structure of bovine odorant binding protein and its mechanism of odor recognition. Nat Struct Biol 3:934–939

Bittova L, Stahelin RV, Cho W (2001) Roles of ionic residues of the C1 domain in protein kinase C-alpha activation and the origin of phosphatidylserine specificity. J Biol Chem 276:4218–26

Böcskei Z, Groom CR, Flower DR, Wright CE, Phillips SE, Cavaggioni A, Findlay JB, North AC (1992) Pheromone binding to two rodent urinary proteins revealed by X-ray crystallography. Nature 360:186–188

Bogdanov M, Dowhan W (1999) Lipid-assisted protein folding. J Biol Chem 274:36827–36830

Bowie JU (2001) Stabilizing membrane proteins. Curr Opin Struct Biol 11:397–402

Brady L, Brzozowski AM, Derewenda ZS, Dodson E, Dodson G, Tolley S, Turkenburg JP, Christiansen L, Hugejensen B, Norskov L, Thim L, Menge U (1990) A serine protease triad forms the catalytic center of a triacylglycerol lipase. Nature 343:767–770

Brownlow S, Morais Cabral JH, Cooper R, Flower DR, Yewdall SJ, Polikarpov I, North AC, Sawyer L (1997) Bovine beta-lactoglobulin at 1.8 Å resolution – still an enigmatic lipocalin. Structure 5:481–95

Brzozowski AM, Derewenda U, Derewenda ZS, Dodson GG, Lawson DM, Turkenburg JP, Bjorkling F, Hugejensen B, Patkar SA, Thim L (1991) A model for interfacial activation in lipases from the structure of a fungal lipase-inhibitor complex. Nature 351:491–494

Buchanan S, Smith BS, Venkatramani L, Xia D, Esser L, Palnitkar M, Chakraborty R, van der Helm D, Deisenhofer J (1999) Crystal structure of the outer membrane active transporter FepA from Escherichia coli. Nat Struct Biol 6:56–63

Burley SK, Petsko GA (1985) Aromatic–aromatic interaction: a mechanism of protein structure stabilization. Science 229:23–28

Byrne B, Iwata S (2002) Membrane protein complexes. Curr Opin Struc Biol 12:239–243

Charvolin D, Douliez JP, Marion D, Cohen-Addad C, Pebay-Peyroula E (1999) The crystal structure of a wheat nonspecific lipid transfer protein (ns-LTP1) complexed with two molecules of phospholipid at 2.1 Å resolution. Eur J Biochem 264:562–568

Chaudhuri BN, Kleywegt GJ, Bjorkman J, Lehman-McKeeman LD, Oliver JD, Jones TA (1999) The structures of alpha 2u-globulin and its complex with a hyaline droplet inducer. Acta Crystallogr D 55:753–762

Chayen NE (2004) Turning protein crystallisation from an art into a science. Curr Opin Struct Biol 14:577–583

Cheng HC, Cheng PT, Peng P, Lyu PC, Sun YJ (2004) Lipid binding in rice nonspecific lipid transfer protein-1 complexes from Oryza sativa. Prot Sci 13:2304–2315

Cherezov V, Avinash P, Muthusubramaniam L, Zheng YF, Caffrey M (2004) A robotic system for crystallizing membrane and soluble proteins in lipidic mesophases. Acta Cryst D60:1795:1807

Chiu M, Nollert P, Loewen M, Belrhali H, Pebay-Peyroula E, Rosenbusch JP, Landau EM (2000) Crystallization in lipidic cubic phases: General applicability to membrane proteins. Acta crystallogr D56:781–784

Cho W (2001) Membrane targeting by C1 and C2 domains. J Biol Chem 276:32407–32410

Choe S, Bennett MJ, Fujii G, Curmi PM, Kantardjieff KA, Collier RJ, Eisenberg D (1992) The crystal structure of diphtheria toxin. Nature 357:216–222

Choinowski T, Hauser H, Piontek K (2000) Structure of sterol carrier protein 2 at 1.8 Å resolution reveals a hydrophobic tunnel suitable for lipid binding. Biochemistry 39:1897–1902

Cole AR, Gibert M, Popoff M , Moss DS, Titball RW, Basak AJ (2004) Clostridium perfringens -toxin shows structural similarity to the pore-forming toxin aerolysin. Nat Struct Molec Biol 11:797–798

Cowan SW, Newcomer ME, Jones TA (1990) Crystallographic refinement of human serum retinol binding protein at 2 Å resolution. Proteins: Struct Funct Genet 8:44–61

Cowan SW, Schirmer T, Rummel G, Steiert M, Ghosh R, Pauptit RA, Jansonius JN, Rosenbusch JP (1992) Crystal structures explain functional properties of two E. coli porins. Nature 358:727–733

Curry S, Mandelkow H, Brick P, Franks N (1998) Crystal structure of human serum albumin complexed with fatty acid reveals an asymmetric distribution of binding sites. Nat Struct Biol 5:827–835

Dahout-Gonzalez C, Brandolin G, Pebay-Peyroula E (2003) Crystallization of the bovine ADP/ATP carrier is critically dependent upon detergent-to-protein ratio. Acta Cryst D59:2353–2355

Deisenhofer J, Epp O, Miki K, Huber R, Michel H (1985) Structure of the protein subunits in the photosynthetic reaction centre of Rhodopseudomonas viridis at 3 Å resolution. Nature 318:618–624

De los Ríos V, Mancheño JM, Lanio ME, Oñaderra M, Gavilanes JG (1998) Mechanism of the leakage induced on lipid model membranes by the haemolytic protein sticholysin II from the sea anemone Stichodactyla helianthus. Eur J Biochem 252:284–289

Di Pietro SM, Veerkamp JH, Santome JA (1999) Isolation, amino acid sequence determination and binding properties of two fatty-acid-binding proteins from axolotl (Ambistoma mexicanum) liver. Evolutionary relationship. Eur J Biochem 259:127–134

Elkins P, Bunker A, Cramer WA, Stauffacher CV (1997) A mechanism for toxin insertion into membranes is suggested by the crystal structure of the channel-forming domain of colicin E1. Structure 5:443–448

Eroglu C, Cronet P, Panneels V, Beaufils P, Sinning I (2002) Functional reconstitution of purified metabotropic glutamate receptor expressed in the fly eye. EMBO Reports 3:491–496

Eroglu C, Brügger B, Wieland F, Sinning I (2003) Glutamate-binding affinity of Drosophila metabotropic glutamate receptor is modulated by association with lipid rafts. Proc Natl Acad Sci USA, 100:10219–10224

Ferguson KM, Lemmon MA, Schlessinger J, Sigler PB (1995) Structure of the high affinity complex of inositol trisphosphate with a phospholipase C pleckstrin homology domain. Cell 83:1037–1046

Ferguson AD, Hofmann E, Coulton JW, Diedrichs K, Welte W (1998) Siderophore-mediated iron transport. Science 282:2215–2220

Flower, DR (1996) The lipocalin protein family: structure and function. Biochem J 318:1–14

Gallivan JP, Dougherty DA (1999) Cation- interactions in structural biology. Proc Nat Acad Sci USA 96:9459–9464

Garavito RM, Ferguson-Miller S (2001) Detergents as tools in membrane biochemistry. J Biol Chem 276:32403–32406

Gewold J (2002) Plant scientists see big potential in tiny plastids. Science 295:258–259

Ghosh D, Wawrzak Z, Pletnev VZ, Li N, Kaiser R, Pangborn W, Jörnvall H, Erman M, Duax WL (1995) Structure uncomplexed and linoleate-bound Candida cylindracea cholesterol esterase. Structure 3:279–288

Gohon Y, Popot JL (2003) Membrane protein–surfactant complexes. Curr Opin Colloid Interface Sci 8:15–22

Gordelyi VI, Labahn J, Moukhametzianov R, Efremov R, Granzin J, Schlesinger R, Büldt G, Savopol T, Scheidig AJ, Klare JP, Engelhard M (2002) Molecular basis of transmembrane signalling by sensory rhodopsin II-transducer complex. Nature 419:484–487

Gouaux E (1997) Channel-forming toxins: tales of transformation. Curr Opin Struct Biol 7:566–573

Gouaux E, White SH (2003) Proteins and membranes – a fusion of new ideas. Curr Opin Struct Biol 13:401–403

Grigorieff N, Ceska TA, Downing KH, Baldwin JM, Henderson R (1996) Electron-crystallographic refinement of the structure of bacteriorhodopsin. J Mol Biol 259:393–421

Grobler JA, Essen L-O, Williams RL, Hurley JH (1996) C2 domain conformational changes in phospholipase Cδ1. Nat Struc Biol 3:788–795

Grochulski P, Masson L, Borisova S, Pusztai-Carey M, Schwartz JL, Brousseau R, Cygler M (1995) Bacillus thuringiensis CryIA(a) insecticidal toxin: crystal structure and channel formation. J Mol Biol 254:447–464

Han GW, Lee JY, Song HK, Chang C, Min K, Moon J, Shin DH, Kopka ML, Sawaya MR, Yuan HS, Kim TD, Choe J, Lim D, Moon HJ, Suh SW (2001) Structural basis of non-specific lipid binding in maize lipid-transfer protein complexes revealed by high-resolution X-ray crystallography. J Mol Biol 308:263–278

Hanhoff T, Lücke Ch, Spener F (2002) Insights into binding of fatty acids by fatty acid binding proteins. Mol Cell Biochem 239:45–54

Haunerland NH, Spener F (2004) Fatty acid-binding proteins – insights from genetic manipulations. Prog Lipid Res 43:328–349

Hermoso J, Pignol D, Penel S, Roth M, Chapus C, Fontecilla-Camps JC (1997) Neutron crystallographic evidence of lipase/colipase complex activation by a micelle. EMBO J 18:5531–5536

Heuck AP, Tweten RK, Johnson AE (2001) -barrel pore-forming toxins: intriguing dimorphic proteins. Biochemistry 40:9065–9073

Heymann JB, Zakharov SD, Zhang YL, Cramer WA (1996) Characterization of electrostatic and nonelectrostatic components of protein–membrane binding interactions. Biochemistry 35:2717–2725

Hohoff C, Borchers T, Rustow B, Spener F, van Tilbeurgh H (1999) Expression, purification, and crystal structure determination of recombinant human epidermal-type fatty acid binding protein. Biochemistry 38:12229–12239

Holden HM, Rypniewski WR, Law JH, Rayment I (1987) The molecular structure of insecticyanin from the tobacco hornworm Manduca sexta L. at 2.6 Å resolution. EMBO J 6:1565–1570

Hommel U, Zurini M, Luyten M (1994) Solution structure of a cysteine-rich domain of rat protein kinase C. Nat Struct Biol 1:383–387

Hong Q, Gutiérrez-Aguirre I, Barlic A, Malovrh P, Kristan K, Podlesek Z, Macek P, Turk D, González-Mañas JM, Lakey JH, Anderluh, G (2002) Two-step membrane binding by Equinatoxin II, a pore-forming toxin from the sea anemone, involves an exposed aromatic cluster and a flexible helix. J Biol Chem 277:41916–41924

Hunte C, Kannt A (2003) Antibody fragment mediated crystallization of membrane proteins. In: Hunte C, Schägger H, von Jagow G (eds) Membrane protein purification and crystallization, 2nd edn. Academic Press/Elsevier Science, San Diego, p 143–160

Hunte C, Michel H (2003) Membrane protein crystallization. In: Hunte C, Schägger H, von Jagow G (eds) Membrane protein purification and crystallization, 2nd edn. Academic Press/Elsevier Science, San Diego, p 205–218

Hurley JH, Misra S (2000) Signalling and subcellular targeting by membrane-binding domains. Annu Rev Biophys Biomol Struct Biol 29:49–79

Hurley JH, Newton AC, Parker PJ, Blumberg PM, Nishizuka Y (1997) Taxonomy and function of C1 protein kinase C homology domains. Protein Sci 6:477–80

Jormakka M, Törnroth S, Byrne B, Iwata S (2002) Molecular basis of proton motive force generation: structure of formate dehydrogenase-N. Science 295:1863–1868

Katona K, Andreasson U, Landau EM, Andreasson L-K, Neutze R (2003) Lipidic cubic phase crystal structure of the photosynthetic reaction centre from Rhodobacter sphaeroides at 2.35 Å resolution. J Mol Biol 331:681–692

Killian JA, von Heijne G (2000) How proteins adapt to a membrane–water interface. Trends Biochem Sci 25:429–434

Kolbe M, Besir H, Essen L-O, Oesterhelt D (2000) Structure of the light-driven chloride pump halorhodospin at 1.8 Å resolution. Science 288:1390–1396

Landau EM, Rosenbusch JP (1996) Lipidic cubic phases: A novel concept for the crystallization of membrane proteins. Proc Natl Acad Sci USA 93:14532–14535

Lassen D, Lucke C, Kveder M, Mesgarzadeh A, Schmidt JM, Specht B, Lezius A, Spener F, Ruterjans H (1995) Three-dimensional structure of bovine heart fatty-acid-binding protein with bound palmitic acid, determined by multidimensional NMR spectroscopy. Eur J Biochem 230:266–280

Lee JY, Min K, Cha H, Shin DH, Hwang KY, Suh SW (1998) Rice non-specific lipid transfer protein: the 1.6 Å crystal structure in the unliganded state reveals a small hydrophobic cavity. J Mol Biol 276:437–448

Lemmon MA, Falasca M, Ferguson KM, Schlessinger J (1997) Regulatory recruitment of signalling molecules to the cell membrane by pleckstrin-homology domains. Trends Cell Biol 7:237–242

Lerche MH, Poulsen F (1998) Solution structure of barley lipid transfer protein complexed with palmitate. Two different binding modes of palmitate in the homologous maize and barley nonspecific lipid transfer proteins. Protein Sci 7:2490–2498

Lemieux MJ, Song J, Kim MJ, Huang Y, Villa A, Auer M, Li X-D, Wang D-N (2003) Three-dimensional crystallization of the Escherichia coli glycerol-3-phosphate transporter: a member of the major facilitator superfamily. Protein science 12:2748–2756

Li J, Carroll J, Ellar DJ (1991) Crystal structure of insecticidal δ-endotoxin from Bacillus thuringiensis at 2.5 Å resolution. Nature 353:815–821

Li J, Koni PA, Ellar DJ (1996) Structure of the mosquitocidal δ-endotoxin CytB from Bacillus thuringiensis sp. kyushuensis and implications for membrane pore formation. J Mol Biol 257:129–152

Locher KP, Rees B, Koebnik R, Mitschler A, Moulinier L, Rosenbusch JP, Moras D (1998) Transmembrane signaling across the ligand-gated FhuA receptor: crystal structures of free and ferrichrome-bound states reveal allosteric changes. Cell 11:771–778

Lowe ME (2002) The triglyceride lipases of the pancreas. J Lip Res 43:2007–2016

Luecke H, Schobert B, Richter H-T, Cartailler J-P, Lanyi JK (1999) Structure of bacteriorhodopsin at 1.55 Å resolution. J Mol Biol 291:899–911

Luft JR, Collins RJ, Fehrman NA, Lauricella AM, Veatch CK, DeTitta GT (2003) A deliberate approach to screening for initial crystallization conditions of biological macromolecules. J Struct Biol 142:170–179

McAuley KE, Fyfe PK, Ridge JP, Isaacs NW, Cogdell RJ, Jones MR (1999) Structural details of an interaction between cardiolipin and an integral membrane protein. Proc Natl Acad Sci USA 96:14706–14711

Malovrh P, Viero G, Serra MD, Podlesek Z, Lakey JH, Macek P, Menestrina G, Anderluh G (2003) A novel mechanism of pore formation: membrane penetration by the N-terminal amphipathic region of equinatoxin. J Biol Chem 278:22678–22685

Mancheño JM, Martín-Benito J, Martínez-Ripoll M, Gavilanes JG, Hermoso JA (2003) Crystal and electron microscopy structures of sticholysin II actinoporin reveal insights into the mechanism of membrane pore formation. Structure 11:1319–1328

Mancheño JM, Pernas MA, Rúa ML, Hermoso JA (2003) Structural insights into the lipase/esterase behavior in the Candida rugosa lipase family: crystal structure of the lipase 2 isoenzyme at 1.97 Å resolution. J Mol Biol 332:1059–1069

Mancheño JM, Tateno H, Goldstein IJ, Martínez-Ripoll M, Hermoso JA (2005) Structural analysis of the Laetiporus sulphureus hemolytic pore-forming lectin in complex with sugars. J Biol Chem (in press) 280:17251–17259

Mann RK, Beachy PA (2004) Novel lipid modifications of secreted protein signals. Annu Rev Biochem 73:891–923

Marsh D (1993) New comprehensive biochemistry: protein–lipid interactions. Elsevier, Amsterdam

Martín-Benito J, Gavilanes F, de los Ríos V, Mancheño JM, Fernández JJ, Gavilanes JG (2000) Two-dimensional crystallization on lipid monolayers and three-dimensional structure

of sticholysin II, a cytolysin from the sea anemone Stichodactyla helianthus. Biophys J 78:3186–3194

Michel H (1983) Crystallization of membrane proteins. Trends Biochem Sci 8:56–59

Misra S, Hurley JH (1999) Crystal structure of a phosphatidylinositol 3-phosphate-specific membrane targeting motif, the FYVE domain of Vps27p. Cell 97:657–666

Monaco HL, Zanotti G, Spadon P, Bolognesi M, Sawyer L, Eliopoulos EE (1987) Crystal structure of the trigonal form of bovine beta-lactoglobulin and of its complex with retinol at 2.5 Å resolution. J Mol Biol 197:695–706

Montoya M, Gouaux E (2003) β-barrel membrane protein folding and structure viewed through the lens of α-hemolysin. Biochim Biophys Acta 1609:19–27

Mosior M, Newton AC (1996) Calcium-independent binding to interfacial phorbol esters causes protein kinase C to associate with membranes in the absence of acidic lipids. Biochemistry 35:1612–1623

Muga A, González-Mañas JM, Lakey JH, Pattus FP, Surewicz WK (1993) pH-dependent stability and membrane interaction of the pore-forming domain of colicin A. J Biol Chem 268:1553–1557

Nalefski EA, McDonagh T, Somers W, Seehra J, Falke JJ, Clark JD (1998) Independent folding and ligand specificity of the C2 calcium-dependent lipid binding domain of cytosolic phospholipase A2. J Biol Chem 273:1365–1372

Newcomer ME (1993) Structure of the epididymal retinoic acid binding protein at 2.1 Å resolution. Structure 1:7–18

Newcomer ME, Jones TA, Aqvist J, Sundelin J, Eriksson U, Rask L Peterson PA (1984) The three-dimensional structure of retinol-binding protein. EMBO J 3:1451–1454

Nishizuka Y (1988) The molecular heterogeneity of protein kinase C and its implications for cellular regulation. Nature 334:661–665

Nollert P, Qiu M, Caffrey M, Rosenbusch JP, Landau EM (2001) Molecular mechanism for the crystallization of bacteriorhodopsin in lipidic cubic phases. FEBS Lett 504:179–186

Ockner RK, Manning JA, Poppenhausen RB, Ho WK (1972) A binding protein for fatty acids in cytosol of intestinal mucosa, liver, myocardium, and other tissues. Science 177:56–58

Ollis DL, Cheah E, Cygler M, Dijkstra B, Frolow F, Franken SM, Harel M, Remington SJ, Silman I, Schrag J, Sussman JL, Verschueren KHG, Goldman A (1992) The alpha/beta hydrolase fold. Protein Eng 5, 197–211

Olson R, Nariya H, Yokota K, Kamio Y, Gouaux E (1999) Crystal structure of staphylococcal LukF delineates conformational changes accompanying formation of a transmembrane channel. Nature Struct Biol 6:134–140

Ostermeier C, Michel H (1997) Crystallization of membrane proteins. Curr Opin Struct Biol 7:697–701

Papiz MZ, Sawyer L, Eliopoulos EE, North AC, Findlay JB, Sivaprasadarao R, Jones TA, Newcomer ME, Kraulis PJ (1986) The structure of beta-lactoglobulin and its similarity to plasma retinol-binding protein. Nature 324:383–385

Parker MW, Feil SC (2005) Pore-forming protein toxins: from structure to function. Prog Biophys Mol Biol 88:91–142

Parker MW, Tucker AD, Tsernoglou D, Pattus F (1990) Insights into membrane insertion based on studies of colicins. Trends Biochem Sci 15:126–129

Parker MW, Buckley JT, Postma JP, Tucker AD, Leonard K, Pattus F, Tsernoglou D (1994) Structure of the Aeromonas toxin proaerolysin and the membrane-channel states. Nature 367:292–295

Parker MW, Postma JP, Pattus F, Tucker AD, Tsernoglou D (1996) Refined structure of the pore-forming domain of colicin A at 2.4 Å resolution. J Mol Biol 224:639–657

Pebay-Peyroula E, Garavito M, Rosenbusch JP, Zulauf M, Timmins PA(1995) Detergent structure in tetragonal crystals of porin from the outer membrane of E. coli. Structure 3:1051–1059

Pebay-Peyroula E, Rummel G, Rosenbusch JP, Landau EM (1997) High resolution X-ray structure of bacteriorhodopsin from microcrystals grown in lipidic cubic phases. Science 277:1676–1681

Pebay-Peyroula E, Myles D (2000) Neutron crystallography of biological molecules. In: Fanchon E, Geissler E, Hodeau J-L, Regnard J-R, Timmins PA (eds) Structure and dynamics of biomolecules. Oxford University Press, pp 102–115

Pebay-Peyroula E, Rosenbusch JP (2001) High-resolution structures and dynamics of membrane protein-lipid complexes. Curr Opin Struc Biol 11:427–432

Pebay-Peyroula E, Dahout-Gonzalez C, Kahn R, Trézéguet V, Lauquin GJ-M, Brandolin G (2003) Structure of mitochondrial ADP/AP carrier in complex with carboxyatractyloside. Nature 426:39–44

Pebay-Peyroula E, Brandolin G (2004) Nucleotide exchange in mitochondria: insight at a molecular level. Curr Opin Struct Biol 14:420–425

Pèdelacq J-D, Maveyraud L, Prèvost G, Baba-Moussa L, González A, Courcelle E, Shepard W, Monteil H, Samama J-P, Mourey L (1999) The structure of a Staphylococcus aureus leucocidin component (LukF-PV) reveals the fold of the water-soluble species of a family of transmembrane pore-forming toxins. Structure 7:277–287

Penel S, Pebay-Peyroula E, Rosenbusch JP, Rummel G, Schirmer T, Timmins PA (1998) Detergent binding in trigonal crystals of OmpF porin from Escherichia coli. Biochimie 80:543–551

Perisic O, Paterson HF, Mosedale G, Lara-Gonzalez S, Williams RL (1999) Mapping the phospholipid-binding surface and translocation determinants of the C2 domain from cytosolic phospholipase A2. J Biol Chem 274:14979–14987

Petitpas I, Grune T, Bhattacharya AA, Curry S (2001) Crystal structures of human serum albumin complexed with monounsaturated and polyunsaturated fatty acids. J Mol Biol 314:955–960

Petosa C, Collier RJ, Klimpel KR, Leppla SH, Liddington RC (1997) Crystal structure of the anthrax toxin protective antigen. Nature 385:833–838

Prince SM, Howard TD, Myles DAA, Wilkinson C, Papiz MZ, Freer AA, Cogdell RJ, Isaacs NW (2003) Detergent structure in crystals of the integral membrane light-harvesting complex LH2 from Rhodopseudomonas acidophila strain 10050. J Mol Biol 326:307–315

Qutub Y, Reviakine I, Maxwell C, Navarro J, Landau EM, Vekilov PG (2004) Crystallization of transmembrane proteins in cubo: mechanisms of crystal growth and defect formation. J Mol Biol 343:1243–1254

Rebecchi MJ, Scarlata S (1998) Pleckstrin homology domains: a common fold with diverse functions. Annu Rev Biophys Biomol Struct 27:503–528

Reiss-Husson F, Picot D (1999) Crystallization of membrane proteins. In: Ducruix A, Giégé R, (eds) Crystallization of nucleic acids and proteins. A practical approach. Oxford University Press, pp 245–268

Ringom R, Axem E, Uppenberg J, Lundback T, Rondahl L, Barf T (2004) Substituted benzylamino-6-(trifluoro methyl) pyrimidin-4(1H)-ones: a novel class of selective human A-Fabp inhibitors. Bioorg Med Chem Lett 14:4449

Rizo J, Sudhof TC (1998) C2 domains, structure and function of a universal Ca 2+ binding domain. J Biol Chem 273:15879–15882

Roderick SL, Chan WW, Agate DS, Olsen LR, Vetting MW, Rajashankar KR, Cohen DE (2002) Structure of human phosphatidylcholine transfer protein in complex with its ligand. Nat Struct Biol 9:507–511

Romanowski MJ, Soccio RE, Breslow JL, Burley SK (2002) Crystal structure of the Mus musculus cholesterol-regulated START protein 4 (StarD4) containing a StAR-related lipid transfer domain. Proc Nat Acad Sci USA 99:6949–6954

Ross AC (1993) Cellular metabolism and activation of retinoids – roles of cellular retinoid-binding proteins. FASEB J 7:317–327

Rossjohn J, Feil SC, McKinstry WJ, Tweten RK, Parker MW (1997) Structure of a cholesterol-binding,thiol-activated cytolysin and a model of its membrane form. Cell 89:685–692

Roth M, Lewit-Bentley A, Michel H, Deisenhofer J, Huber R, Oesterhelt D (1989) Detergent structure in crystals of a bacterial photosynthetic reaction centre. Nature 340:659–662

Royant A, Nollert P, Edman K, Neutze R, Landau EM, Pebay-Peyroula E, Navarro J (2001) X-ray structure of sensory rhodopsin II at 2.1 Å resolution. Proc Natl Acad Sci USA 98:10131–10136

Rubin B, Dennis EA (eds.) (1997) Lipases. Methods in enzymology, Vol. 284. Academic Press, New York

Rueckert DG, Schmidt K (1990) Lipid-transfer proteins. Chem Phys Lip 56:1–20

Sacchettini JC, Scapin G, Gopaul D, Gordon JI (1992) Refinement of the structure of Escherichia coli-derived rat intestinal fatty acid binding protein with bound oleate to 1.75-Å resolution. Correlation with the structures of the apoprotein and the protein with bound palmitate. J Biol Chem 267:23534–23545

Santelli E, Bankston LA, Leppla SH, Liddington RC (2004) Crystal structure of a complex between anthrax toxin and its host cell receptor. Nature 430:905–908

Schulz GE (2000) β-barrel membrane proteins. Curr Opin Struct Biol 10:443–447

Shin DH, Lee JY, Hwang KY, Kim KK, Suh SW (1995) High-resolution crystal structure of the non-specific lipid-transfer protein from maize seedlings. Structure 3:189–199

Skerra A (2000) Lipocalins as a scaffold. Biochim Biophys Acta 1482:337–350

Snijder HJ, Timmins PA, Kalk KH, Dijkstra BW (2003) Detergent organisation in crystals of monomeric outer membrane phospholipase A. J Struct Biol 141:122–131

Song L, Hobaugh MR, Shustak C, Cheley S, Bayley H, Gouaux JE (1996) Structure of Staphylococcal α-hemolysin, a heptameric transmemabrane pore. Science 274:1859–1866

Staub JM, Garcia B, Graves J, Hajdukiewicz PT, Hunter P, Nehra N, Paradkar V, Schlittler M, Carroll JA, Spatola L, Ward D, Ye G, Russell DA (2000) High-yield production of a human therapeutic protein in tobacco chloroplasts. Nat Biotechnol 18:333–338

Stenmark H, Asaland R, Toh B, D'Arrigo A (1996) Endosomal localization of the autoantigen EEA1 is mediated by a zinc-binding FYVE finger. J Biol Chem 271:24048–24054

Stroud RM, Reiling K, Wiener M, Freymann D (1998) Ion-channel colicins. Curr Opin Struct Biol 8:525–533

Sussman JL, Harel M, Frolow F, Oefner C, Goldman A, Toker L, Silman I (1991) Atomic structure of acetylcholinesterase from Torpedo californica: a prototypic acetylcholine-binding protein. Science 253:872–879

Tate CG (2001) Overexpression of mammalian integral membrane proteins for structural studies. FEBS Lett 504:94–98

Tassin-Moindrot S, Caille A, Douliez JP, Marion D, Vovelle F (2000) The wide binding properties of a wheat nonspecific lipid transfer protein. Solution structure of a complex with prostaglandin B2. Eur J Biochem 267:1117–1124

Tegoni M, Ramoni R, Bignetti E, Spinelli S, Cambillau C (1996) Domain swapping creates a third putative combining site in bovine odorant binding protein dimer. Nat Struct Biol 3:863–867

Teruel MN, Meyer T (2000) Translocation and reversible localization of signaling proteins: a dynamic future for signal transduction. Cell 103:181–184

Thompson J, Winter N, Terwey D, Bratt J, Banaszak L (1997) The crystal structure of the liver fatty acid-binding protein. A complex with two bound oleates J Biol Chem 272:7140–7150

Timmins P, Pebay-Peyroula E, Welte W (1994) Detergent organisation in solutions and in crystals of membrane proteins. Biophys Chem 53:27–36

Toyoshima C, Nakasako M, Nomura H, Ogawa H (2000) Crystal structure of the calcium pump of sarcoplasmic reticulum at 2.6 Å resolution. Nature 405:647–655

Tweten RK, Parker MW, Johnson AE (2001) The cholesterol-dependent cytolysins. Curr Top Microbiol Immunol 257:13–33

Tsujishima Y, Hurley JH (2000) Structure and lipid transport mechanism of a StAR-related domain. Nat Struc Biol 7:408–414

Van der Goot FG, González-Mañas JM, Lakey JH, Pattus F (1991) A 'molten-globule' membrane-insertion intermediate of the pore-forming domain of colicin A. Nature 354:408–410

Vogeley L, Sineshchekov OA, Trivedi VD, Sasaki J, Spudich JL, Luecke H (2004) Anabena sensory rhodopsin: a photochromic color sensor at 2.0 Å resolution. Science 306:1390–1393

Wallin E, von Heijne G (1998) Genome-wide analysis of integral membrane proteins from eubacterial, archaean, and eukarytic organisms. Prot Sci 7:1029–1038

Welte W, Wacker T (1991) Protein–detergent micellar solutions for the crystallization of membrane proteins. In: Michel H (ed) Crystallization of membrane proteins. CRC Press, pp 107–123

Weik M, Patzelt H, Zaccai J, Oesterhelt D (1998) Localization of glycolipids in membranes by in vivo labeling and neutron diffraction. Mol Cell 1:411–419

Werten PJL, Rémigy H-W, de Groot BL, Fotiadis D, Philippsen A, Stahlberg H, Grubmüller H, Engel A (2002) Progress in the analysis of membrane protein structure and function. FEBS Lett 529:67–72

White SH (2004) The progress of membrane protein structure determination. Prot Sci 13:1948–1949

Wiener M, Freymann D, Ghosh P, Stroud RM (1997) Crystal structure of colicin Ia. Nature 385:155–163

Wimley WC (2003) The versatile β-barrel membrane protein. Curr Opin Struct Biol 13:404–411

Wurmser AE, Gary JD, Emr SD (1999) Phosphoinositide 3-kinases and their FYVE domain-containing effectors as regulators of vacuolar/lysosomal membrane trafficking pathways. J Biol Chem 274:9129–9132

Xu RX, Pawelczyk T, Xia T-H, Brown SC (1997) NMR structure of a protein kinase C-phorbol-binding domain and study of protein–lipid micelle interactions. Biochemistry 36:10709–10717

Yankovskaya V, Horesefield R, Törnroth S, Luna-Chavez C, Miyoshi H, Léger C, Byrne B, Cecchini G, Iwata S (2003) Architecture of succinate dehydrogenase and reative oxygen species generation. Science 299:700–704

Zakharov SD, Heymann JB, Zhang YL, Cramer WA (1996) Membrane binding of the colicin E1 channel: activity requires an electrostatic interaction of intermediate magnitude. Biophys J 70:2774–2783

Zanotti G, Berni R, Monaco HL (1993) Crystal structure of liganded and unliganded forms of bovine plasma retinol-binding protein. J Biol Chem 268:10728–10738

Zanotti G, Marcello M, Malpeli G, Folli C, Sartori G, Berni R (1994) Crystallographic studies on complexes between retinoids and plasma retinol-binding protein. J Biol Chem 269:29613–29620

Zasloff M (2002) Antimicrobial peptides of multicellular organisms. Nature 415:389–395

Zhang G, Kazanietz MG, Blumberg PM, Hurley JH (1995) Crystal structure of the cys2 activator-binding domain of protein kinase C delta in complex with phorbol ester. Cell 81:917–924

Zimmerman AW, Veerkamp JH (2002) New insights into the structure and function of fatty acid-binding proteins. Cell Mol Life Sci 59:1096–1116

Zulauf M (1991) Detergent phenomena in membrane protein crystallization. In: Michel H (ed) Crystallization of membrane proteins. CRC Press, Boston, pp 53–72

The Role of Proteins in the Formation of Domains in Membranes

Richard M. Epand

4.1 Domains

There has been increased interest in recent years in the formation of domains in biological membranes. This has resulted from the challenges in defining the structure and properties of "raft" domains and their possible biological roles (Munro 2003). In October, 2004 the Biophysical Society sponsored a four-day meeting "Probing Membrane Microdomains" which was largely devoted to discussing the existence and characteristics of rafts (http://www.netbriefings.com/event/biophysics/Archives/discussions2004/). One characteristic of raft domains in biological membranes is that their lipid composition is enriched in cholesterol and sphingomyelin (Brown and London 2000).

The phase behavior of mixtures of cholesterol, sphingomyelin and phosphatidylcholine is reasonably well understood from both the thermodynamic (de Almeida et al. 2003) and morphological (Veatch and Keller 2003; Veatch et al. 2004; Veatch and Keller 2002) points of view. These mixtures can give rise to a domain that is in the liquid-ordered phase, defined as a region of the membrane in which there is an increase in the ratio of trans to gauche rotomers in the acyl chain, as occurs in the gel state, but the rate of lateral diffusion of the lipid is more characteristic of the fluid phase. Surprisingly, there is not a large enrichment of cholesterol in these domains (Veatch et al. 2004). The separation of a domain enriched in cholesterol and sphingomyelin is dependent on the ratio of lipid components, temperature and the nature of the acyl chains in phosphatidylcholine as well as sphingomyelin. Dioleoylphosphatidylcholine (DOPC) is particularly effective in promoting phase separation of a liquid-ordered domain. Species of phosphatidylcholine with two unsaturated acyl chains is not abundant found in mammalian cell membranes but DOPC has been commonly used to promote raft formation in lipid mixtures. Phosphatidylcholines with polyunsaturated acyl chains are even more effective in promoting domain formation in mixtures with cholesterol even when the acyl chain on the C1 of glycerol is saturated (Brzustowicz et al. 2002a,b). The major fraction of acyl chains in sphingomyelin from biological sources is saturated and can form liquid-ordered domains with cholesterol. One exception to this generalization is the finding of unsaturated sphingomyelins during the life-cycle of the moth *Manduca sexta* (Abeytunga et al. 2004). There is a greatly reduced tendency of sphingomyelin to form cholesterol-rich domains when its acyl chain is an oleoyl moiety (Mattjus and Slotte 1996; Waarts et al. 2002), possibly because sphingomyelins with oleoyl chains are more miscible with phos-

Springer Series in Biophysics
C.R. Mateo et al. (Ed.)
Protein-Lipid Interactions

phatidylcholine than are sphingomyelins with saturated acyl chains (Epand and Epand 2004).

There are two terms that describe the formation of distinct areas in the membrane that have different chemical and physical characteristics. These are the terms "domain" and "phase". Often these two terms can be used interchangeably when the phase diagram indicates the coexistence of more than one phase. However, as the size and lifetime of an area decreases the segregated area will no longer be a phase, but can still be considered a domain. Very small or transient domains might better be described as non-ideal mixing of membrane components (Huang and Feigenson 1993; Huang et al. 1993; Metso et al. 2004), rather than as a discrete physical structure. The exact criterion for describing something as a phase, a domain or as non-uniform mixing is not well defined.

The distribution of lipid molecules in the plane of the membrane will be altered when proteins or peptides are incorporated into the membrane. The raft domains of biological membranes are generally thought of as forming as a result of the stabilizing interactions between cholesterol and sphingomyelin. Although this may be largely true in model membrane systems composed only of lipids, about half of the material in biological membranes is protein in nature. There will be interactions among proteins, among lipids and between proteins and lipids. In general, proteins will have different affinities for different lipids. One contribution to the interaction between proteins and lipids is charge. Proteins can have segments that are highly charged that will either attract or repel negatively charged lipids. In addition, cholesterol is a major lipid component of the surface membrane of mammalian cells. This lipid has a more rigid structure because of its fused ring system and is more hydrophobic that the phospholipid component of the membrane. As a result different proteins will either favor or disfavor interactions with cholesterol vs. phospholipids. Interestingly, both cases will lead to the formation of cholesterol-rich domains. This is because the binding of a protein to a lipid will lower the chemical potential of the lipid, i.e. it will stabilize that lipid component. If the protein favors binding to a phospholipid over cholesterol the protein will cause cholesterol to be depleted from its surroundings and consequently be redistributed into cholesterol-rich domains. The system should come to an energy minimum. Of course the opposite is also true, and is more intuitively obvious: if a protein binds preferentially to cholesterol, it will cause cholesterol to be sequestered into a cholesterol-rich raft-like domain. Domain formation in membranes is not the result of only charged interactions and of preferential interactions of proteins with cholesterol or phospholipids. Each lipid structure, including the nature of the acyl chain, will generally have a somewhat different interaction with a protein and not all domains involve the formation of a liquid-ordered phase. In this review, however, we will focus particularly on the role of cholesterol in membrane domain formation because it relates to the formation of rafts and caveolae in biological membranes and is also likely to be one of the more common driving forces for domain formation because of the large differences between the properties of cholesterol and polar lipids.

4.2 Proteins that Bind Specific Lipids

There are several protein-folding domains that recognize specific lipids. Many of these bind specifically to one or more forms of phosphorylated phosphatidylinositol through interactions that are more specific than simple electrostatic interactions. These domains are often found in proteins involved in signal transduction. Their function has been considered largely on the basis of specific subcellular localization (Hurley and Meyer 2001; Misra et al. 2001). These domains, such as the PH, FYVE or FERM domains, bind stoichiometric amounts of specific lipids that would not be considered in itself a domain. However, the lipids they bind are highly charged, minor components of the membrane and their sequestration by proteins may be coupled with other rearrangements in the organization of membrane lipids.

There are also proteins and peptides that bind to specific lipid components of raft and caveolae domains in membranes, e.g. gangliosides, sphingomyelin and cholesterol. Gangliosides are among the sphingolipids found in rafts. The B chain of cholera toxin has specific affinity for the ganglioside GM_1 (Lanne et al. 1999) and has been used as a marker for raft domains (Kenworthy et al. 2000). Binding of a fluorescently labeled cholera toxin to the ganglioside GM_1 results in clustering of the ganglioside (Antes et al. 1992; Mitchell et al. 2002; Nagy et al. 2002). Thus, specific binding between a protein and lipid component can result in the lateral redistribution of lipid components in a membrane. A further complexity is the role of the cytoskeleton in affecting the lateral diffusion of ganglioside-containing domains in cell membranes, but not in model liposomal membranes (Bacia et al. 2004). Lysenin is a sphingomyelin-specific toxin (Yamaji-Hasegawa et al. 2003; Ishitsuka et al. 2004) that would also be expected to locate in rafts (Shakor et al. 2003). Another cytolysin, pleurotolysin A, also binds specifically to sphingomyelin (Sakurai et al. 2004; Tomita et al. 2004). In addition, there are cholesterol-binding peptides and proteins, including a toxic peptides perfringolysin O (Ramachandran et al. 2002; Shimada et al. 2002; Waheed et al. 2001) and ostreolysin (Sepcic et al. 2004), that bind to cholesterol-rich domains in membranes. In model membranes at least, the properties of the lipids in a mixture of DOPC with sphingomyelin, cholesterol and GM_1 would result in the formation of a raft-like domain in the absence of any protein. However, the addition of a protein that binds specifically to a lipid component of the raft, liquid-ordered domain would stabilize that domain. In the case of biological membranes the size of raft domains in resting cells is too small to be observed by light microscopy, if they exist at all, but the presence of proteins that bind specifically to the raft lipid components would stabilize these domains and increase their lifetime and size.

4.3 Non-Specific Interactions of Proteins with Membranes

Dividing protein–lipid interactions into "specific" and "non-specific" is somewhat arbitrary. The degree of specificity can be described quantitatively in terms

of affinity constants that can span a range of values. Nevertheless, there is a qualitative difference in affinity and specificity between a specific protein-folding domain that recognizes a lipid structure and proteins or peptides that interact with membranes in a less discriminate manner through electrostatic or hydrophobic interactions. We will focus on electrostatic interactions and on hydrophobic interactions that result in proteins or peptides forming cholesterol-rich domains.

4.3.1 Electrostatic Interactions

Electrostatic interactions can promote domain formation in membranes. In mammalian plasma membranes, anionic lipid components are found almost exclusively on the cytoplasmic leaflet. These lipids can interact with cationic proteins or clusters of cationic residues in a protein sequence. Anionic lipids will attract cations into the electrical double layer of the membrane. When polycationic peptides are bound to the membrane it will reduce the surface charge and hence the extent of the electrical double layer. This collapse of the electrical double layer will result in a stabilization of the region of the membrane where the peptide binds and as a consequence the area of this domain will grow by recruiting more peptide and anionic lipid (Denisov et al. 1998). It has been suggested that proteins with clusters of cationic residues bind a significant fraction of the phosphatidylinositol (4,5) bisphosphate (PIP2) in a cell, helping to sequester it in lateral membrane domains.

The sequestering of anionic lipids by cationic peptides is more effective when the lipid has multiple negative charges. Phosphorylated phosphatidylinositols have several negative charges at neutral pH. One of these lipids, phosphatidylinositol 4,5-bisphosphate (PIP2), is a component of raft domains (Parmryd et al. 2003; Klopfenstein et al. 2002; Pike and Casey 1996; Liu et al. 1998). Although PIP2 is a minor lipid component of these domains it can still be sequestered by proteins having cationic clusters. This PIP2 can then be released in response to local signals such as an increased concentration of Ca^{2+} or by activation of protein kinase C that can decrease the positive charge on the protein by catalyzing the phosphorylation of a Ser or Thr residue in its cationic segment (McLaughlin et al. 2002). This can have important functional consequences in signal transduction. PIP2 plays an important role in the attachment between the membrane and the actin cytoskeleton and is involved in the rearrangement of the cytoskeleton (Caroni 2001; Rozelle et al. 2000). Proteins such as GAP-43, MARCKS and CAP-23/NAP-22 have a cluster of cationic residues in their amino-acid sequence. CAP-23 is a protein with a high sequence homology to NAP-22 and likely with very similar properties; it was first identified by Widmer and Caroni (1990). Along with GAP-43 and MARCKS, CAP-23 accumulates in rafts, where it co-localizes with PIP2 (Laux et al. 2000). In the case of the MARCKS peptide, it has been shown that in liposomes the sequestering of PIP2 is not cholesterol-dependent (Gambhir et al. 2004). However, the sequestering of PIP2 by a NAP-22 peptide is cholesterol-dependent (Epand et al. 2004). Compared with MARCKS, NAP-22 has fewer cationic residues in the cationic cluster, and thus may be less effective in promoting the

segregation of PIP2. We suggest that the role of cholesterol, in the case of the NAP-22 peptide, is related to its effect of increasing line tension (Karatekin et al. 2003; Zhelev and Needham 1993). An increase in line tension will favor the growth of domains so as to minimize the interfacial boundary. This would also be a factor for the MARCKS peptide, but apparently the electrostatic interactions in this case are sufficiently strong that this factor is not required for the sequestering of PIP2 by MARCKS. PIP2 stimulates actin polymerization by causing the dissociation of gelsolin-actin complexes (Janmey and Stossel 1987), establishing a linkage between the plasma membrane and the cytoskeleton. The model helps to explain the physiological action of NAP-22, a protein found in rafts (Terashita et al. 2002), in reorganizing the actin cytoskeleton (Caroni 2001).

4.3.2 Hydrophobic Interactions with Acyl Chains

4.3.2.1 Transmembrane Helices

The nature of the transmembrane helical segment of integral membrane proteins will also contribute to determining the partitioning of the protein between raft and non-raft domains. It is possible that a smooth, uniform surface contour of a transmembrane helix would more readily mix with a rigid cholesterol-rich domain. Another factor is the possible length mismatch between the transmembrane helix and the bilayer thickness. Cholesterol will contribute to increasing the thickness of the bilayer by restricting acyl chain motions of neighboring phospholipids. However, many transmembrane helices are excluded from raft-like domains not because of a change in bilayer thickness, but rather because of an increased area compressibility modulus in the cholesterol-rich domains (McIntosh 2004; McIntosh et al. 2003). Nevertheless, the length of the hydrophobic segment of the bilayer has been suggested to be a factor in favoring interaction with transmembrane helices of specific lengths, both for certain model peptides (Ren et al. 1997) as well as with the M2 channel protein from influenza virus (Cristian et al. 2003). If these integral membrane proteins distribute preferentially into cholesterol-rich or cholesterol-depleted domains they will contribute to the formation of cholesterol-rich domains.

4.3.2.2 Lipidation

Lipids that are covalently attached to proteins will insert into the membrane and will partition preferentially into certain membrane domains. Many proteins that are acylated with saturated fatty acids, particularly with palmitic acid on cysteine residues or myristic acid on the N-terminal amino group, partition into membrane rafts (Brown and London 2000; Resh 2004). This is not the case with prenylated proteins that are commonly excluded from raft domains (Melkonian

et al. 1999). Another form of protein lipidation is by attachment to a glycosylphosphatidylinositol (GPI)-anchor that results in the protein being found in the low-density detergent-insoluble fraction (Morandat et al. 2002; Sharom and Lehto 2002), suggesting incorporation into rafts. Alkaline phosphatase is a relatively abundant GPI-anchored protein. AFM studies have demonstrated its sequestering into raft domains (Milhiet et al. 2002). Quantitative affinity purification has been used to demonstrate that different GPI-anchored proteins are sequestered into different raft-like domains (Wang et al. 2002) indicating a greater specificity for domain formation in biological systems than simple recognition of a lipidic moiety. Using homo- and hetero-FRET (fluorescence resonance energy transfer)-based experiments, combined with theoretical modeling in live cells, it was demonstrated that GPI-anchored proteins are present as monomers as well as a smaller fraction (20–40%) as nanoscale (<5 nm) cholesterol-sensitive clusters. These clusters are composed of at most four molecules and accommodate diverse GPI-anchored proteins (Sharma et al. 2004).

An interesting example of a myristoylated protein that preferentially binds to cholesterol-rich domains is the neuronal protein, NAP-22. NAP-22 itself is a highly acidic protein that is water-soluble. It exhibits the property of binding to liposomes containing cholesterol but not to pure phospholipid liposomes (Epand et al. 2001; Maekawa et al. 1999). NAP-22 was mentioned earlier in this chapter in connection with the clustering of PIP2. Calorimetry results indicate that the protein also induces the segregation of cholesterol into domains (Epand et al. 2001). In membranes with pre-existing domains, it has been shown by fluorescence microscopy that NAP-22 partitions into raft-like domains (Khan et al. 2003).

4.4 Juxta-Membrane Domains

Juxta-membrane domains can be distinguished from transmembrane helices or lipidation in that these segments do not penetrate deeply into the bilayer. One type of juxta-membrane domain is a cluster of cationic amino-acid residues that can bind to the surface of anionic membranes (Ellena et al. 2004). There are some lipoproteins, such as NAP-22, in which a smaller cationic cluster on the protein is found close to the amino terminus that is post translationally modified by myristoylation. In such cases the cationic cluster may sequester adjacent to the membrane surface because of a combination of lipid anchoring and electrostatic interactions. In addition, many of these cationic clusters, such as MARCKS, also contain aromatic amino-acid residues that will also contribute to membrane binding. The consequence of electrostatic interactions between cationic segments of proteins and anionic lipids has been described in Sect. 4.3.1.

There are also a few examples of protein segments that are adjacent to transmembrane domains that have been shown to be important in sequestering the protein to raft domains in membranes. One example of this is the so-called scaffolding domain of caveolin-1. Caveolin-1 is a major protein component of caveolae which are small structures of 50–100 nm in the plasma membrane that bud inward toward the cell (Anderson 1998). The lipid composition of caveolae

is enriched in cholesterol and sphingomyelin, the principal components of raft domains. The protein caveolin-1 has three palmitoyl chains that would facilitate its incorporation into raft-like domains. However, when the three sites of palmitoylation are mutated, the resulting protein still translocates to caveolae (Dietzen et al. 1995). This suggests that segments of the protein itself facilitate the interaction of caveolin-1 with cholesterol-rich domains. Mutational studies indicate that the segment comprising residues 82–101 is necessary and sufficient for membrane binding and has been termed the scaffolding domain (Schlegel et al. 1999). A recent fluorescence microscopy study has shown that a synthetic peptide corresponding to the scaffolding domain of caveolin can recruit NBD-labeled forms of cholesterol and acidic lipids (Wanaski et al. 2003).

Another example of a juxta-membrane domain, adjacent to a transmembrane segment, is the Trp-rich region of the gp41 protein of HIV. This region has been shown to be important for the infectivity of the virus (Salzwedel et al. 1999) and for sequestering the protein to cholesterol-rich domains (Saez-Cirion et al. 2002; Epand et al. 2003). Evidence that HIV also buds from raft domains includes the finding that the viral envelope is enriched in both lipids (Aloia et al. 1993) and GPI-anchored proteins (Esser et al. 2001; Nguyen and Hildreth 2000) found in "raft" domains of mammalian membranes. Several components that facilitate the entry of HIV into cells are suggested to be associated with raft domains in membranes, including cholesterol, CD4, the coreceptors CXCR4 and CCR5, as well as glycosphingolipids (Viard et al. 2004). However, viral entry into cells does not necessarily require the presence of cholesterol (Viard et al. 2002), but the removal of cholesterol with methyl-β-cyclodextrin from cells with relatively low receptor densities reduces the capacity of HIV-1 to trigger fusion (Viard et al. 2002). Extraction of cholesterol from the envelope of HIV-1 or SIV also results in reduced infectivity (Graham et al. 2003).

There is a relationship between the juxta-membrane regions of caveolin-1 and of the gp41 of HIV. Both segments conform to the requirements for a Cholesterol Recognition/interaction Amino acid Consensus (CRAC) motif (Li and Papadopoulos 1998) that was developed by analyzing amino acid sequences of proteins that interact with cholesterol (Li et al. 2001). A CRAC sequence is defined by having the pattern -L/V-(X)(1-5)-Y-(X)(1-5)-R/K-, in which (X)(1-5) represents between one and five residues of any amino acid.

Caveolin-1 has a juxta-membrane segment, residues 94–101, with the sequence VTKYWFYR that conforms to a CRAC motif. A shortened version of this segment that does not fulfill the requirements of the consensus sequence, KYWFYR, was found to sequester the protein to membranes, but is not sufficient to target the protein to the cholesterol-rich domain of caveolae (Woodman et al. 2002). In addition, the synthetic peptide, N-acetyl-KYWFYR-amide did not induce the formation of cholesterol-rich domains in liposomes despite the segment having four sequential aromatic residues (Epand et al. 2003). The segment N-acetyl-FTVTKYWFYR-amide was shown to bind weakly to lipid bilayers in the absence of cholesterol (Arbuzova et al. 2000). Two longer peptide segments of caveolin that do correspond to the requirements of the consensus sequence of Li and Papadopolus (1998), i.e. N-acetyl-VTKYWFYR-amide (residues 94–101) and

N-acetyl-GIWKASFTTFTVTKYWFYRL-amide (residues 83–102), exhibit preferential interaction with cholesterol (Epand et al. 2005c).

The Trp-rich juxta-membrane domain of the gp41 of HIV has the sequence LWYIK. The peptide N-acetyl-LWYIK-amide, also having a CRAC motif, has preferential interaction with cholesterol-rich domains (Epand et al. 2003). The sequence LWYIK is located at the carboxyl-terminus of a longer membrane-proximal region that is rich in Trp. It has been shown by mutational studies that this region is important for membrane fusion and virus infectivity (Salzwedel et al. 1999). This longer membrane-proximal sequence has also been studied as an isolated 20 amino acid, synthetic peptide and found to aggregate and promote fusion of liposomes containing sphingomyelin and cholesterol, the principal lipid components of membrane rafts (Saez-Cirion et al. 2002; Shnaper et al. 2004). The amino-terminal region of this peptide is responsible for the formation of peptide oligomers (Saez-Cirion et al. 2003).

There is not a great deal of information regarding the nature of the molecular interactions of the various residues of the CRAC motif with membranes. To begin with, the consensus sequence is rather general, having two segments that vary in length between one and five amino acid residues. This would suggest that the CRAC motif does not have a specific conformation since a unique folding pattern would require that there be a certain number of amino acids between one required residue and another. There are only three required residues, L/V, Y and R/K. In the case of LWYIK it was suggested that the Y residue interacts with the A ring of cholesterol (Epand et al. 2003), possibly through hydrophobic interactions of two conformationally restrained moieties. It is not known, however, if the Y can be replaced by another aromatic amino-acid residue. With regard to the requirement for an L or a V at the amino terminal side of the CRAC sequence, it is possible that this facilitates non-specific sequestering to a membrane by increasing the hydrophobicity of the segment. Might then an I also be able to substitute in this position? The last requirement, an R or K on the carboxyl side of the CRAC motif, suggests that a charge interaction is important. We have shown that peptides with a CRAC motif will promote the formation of cholesterol-rich domains even in the absence of anionic lipids. It is possible that on the cytoplasmic surface of mammalian cell membranes the cationic residue in the CRAC motif is important for interacting with anionic lipids; alternatively this group may play a role in modulating the depth of insertion of the peptide into the membrane. In that regard, the fact that the CRAC motif allows up to 10 residues of any type (as many as five before and five after the Y) without restriction, would allow for a wide range of peptide hydrophobicities. It seems likely that these 10 residues are not completely undetermined, but that the requirements for these segments have not yet been elucidated.

We have studied several peptides with variations of the CRAC motifs of the scaffolding region of caveolin-1 and of Trp-rich region of the gp41 of HIV. In the case of caveolin-1, shortening the segment to KYWFYR, a sequence that has four successive aromatic amino acids and a C-terminal R, does not result in preferential interaction with cholesterol (Epand et al. 2003) and this segment is not sufficient to target caveolin to the cholesterol-rich domain of caveolae (Woodman et al. 2002). Lengthening this segment to make N-acetyl-VTKYWFYR-amide re-

sults in a peptide that exhibits some preference for cholesterol-rich domains. This peptide, unlike N-acetyl-KYWFYR-amide, fulfills the requirements of a CRAC sequence (Li and Papadopoulos 1998). A longer peptide, N-acetyl-GIWKASFT-TFTVTKYWFYRL-amide, is even more potent in promoting the formation of cholesterol crystals compared with N-acetyl-VTKYWFYR-amide. The ability of CRAC sequences to promote the formation of cholesterol crystals cannot be a consequence of the peptide binding to cholesterol. Such an interaction would inhibit formation of cholesterol crystals by stabilizing the cholesterol that is bound to the peptide. Apparently, however, the CRAC peptide can alter the properties of the membrane in such a manner as to recruit more molecules of cholesterol to a specific domain, thus passing its solubility limit in the membrane. In the case of the Trp-rich region of the gp41 of HIV, we find the opposite, i.e. the longer the segment of the juxta-membrane region, the less able is the peptide to sequester cholesterol into domains. We find that the short peptide N-acetyl-LWYIK-amide is more effective than a peptide, N-acetyl-KWASLWNWFNITNWLWYIK-amide, corresponding to the full Trp-rich, membrane-proximal segment of HIV-1_{HXB2}, residues 665–683 of the gp41 protein, in promoting the formation of cholesterol-rich domains (Epand et al. 2005a). The results with the membrane proximal region of HIV gp41 are opposite to thoes found with the caveolin scaffolding domain. In the case of gp41, the longer peptide, N-acetyl-KWASLWNWFNITNWL-WYIK-amide, with more aromatic groups present, is less capable of promoting the formation of cholesterol-rich domains. Perhaps being more hydrophobic it can no longer distinguish between specific lipid molecules in sequestering to membranes (Epand et al. 2005a).

In the HIV-1 sequence database there are variants having a Ser at position 681 and that therefore do not formally have a CRAC motif. In addition, HIV-2 as well as several strains of SIV are also devoid of a CRAC motif. For example, for HIV-2CBL24, $SIV_{cpz(Q88004)}$, SIV_{mac251}, SIV_{agm} and SIVsm84, the segment 679–683, adjacent to the transmembrane segment, has the sequence LASWIK (Vincent et al. 2002), similar to the sequence LWYIK of HIV-1, but not fulfilling the requirements of the CRAC motif because it has no Tyr (Li and Papadopoulos 1998). Altering the sequence of LWYIK to LASWIK reduced the lipid preference of the peptide (Epand et al. 2005a).

The presence of a CRAC motif does not strictly correlate with the ability of a peptide to sequester cholesterol into a domain. Nevertheless, a CRAC motif is found in the juxta-membrane region of two proteins that associate with cholesterol-rich domains of biological membranes, i.e. caveolin-1 and HIV gp41. This suggests that segments that conform to the CRAC motif may have greater cholesterol-sequestering ability than similar peptides, such as LASWIK, that do not conform to the requirements of this domain. Of course, LASWIK is very similar to a CRAC sequence and it has partial cholesterol-sequestering activity. There are also caveats in comparing the results of isolated peptides with liposomes and the interaction of full-length proteins with biological membranes. The peptide may fold into a different conformation in the full-length protein. In the case of the gp41 fragment, N-acetyl-KWASLWNWFNITNWLWYIK-amide, the amino-terminal region of this peptide is responsible for the formation of oligomers (Saez-Cirion

et al. 2003). This may occur more readily in the intact proteins, whereas in the isolated peptide this region is freer to interact non-selectively with a membrane.

It is clear that juxta-membrane segments of a protein can cause the sequestering of cholesterol into domains. The precise correlation between amino acid sequence and length and the ability to recruit cholesterol is yet to be determined, as is the functional role of each amino-acid side-chain. Although the interaction does not appear to be very specific, the peptide N-acetyl-LWYIK-amide exhibits chiral specificity for cholesterol (Epand et al. 2005b). The aromatic side-chains by themselves are not chiral. One would therefore, a priori, not expect an effect of peptide chirality on the interaction with cholesterol. This is supported by the finding that the chirality of the LWYIK peptide has little to do with the extent of segregation of cholesterol. Cholesterol chirality has a small effect on lipid–lipid interactions that give rise to the formation of cholesterol-rich domains in the absence of peptide (Lalitha et al. 2001a,b). However, the ability of the L-enantiomer of N-acetyl-LWYIK-amide to sequester cholesterol into domains is strongly dependent on the chirality of the sterol (Epand et al. 2005b). Our results indicate that the membrane interactions of peptides and proteins that induce the formation of cholesterol-rich domains are altered by the small change in the arrangement and physical properties of cholesterol-containing bilayers as a result of changes in cholesterol chirality. As a consequence, the peptide-induced segregation of cholesterol into domains is strongly affected by cholesterol chirality, even though the peptide–lipid interactions that are involved are not very specific.

4.5 Energy Minimization as a Driving Force for Domain Formation

Biological membranes are in a steady state with continual cycling of membrane components and membrane vesicles. Nevertheless, it is likely that these membranes are not far from equilibrium. Their arrangement does not change drastically when the membranes are isolated and there is no longer cycling of membrane materials. With regard to organization of domains in model membranes, this occurs spontaneously when a peptide or protein is added to a liposome. The formation of these domains is thus a more stable arrangement. Raft domains are often described as the lipids forming domains and the peptides and proteins partitioning between cholesterol-rich and cholesterol-poor regions. However, the preferential interaction of a protein with one of the two domains will in itself alter the distribution of lipids between the two domains. The system is expected to come to thermodynamic equilibrium that will be determined by the sum of all of the interactions including those among lipids, among proteins and between lipids and proteins. There will be cases in which the protein is excluded from cholesterol-rich domains. This will indirectly stabilize the formation of cholesterol-rich domains by lowering the energy of those domains that are depleted of cholesterol and hence forcing the cholesterol into another region of the membrane where it will become enriched. This is likely to be a common situation. Cholesterol condenses the membrane, increasing the tightness of packing of the lipids, preventing peptides and proteins from entering the bilayer. The only proteins

that will not alter cholesterol distribution in the membrane are those that interact equally well with cholesterol-rich and cholesterol-depleted membrane regions. Hence in biological membranes it would be anticipated that most proteins facilitate the formation of cholesterol domains.

References

Abeytunga DTU, Glick JJ, Gibson NJ, Oland LA, Somogyi A, Wysocki VH, Polt R (2004) Presence of unsaturated sphingomyelins and changes in their composition during the life cycle of the moth Manduca sexta. J Lipid Res 45:1221–1231

Aloia, RC, Tian H, Jensen FC (1993) Lipid composition and fluidity of the human immunodeficiency virus envelope and host cell plasma membranes. Proc Natl Acad Sci USA 90:5181–5185

Anderson, RG (1998) The caveolae membrane system. Annu Rev Biochem 67:199–225

Antes P, Schwarzmann G, Sandhoff K (1992) Detection of protein mediated glycosphingolipid clustering by the use of resonance energy transfer between fluorescent labelled lipids A method established by applying the system ganglioside GM1 and cholera toxin B subunit. Chem Phys Lipids 62:269–280

Arbuzova A, Wang L, Wang J, Hangyas-Mihalyne G, Murray D, Honig B, McLaughlin S (2000) Membrane binding of peptides containing both basic and aromatic residues Experimental studies with peptides corresponding to the scaffolding region of caveolin and the effector region of MARCKS. Biochemistry 39:10330–10339

Bacia K, Scherfeld D, Kahya N, Schwille P (2004) Fluorescence correlation spectroscopy relates rafts in model and native membranes. Biophys J 87:1034–1043

Brown DA and London E (2000) Structure and function of sphingolipid- and cholesterol-rich membrane rafts. J Biol Chem 275:17221–17224

Brzustowicz MR, Cherezov V, Caffrey M, Stillwell W, Wassall SR (2002a) Molecular organization of cholesterol in polyunsaturated membranes: microdomain formation. Biophys J 82:285–298

Brzustowicz MR, Cherezov V, Zerouga M, Caffrey M, Stillwell W, Wassall SR (2002b) Controlling membrane cholesterol content a role for polyunsaturated (docosahexaenoate) phospholipids. Biochemistry 41:12509–12519

Caroni P (2001) New EMBO members' review: actin cytoskeleton regulation through modulation of PI(4, 5)P(2) rafts. EMBO J 20:4332–4336

Cristian L, Lear JD, DeGrado WF (2003) Use of thiol-disulfide equilibria to measure the energetics of assembly of transmembrane helices in phospholipid bilayers. Proc Natl Acad Sci USA 100:14772–14777

de Almeida RF, Fedorov A, Prieto M (2003) Sphingomyelin/phosphatidylcholine/cholesterol phase diagram: boundaries and composition of lipid rafts. Biophys J 85:2406–2416

Denisov G, Wanaski S, Luan P, Glaser M, McLaughlin S (1998) Binding of basic peptides to membranes produces lateral domains enriched in the acidic lipids phosphatidylserine and phosphatidylinositol 4, 5-bisphosphate: an electrostatic model and experimental results. Biophys J 74:731–744

Dietzen DJ, Hastings WR, Lublin DM (1995) Caveolin is palmitoylated on multiple cysteine residues Palmitoylation is not necessary for localization of caveolin to caveolae. J Biol Chem 270:6838–6842

Ellena JF, Moulthrop J, Wu J, Rauch M, Jaysinghne S, Castle JD, Cafiso DS (2004) Membrane position of a basic aromatic peptide that sequesters phosphatidylinositol 4, 5 bisphosphate determined by site-directed spin labeling and high-resolution NMR. Biophys J 87:3221–3233

Epand RF, Sayer BG, Epand RM (2005a) The tryptophan-rich region of HIV gp41 and the promotion of cholesterol-rich domains. Biochemistry 44:5525–5531

Epand RM, Rychnovsky S, Belani J, Epand RF (2005b) Role of chirality in peptide-induced formation of cholesterol-rich domains. Biochemical J 390:541–548

Epand RM, Epand RF (2004) Non-raft forming sphingomyelin-cholesterol mixtures. Chem Phys Lipids 132:37–46

Epand RM, Maekawa S, Yip CM, Epand RF (2001) Protein-induced formation of cholesterol-rich domains. Biochemistry 40:10514–10521

Epand RM, Sayer BG, Epand RF (2003) Peptide-induced formation of cholesterol-rich domains. Biochemistry 42:14677–14689

Epand RM, Sayer BG, Epand RF (2005c) Caveolin scaffolding region and cholesterol-rich domains in membranes. J Mol Biol 345:339–350

Epand RM, Vuong P, Yip CM, Maekawa S, Epand RF (2004) Cholesterol-dependent partitioning of Ptdlns(4,5)P-2 into membrane domains by the N-terminal fragment of NAP-22 (neuronal axonal myristoylated membrane protein of 22 kDa). Biochemical Journal 379:527–532

Esser MT, Graham DR, Coren LV, Trubey CM, Bess JW, Jr, Arthur LO, Ott DE, Lifson JD (2001) Differential incorporation of CD45, CD80 (B7-1), CD86 (B7-2), major histocompatibility complex class I and II molecules into human immunodeficiency virus type 1 virions and microvesicles: implications for viral pathogenesis and immune regulation. J Virol 75:6173–6182

Gambhir A, Hangyas-Mihalyne G, Zaitseva I, Cafiso DS, Wang J, Murray D, Pentyala SN, Smith SO, McLaughlin S (2004) Electrostatic sequestration of PIP2 on phospholipid membranes by basic/aromatic regions of proteins. Biophys J 86:2188–2207

Graham DR, Chertova E, Hilburn JM, Arthur LO, Hildreth JE (2003) Cholesterol depletion of human immunodeficiency virus type 1 and simian immunodeficiency virus with beta-cyclodextrin inactivates and permeabilizes the virions: evidence for virion-associated lipid rafts. J Virol 77:8237–8248

Huang J and Feigenson GW (1993) Monte Carlo simulation of lipid mixtures: finding phase separation. Biophys J 65:1788–1794

Huang J, Swanson JE, Dibble AR, Hinderliter AK, Feigenson GW (1993) Nonideal mixing of phosphatidylserine and phosphatidylcholine in the fluid lamellar phase. Biophys J 64:413–425

Hurley JH and Meyer T (2001) Subcellular targeting by membrane lipids. Curr Opin Cell Biol 13:146–152

Ishitsuka R, Yamaji-Hasegawa A, Makino A, Hirabayashi Y, Kobayashi T (2004) A lipid-specific toxin reveals heterogeneity of sphingomyelin-containing membranes. Biophys J 86:296–307

Janmey PA and Stossel TP 1987 Modulation of gelsolin function by phosphatidylinositol 4, 5-bisphosphate. Nature 325:362–364

Karatekin E, Sandre O, Guitouni H, Borghi N, Puech PH, Brochard-Wyart F (2003) Cascades of transient pores in giant vesicles: line tension and transport. Biophys J 84:1734–1749

Kenworthy AK, Petranova N, Edidin M (2000) High-resolution FRET microscopy of cholera toxin B-subunit and GPI-anchored proteins in cell plasma membranes. Mol Biol Cell 11:1645–1655

Khan TK, Yang B, Thompson NL, Maekawa S, Epand RM, Jacobson K (2003) Binding of NAP-22, a calmodulin-binding neuronal protein, to raft-like domains in model membranes. Biochemistry 42:4780–4786

Klopfenstein DR, Tomishige M, Stuurman N, Vale RD (2002) Role of phosphatidylinositol(4, 5)bisphosphate organization in membrane transport by the Unc104 kinesin motor. Cell 109:347–358

Lalitha S, Kumar AS, Stine KJ, Covey DF (2001a) Chirality in membranes: first evidence that enantioselective interactions between cholesterol and cell membrane lipids can be a determinant of membrane physical properties. J Supramol Chem 1:53–61

Lalitha S, Kumar AS, Stine KJ, Covey DF (2001b) Enantiospecificity of sterol–lipid interactions: first evidence that the absolute configuration of cholesterol affects the physical properties of cholesterol-sphingomyelin membranes. Chem Commun 1192–1193

Lanne B, Schierbeck B, Angstrom J (1999) Binding of cholera toxin B-subunits to derivatives of the natural ganglioside receptor, GM1. J Biochem (Tokyo) 126:226–234

Laux T, Fukami K, Thelen M, Golub T, Frey D, Caroni P (2000) GAP43, MARCKS, and CAP23 modulate PI(4, 5)P(2) at plasmalemmal rafts, and regulate cell cortex actin dynamics through a common mechanism. J Cell Biol 149:1455–1472

Li H, Papadopoulos V (1998) Peripheral-type benzodiazepine receptor function in cholesterol transport Identification of a putative cholesterol recognition/interaction amino acid sequence and consensus pattern. Endocrinology 139:4991–4997

Li H, Yao Z, Degenhardt B, Teper G, Papadopoulos V (2001) Cholesterol binding at the cholesterol recognition/ interaction amino acid consensus (CRAC) of the peripheral-type benzodiazepine receptor and inhibition of steroidogenesis by an HIV TAT-CRAC peptide. Proc Natl Acad Sci USA 98:1267–1272

Liu Y, Casey L, Pike LJ (1998) Compartmentalization of phosphatidylinositol 4,5-bisphosphate in low-density membrane domains in the absence of caveolin. Biochem Biophys Res Commun 245:684–690

Maekawa S, Sato C, Kitajima K, Funatsu N, Kumanogoh H, Sokawa Y (1999) Cholesterol-dependent localization of NAP-22 on a neuronal membrane microdomain (raft). J Biol Chem 274:21369–21374

Mattjus P, Slotte JP (1996) Does cholesterol discriminate between sphingomyelin and phosphatidylcholine in mixed monolayers containing both phospholipids? Chem Phys Lipids 81:69–80

McIntosh TJ (2004) The (2004) Biophysical Society – Avanti Award in Lipids address: roles of bilayer structure and elastic properties in peptide localization in membranes. Chem Phys Lipids 130:83–98

McIntosh TJ, Vidal A, Simon SA (2003) Sorting of lipids and transmembrane peptides between detergent-soluble bilayers and detergent-resistant rafts. Biophys J 85:1656–1666

McLaughlin S, Wang J, Gambhir A, Murray D (2002) PIP(2) and proteins: interactions, organization, and information flow. Annu Rev Biophys Biomol Struct 31:151–175

Melkonian KA, Ostermeyer AG, Chen JZ, Roth MG, Brown DA (1999) Role of lipid modifications in targeting proteins to detergent-resistant membrane rafts Many raft proteins are acylated, while few are prenylated. J Biol Chem 274:3910–3917

Metso AJ, Mattila JP, Kinnunen PK (2004) Characterization of the main transition of dinervonoylphosphocholine liposomes by fluorescence spectroscopy. Biochim Biophys Acta 1663:222–231

Milhiet PE, Giocondi MC, Le Grimellec C (2002) Cholesterol is not crucial for the existence of microdomains in kidney brush-border membrane models. J Biol Chem 277:875–878

Misra S, Miller GJ, Hurley JH (2001) Recognizing phosphatidylinositol 3-phosphate. Cell 107:559–562

Mitchell JS, Kanca O, McIntyre BW (2002) Lipid microdomain clustering induces a redistribution of antigen recognition and adhesion molecules on human T lymphocytes. J Immunol 168:2737–2744

Morandat S, Bortolato M, Roux B (2002) Cholesterol-dependent insertion of glycosylphosphatidylinositol-anchored enzyme. Biochim Biophys Acta 1564:473–478

Munro S (2003) Lipid rafts: elusive or illusive? Cell 115:377–388

Nagy P, Vereb G, Sebestyen Z, Horvath G, Lockett SJ, Damjanovich S, Park JW, Jovin TM, Szollosi J (2002) Lipid rafts and the local density of ErbB proteins influence the biological role of homo- and heteroassociations of ErbB2. J Cell Sci 115:4251–4262

Nguyen DH, Hildreth JE (2000) Evidence for budding of human immunodeficiency virus type 1 selectively from glycolipid-enriched membrane lipid rafts. J Virol 74:3264–3272

Parmryd I, Adler J, Patel R, Magee AI (2003) Imaging metabolism of phosphatidylinositol 4,5-bisphosphate in T-cell GM1-enriched domains containing Ras proteins. Exp Cell Res 285:27–38

Pike LJ, Casey L (1996) Localization and turnover of phosphatidylinositol 4,5-bisphosphate in caveolin-enriched membrane domains. J Biol Chem 271:26453–26456

Ramachandran R, Heuck AP, Tweten RK, Johnson AE (2002) Structural insights into the membrane-anchoring mechanism of a cholesterol-dependent cytolysin. Nat Struct Biol 9:823–827

Ren J, Lew S, Wang Z, London E (1997) Transmembrane orientation of hydrophobic alpha-helices is regulated both by the relationship of helix length to bilayer thickness and by the cholesterol concentration. Biochemistry 36:10213–10220

Resh MD (2004) Membrane targeting of lipid modified signal transduction proteins. Subcell Biochem 37:217–232

Rozelle AL, Machesky LM, Yamamoto M, Driessens MH, Insall RH, Roth MG, Luby-Phelps K, Marriott G, Hall A, Yin HL (2000) Phosphatidylinositol 4,5-bisphosphate induces actin-based movement of raft-enriched vesicles through WASP-Arp2/3. Curr Biol 10:311–320

Saez-Cirion A, Arrondo JL, Gomara MJ, Lorizate M, Iloro I, Melikyan G, Nieva JL (2003) Structural and functional roles of HIV-1 gp41 pretransmembrane sequence segmentation. Biophys J 85:3769–3780

Saez-Cirion A, Nir S, Lorizate M, Agirre A, Cruz A, Perez-Gil J, Nieva JL (2002) Sphingomyelin and cholesterol promote HIV-1 gp41 pretransmembrane sequence surface aggregation and membrane restructuring. J Biol Chem 277:21776–21785

Sakurai N, Kaneko J, Kamio Y, Tomita T (2004) Cloning, expression, and pore-forming properties of mature and precursor forms of pleurotolysin, a sphingomyelin-specific two-component cytolysin from the edible mushroom Pleurotus ostreatus. Biochim Biophys Acta 1679:65–73

Salzwedel K, West JT, Hunter E (1999) A conserved tryptophan-rich motif in the membrane-proximal region of the human immunodeficiency virus type 1 gp41 ectodomain is important for Env-mediated fusion and virus infectivity. J Virol 73:2469–2480

Schlegel A, Schwab RB, Scherer PE, Lisanti MP (1999) A role for the caveolin scaffolding domain in mediating the membrane attachment of caveolin-1 The caveolin scaffolding

domain is both necessary and sufficient for membrane binding in vitro. J Biol Chem 274:22660–22667

Sepcic K, Berne S, Rebolj K, Batista UK, Plemenitas A, Sentjurc M, Macek P (2004) Ostreolysin, a pore-forming protein from the oyster mushroom, interacts specifically with membrane cholesterol-rich lipid domains. FEBS Lett 575:81–85

Shakor ABA, Czurylo EA, Sobota A (2003) Lysenin, a unique sphingomyelin-binding protein. FEBS Lett 542:1–6

Sharma P, Varma R, Sarasij RC, Ira, Gousset K, Krishnamoorthy G, Rao M, Mayor S (2004) Nanoscale organization of multiple GPI-anchored proteins in living cell membranes. Cell 116:577–589

Sharom FJ, Lehto MT (2002) Glycosylphosphatidylinositol-anchored proteins: structure, function, and cleavage by phosphatidylinositol-specific phospholipase C. Biochem Cell Biol 80:535–549

Shimada Y, Maruya M, Iwashita S, Ohno-Iwashita Y (2002) The C-terminal domain of perfringolysin O is an essential cholesterol-binding unit targeting to cholesterol-rich microdomains. Eur J Biochem 269:6195–6203

Shnaper S, Sackett K, Gallo SA, Blumenthal R, Shai Y (2004) The C- and the N-terminal regions of glycoprotein 41 ectodomain fuse membranes enriched and not enriched with cholesterol, respectively. J Biol Chem 279:18526–18534

Terashita A, Funatsu N, Umeda M, Shimada Y, Ohno-Iwashita Y, Epand RM, Maekawa S (2002) Lipid binding activity of a neuron-specific protein NAP-22 studied in vivo and in vitro. J Neurosci Res 70:172–179

Tomita T, Noguchi K, Mimuro H, Ukaji F, Ito K, Sugawara-Tomita N, Hashimoto Y (2004) Pleurotolysin, a novel sphingomyelin-specific two-component cytolysin from the edible mushroom Pleurotus ostreatus, assembles into a transmembrane pore complex. J Biol Chem 279:26975–26982

Veatch SL, Keller SL (2002) Organization in lipid membranes containing cholesterol. Phys Rev Lett 89:268101

Veatch SL, Keller SL (2003) A closer look at the canonical 'raft mixture' in model membrane studies. Biophys J 84:725–726

Veatch SL, Polozov IV, Gawrisch K, Keller SL (2004) Liquid domains in vesicles investigated by NMR and fluorescence microscopy. Biophys J 86:2910–2922

Viard M, Parolini I, Rawat SS, Fecchi K, Sargiacomo M, Puri A, Blumenthal R (2004) The role of glycosphingolipids in HIV signaling, entry and pathogenesis. Glycoconj J 20:213–222

Viard M, Parolini I, Sargiacomo M, Fecchi K, Ramoni C, Ablan S, Ruscetti FW, Wang JM, Blumenthal R (2002) Role of cholesterol in human immunodeficiency virus type 1 envelope protein-mediated fusion with host cells. J Virol 76:11584–11595

Vincent N, Genin C, Malvoisin E (2002) Identification of a conserved domain of the HIV-1 transmembrane protein gp41 which interacts with cholesteryl groups. Biochim Biophys Acta 1567:157–164

Waarts BL, Bittman R, Wilschut J (2002) Sphingolipid and cholesterol dependence of alphavirus membrane fusion Lack of correlation with lipid raft formation in target liposomes. J Biol Chem 277:38141–38147

Waheed AA, Shimada Y, Heijnen HF, Nakamura M, Inomata M, Hayashi M, Iwashita S, Slot JW, Ohno-Iwashita Y (2001) Selective binding of perfringolysin O derivative to cholesterol-rich membrane microdomains (rafts). Proc Natl Acad Sci USA 98:4926–4931

Wanaski SP, Ng BK, Glaser M (2003) Caveolin scaffolding region and the membrane binding region of SRC form lateral membrane domains. Biochemistry 42:42–56

Wang J, Gunning W, Kelley KM, Ratnam M (2002) Evidence for segregation of heterologous GPI-anchored proteins into separate lipid rafts within the plasma membrane. J Membr Biol 189:35–43

Widmer F, Caroni P (1990) Identification, localization, and primary structure of CAP-23, a particle-bound cytosolic protein of early development. J Cell Biol 111:3035–3047

Woodman SE, Schlegel A, Cohen AW, Lisanti MP (2002) Mutational analysis identifies a short atypical membrane attachment sequence (KYWFYR) within caveolin-1. Biochemistry 41:3790–3795

Yamaji-Hasegawa A, Makino A, Baba T, Senoh Y, Kimura-Suda H, Sato SB, Terada N, Ohno S, Kiyokawa E, Umeda M, Kobayashi T (2003) Oligomerization and pore formation of a sphingomyelin-specific toxin, lysenin. J Biol Chem 278:22762–22770

Zhelev DV, Needham D (1993) Tension-stabilized pores in giant vesicles: determination of pore size and pore line tension. Biochim Biophys Acta 1147:89–104

Lateral Membrane Structure and Lipid–Protein Interactions

Jesús Pérez-Gil, Antonio Cruz, Jorge Bernardino de la Serna

5.1 Introduction

The assembly of lipid-based membranes was a crucial step for triggering the evolution of living cells in the prebiotic scenario. The hydrophobic barrier imposed by the lipid bilayers was essential for the isolation of different protocellular compartments and allowing for an independent and progressively complex evolution of small portions of the primordial soup (Deamer 1986; Szostak et al. 2001; Orgel 2004). These protomembranes were likely to be compositionally complex and functionally imperfect at first and their main role was to ensure and preserve compartmentalization. The subsequent coevolution of membranes and compartmentalized biomolecules, such as nucleic acids and polypeptides, may have utilized the membrane as a potential support structure for new functions. One can envision the adsorptive processes of the membrane surface as an important component of primitive catalysis (Pohorille and Wilson 1995; Orgel 2004). If proteins were the chosen molecules to carry out most of the chemical transformations, the association of proteins with the membrane surely played a major part in the development of their efficiency. Membrane interacting properties were probably selectable traits because they allowed proteins to localize, orientate, and accumulate in defined microenvironments where finding the proper counterparts introduced a significant entropic component to the cellular processes. Coevolution of membrane-associated proteins and the membranes themselves could progressively initiate the whole variety of protein promoted membrane activities we can identify in modern cells, including membrane enzymes, signaling pathways, or the crucial establishment of transport mechanisms to ensure transference of mass and energy between the cell and the environment in a regulated way.

The model proposed for the structure of membranes by Singer and Nicholson in the 1970s provided a simplified picture of the final portrait of those protein–lipid coevolutive processes (Singer and Nicolson 1972). Phospholipids may be organized in bilayers and these bilayers may be the structural support for proteins embedded to different extents. Both proteins and lipids freely diffuse in the plane of the membrane, but the proteins are the real role players of most membrane-associated functions. This model has been refined to incorporate, for instance, the role of the cytoskeleton in organizing membrane-confined compartments (Kusumi et al. 1993) through the direct participation of proteins via lipid–protein and protein–protein interactions. This view of the lipid moiety of the membranes as a mere structural element that creates an impermeable space between proteins

Springer Series in Biophysics
C.R. Mateo et al. (Ed.)
Protein-Lipid Interactions

has persisted until recent years. The proposal of the existence in the membranes of specialized lipid platforms or "rafts" has challenged this paradigm and has brought into question the fundamental role of lipids in organizing and regulating membrane complexity (Simons and Ikonen 1997; Edidin 2003).

Most membrane processes and the function of many membrane proteins are now being re-evaluated after considering the concept of a non-homogeneous membrane structure. However, the mechanism of the formation and the dynamics of these lipid domains in biological membranes is not well understood. In particular, there is considerable controversy concerning the kind of domains that exist in real membranes and the role of lipid composition in imposing domain segregation, with or without the necessary participation of defined proteins. Although the raft hypothesis is very much centered on the behavior of particular lipid segregates, such as those triggered by sphingolipid/cholesterol complexation, there are probably many other events in the cell membrane leading to lipid lateral self-organization. Furthermore, the concept of rafts, as discussed in cell biology, has probably little to do with the properties defining domain segregation under a more physico-chemical view of the membranes.

Returning to the evolutionary perspective, the establishment of protein–lipid interactions would be expected to provide an advantage in those early times of inhomogeneous membranes. If the membrane offered a surface where proteins and substrates could concentrate and where potential protein–protein interactions and formation of complexes would be favored, the existence of lipid domains or clusters in the membrane would be even more effective provided that some molecules showed selective association with particular lipid regions. Such specialized domain-promoted lipid–protein interactions could have been further optimized to form the basis of molecular mechanisms occurring in modern membranes. If this is true, both a heterogeneous lipid composition of membranes producing complex in-plane organizations and selective domain-dependent protein–lipid interactions should have persisted and be present in modern membranes and membrane proteins. The present review summarizes the evidence pointing to the existence of such traits both in model and natural membranes, and demonstrates the importance of lipid lateral organization in defining membrane structure and membrane protein structure–function relationships.

5.2 Lateral Lipid Organization in Membranes

Several processes have been proposed for producing non-homogeneous in-plane organization of different lipid species in membranes (Binder et al. 2003). Some of these processes suggest self-organization due to equilibration of the membrane system towards thermodynamically favorable states, without a necessary major participation of specific lipid–lipid interactions. An example of this type of process is the phase separation that spontaneously occurs in bilayers made from a mixture of lipids with significantly different gel-to-fluid transition temperatures (Tm), where segregation of phases occurs at temperatures between the Tm's of the different lipids (Fig. 5.1b) (Bagatolli and Gratton 2000; 2000a,b).

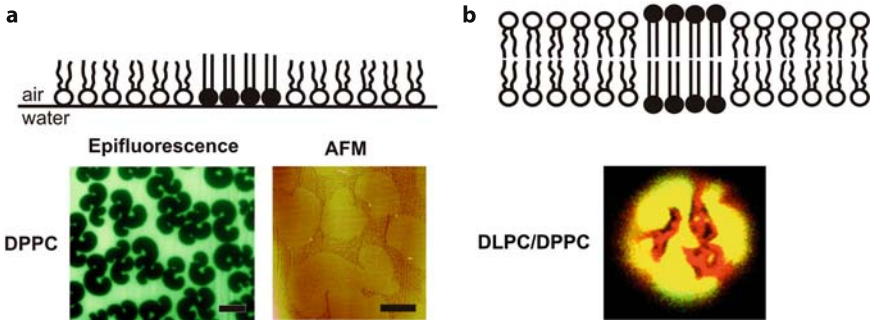

Fig. 5.1. Gel/fluid-like phase coexistence in phospholipid monolayers and bilayers. (**a**) Liquid-condensed/liquid-expanded regions coexist in interfacial films of dipalmitoylphosphatidylcholine (DPPC) compressed to 11 mN/m, at 25°C. Condensed domains were visualized either by exclusion of 1 mol% of the fluorescent probe NBD-PC in the epifluorescence images (scale bar, 25 μm), or by their greater thickness visualized with AFM of films transferred onto mica supports (scale bar, 10 μm). (**b**) Gel/liquid crystalline phase coexistence in giant unilamellar vesicles (GUVs) made of an equimolar mixture of dilauroylphosphatidylcholine (DLPC) and DPPC at 25°C in the presence of 0.5 mol% fluorescent probe rhodamine-dipalmitoylphosphatidylethanolamine (Rh-DPPE) (Bagatolli and Gratton 2000a)

The molecules of the component with the higher Tm nucleate and segregate into highly packed ordered regions excluding the more disordered molecules of the lipid with lower Tm, which still have chains with a high number of spontaneous *trans-gauche* isomerizations, at these intermediate temperatures. Phase separation can be envisaged as a typical entropically driven phenomenon. The process can be easily modeled in interfacial monolayers where the packing state of the lipids can be controlled by compressing or expanding the films in a surface balance (Fig. 5.1a) (Nag and Keough 1993; Mohwald et al. 1995). Single phospholipid monolayers compressed to pressures into the liquid-expanded to liquid-condensed transition plateau show coexistence of condensed highly packed regions with disordered loosely packed areas. Films made from a mixture of two lipids with significantly different Tm's show two-dimensional phase segregation at a wide range of lateral pressures, including those thought to be equivalent to the ones occurring in cellular membranes (around 30 mN/m). Phase separation has also been observed in membrane bilayers made of phospholipids with very different chain lengths, especially, although not exclusively, at temperatures inducing gel-like solid phases (Fig. 5.1b). This should also be considered an entropy-driven process because the phase separation minimizes the amount of hydrophobic segments, arising from the hydrophobic mismatch of the different lipids, which are potentially exposed to the polar solvent.

Alternatively, certain lipid complexes could be established by selective or preferential molecular interactions that also induce lateral organization of lipids in processes that may be considered not only entropic, but also enthalpically driven. For instance, this would be the case for the lipid–lipid interactions that

induce the formation of the sphingolipid/cholesterol complexes thought to be the basis for the organization of rafts (Veiga et al. 2001; Collado et al. 2005). In this case, hydrogen bonding between the amide of the sphingomyelin skeleton and the hydroxyl of cholesterol would supply an important stabilizing energy. Formation of other lipid condensates, such as the phosphatidylcholine/cholesterol condensed complexes proposed by McConnell (McConnell and Vrljic 2003; McConnell 2005), would still have a mainly entropic origin. This demonstrates that entropic and enthalpic contributions for membrane domain triggering cannot be easily separated. Simple ternary mixtures containing variable proportions of saturated and unsaturated phospholipid species and cholesterol show that two fluid phases exist in both interfacial monolayers and bilayers (Fig. 5.2) (Dietrich et al. 2001; Veatch and Keller 2002; Veatch and Keller 2003).

The saturated lipid molecules tend to pack with cholesterol and form what is called a liquid-ordered (lo) phase. The lipid acyl chains are mostly extended and tightly packed against the planar structure of the sterol forming an "ordered phase", while the unsaturated lipid molecules maintain a high degree of translational mobility forming a "fluid phase". The ability of the sphingomyelin backbone to form a hydrogen bond with the cholesterol molecule increases the affinity between these two components, favoring segregation of the sphingolipid/cholesterol complexes from unsaturated lipid-enriched regions in membranes. These complexes are extraordinarily resistant to detergent solubilization (Shogomori and Brown 2003; Chamberlain 2004). Other processes can also produce lateral organization via a major enthalpic contribution, for instance, the segregation that occurs in mixtures of charged and non-charged lipids in the presence of proper counter-charged molecules (Russ et al. 2003; Mbamala et al. 2005).

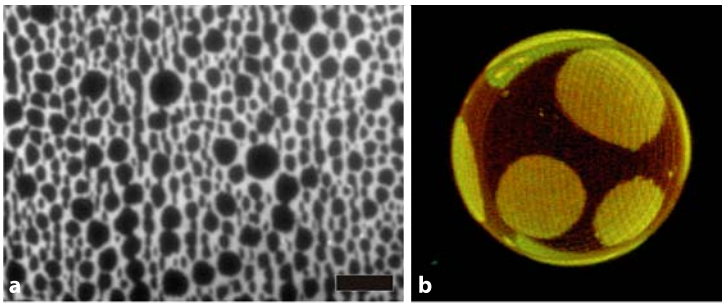

Fig. 5.2. Fluid/fluid-like phase coexistence in lipid monolayers and bilayers. (**a**) Fluid-ordered/fluid-disordered coexistence in interfacial films made of egg yolk phosphatidylcholine (PC)/bovine brain sphingomyelin (SM)/Cholesterol (Chol) (25:45:30, w/w/w) compressed to 17 mN/m at 25°C. (**b**) Liquid-ordered/liquid-disordered phase coexistence in GUVs made of the ternary mixture dioleoylphosphatidylcholine (DOPC)/DPPC/Chol (30:30:40, w/w/w) in the presence of 0.5 mol% BODIPY-PC and 0.5 mol% $DiIC_{18}$. Scale bar in the left panel represents 25 μm and image in the right panel also have 25 μm width

Simplistic molecular mechanisms for producing lateral sorting of lipids in membranes are often invoked to explain the nature of membrane domains. However, the compositional complexity of the real membranes could sustain simultaneous processes, perhaps synergistically potentiated or mutually influenced, that promote membrane lateral organization to different extents and lead to the coexistence of many different types of lipid domains. In this context, the notion of rafts, as is often used in the literature, can be misleading.

Lateral separation of domains or phases in lipid membranes due to some of these different processes has been mostly documented in simple model systems such as vesicles or interfacial monolayers made of structurally different lipids. Under the appropriate environmental conditions, spontaneous self-organized micrometer-sized domains can be visualized in model bilayers or monolayers (Binder et al. 2003). The study of these models demonstrates that pure lipid systems may have defined intrinsic properties for lateral self-organization, providing a structural scaffold that is probably very sensitive to compositional complexity. Microscopic techniques such as epifluorescence or Brewster angle microscopy are suitable to detect and analyze lateral domains in the microscopic size range, while atomic or scanning force microscopy (AFM, SFM) has produced pictures showing lipid domains from micrometer to hundreds of nanometer size. Other techniques, such as fluorescence resonance energy transfer (FRET), fluorescence quenching (Silvius 2003; de Almeida et al. 2005), or more recently, fluorescence correlation spectroscopy (FCS) (Kahya et al. 2004) have provided indirect evidence for the existence of membrane domains in the size range of a few nanometers. However, little is known about the occurrence of lipid self-organizing processes in the context of compositionally complex cellular membranes. Recent studies have shown that native membranes from the pulmonary surfactant system maintain a stable

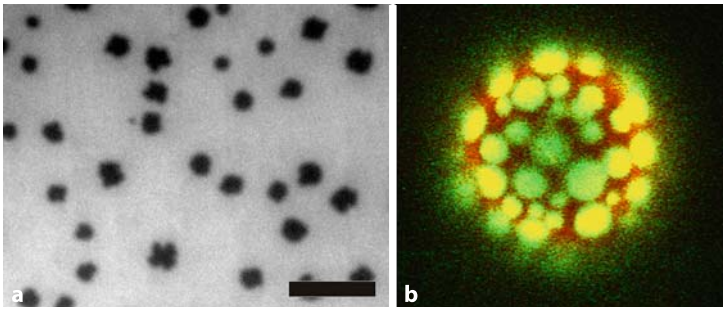

Fig. 5.3. Presence of condensed regions in pulmonary surfactant monolayers and bilayers. (**a**) Dark condensed domains in interfacial monolayers made from an organic extract of porcine pulmonary surfactant, containing all the lipid components plus the hydrophobic proteins SP-B and SP-C with 1 mol% NBD-PC added and compressed to 35 mN/m at 25°C. (**b**) Coexistence of fluid-ordered (*red*) and fluid-disordered (*yellow*) regions in GUVs made from organic extracted material from porcine pulmonary surfactant doped with 0.5 mol% BODIPY-PC and 0.5 mol% $DiIC_{18}$. Scale bars in left panels represent 25 μm and images in right panels also have 25 μm width

coexistence of two fluid phases in the form of micrometer-sized fluid disordered domains immersed in a cholesterol-enriched fluid-ordered background (Fig. 5.3) (Bernardino de la Serna et al. 2004).

Liposomes made from the full lipid fraction extracted from certain membranes also show the coexistence of ordered and disordered regions (Dietrich et al. 2001; Nag et al. 2002). These experiments indicate that the lipid fraction of membranes plays a major role in determining their lateral structure. Considerable effort is being directed toward the detection of membrane domains in the membranes of whole cells. Several studies have shown the existence of large micrometer sized domains in certain cell membranes (Gousset et al. 2002; Gaus et al. 2003). Other studies suggest that domains in intact cell membranes could be very small and highly dynamic, thus making their detection and morphological characterization a technical challenge (Helms and Zurzolo 2004; Kusumi et al. 2004; Simons and Vaz 2004). It may be difficult to distinguish between the presence of real "domains" with a defined lifetime and what could be considered transient lipid fluctuations caught in a given instant (Nielsen et al. 2000).

5.3 Membrane Lateral Organization and Lipid–Protein Interactions

As suggested from an evolutionary perspective, proteins could have sensed in different ways the lateral structure imposed by the heterogeneous composition of the lipid matrix when interacting with the membrane. Partition of a protein from the aqueous bulk phase into the membrane interface requires the initial establishment of thermodynamically favorable interactions of specific protein regions with groups at the interfacial environment. Structural contributions to membrane partitioning, both at the sequence and at the conformational level, of membrane-associating proteins have been extensively analyzed in recent years (Wimley and White 1996; White and Wimley 1998). Once at the membrane interface, the properties of particular protein regions could define their eventual insertion or translocation into the most hydrophobic regions of the membrane. Lipid packing and lateral pressure are likely additional determinants influencing the interaction and insertion of proteins into the membrane (Marsh 1996; Tillman and Cascio 2003; van den Brink-van der Laan et al. 2004). Common experiments have used monolayer models for the determination of the maximal pressure permitting interaction of any given protein or peptide with a lipid layer. Only proteins increasing the surface pressure above 30 mN/m are typically considered as potentially competent to interact with deep regions of the membranes (Brockman 1999). Lateral heterogeneities in the membrane could regionally differ in properties such as: (1) the chemical interfacial environment that defines the initial partitioning of polypeptides from the bulk phase, (2) the transient exposure and accessibility of hydrophobic regions of the membrane, (3) the lipid packing and lateral pressure, or (4) the thickness of the membrane.

There are several examples in the literature of proteins that seem to show preferential interaction with defined membrane regions of a particular lipid compo-

sition or structure. It is difficult to evaluate what is the most prominent factor for such discrimination. Different membrane proteins have different membrane requirements for both initiating the lipid–protein interaction and stabilizing a

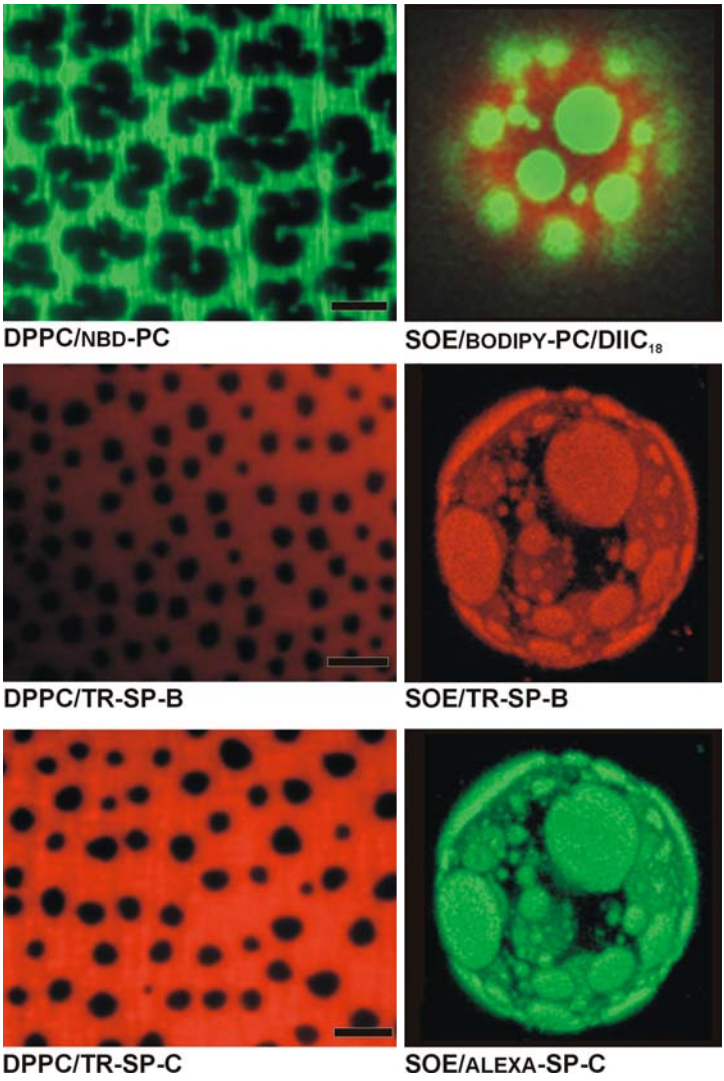

Fig. 5.4. Lateral distribution of hydrophobic proteins SP-B and SP-C in monolayers and bilayers of pulmonary surfactant. Lateral separation of ordered and disordered regions in pulmonary surfactant layers results in accumulation of proteins SP-B and SP-C in the most disordered phases in both interfacial phospholipid films (*left images*) or giant vesicles formed with material from surfactant organic extract (SOE) (*right images*). Scale bars in left panels represent 25 μm and images in right panels also have 25 μm width

given disposition. For example, the thickness of particular membrane patches has been proposed to be a major determinant for promoting proper protein sorting during intracellular trafficking (Harder 2003). Regulated post-translational modifications, such as acylation, seem to direct specific proteins to particular membrane domains (Mukherjee et al. 2003; Neumann-Giesen et al. 2004; Shogomori et al. 2005). Therefore, the lateral structure of the lipid matrix could impose major restrictions on the lateral distribution and sorting of the membrane proteome. Preferential distribution of any given membrane protein into a particular region or phase of the membrane presumably defines important functional features, such as local protein densities or the probability of the protein encountering homologous or heterologous counterparts (Fig. 5.4).

As a consequence, environmental conditions producing alterations in the lateral structure of the membrane could lead to profound rearrangements of membrane-associated protein distributions. This would have major implications on the establishment and organization of selective protein–protein interaction networks. It remains to be demonstrated whether cellular membranes actually support such dynamic behavior under physiologically relevant conditions. A recent study has demonstrated that the transfer of transmembrane protein segments into the membrane of the endoplasmic reticulum, as it passes through the translocon, is predominantly mediated by the thermodynamic rules governing lipid–protein interactions (Hessa et al. 2005). It still remains to be determined how the structure of the membrane itself, including the existence of compositional and structural heterogeneities, influences membrane protein assembly *in vivo*. It has been proposed that the composition of natural membranes may have been optimized to maintain the membranes close to the edge of an abrupt structural transition. This would have potentially major effects on the membrane lateral structure and domain organization (Grabitz et al. 2002). Membranes at that "edge" might show a very dynamic behavior that is sensitive to respond, perhaps via redistribution of the protein network, to environmental demands.

Membrane regions at the boundaries between different phases or domains could be especially amenable for supporting lipid–protein interactions. These boundaries have been proposed to posses lipid packing defects, which could be used by certain protein motifs to access deeper regions of the membrane interface (Saez-Cirion et al. 2002; Barlic et al. 2004; Cruz et al. 2004). Therefore, some proteins might require the presence of membrane heterogeneities to initiate partitioning into the membrane surface. Experiments with monolayers suggest that the boundaries between different phases, in systems showing liquid-expanded/liquid-condensed phase coexistence, act as thermodynamic "sinks", trapping proteins or other molecules, virtual "impurities", that do not mix well with the lipid matrix (Fig. 5.5) (Ruano et al. 1998).

Some membrane-associated proteins may accumulate into these boundaries, where the dynamics may directly regulate important structural and functional protein features. It has been suggested that association of certain protein segments with the boundaries of some membrane domains could precede protein accumulation and membrane translocation (Saez-Cirion et al. 2002; Barlic et al. 2004).

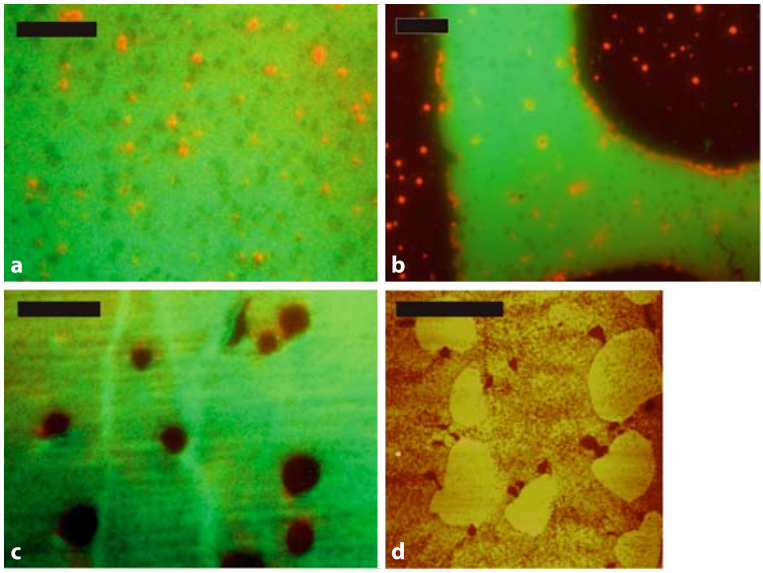

Fig. 5.5. Examples observed in interfacial films of preferential association of proteins with the boundaries of condensed domains. (**a**) Formation of clusters of pretransmembrane peptide from HIV protein gp41 associated with raft-like domains of monolayers made from POPC/SM/Chol (2/1/1, mole ratio) at 32 mN/m and 25°C. Green fluorescence is emitted by the probe fluorescein-dipalmitoylphosphatidylethanolamine (FL-DPPE) and red fluorescence from rhodamine-labeled peptide (Saez-Cirion et al. 2002). (**b**) Accumulation of the cytolysin equinatoxin-II at the boundaries between ordered and disordered phases in the monolayers of SM/PC/Chol (50/14/35, mol ratios) compressed to 25 mN/m at 25°C. Green fluorescence was emitted from NBD-PC and red fluorescence from Texas Red-labeled protein (Barlic et al. 2004). (**c**) Accumulation of Texas Red-labeled surfactant protein SP-C in the surroundings of liquid-condensed domains of DPPC compressed to 11 mN/m. (**d**) Two-dimensional clusters of surfactant protein SP-B segregated to the boundary regions close to liquid-condensed domains of DPPC interfacial films observed by AFM (Cruz et al. 2004)

A specialized case may exist for proteins possessing structural motifs with the ability to recognize specific lipid species, such as occurs with the increasing number of cholesterol-binding proteins (Shimada et al. 2002; Khan et al. 2003). Aromatic side-chains in these cholesterol-binding motifs seem to associate favorably with the planar cholesterol rings and form clusters that mutually potentiate both lipid and protein segregation. Interaction of these proteins with membranes would occur predominantly in cholesterol-enriched domains, where proteins with such motifs could accumulate.

It is debatable whether the selective interaction of certain membrane proteins with selected lipid species is sufficient to initiate organization of lipid domains in the plane of the membrane, which might consequently produce further lipid and protein sorting. It has been shown that the acetylcholine receptor accretes a

phosphatidic acid-enriched membrane environment (Poveda et al. 2002). Likewise, some cholesterol-binding proteins have been proposed to nucleate formation of cholesterol segregates that, by virtue of selective cholesterol–sphingolipid interactions, could progress towards producing a raft-like membrane structure (Epand et al. 2001; Epand et al. 2003). Protein initiated reorganization of the lateral structure of the membrane could be the signal to recruit other lipid and protein partners. This has been proposed for the molecular mechanisms behind certain signaling platforms (Zhang et al. 1998; Bunnell et al. 2002). While the literature suggests apparently contradictory models confronting lipid-directed versus protein-directed mechanisms for organization of in-plane membrane structure, there is no doubt that an intense "lateral" cross-talk between lipids and proteins occurs and is responsible for the complex structure of real cellular membranes. The lateral cross-talk between lipids and proteins as potential regulatory mechanisms of cellular function is only starting to be envisaged.

5.4 Lipid Domains and Protein–Protein Interactions

The study of cellular membrane lateral structure has gained considerable interest in the last few years. It has been proposed that organization of membrane domains could be the basis for the assembly of functional platforms that promote the selective encounter of certain proteins and the subsequent activation of specific processes. A well-known example of these platforms is the raft-like domains. Raft-like domains are supposed to promote accumulation and association of certain transmembrane proteins (Coffin et al. 2003), proteins anchored to membranes via phosphatidylinositol (Cordy et al. 2003), or proteins covalently modified with long acyl chains (Zhang et al. 1998; Shogomori et al. 2005). On the other hand, domains accumulating lipids with a high prevalence of saturated long chains have been proposed to favor the accumulation of membrane proteins with particularly long transmembrane domains (Ait Slimane and Hoekstra 2002; Bonifacino and Traub 2003; Helms and Zurzolo 2004). The opposite rationalization has also been proposed in some cases. Association and accumulation of specific membrane proteins in selected populations of lipids might constitute a driving force for inducing compositional and structural regionalization of particular membrane forms (Zhang et al. 2000; Kropshofer et al. 2002).

Whatever the initiating force, several models have been proposed for the regulatory mechanisms that link protein clustering and activation with the localization of protein complexes in defined membrane domains. Integrin-mediated adhesion (Hogg et al. 2002) or platelet activation (Tablin et al. 2001), the assembly of the so-called "immunological synapse" (Cherukuri et al. 2001), caveolae-mediated endocytosis (Nabi and Le 2003), and the coupling and budding of viral particles (Chazal and Gerlier 2003; Nayak et al. 2004) are all processes putatively triggered, regulated, and optimized within the framework of specialized lateral membrane domains. The study of environmental factors and molecules directed to modify membrane lateral organization should contribute to confirming the role of the

membrane as a major element regulating cellular functions and identify new classes of targets in the search for therapeutic drugs.

Acknowledgements. We sincerely thank Dr. Luis Bagatolli, from the University of Southern Denmark, Odense, for fruitful scientific discussions and for providing us with pictures of giant unilamellar vesicles. We are also grateful to Drs. Jose Luis Nieva and Juan Manuel Gonzalez-Mañas, from Basque Country University, for their valuable comments and help in obtaining the pictures of the HIV pretransmembrane peptide and the cytotoxin equinatoxin interacting with membrane domains. Research in the laboratory of the authors is being funded by a grant from the Spanish Ministry of Science and Education (BIO2003-09056).

References

Ait Slimane T, Hoekstra D (2002) Sphingolipid trafficking and protein sorting in epithelial cells. FEBS Lett 529:54–9

Bagatolli LA, Gratton E (2000a) A correlation between lipid domain shape and binary phospholipid mixture composition in free standing bilayers: A two-photon fluorescence microscopy study. Biophys. J 79:434–47

Bagatolli LA, Gratton E (2000b) Two photon fluorescence microscopy of coexisting lipid domains in giant unilamellar vesicles of binary phospholipid mixtures. Biophys J 78:290–305

Barlic A, Gutierrez-Aguirre I, Caaveiro JM, Cruz A, Ruiz-Arguello MB, Perez-Gil J, Gonzalez-Manas JM (2004) Lipid phase coexistence favors membrane insertion of equinatoxin-II, a pore-forming toxin from Actinia equina. J Biol Chem 279:34209–16

Bernardino de la Serna J, Perez-Gil J, Simonsen AC, Bagatolli LA (2004) Cholesterol rules: direct observation of the coexistence of two fluid phases in native pulmonary surfactant membranes at physiological temperatures. J Biol Chem 279:40715–22

Binder WH, Barragan V, Menger FM (2003) Domains and rafts in lipid membranes. Angew Chem Int Ed Engl 42:5802–27

Bonifacino JS, Traub LM (2003) Signals for sorting of transmembrane proteins to endosomes and lysosomes. Annu Rev Biochem 72:395–447

Brockman H (1999) Lipid monolayers: why use half a membrane to characterize protein–membrane interactions? Curr Opin Struct Biol 9:438–43

Bunnell SC, Hong DI, Kardon JR, Yamazaki T, McGlade CJ, Barr VA, Samelson LE (2002) T cell receptor ligation induces the formation of dynamically regulated signaling assemblies. J Cell Biol 158:1263–75

Chamberlain LH (2004) Detergents as tools for the purification and classification of lipid rafts. FEBS Lett 559:1–5

Chazal N, Gerlier D (2003) Virus entry, assembly, budding, and membrane rafts. Microbiol Mol Biol Rev 67:226–37, table of contents

Cherukuri A, Dykstra M, Pierce SK (2001) Floating the raft hypothesis: lipid rafts play a role in immune cell activation. Immunity 14:657–60

Coffin WF, 3rd, Geiger TR, Martin JM (2003) Transmembrane domains 1 and 2 of the latent membrane protein 1 of Epstein–Barr virus contain a lipid raft targeting signal and play a critical role in cytostasis. J Virol 77:3749–58

Collado MI, Goni FM, Alonso A, Marsh D (2005) Domain formation in sphingomyelin/cholesterol mixed membranes studied by spin-label electron spin resonance spectroscopy. Biochemistry 44:4911–8

Cordy JM, Hussain I, Dingwall C, Hooper NM, Turner AJ (2003) Exclusively targeting beta-secretase to lipid rafts by GPI-anchor addition up-regulates beta-site processing of the amyloid precursor protein. Proc Natl Acad Sci USA 100:11735–40

Cruz A, Vazquez L, Velez M, Perez-Gil J (2004) Effect of pulmonary surfactant protein SP-B on the micro- and nanostructure of phospholipid films. Biophys J 86:308–20

de Almeida RF, Loura LM, Fedorov A, Prieto M (2005) Lipid rafts have different sizes depending on membrane composition: a time-resolved fluorescence resonance energy transfer study. J Mol Biol 346:1109–20

Deamer DW (1986) Role of amphiphilic compounds in the evolution of membrane structure on the early earth. Orig Life Evol Biosph 17:3–25

Dietrich C, Bagatolli LA, Volovyk ZN, Thompson NL, Levi M, Jacobson K, Gratton E (2001) Lipid rafts reconstituted in model membranes. Biophys J 80:1417–28

Edidin M (2003) The state of lipid rafts: from model membranes to cells. Annu Rev Biophys Biomol Struct 32:257–83

Epand RM, Maekawa S, Yip CM, Epand RF (2001) Protein-induced formation of cholesterol-rich domains. Biochemistry 40:10514–21

Epand RM, Sayer BG, Epand RF (2003) Peptide-induced formation of cholesterol-rich domains. Biochemistry 42:14677–89

Gaus K, Gratton E, Kable EP, Jones AS, Gelissen I, Kritharides L, Jessup W (2003) Visualizing lipid structure and raft domains in living cells with two-photon microscopy. Proc Natl Acad Sci USA 100:15554–9

Gousset K, Wolkers WF, Tsvetkova NM, Oliver AE, Field CL, Walker NJ, Crowe JH, Tablin F (2002) Evidence for a physiological role for membrane rafts in human platelets. J Cell Physiol 190:117–28

Grabitz P, Ivanova VP, Heimburg T (2002) Relaxation kinetics of lipid membranes and its relation to the heat capacity. Biophys J 82:299–309

Harder T (2003) Formation of functional cell membrane domains: the interplay of lipid- and protein-mediated interactions. Phil Trans R Soc Lond B Biol Sci 358:863–8

Helms JB, Zurzolo C (2004) Lipids as targeting signals: lipid rafts and intracellular trafficking. Traffic 5:247–54

Hessa T, Kim H, Bihlmaier K, Lundin C, Boekel J, Andersson H, Nilsson I, White SH, von Heijne G (2005) Recognition of transmembrane helices by the endoplasmic reticulum translocon. Nature 433:377–81

Hogg N, Henderson R, Leitinger B, McDowall A, Porter J, Stanley P (2002) Mechanisms contributing to the activity of integrins on leukocytes. Immunol Rev 186:164–71

Kahya N, Scherfeld D, Bacia K, Schwille P (2004) Lipid domain formation and dynamics in giant unilamellar vesicles explored by fluorescence correlation spectroscopy. J Struct Biol 147:77–89

Khan TK, Yang B, Thompson NL, Maekawa S, Epand RM, Jacobson K (2003) Binding of NAP-22, a calmodulin-binding neuronal protein, to raft-like domains in model membranes. Biochemistry 42:4780–6

Kropshofer H, Spindeldreher S, Rohn TA, Platania N, Grygar C, Daniel N, Wolpl A, Langen H, Horejsi V, Vogt AB (2002) Tetraspan microdomains distinct from lipid rafts enrich select peptide-MHC class II complexes. Nat Immunol 3:61–8

Kusumi A, Koyama-Honda I, Suzuki K (2004) Molecular dynamics and interactions for creation of stimulation-induced stabilized rafts from small unstable steady-state rafts. Traffic 5:213–30

Kusumi A, Sako Y, Yamamoto M (1993) Confined lateral diffusion of membrane receptors as studied by single particle tracking (nanovid microscopy). Effects of calcium-induced differentiation in cultured epithelial cells. Biophys J 65:2021–40

Marsh D (1996) Lateral pressure in membranes. Biochim Biophys Acta 1286:183–223

Mbamala EC, Ben-Shaul A, May S (2005) Domain formation induced by the adsorption of charged proteins on mixed lipid membranes. Biophys J 88:1702–14

McConnell H (2005) Complexes in ternary cholesterol–phospholipid mixtures. Biophys J 88: L23–5

McConnell HM, Vrljic M (2003) Liquid–liquid immiscibility in membranes. Annu Rev Biophys Biomol Struct 32:469–92

Mohwald H, Dietrich A, Bohm C, Brezesinski G, Thoma M (1995) Domain formation in monolayers. Mol Membr Biol 12:29–38

Mukherjee A, Arnaud L, Cooper JA (2003) Lipid-dependent recruitment of neuronal Src to lipid rafts in the brain. J Biol Chem 278:40806–14

Nabi IR, Le PU (2003) Caveolae/raft-dependent endocytosis. J Cell Biol 161:673–7

Nag K, Keough KM (1993) Epifluorescence microscopic studies of monolayers containing mixtures of dioleoyl- and dipalmitoylphosphatidylcholines. Biophys J 65:1019–26

Nag K, Pao JS, Harbottle RR, Possmayer F, Petersen NO, Bagatolli LA (2002) Segregation of saturated chain lipids in pulmonary surfactant films and bilayers. Biophys J 82:2041–51

Nayak DP, Hui EK, Barman S (2004) Assembly and budding of influenza virus. Virus Res 106:147–65

Neumann-Giesen C, Falkenbach B, Beicht P, Claasen S, Luers G, Stuermer CA, Herzog V, Tikkanen R (2004) Membrane and raft association of reggie-1/flotillin-2: role of myristoylation, palmitoylation and oligomerization and induction of filopodia by overexpression. Biochem J 378:509–18

Nielsen LK, Bjornholm T, Mouritsen OG (2000) Fluctuations caught in the act. Nature 404:352

Orgel LE (2004) Prebiotic chemistry and the origin of the RNA world. Crit Rev Biochem Mol Biol 39:99–123

Pohorille A, Wilson MA (1995) Molecular dynamics studies of simple membrane–water interfaces: structure and functions in the beginnings of cellular life. Orig Life Evol Biosph 25:21–46

Poveda JA, Encinar JA, Fernandez AM, Mateo CR, Ferragut JA, Gonzalez-Ros JM (2002) Segregation of phosphatidic acid-rich domains in reconstituted acetylcholine receptor membranes. Biochemistry 41:12253–62

Ruano ML, Nag K, Worthman LA, Casals C, Perez-Gil J, Keough KM (1998) Differential partitioning of pulmonary surfactant protein SP-A into regions of monolayers of dipalmitoylphosphatidylcholine and dipalmitoylphosphatidylcholine/dipalmitoylphosphatidylglycerol. Biophys J 74:1101–9

Russ C, Heimburg T, von Grunberg HH (2003) The effect of lipid demixing on the electrostatic interaction of planar membranes across a salt solution. Biophys J 84:3730–42

Saez-Cirion A, Nir S, Lorizate M, Agirre A, Cruz A, Perez-Gil J, Nieva JL (2002) Sphingomyelin and cholesterol promote HIV-1 gp41 pretransmembrane sequence surface aggregation and membrane restructuring. J Biol Chem 277:21776–85

Shimada Y, Maruya M, Iwashita S, Ohno-Iwashita Y (2002) The C-terminal domain of perfringolysin O is an essential cholesterol-binding unit targeting to cholesterol-rich microdomains. Eur J Biochem 269:6195–203

Shogomori H, Brown DA (2003) Use of detergents to study membrane rafts: the good, the bad, and the ugly. Biol Chem 384:1259–63

Shogomori H, Hammond AT, Ostermeyer-Fay AG, Barr DJ, Feigenson GW, London E, Brown DA (2005) Palmitoylation and intracellular-domain interactions both contribute to raft targeting of linker for activation of T cells (LAT). J Biol Chem 280:18931–18942

Silvius JR (2003) Role of cholesterol in lipid raft formation: lessons from lipid model systems. Biochim Biophys Acta 1610:174–83

Simons K, Ikonen E (1997) Functional rafts in cell membranes. Nature 387:569–72

Simons K, Vaz WL (2004) Model systems, lipid rafts, and cell membranes. Annu Rev Biophys Biomol Struct 33:269–95

Singer SJ, Nicolson GL (1972) The fluid mosaic model of the structure of cell membranes. Science 175:720–31

Szostak JW, Bartel DP, Luisi PL (2001) Synthesizing life. Nature 409:387–90

Tablin F, Wolkers WF, Walker NJ, Oliver AE, Tsvetkova NM, Gousset K, Crowe LM, Crowe JH (2001) Membrane reorganization during chilling: implications for long-term stabilization of platelets. Cryobiology 43:114–23

Tillman TS, Cascio M (2003) Effects of membrane lipids on ion channel structure and function. Cell Biochem Biophys 38:161–90

van den Brink-van der Laan E, Killian JA, de Kruijff B (2004) Nonbilayer lipids affect peripheral and integral membrane proteins via changes in the lateral pressure profile. Biochim Biophys Acta 1666:275–88

Veatch SL, Keller SL (2002) Organization in lipid membranes containing cholesterol. Phys Rev Lett 89:268101

Veatch SL, Keller SL (2003) Separation of liquid phases in giant vesicles of ternary mixtures of phospholipids and cholesterol. Biophys J 85:3074–83

Veiga MP, Arrondo JL, Goni FM, Alonso A, Marsh D (2001) Interaction of cholesterol with sphingomyelin in mixed membranes containing phosphatidylcholine, studied by spin-label ESR and IR spectroscopies. A possible stabilization of gel-phase sphingolipid domains by cholesterol. Biochemistry 40:2614–22

White SH, Wimley WC (1998) Hydrophobic interactions of peptides with membrane interfaces. Biochim Biophys Acta 1376:339–52

Wimley WC, White SH (1996) Experimentally determined hydrophobicity scale for proteins at membrane interfaces. Nat Struct Biol 3:842–8

Zhang J, Pekosz A, Lamb RA (2000) Influenza virus assembly and lipid raft microdomains: a role for the cytoplasmic tails of the spike glycoproteins. J Virol 74:4634–44

Zhang W, Trible RP, Samelson LE (1998) LAT palmitoylation: its essential role in membrane microdomain targeting and tyrosine phosphorylation during T cell activation. Immunity 9:239–46

The Membrane as a System: How Lipid Structure Affects Membrane Protein Function

Anthony G. Lee

6.1 Introduction

A proper understanding of how lipids and proteins interact in a membrane requires a prior knowledge of the properties of the lipid bilayer component of the membrane. Previous reviews have considered the structures of membrane proteins and how membrane proteins sit in the surrounding lipid bilayer (Lee 2003), and how lipid binding to membrane proteins might affect protein function (Lee 2004). The aim of this review is to summarize some of the key information we have about lipid bilayers and show how this helps us to identify the interactions that are likely to be most important for membrane protein structure and function.

6.2 The Structure of a Lipid Bilayer

High-resolution structures cannot be obtained for bilayers in the liquid crystalline phase because the thermal motion and disorder in the bilayer means that the positions of the atoms are relatively ill-defined. Nevertheless, a picture of the bilayer can be developed, showing the average spatial distribution of atoms or groups of atoms, projected along the direction normal to the bilayer surface (White and Wiener 1995). The structure of a bilayer of dioleoylphosphatidylcholine (di(C18:1)PE) in the liquid crystalline phase at relatively low hydration (5.4 water molecules per lipid molecule), determined by a combination of X-ray and neutron diffraction methods, is shown in Fig. 6.1 (Wiener and White 1992). The structure is represented by a number of fragments, and Fig. 6.1 shows the fraction of each fragment to be found (the probability of finding the fragment) at any given position along the direction of the bilayer normal. The width of the peak representing each fragment provides an estimate of the range of thermal motion for the fragment, in the direction of the bilayer normal. The narrowest of the regions is that corresponding to the glycerol backbone region, indicating that this is the most rigid part of the structure. Extents of motion generally increase with increasing distance from the backbone, both out to the choline of the headgroup and down the fatty acyl chains to the terminal methyl groups, but the wider distribution for the C=C double bonds than for either the carbonyl or the terminal

Springer Series in Biophysics
C.R. Mateo et al. (Ed.)
Protein-Lipid Interactions

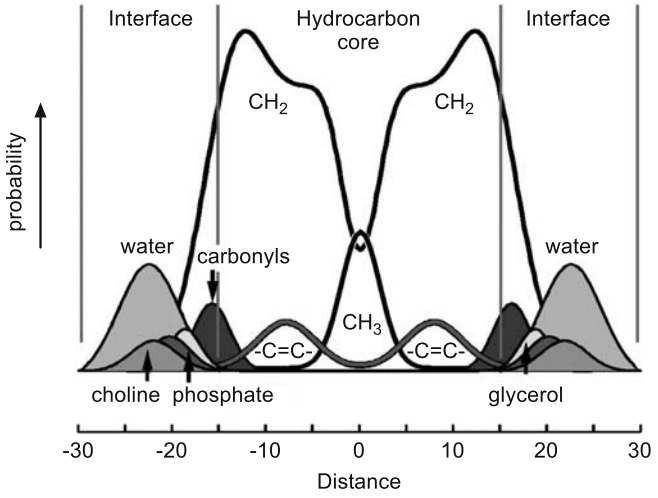

Fig. 6.1. The structure of a bilayer of di(C18:1)PC at 23°C at low hydration. The figure shows projections onto the bilayer normal of the time-averaged transbilayer distributions of the principal structural groups. Fragments shown are the methyls (CH_3), methylenes (CH_2), double bonds (C=C), carbonyls, the glycerol backbone, the phosphate and choline groups of the headgroup, and water. Modified from White et al. (2001)

methyl groups implies increased thermal motion in this region of the fatty acyl chain (Wiener and White 1992).

The glycerol backbone region lies at the extreme boundaries of both the methylene and water distributions and thus marks the water–hydrocarbon interface. The combined thicknesses of the interface regions on the two sides of the bilayer, defined as the distance from the choline to the glycerol group, are comparable to that of the hydrocarbon core of the bilayer (Fig. 6.1), so that it is clear that the bilayer cannot be represented as just a "slab" of hydrocarbon. As described later, the hydrophobic thickness of a fully hydrated bilayer of di(C18:1)PC is significantly less than that for the partially hydrated sample represented in Fig. 6.1.

6.2.1 Glycerol Backbone and Headgroup Structures

Useful information about glycerol backbone and headgroup structures in a liquid crystalline bilayer can be deduced from X-ray diffraction studies of crystalline lipids (Pascher et al. 1992). The crystal structures for dilauroylphosphatidylethanolamine [di(C12:0)PE] and dimyristoylphosphatidylcholine [di(C14:0)PC] are shown in Fig. 6.2; the lipid headgroups lie parallel to the bilayer surface with very similar conformations. These conformations reflect the tendency of the ammonium nitrogen to fold back towards the phosphate groups so as to minimize the distance between the groups of opposite charge. The conformation of the glycerol

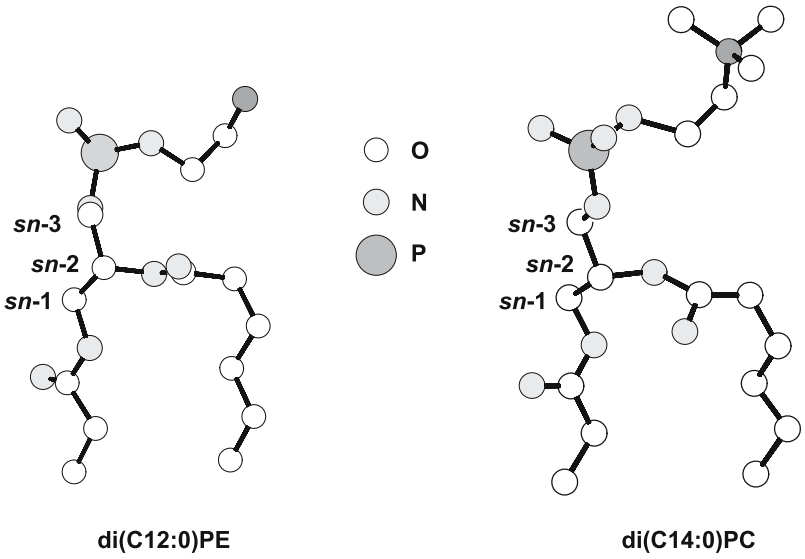

Fig. 6.2. Headgroup conformations of phosphatidylethanolamine [di(C12:0)PE] and phosphatidylcholine [di(C14:0)PC; molecule 2 in the unit cell]. The three glycerol carbons are marked *sn*-1 to *sn*-3. Coordinates from Harlos et al. (1984) and Pearson and Pascher (1979)

diester group is such that the initial part of the *sn*-2 fatty acyl chain extends parallel to the bilayer surface but then bends sharply at the second carbon atom (Fig. 6.2). As a consequence, the *sn*-1 chain extends further into the bilayer than the *sn*-2 chain. The axial displacement of the two chains, 3.7 Å, is equivalent to three methylene groups. In natural lipids, this difference is minimized since longer fatty acyl chains are normally found at the *sn*-2 position rather than at the *sn*-1 position. The glycerol backbone is oriented almost perpendicular to the bilayer surface with the *sn*-1 chain continuing in this direction forming an antiplanar zigzag chain together with the glycerol moiety (Fig. 6.2).

In the crystal of di(C12:0)PE the headgroups are arranged in antiparallel rows, with hydrogen bonds between the nitrogen atoms and the non-esterified phosphate oxygen atoms of neighbouring molecules (Pascher et al. 1992). The small separations between the nitrogen and oxygen atoms (2.7–2.9 Å) have the character of both hydrogen bonds and ionic interactions. The structure of the di(C14:0)PC dihydrate is more complex (Pearson and Pascher 1979). The molecular area occupied by di(C14:0)PC is the same as that occupied by di(C12:0)PE (39 $Å^2$), but this is too small for the more bulky phosphorylcholine headgroup. The phosphatidylcholine molecules therefore pack in pairs, mutually displaced in the direction perpendicular to the bilayer surface. This means that the effective surface area per molecule is kept small. The headgroup conformations of the two crystallographically independent molecules making up each pair are very similar, being approximately mirror images of each other. Hydrogen bonding of the type observed in phosphatidylethanolamine between the ammonium and phosphate

groups is not possible with the $-N(CH_3)_3^+$ group in a phosphatidylcholine. Indeed, because of the bulky nature of the choline group, the nitrogen atom comes no closer than 4.5 Å to the phosphate oxygens. Instead, the negatively charged phosphate groups are separated and shielded by water molecules of hydration. In the dihydrate, two water molecules are located between neighbouring phosphate ester groups, forming an infinite hydrogen bonded ribbon: phosphate(1)–water–phosphate(2)–water. Lateral interactions between phosphatidylcholine molecules can thus be expected to be weaker than those between molecules of phosphatidylethanolamine.

Very similar backbone and headgroup structures have been suggested from NMR and neutron diffraction studies for phosphatidylethanolamines and phosphatidylcholines in liquid crystalline phase bilayers in the presence of excess water. The conformational inequivalence of the two chains is maintained, with the glycerol backbone lying parallel to the bilayer normal (Seelig and Seelig 1975; Zaccai et al. 1979), although the chain equivalence is reduced compared to that in the crystal, and the terminal methyl ends of the two chains are out of step by only about 1.8 Å (Zaccai et al. 1979). X-ray diffraction studies of di(C18:1)PC and a brominated analogue show that, in the liquid crystalline phase, the positions of the double bonds in the *sn*-1 and *sn*-2 chains, when projected onto the bilayer normal, can be no more than 1 Å apart (Wiener et al. 1991).

Studies using neutron scattering have shown that the lipid headgroups in phosphatidylcholines and phosphatidylethanolamines are oriented roughly parallel to the bilayer surface in the liquid crystalline phase in excess water (Buldt and Wohlgemuth 1981), as in the crystal structures. These headgroup structures represent average orientations, since molecular dynamics simulations show that there is considerable motion in the headgroup region of the bilayer, the orientation of the P–N vector in a phosphatidylcholine, for example, varying, for individual molecules, from an angle of zero with respect to the bilayer normal, so that the NMe_3^+ group is pointing out into the solvent, to values greater than 90°, so that the NMe_3^+ group is pointing into the hydrocarbon core of the bilayer (Heller et al. 1993; Stouch et al. 1994; Hyvonen et al. 1997). The conformation of the phosphorylcholine headgroup is affected by the charge on the membrane, the headgroup acting as a molecular voltmeter (Seelig et al. 1987). Incorporation of positive charge into the membrane results in repulsion of the positively charged choline group, with a tilting of the $^-P–N^+$ dipole away from the surface of the membrane; conversely, introduction of negative charge attracts the choline group, pulling the $^-P–N^+$ dipole towards the surface (Seelig et al. 1987).

For phosphatidylserines, the glycerol backbone and headgroup structures are dependent on pH (Sanson et al. 1995). At acid pH, when the phosphatidylserine headgroup is zwitterionic with no net charge, the glycerol backbone conformation is very similar to that in a phosphatidylcholine or phosphatidylethanolamine, lying parallel to the bilayer normal. However, this changes at neutral pH, when the headgroup becomes negatively charged; the glycerol backbone is now oriented perpendicular to the bilayer normal, the conformation observed for negatively charged phospholipids in crystals. Whereas the headgroup lies parallel to the bilayer surface at acid pH (again as for phosphatidylcholine or phosphatidylethanolamine), at neutral pH it is more extended; this increases the distance

between the serine carboxylate group and the layer of negatively charged phosphate groups, minimizing electrostatic interactions.

The ceramide backbone of glycosphingolipids in liquid crystalline bilayers also adopts a structure with a sharp bend in the fatty acyl chain away from the bilayer surface at C2, comparable to the bend in the *sn*-2 chain of the phosphatidylcholines (Johnston and Chapman 1988). However, it has been suggested that dialkylphospholipids adopt a structure in the liquid crystalline state in which the *sn*-2 chain is fully extended with no bend at C2 (Lohner 1996); the presence of two ester groups (in the diacylphospholipids and diacylglycerol) or an ester and an –OH group (in the glycosphingolipids) would seem to determine packing in the lipid backbone region of the bilayer. Despite the differences in the glycerol backbone region for the ester and ether linked phosphatidylcholines, the time-averaged conformations of the phosphorylcholine headgroups are the same (Paltauf 1994).

Our knowledge of the water structure close to a lipid bilayer surface is rather limited. This is unfortunate since interactions between lipid headgroups and water is likely to have a major effect on packing in the headgroup region, and possibly on interactions with membrane proteins. There are three regions in a phospholipid headgroup that are likely to be involved in interaction with water: the ester oxygens, the phosphate oxygens, and the carboxyl, amino, or tetramethylammonium groups of phosphatidylserine, phosphatidylethanolamine and phosphatidylcholine, respectively, although interaction of water with the tetramethylammonium group may be relatively weak. The extent of hydration is very different for phosphatidylcholines and phosphatidylethanolamines. At full hydration, a bilayer of dipalmitoylphosphatidylcholine [di(C16:0)PC] takes up about 23 molecules of water per molecule of lipid (Nagle and Wiener 1988), whereas a bilayer of di(C12:0)PE takes up only about 10 molecules of water per molecule of lipid (McIntosh and Simon 1986). The first few water molecules to bind, bind tightly to the phosphate group and are motionally restricted (Volke et al. 1994). Further water molecules, although distinct from bulk water, are in fast exchange with bulk water. Measurements of NMR spin lattice relaxation times for deuterated water as a function of lipid hydration suggest that between about 11 and 16 water molecules occupy the first hydration shell around a phosphatidylcholine headgroup (Borle and Seelig 1983). In a molecular dynamics simulation of di(C16:0)PC, an average of 10.2 water molecules were found hydrating the $-NMe_3^+$ group in a clathrate-like cluster, 4.0 water molecules hydrating the phosphate, and one water molecule hydrating a carbonyl group (Marrink and Berendsen 1994). NMR studies, however, suggest, at least at low temperatures, that only five water molecules are needed to form a solvation shell around the $-NMe_3^+$ group (Hsieh and Wu 1997).

Molecular dynamic simulations of bilayers of di(C14:0)PC show that the headgroups are linked into clusters by water molecules and by charge interactions between the positively charged choline groups of one di(C14:0)PC molecule and the phosphate or carbonyl oxygen atoms of another molecule (Pasenkiewicz-Gierula et al. 1999). Strong intermolecular interactions between choline and phosphate groups on neighbouring molecules has been demonstrated in $^{31}P-^{1}H$ nuclear Overhauser experiments on phospholipid bilayers (Yeagle 1978) and molecular

dynamics simulations suggest that intermolecular charge interactions are much more important than intramolecular interactions between the choline and phosphate and carbonyl oxygens on the same molecule (Pasenkiewicz-Gierula et al. 1999). As well as salt bridges, the headgroups are linked by multiple water bridges, the water molecules hydrogen bonding mostly to the phosphate and carbonyl oxygens (Pasenkiewicz-Gierula et al. 1999). Individual water molecules exchange in and out of the lipid clusters relatively rapidly. The presence of an unsaturated fatty acyl chain increases the area occupied by the phospholipid molecule and increases the distance between the headgroups, leading to less interaction between the headgroups and increased accessibility of carbonyl and phosphate oxygens to water, with increased hydration of the lipid headgroup (Murzyn et al. 2001).

The pattern of hydration observed in simulations of a bilayer of a phosphatidylethanolamine was distinctly different to that observed for a phosphatidylcholine (Damodaran and Merz 1994; Zhou and Schulten 1995). Whereas the hydrophobic $-NMe_3^+$ group induced formation of a clathrate-like hydration shell around the headgroups in order to optimize interwater hydrogen bonding, direct hydrogen bonds are formed between the $-NH_3^+$ group and the water molecules. Although interlipid hydrogen bonds are observed in the headgroup region of the phosphatidylethanolamine, more hydrogen bonds are formed with water; the hydrogen bonding interlipid network is much weaker than that observed in the crystal (Zhou and Schulten 1995).

6.2.2 Fatty Acyl Chain Region of the Bilayer

One characteristic of the liquid crystalline phase is the considerable intramolecular motion of the lipid fatty acyl chains, due to rotation about C–C bonds in the chains. The change in steric energy that results from rotation about the C_6–C_7 single bond in dodecane is shown in Fig. 6.3. The minimum potential energy occurs when the two neighbouring methylene groups are related by a dihedral angle of 0°, in the *trans* conformation. Two other minima are obtained at torsion angles of 115 and 245°, corresponding to the *gauche*+ and *gauche*– conformations, respectively. These conformations have energies 3.7 kJ mol^{-1} above that of the all-*trans* conformation, and to reach the *gauche*+ or gauche– conformations from the *trans* conformation the molecule has to move over an energy barrier of 14.0 kJ mol^{-1}. The relative sharpness of the minima and the quite high barriers to rotation mean that the molecule will remain for most of the time in the vicinity of the minima, carrying out torsional oscillations.

Introduction of a *cis*-double bond into a fatty acyl chain has a significant effect on motion in the chain (Rich 1993; Li et al. 1994). Figure 6.3 also shows the steric energy as a function of the torsion angle α_1 describing rotation about the C_7–C_8 bond adjacent to the carbon–carbon double bond in *cis*-dodecene-6. The energy profile is characterized by a very broad peak from 120 to 240° and a narrower and smaller peak centred at 0°. Two broad minima are observed centred at 65 and 295°. The energy barrier to rotation between these two minima is just 8.1 kJ mol^{-1}, 5.9 kJ mol^{-1} less than the corresponding energy in a saturated chain. Thus the car-

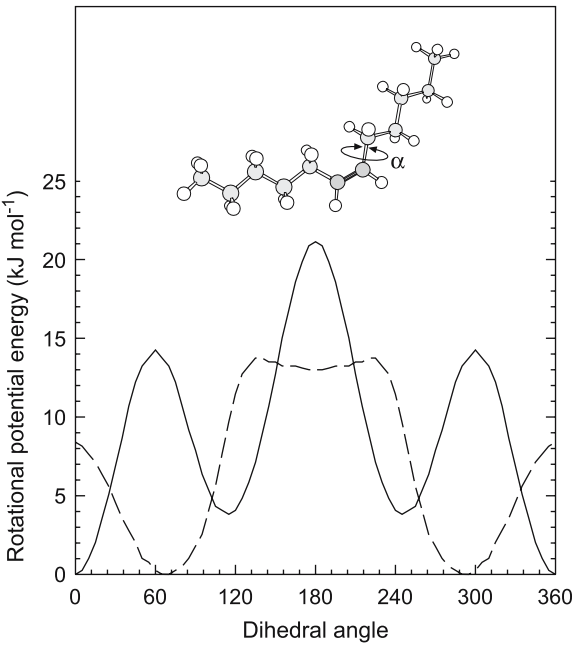

Fig. 6.3. Steric energy changes as a function of the torsion angle about the C6–C7 bond in dodecane (*solid line*) or about the C7–C8 bond in cis-dodecene-6 (broken line). Calculations were performed using MM3 force fields (Allinger et al. 1989)

bon–carbon single bond adjacent to a rigid *cis* double bond has more freedom of motion than the corresponding bond in a saturated chain. The shallowness of the potential energy wells around 65° suggests that the C–C bond adjacent to a double bond can readily adopt a wide range of torsion angles (Li et al. 1994).

The extent or range of motion in a fatty acyl chain can be described by an *order parameter* that defines the time-averaged disposition in space of each group of atoms in the fatty acyl chain. The rate of motion can be described in terms of a *correlation time*, a measure of the rate of movement of a group of atoms between its various possible positions in space. Formally, fluidity (and its inverse, viscosity) corresponds solely to rate of motion. The most powerful technique for measuring order parameters is ^{2}H-NMR, studying the motion of C–D groups introduced at specific positions in the chains (Seelig and Seelig 1980; Bloom et al. 1991). Order parameter profiles for all phospholipid bilayers in the liquid crystalline phase are remarkably similar; that for the saturated palmitoyl chain in 1-palmitoyl-2-oleoylphosphatidylcholine [(C16:0, C18:1)PC] is shown in Fig. 6.4 (Seelig and Seelig 1980). The magnitudes of the order parameters are observed to lie between the values expected for an all-*trans* chain rotating about its long axis ($S_{CD} = -0.5$) and for complete orientational disorder, as found in an isotropic liquid ($S_{CD} = 0$). Thus the fatty acyl chain region exists in a state of intermediate order, with some order persisting despite the liquid-like state of the chains. The degree of order varies along the chain; an initial plateau region of constant order is followed by a region of rapidly decreasing order towards the centre of the bilayer. The plateau region has its origin in the intermolecular restrictions on chain motion. In the upper part of the chain excluded volume effects are very important since rotation

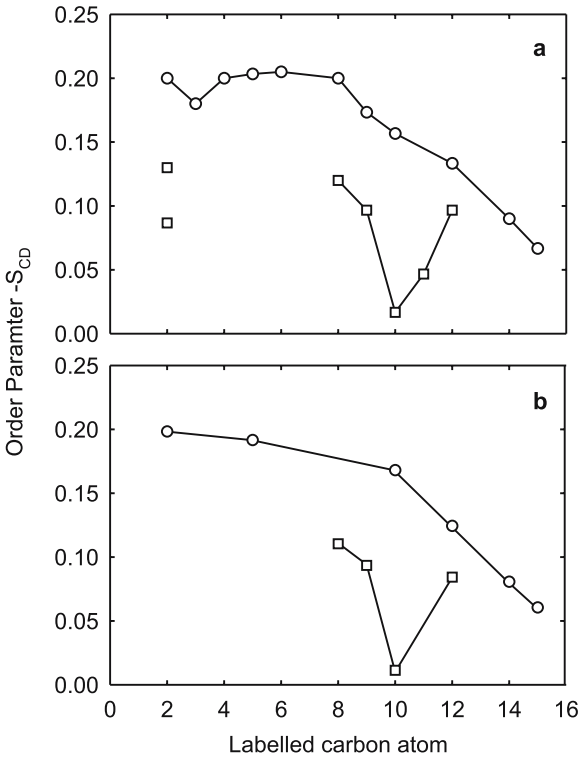

Fig. 6.4. The experimental order parameters ($-S_{CD}$) for the palmitoyl (○) and oleoyl (□) chains of: (**a**) (C16:0,C18:1)PC (POPC); (**b**) lipids of *E. coli* labelled in the palmitoyl (○) and oleoyl (□) chains. Modified from Seelig and Seelig (1980)

about a single C–C bond results in a large bend in the chain. Lower down the chain, lateral displacements resulting from rotations about single C–C bonds are very much smaller, and, therefore, steric restrictions on motion become less important. The order parameter profile for the palmitoyl chain in (C16:0, C18:1)PC is very similar to that observed in di(C16:0)PC, but with order being slightly higher in bilayers of di(C16:0)PC than in bilayers of (C16:0,C18:1)PC, suggesting that introduction of a *cis* double bond results in a slight disordering of the bilayer (Seelig and Seelig 1980). This effect could follow from the effect of the "bent" *cis*-double bond on motion in the bilayer, but it could also reflect the fact that at 42°C, the temperature of the experiment shown in Fig. 6.4, (C16:0,C18:1)PC is about 50°C above its phase transition temperature, whereas di(C16:0)PC with a phase transition temperature of 42°C would only just have entered the liquid crystalline phase.

Interpretation of the order parameter profile for the unsaturated chain in (C16:0,C18:1)PC is more complex than for the saturated chain (Fig. 6.4). The experimental order parameters for carbons atoms 10 and 11 are low in the oleoyl chain. This does not, however, indicate a high degree of motional disorder for these carbons, but rather follows from effects of the *cis* double bond on the orientation of C–D bonds with respect to the bilayer normal. Since the measured spectra for a C–D bond depend not only on the true molecular order parameter

but also on the angle between the C–D bond and the applied magnetic field direction (or bilayer normal), this will have a large effect on the measured spectra; the dip in order parameter following the *cis* double bond shown in Fig. 6.4 follows largely from the special geometry of the *cis* double bond (Heller et al. 1993). Nevertheless, molecular dynamics simulations do show an increased motion for the C=C double bond and the methylene groups next to it, particularly for that on the terminal methyl side (Heller et al. 1993; Huang et al. 1994). Increased disorder in the region of the double bond could follow from a cooperative effect of the double bond on the way that lipid molecules pack within the bilayer or could be a result of the shallow energy barriers for rotation about C–C bonds adjacent to a double bond, as described above (Fig. 6.3).

In conclusion we can say that the effects of a single *cis* C=C double bond on motion of fatty acyl chains in a bilayer are rather modest. It might have been thought that the presence of a single *cis* double bond towards the middle of a fatty acyl chain would have led to a significant packing problem because of the sharp bend in the chain at the double bond. This indeed is the basis of the large decrease in phase transition temperature observed on introduction of a single double bond into phosphatidylcholines or phosphatidylethanolamines. However, the data in Fig. 6.4 suggest that in a liquid crystalline bilayer the oleoyl chain is unlikely to contain a sharp bend; by C12 the order parameter has a value very similar to that observed in the corresponding position of a saturated chain.

Larger effects of unsaturation can be expected for polyunsaturated chains. As for monounsaturated chains, description of chain motion for a polyunsaturated chain is more difficult than for a saturated chain. The effects of polyunsaturation have been studied in a series of phosphatidylcholines with a deuterated stearoyl chain at the *sn*-1 position and an unsaturated chain at the *sn*-2 position. Effects are rather small, with the *sn*-1 chain becoming slightly more disordered as the unsaturation of the *sn*-2 chain is increased, the effect of unsaturation reaching a maximum at three double bonds (Holte et al. 1995). The largest changes in order occur around the centre of the chain, with relatively little change in the top part of the chain close to the glycerol backbone. The effects of a polyunsaturated chain have been shown to depend slightly on the position of unsaturation (McCabe et al. 1994).

It had been suggested that chains such as linoleic acid or docosahexaenoic acid (DHA) containing a 1,4-pentadiene structure might have unique conformational properties and that the presence of six *cis*-double bonds in DHA might reduce chain flexibility (Applegate and Glomset 1986). However, the DHA chain in fact shows considerable flexibility with a greater lateral compressibility than a saturated chain because the presence of the *cis*-double bonds leads to increased rates of interconversion between torsional states, because of a decrease in energy barriers (Feller et al. 2002). It has been suggested that the extreme flexibility for the DHA chain could be important for interaction with membrane proteins. A molecular dynamics simulation of rhodopsin in a bilayer of 1-stearoyl-2-docosohexaenoyl-phosphatidylcholine showed that the DHA chains penetrate deeper into the protein interface than do the stearic acid chains (Feller et al. 2003). It was suggested that the extreme flexibility of the DHA chain could allow it to adapt better to the rugged surface of the protein (Feller et al. 2003).

Profiles of chain order are almost unaffected by the lipid headgroup, although absolute values of order parameters can be affected. Thus order parameters for phosphatidylethanolamines in the liquid crystalline phase are almost constant for the first part of the chain, but decrease rapidly towards the terminal methyl group, as for the phosphatidylcholines, but the order parameters are higher for phosphatidylethanolamines than for phosphatidylcholines, at all positions of the chain (Perly et al. 1985; Lafleur et al. 1990). The higher order parameters in phosphatidylethanolamines can be attributed to the smaller headgroup of the phosphatidylethanolamine and to strong intermolecular hydrogen bonding between the headgroups, both factors leading to a greater packing density throughout the bilayer. However, differences in packing density in the chain region between phosphatidylcholines and phosphatidylethanolamines must be quite small since the thicknesses of bilayers of di(C18:1)PC and di(C18:1)PE are equal (Fenske et al. 1990).

The chain order parameter profile for dipalmitoylphosphatidylserine [di(C16:0)PS] is also very similar to that for di(C16:0)PC along most of the length of the chain; order parameters are, however, slightly less in di(C16:0)PS than for

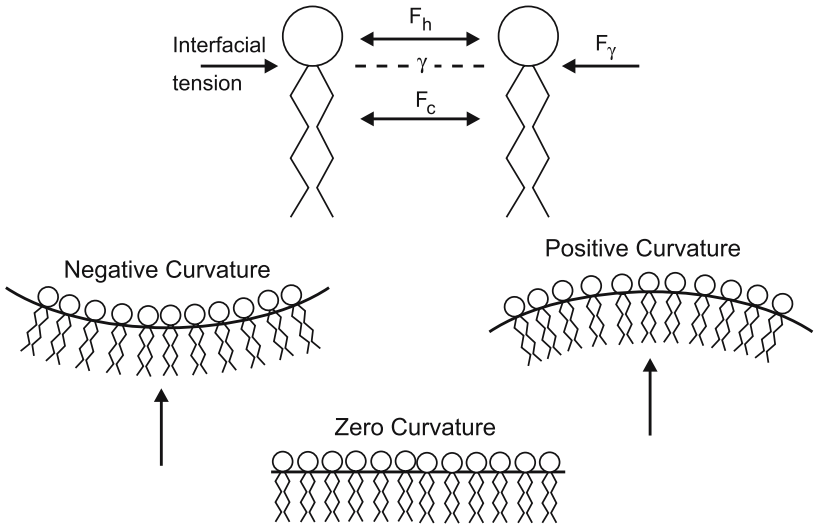

Fig. 6.5. The forces present in a lipid bilayer. At the top is shown the distribution of lateral pressures and tensions across a lipid monolayer. The repulsive lateral pressure F_c in the chain region is due to thermally activated bond rotational motion. The interfacial tension γ, tending to minimize the interfacial area, arises from the hydrophobic effect (unfavourable hydrocarbon–water contacts). Finally, the lateral pressure F_h in the headgroup region arises from steric, hydrational and electrostatic effects; it is normally repulsive, but may contain attractive contributions from, for example, hydrogen bonding interactions. After Seddon (1990). Below is shown the tendency for spontaneous curvature of a lipid monolayer arising from an imbalance in the distribution of lateral forces across the monolayer. The arrows show the direction of observation used in the definition of negative and positive curvature

di(C16:0)PC for the first few carbon atoms of the chain (Seelig and Seelig 1975). The order parameter profile for dimyristoylphosphatidic acid [di(C14:0)PA] is also very like that for di(C16:0)PC (Laroche et al. 1990; Pott et al. 1995).

6.2.2.1 How Similar is the Hydrocarbon Core of a Lipid Bilayer to that of a Simple Liquid Alkane?

The stability of a lipid bilayer is determined largely by the balance between hydrophobic interactions, which tend to decrease the interfacial area between the lipids and water, and inter- and intramolecular interactions, including headgroup hydration, which give rise to a net repulsion, tending to increase the surface area of the bilayer (Marsh 1996). The lateral stresses involved have been illustrated by Seddon (1990) as in Fig. 6.5. At about the position of the glycerol backbone region, an attractive force F_Y arises from the unfavourable contact of the hydrocarbon chains with water (the hydrophobic effect). Tight packing in this region ensures the minimum exposure of the hydrocarbon interior of the membrane to water, leading to a negative lateral pressure (a positive membrane tension), tending to contract the bilayer. A repulsive lateral pressure F_h arises in the headgroup region because of steric, hydrational and electrostatic effects. Similarly, in the hydrocarbon interior of the membrane, attractive van der Waals interactions between the chains will be opposed by the repulsive interactions due to the thermal motions of the chains.

An important question is whether anchoring of lipid fatty acyl chains to the glycerol backbone leads to unusually high "pressures" within the hydrocarbon core of a lipid bilayer. Comparisons between the properties of lipid bilayers and simple alkanes suggest that this is not so. An analysis of NMR spin–lattice relaxation times has suggested that *trans–gauche* isomerization rates (10^9–10^{10} s^{-1}) in fatty acyl chains in a lipid bilayer are very similar to those in a free chain, and that the effective viscosity for the bilayer is ca. 0.01 P (Poastor et al. 1988). This can be compared with the viscosity of neat hexadecane at 50°C, which is 0.019 P (Small 1986). Thus the internal dynamics of a fatty acyl chain in a membrane are very similar to those in a neat alkane, despite the reduction in orientational freedom for the chain. Despite the highly anisotropic motion of the acyl chains, the molecular packing of the chains in the liquid crystalline bilayer is also equivalent to that of a liquid alkane, with average methylene and methyl group volumes in the bilayer interior of 28 and 54 $Å^3$, respectively (Petrache et al. 1997), comparable to the methylene and methyl group volumes in a liquid alkane of 27 and 57 $Å^3$, respectively (Nagle and Wiener 1988). Methylene and methyl group volumes are almost identical for bilayers of di(C18:1)PC, di(C16:0)PC, and di(C12:0)PE in the liquid crystalline phase (Armen et al. 1998; Nagle and Tristram-Nagle 2000). Further, it has been suggested that the average volume occupied by a methylene group varies little with transverse distance from the bilayer centre (Armen et al. 1998; Nagle and Tristram-Nagle 2000). Thus it is clear that the large hydration and van der Waals pressures in the bilayer have little effect on the packing of the chains.

6.2.3 Dimensions of a Lipid Bilayer

The hydrophobic thickness of a membrane has been taken to be the thickness of the central hydrocarbon slab up to the C2 carbons of the chains (Lewis and Engelman 1983). This definition corresponds closely to the separation between the positions of the carbonyl groups in Fig. 6.1 (Wiener and White 1992). The positions of the carbonyls therefore mark the hypothetical hydrocarbon slab boundaries – hypothetical because the extent of the thermal motions is such that there is a significant overlap between the distributions of the various fragments making up the bilayer, with a number of methylene groups extending beyond the edge of the interface defined by the position of the carbonyl groups (Fig. 6.1).

The hydrophobic thickness d of a lipid bilayer of a saturated phosphatidylcholine in the liquid crystalline phase in excess water is related to fatty acyl chain length by the equation

$$d = 1.75\ (n - 1) \tag{6.1}$$

where n is the number of carbon atoms in the fatty acyl chain (Lewis and Engelman 1983; Sperotto and Mouritsen 1988). The thickness of a bilayer of a phosphatidylcholine with two monounsaturated chains was estimated by Lewis and Engelman (1983) to be about 2.5 Å less than that of the corresponding phosphatidylcholine with two saturated chains estimated from (6.1). The thickness of a bilayer of di(C18:0)PC calculated from (6.1) is 29.7 Å, giving a thickness for a bilayer of di(C18:1)PC of about 27.2 Å, in good agreement with the estimated thickness given by Nagle and Tristram-Nagle (2000), which is 27.1 Å. The hydrophobic thickness of a bilayer of di(C18:1)PC at low hydration estimated from the data shown in Fig. 6.1 is 32 Å, (Lewis and Engelman 1983; Wiener and White 1992); the thickness of a bilayer is known to increase with decreasing hydration (Nagle and Tristram-Nagle 2000). The hydrophobic thickness of a bilayer of (C18:0,C22:6)PC is 30.5 Å (Eldho et al. 2003) very close to the value calculated from (6.1) for a bilayer of an unsaturated PC with the average chain length of C20 (30.7 Å). Changing headgroup structure has only a small effect on hydrophobic thickness (Rand et al. 1988). The hydrophobic thickness of a bilayer of di(C18:1)PE (30.8 Å) is just 3.6 Å greater than that of a bilayer of di(C18:1)PC (Petrache et al. 2004).

The area per lipid molecule is an important parameter in theoretical models of lipid bilayers. The area occupied in the bilayer surface by a molecule of di(C16:0)PC in the liquid crystalline phase at 50°C has been determined to be 64 $Å^2$ (Nagle and Tristram-Nagle 2000). This compares with an area of 72.5 $Å^2$ for di(C18:1)PC in the liquid crystalline state (Nagle and Tristram-Nagle 2000); the greater area occupied by di(C18:1)PC follows from effects of the unsaturated oleoyl chains. For liquid crystalline bilayers of di(C12:0)PE, the surface area per lipid is 51.2 $Å^2$ (Nagle and Tristram-Nagle 2000). This compares to a value of 56 $Å^2$ for 1-palmitoyl-2-oleoylphosphatidylethanolamine ((C16:0,C18:1)PE) (Rand et al. 1988); the greater area occupied by (C16:0,C18:1)PE can again be attributed to the presence of the bulky *cis* unsaturated chain. Values in the range 50–55 $Å^2$ have been reported for the surface area of di(C16:0)PS in the liquid crystalline

phase (Cevc et al. 1981; Demel et al. 1987). This is about 10% smaller than for di(C16:0)PC, an effect attributed to strong intermolecular interaction between the phosphatidylserine headgroups (Lopez Cascales et al. 1996).

6.2.4 Mixing of Lipids in the Liquid Crystalline Phase

The fluid nature of the liquid crystalline phase means that lipid molecules mix well in the liquid crystalline phase (Lee 1977). Thus there is no evidence for immiscibility in the liquid crystalline phase, even for mixtures of two lipids with very different fatty acyl chain lengths such as di(C12:0)PC and di(C18:0)PC, where phase separation in the gel phase is very extensive (Shimshick and McConnell 1973). Mixtures of branched chains phosphatidylcholines are also miscible in the liquid crystalline phase (Dorfler and Miethe 1990). The small degree of non-ideality in mixing that is observed is such that like molecules will be slightly more likely to be neighbours than expected for totally random mixing (Lee 1977). This is consistent with the results of small-angle neutron scattering studies, which show random mixing in the liquid crystalline phase for mixtures of di(C14:0)PC and di(C16:0)PC, but a significant non-random distribution for mixtures of di(C14:0)PC and di(C18:0)PC, the non-random mixing favouring the clustering of like molecules (Knoll et al. 1981, 1983). The mixing properties of phosphatidylethanolamines with different chain lengths are very similar to those described above for the phosphatidylcholines (Lee 1977).

6.2.5 Non-Bilayer Phases

Most, if not all, biological membranes contain lipids that, in isolation, prefer to adopt a curved, hexagonal H_{II} phase rather than the normal, planar, bilayer phase (Cullis and de Kruijff 1979; Rietveld et al. 1993). Sometimes such lipids can be the major lipids in a membrane: for example, monogalactosyl diacylglycerol makes up about 50% of the total lipid in the chloroplast membrane (Shipley et al. 1973) and the *E. coli* inner membrane contains about 70% phosphatidylethanolamine (Harwood and Russell 1984). It has been suggested that bacteria control the lipid compositions of their membranes to maintain a constant proportion of lipids favouring the hexagonal H_{II} phase (for a recent review, see Cronan 2003).

The tendency of phospholipids such as phosphatidylethanolamines to adopt a curved structure can be understood in terms of the forces present in a lipid bilayer, as shown in Fig. 6.5 (Gruner 1985; Seddon 1990; Lindahl and Edholm 2000). For a lipid monolayer to stay flat, the pressures illustrated in Fig. 6.5 must be in balance across the monolayer. If the lateral pressure in the chain region becomes greater than that between the headgroups, the monolayer will curl towards the aqueous region (Fig. 6.5). This is defined as a negative curvature. Conversely, if the lateral pressure between the headgroups becomes greater than that between the chains, the monolayer will curl towards the chain regions, a positive curvature (Fig. 6.5). A lip-

id such as a phosphatidylethanolamine has a tendency to adopt a negatively curved, hexagonal H_{II} phase because the small size of the phosphatidylethanolamine headgroup relative to the cross-sectional area of the two fatty acyl chains gives the lipid an overall conical shape (Seddon 1990).

The tendency to curl becomes frustrated in a lipid bilayer. In a symmetrical bilayer (with identical conditions on each side) the two monolayers will both want to curve in the same way (either positive or negative) and so will counteract each other; the two monolayers cannot both curve in the same direction since this would create free volume in the interior of the bilayer. Thus the bilayer has to remain flat, in a state of physical frustration. Confining a monolayer with a non-zero spontaneous curvature to a planar form results in an elastic free energy stored in the bilayer. If the stresses in the bilayer become too great, the bilayer structure will become unstable and a non-bilayer phase will form.

Of course, in a real biological membrane it is essential that a lipid bilayer structure is maintained, and a lipid bilayer structure is maintained because the presence of intrinsic membrane proteins and bilayer-preferring lipids overcomes the tendency of lipids such as phosphatidylethanolamines to adopt a non-bilayer structure. Thus mixtures of di(C18:1)PC and di(C18:1)PE containing 15% or more di(C18:1)PC adopt a bilayer structure (Boni and Hui 1983), and a number of intrinsic membrane proteins (glycophorin A, cytochrome oxidase, the light-harvesting complex of photosystem II) have also been shown to stabilize a bilayer structure (de Kruijff et al. 1985; Simidjiev et al. 2000).

It is worth exploring further the idea that a lipid such as a phosphatidylethanolamine has an overall conical shape. If the "conical" shape of the phosphatidylethanolamine molecule were to be an accurate description of the overall shape of the phosphatidylethanolamine molecule in a lipid bilayer, incorporation of phosphatidylethanolamine into bilayers of phosphatidylcholine would have significant effects on the order parameter profile for the fatty acyl chains of the phosphatidylcholine molecule; inclusion of phosphatidylethanolamine would create a greater packing density toward the centre of the bilayer and a smaller packing density near the glycerol backbone region and thus increase order parameters for phosphatidylcholine chains at the terminal methyl ends of the chains and decrease order parameters at the carboxyl end. Such effects are not seen, addition of a phosphatidylethanolamine to a bilayer of a phosphatidylcholine increasing order parameters at all positions in the chains of the phosphatidylcholine (Fenske et al. 1990). Thus the phosphatidylethanolamine molecule increases packing density throughout the bilayer, consistent with the observation that order parameters for chains in phosphatidylethanolamines are greater than those in phosphatidylcholines at all positions of the chain (Perly et al. 1985; Lafleur et al. 1990). It has also been shown that, in mixtures of (C16:0,C18:1)PE and (C16:0,C18:1)PC, the order parameters for the palmitoyl chains in (C16:0,C18:1)PE and (C16:0,C18:1)PC are the same (Lafleur et al. 1990). Similarly, it has been shown in molecular dynamics simulations that order parameter profiles for the oleoyl chains in mixtures of di(C18:1)PC and di(C18:1)PE are identical for chains on the two classes of lipid (de Vries et al. 2004). Thus although the idea of a cone-shaped phosphatidylethanolamine molecule is helpful in explaining the preference of phosphatidylethanolamine for the hexagonal H_{II} phase, the acyl chains do not adopt a cone shape

when mixed in a bilayer with phosphatidylcholine. The increase in order parameters seen on addition of a phosphatidylethanolamine to bilayers of a phosphatidylcholine has been attributed to the ability of the phosphatidylethanolamine headgroup to hydrogen bond with phosphatidylcholines or other phosphatidylethanolamines, and to the smaller size of the phosphatidylethanolamine headgroup (de Vries et al. 2004).

6.2.6 Bilayer Deformation Energies

Changes in bilayer shape incur an energetic cost. This can be important when a lipid bilayer is perturbed around a membrane protein. A lipid bilayer can respond to mechanical deformation by changes in its dimensions, up to a point beyond which the bilayer ruptures (Sackmann 1995). The observed changes in dimension are related to the magnitude of the external force (or stress) by a constant, the elastic constant (or modulus). The elastic properties of a lipid bilayer can be described by four elastic moduli that describe the response of a unit area of membrane to compression, expansion, bending, or extension (or shear) (Evans and Hochmuth 1978; Bloom et al. 1991; Sachs and Morris 1998; Hamill and Martinac 2001). The simplest of these is the membrane compression that follows from an increase in pressure. Bilayers are essentially incompressible and the volume of the bilayer will not change significantly under the kinds of pressure change that might be observed physiologically; the bilayer compressibility modulus has been estimated to be between 10^9 and 10^{10} N/m^2 (Evans and Hochmuth 1978; Hamill and Martinac 2001). A lipid bilayer also shows a considerable resistance to area expansion because of the tight lateral packing of the lipid molecules in the bilayer. The linear relationship between membrane tension t (force per unit length, usually measured as mN/m or, equivalently, dynes/cm) and the resulting area expansion of the bilayer is given by

$$t = K_A \Delta A / A_0 \tag{6.2}$$

where ΔA is the increase in surface area, A_0 is the original area, and K_A is the area expansion modulus. Values of K_A vary between 10^2 and 10^3 mN/m depending on the cholesterol content of the bilayer (Table 6.1). Values of K_A for bilayers of phosphatidylethanolamine are very similar to those for phosphatidylcholine in the liquid crystalline phase (Evans and Needham 1987). The area expansion modulus gives a measure of the work required to separate the lipid fatty acyl chains in the plane of the bilayer. Since lipid bilayers rupture at tensions between 3 and 30 mN/m, this means that a bilayer can only expand by about 2–4% before it ruptures (Hamill and Martinac 2001).

Because the bilayer is almost incompressible, any change in area for the bilayer will be accompanied by a corresponding change in thickness, so that the volume remains unchanged. The moduli describing changes in area (K_A) and thickness (K_H) are related by

Table 6.1. Elastic moduli for lipid bilayers[a]

Lipid	K_A pN/nm	K_C pN.nm
(C18:0,C18:1)PC	193	90
(C18:0,C18:1)PC + cholesterol (1:1)	781	246
di(C18:1)PC	188	80
di(C16:0)PC at 50°C	250	50
(C18:0,C22:6)PC	130	120
(C18:0,C22:5)PC	250	110

[a] Data from Nielsen and Andersen (2000), Nagle and Tristram-Nagle (2000) and Eldho et al. (2003)

$$K_A = K_H h \tag{6.-3}$$

where h is the thickness of the membrane (in nm). The value of K_H has been estimated to be about 200×10^7 N/m^2, which would correspond to a value for K_A of about 70 mN/m for a bilayer thickness of 3 nm, in good agreement with the estimate given above (Evans and Hochmuth 1978).

Work also has to be done to bend a lipid bilayer, because bending results in a differential expansion or compression of the two lipid monolayers making up the bilayer (Hamill and Martinac 2001). The bending modulus K_C for a lipid bilayer has been estimated to be about 50–250 pN.nm (Table 6.1) (Sachs and Morris 1998). Finally, a lipid bilayer shows negligible surface shear rigidity in the liquid crystalline phase and will simply flow like a liquid in response to shear (extension).

6.3 Lipid–Protein Interactions

Effects of lipids on the function of membrane proteins can be described either at the microscopic or at the macroscopic level. An explanation at the microscopic level is a "molecular" level interpretation in terms of interactions such as hydrogen bonding, charge–charge interactions, and van der Waals interactions. An explanation at the macroscopic level involves properties of the whole membrane such as membrane viscosity, membrane pressure, and curvature stress. In some cases it is clear that an interpretation at the microscopic level is the most appropriate. In others, explanations at both the microscopic and macroscopic levels are possible, although even in these cases, an explanation at the microscopic level is often the most attractive when a crystal structure for the protein is available.

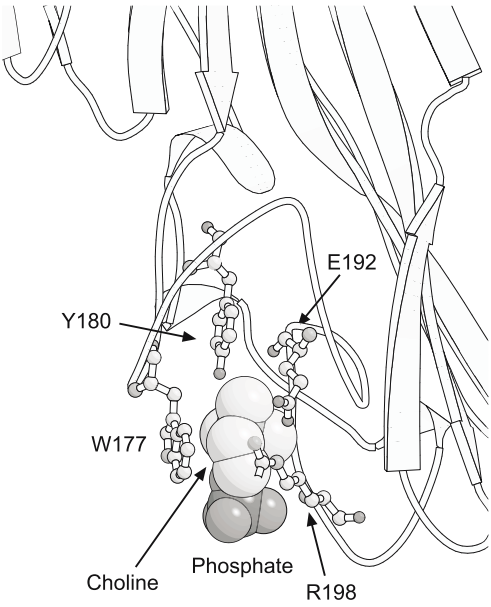

Fig. 6.6. The structure of the phosphatidylcholine binding site on LukF. Only the phosphorylcholine headgroup was resolved in the crystal structure, shown in space fill format. Residues surrounding the headgroup binding site are shown in ball-and-stick format (PDB file 3LKF)

6.3.1 Headgroup Interactions

It has been suggested that binding of extrinsic membrane proteins to lipid bilayer surfaces could be affected by curvature stress in the lipid bilayer, the level of curvature stress being increased by the preference of a phospholipid such as phosphatidylethanolamine for a curved, hexagonal H_{II} phase (Gruner 1985). However, in two cases of extrinsic membrane proteins where crystal structures are available, it is clear that binding specificity is determined by specific molecular interactions rather than by curvature stress. The first case concerns the channel-forming toxins α-hemolysin and LukF of *Staphylococcus aureus* (Olson et al. 1999; Galdiero and Gouaux 2004). α-Hemolysin permeabilizes liposomes of phosphatidylcholine or sphingomyelin, but not those of phosphatidylethanolamine, phosphatidylserine, phosphatidylglycerol, or phosphatidylinositol (Watanabe et al. 1987). The crystal structures make clear the basis of this selectivity (Olson et al. 1999; Galdiero and Gouaux 2004). The crystal structure for LukF crystallized in the presence of dipropanoylphosphatidylcholine is shown in Fig. 6.6. Only the phosphorylcholine headgroup is resolved, this being largely buried. The phosphate group interacts with the side-chain of Arg-198 and its main chain nitrogen, the quaternary ammonium group is in contact with Glu-192 and Tyr-180, and the CH2-CH2 group is near Trp-177 (Fig. 6.6). The specificity of the toxins for phosphatidylcholine or sphingomyelin can, therefore, be understood in terms of the specific molecular interactions between the lipid headgroup and its binding site on the toxin.

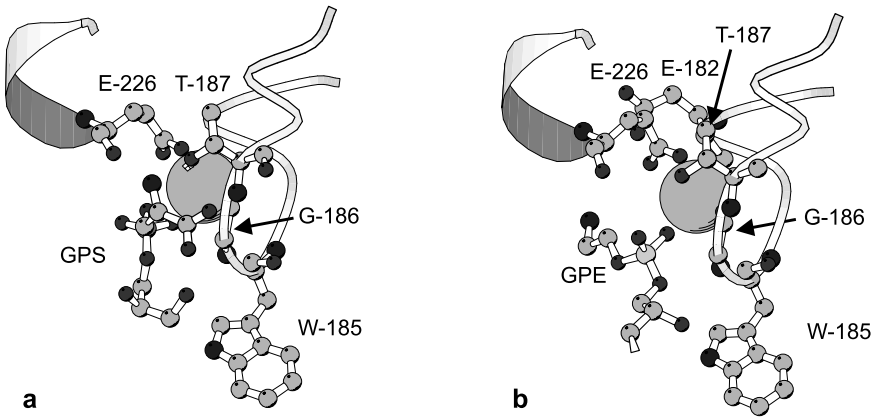

Fig. 6.7. Binding of glycerophosphoserine (GPS) and glycerophosphoethanolamine (GPE) to annexin V. The binding sites for GPS (**a**) and GPE (**b**) are shown. The filled sphere is Ca^{2+}. Some of the residues important for binding are shown in ball-and-stick mode (PDB files 1A8A and 1A8B)

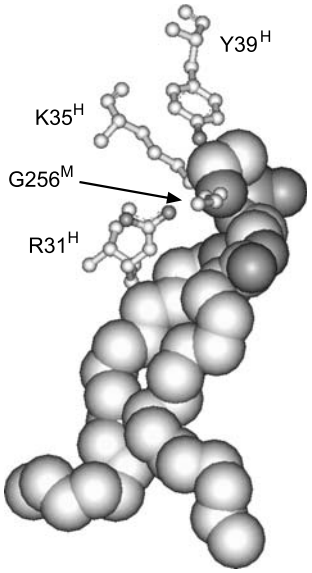

Fig. 6.8. Structure of the phosphatidylethanolamine molecule bound to the photosynthetic reaction centre from *T. tepidum*. The residues from subunits H and M interacting with the lipid headgroup are shown (PDB file 1EYS)

The second case concerns the annexins, which show specificity for phosphatidylethanolamines and phosphatidylserines. Annexin V hardly binds to bilayers of phosphatidylcholine or sphingomyelin but binds to bilayers of phosphatidylethanolamine, and more strongly, to bilayers containing anionic phospholipids such as phosphatidylserine (Schlaepfer et al. 1987; Blackwood and Ernst 1990; Andree

et al. 1990; Raynal and Pollard 1994; Campos et al. 1998). The crystal structure of rat annexin V in the presence of glycerophosphoserine (GPS) and glycerophosphoethanolamine (GPE) (Swairjo et al. 1995) shows the phosphoryl oxygen coordinated to a bound Ca^{2+} ion, with the GPE headgroup extending along the molecular surface in the opposite direction to GPS, in a shallower binding site (Fig. 6.7); the more extensive interactions observed in the crystal structure with GPS than with GPE explains why binding to phosphatidylserine is stronger than to phosphatidylethanolamine. In this case the binding site is too small to accommodate the bulky phosphorylcholine group.

In some cases it is clear that interactions between intrinsic membrane proteins and the surrounding lipid molecules also have to be understood in terms of specific molecular level interactions. For example, Fig. 6.8 shows the structure of a phosphatidylethanolamine molecule resolved in the crystal structure of photosynthetic reaction centre from *Thermochromatium tepidum* (Nogi et al. 2000). The conformation adopted by the phosphatidylethanolamine is very different to that shown in Fig. 6.2; the glycerol backbone is not oriented parallel to the fatty acyl chains, and the headgroup is not oriented perpendicular to the chain axis. Clearly, the adopted structure is determined by specific interactions, particularly between the headgroup and the protein, the headgroup being bent down towards the chain, for example, to allow a hydrogen-bonded interaction between the quaternary ammonium nitrogen and the backbone of Gly-256 in subunit M (Fig. 6.8). Other examples of specific interactions of this type have been presented in Lee (2003) and an analysis of the conformations of bound lipids shows that they are often different from the structures adopted in simple lipid bilayers (Marsh and Pali 2004).

It is likely that the lipid molecules resolved in crystal structures of intrinsic membrane proteins are rather unrepresentative of the bulk of the lipid molecules in contact with a membrane protein, the resolved lipid molecules often being located between transmembrane α-helices, often at protein–protein interfaces in multi-subunit proteins (Lee 2003, 2004). Most of the lipid molecules interacting with the hydrophobic surface of a membrane protein (the boundary or annular lipids) will interact with the protein rather non-specifically, although there is evidence for binding hot-spots on the surface of a protein close, for example, to clusters of positively charged residues where anionic phospholipids will bind relatively strongly (Powl et al. 2005). Hydrogen bonding and charge interactions with the lipid headgroup must also be important for non-specific binding of lipid molecules to a membrane protein. The binding constants for phospholipids to annular sites on membrane proteins will depend on the strengths of the lipid–protein interactions relative to those of lipid–lipid interactions. ESR studies show that the on and off rate constants for annular binding are fast, suggesting that the strength of the lipid–protein interaction is comparable to that of a lipid–lipid interaction (East et al. 1985; Lee 2003) consistent with the general lack of selectivity in binding phospholipids to the annular sites on a membrane protein (Lee 2003). Given the importance of hydrogen bonding and charge interactions between lipid molecules in the headgroup region of a lipid bilayer, this suggests that hydrogen bonding and charge interactions with membrane proteins must also be important. In agreement with this expectation, uncharged molecules such as long-chain

alcohols bind less weakly to membrane proteins than charged molecules such as long-chain amines or acids (Froud et al. 1986; Lee 2003).

The importance of hydrogen bonding has been shown in a molecular dynamics simulation of the mechanosensitive channel of large conductance MscL from *T. tuberculosis* in bilayers of (C16:0,C18:1)PE. The simulation showed a large number of hydrogen bonds between the lipid molecules and MscL, about half involving the NH_3^+ group of the phosphatidylethanolamine headgroup (Elmore and Dougherty 2001). Other lipid headgroups such as phosphatidylcholine and phosphatidylglycerol do not have a hydrogen bond donating group analogous to the NH_3^+ of phosphatidylethanolamine and so show a very different pattern of hydrogen bonding. A molecular dynamics simulation of MscL in bilayers of (C16:0,C18:1)PC suggests that the loss of hydrogen bonding observed on replacement of the phosphatidylethanolamine headgroup by the phosphatidylcholine headgroup is compensated for by a conformational change in the C-terminal region of the protein, bringing the C-terminal region closer to the membrane, leading to stronger interactions with the membrane (Elmore and Dougherty 2003). A molecular dynamics simulation of bacteriorhodopsin also shows the importance of headgroup interactions with the protein, different interactions with the different conformational states of the protein having an important effect on the energetics of the changes between these conformational states (Jang et al. 2004).

It is well established that the conformational equilibrium between the two major intermediates of the rhodopsin photocycle, metarhodopsin I (MI) and metarhodopsin II (MII), depend on lipid structure, and that the presence of phosphatidylethanolamines increases the ratio MII/MI (Litman and Mitchell 1996; Brown 1997). These effects are usually described in terms of the tendency of

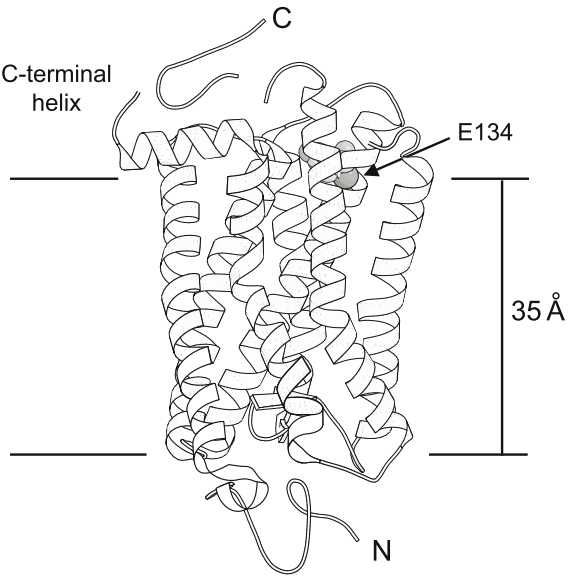

Fig. 6.9. The structure of rhodopsin. The hydrophobic thickness of rhodopsin, defined largely by the positions of Tyr and Trp residues, is shown by the horizontal lines. Residue Glu-134 is shown in space fill format (PDB file 1F88)

phosphatidylethanolamines to adopt a curved, hexagonal H_{II} phase. However, as described in Lee (2003), the results can also be interpreted in terms of headgroup interactions with rhodopsin. The effect of phosphatidylethanolamines on the MII/MI ratio for rhodopsin follows from a shift in the pK describing the pH dependence of this equilibrium (Brown 1994). Mutation of Glu-134 leads to a loss of the pH dependence of the MII/MI ratio, suggesting that the pH dependence of the equilibrium follows from protonation/deprotonation of Glu-134 (Arnis et al. 1994). As shown in Fig. 6.9, Glu-134 is probably located very close to the glycerol backbone region of the surrounding lipid bilayer, so that the pK of this residue is very likely to change with changing lipid structure (Lee 2003). Indeed, calculations of the pK of this residue show that it is environmentally sensitive (Periole et al. 2004).

Further examples of lipid headgroup–protein interactions and their effects on protein function are given in Lee (2003, 2004).

6.3.2 Fatty Acyl Chains

Lipid fatty acyl chain lengths determine the hydrophobic thickness of a lipid bilayer. The hydrophobic thickness of a lipid bilayer is expected to match well the hydrophobic thickness of any protein embedded in the bilayer, because of the high cost of exposing either fatty acyl chains or hydrophobic amino acids to water. The efficiency of hydrophobic matching has been demonstrated experimentally for the potassium channel KcsA where varying the chain length for the surrounding phospholipids from C12 to C24 results in no change in the environment of the Trp residues located at the ends of the transmembrane α-helices (Williamson et al. 2002). Any mismatch between the hydrophobic thicknesses of the lipid bilayer and the protein would be expected to lead to distortion of the lipid bilayer, or the protein, or both, to minimize the mismatch.

The energetics of distortion of the lipid bilayer have been analysed in terms of the bulk bending properties of the lipid bilayer described above, with stretching of the lipid chains being required when the lipid bilayer is too thin and compression when the bilayer is too thick (Fig. 6.10) (Mouritsen and Bloom 1984; Fattal and Ben-Shaul 1993; Nielsen et al. 1998). A comparison of relative lipid binding constants estimated from the results of such a theoretical calculation (Fattal and Ben-Shaul 1993) with experimental data shows that agreement is reasonable for moderate levels of mismatch for the β-barrel protein OmpF but is poor for the α-helical protein MscL (O'Keeffe et al. 2000; Powl et al. 2003) (Fig. 6.11). Presumably, the β-barrel structure of OmpF makes it relatively rigid so that distortion of the lipid bilayer to provide hydrophobic matching is less costly than distortion of the protein. Similarly, the effects of bilayer thickness on the properties of the dimer-channel formed by gramicidin fit well to a model based on elastic deformation of the lipid bilayer around the gramicidin dimer (Lundbaek and Andersen 1999; Nielsen and Andersen 2000) and the presence of gramicidin has been shown to thicken a bilayer of di(C12:0)PC but to compress one of di(C14:0)PC (Harroun et al. 1999). In contrast, an α-helical protein is less rigid, and both distortion of

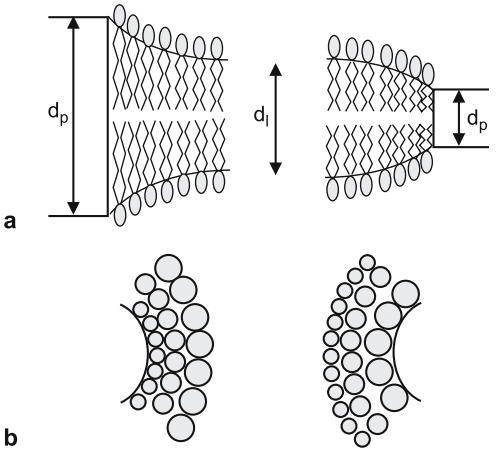

Fig. 6.10. Hydrophobic mismatch. The diagram shows how a lipid bilayer could distort around a membrane protein whose hydrophobic thickness was greater than that of the lipid bilayer (left; $d_p > d_l$) or less than that of the lipid bilayer (right; $d_p < d_l$). (**a**) shows a side view of the membrane and (**b**) shows a view down onto the surface of the membrane. When the hydrophobic thickness of the protein is greater than the hydrophobic thickness of the bilayer, the lipid chains must be stretched so that the surface area occupied by a lipid molecule will be less in the vicinity of the protein than for bulk lipid. Conversely, to match a protein with a thin transmembrane region the fatty acyl chains of neighbouring lipids will be compressed and will therefore occupy a greater surface area

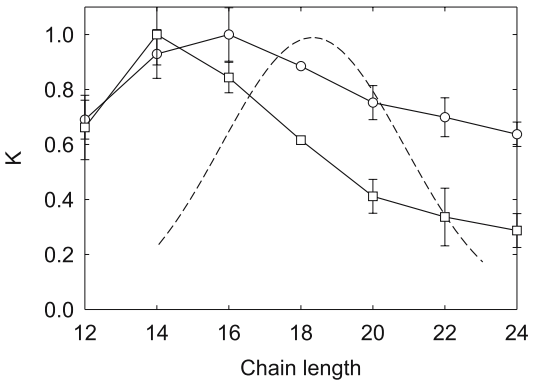

Fig. 6.11. The dependence of lipid binding constants on chain length. Binding constants for phosphatidylcholines relative to di(C16:1)PC for MscL (○) and relative to di(C14:1)PC for the β-barrel protein OmpF (□) are plotted against fatty acyl chain length. The dotted line shows the theoretical dependence of lipid binding constant on chain length calculated from the data of Fattal and Ben-Shaul (1993) for a protein of hydrophobic thickness 30 Å, as described in Powl et al. (2003). Data from O'Keeffe et al. (2000) and Powl et al. (2003)

the lipid bilayer and distortion of the protein is likely (Lee 2004) because the cost of distorting a lipid bilayer is relatively high (Lundbaek et al. 2004). Distortion of α-helical membrane proteins explains the marked dependence of the activities of α-helical membrane proteins on bilayer thickness (Lee 2004).

6.3.3 Effects of Internal Bilayer Pressures and Curvature Stress

Although, as described above, lateral pressures in the headgroup and chain regions of a lipid bilayer must balance, the distribution of lateral pressures within the chain region are not uniform (Lindahl and Edholm 2000; Gullingsrud and Schulten 2004). It has been suggested that the lateral pressure profile in a lipid bilayer could be an important factor in determining the conformational equilibrium of a membrane protein (Cantor 1997). For example, if changes in the cross-sectional area of a membrane protein in going from one conformation to another are different at different depths in the membrane, then it has been suggested that the equilibrium constant describing the conformational change will depend on lateral pressure profile through a series of $P\Delta V$ work terms, where P and ΔV refer, respectively, to pressures and volume changes at particular depths in the bilayer (Cantor 1997). The largest tension in a lipid bilayer is located close to the glycerol backbone region, where close packing is required to prevent exposure of the fatty acyl chains to water (Lindahl and Edholm 2000; Gullingsrud and Schulten 2004). However, it could be argued that expansion of a membrane protein close to the

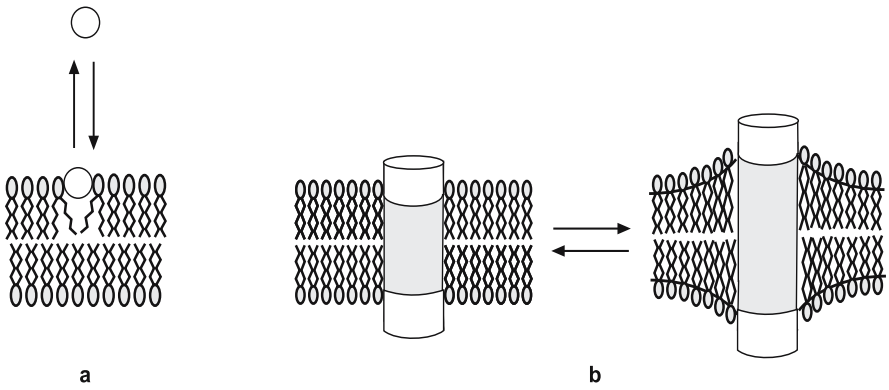

Fig. 6.12. Possible effects of stored curvature elastic energy on the function of membrane proteins. In (**a**) the binding of an extrinsic membrane protein is increased in the presence of lipids favouring the hexagonal H_{II} phase, as the fatty acyl chains of neighbouring lipid molecules can distort to fill the free volume created by insertion of the extrinsic membrane protein into the lipid headgroup region. In (**b**) the presence of lipids favouring the hexagonal H_{II} phase shifts the conformation equilibrium of an intrinsic membrane protein towards the conformation with the greatest hydrophobic thickness

glycerol backbone region need not result in any increased exposure of lipid fatty acyl chains to water, so that expansion of the protein in this region does not require any work against a lipid pressure. Further, it has been argued above, from a comparison of the properties of simple hydrocarbons with the properties of the hydrocarbon core of a lipid bilayer, that the hydrocarbon core of a lipid bilayer is not in any way special as far as its bulk properties are concerned.

It has been suggested that lateral pressure profiles in lipid bilayers will be very dependent on the detailed structure of the phospholipid (Cantor 1997). However, molecular dynamics simulations suggest that the pressure profiles in bilayers of di(C18:1)PC and di(C18:1)PE are rather similar, and differences in pressure profile between di(C18:1)PC and di(C18:1)PE are likely to be too small to be functionally significant (Gullingsrud and Schulten 2004). It has also been shown experimentally that the activity of the Ca^{2+}-ATPase of sarcoplasmic reticulum, although very sensitive to fatty acyl chain length, is not sensitive to features of the fatty acyl chains such as unsaturation (East et al. 1984).

Curvature stress has also been suggested to be a significant factor in the function of membrane proteins. It has been suggested that the stored curvature elastic energy in a bilayer containing a non-bilayer preferring lipid such as phosphatidylethanolamine can be used to increase the binding of a peripheral membrane protein to the membrane (Attard et al. 2000); as shown in Fig. 6.12 insertion of an intrinsic membrane protein into the headgroup region of the bilayer will release some of the stored curvature elastic energy. It has also been suggested that stored curvature elastic energy could alter the conformational equilibrium of an intrinsic membrane protein (Botelho et al. 2002). If the hydrophobic thickness of one conformation of a protein is greater than that of an alternative conformation, then the presence of lipids favouring the hexagonal H_{II} phase could shift the equilibrium in favour of the conformation with the greatest hydrophobic thickness (Fig. 6.12). However, as described in Sect. 6.3.1, it is also possible that any observed effects could be explained in terms of direct lipid–protein interactions.

6.4 Extrapolation from Model Systems to Biological Membranes

It is worth considering how well studies of simple model systems relate to real biological membranes. The amount of unperturbed lipid bilayer present in a biological membrane will be low, because of the high concentration of protein in a biological membrane. For example, the molar ratio of phospholipid to protein in the sarcoplasmic reticulum membrane is about 90:1, sufficient to form about three shells of lipid around each Ca^{2+}-ATPase molecule, the major protein in the membrane (Warren et al. 1974). Despite this, lipid molecules adopt average structures in biological membranes the same as those in simple lipid bilayers. The characteristic ^{2}H-NMR pattern observed for deuterium located on the first methylenes of the *sn*-1 and *sn*-2 chains in *E. coli* membranes suggests that the average orientation of the glycerol backbone is the same as in a simple lipid bilayer (Buldt and Wohlgemuth 1981). Similarly, studies of mouse fibroblasts labelled biosynthetically with deuterated ethanolamine and choline have shown that the

headgroups are again oriented roughly parallel to the membrane surface, as they are in simple bilayers (Scherer and Seelig 1987). Thus the presence of proteins and the other lipids in the membrane has relatively little effect on the average conformations adopted by the lipids in the membrane, although, as described above, the conformations of the protein-bound lipid molecules may be significantly different. The order parameter profiles for intact biological membranes are also the same as for those for simple lipid bilayers. The profiles for *E. coli* membranes labelled in the palmitoyl and oleoyl chains are shown in Fig. 6.4; the values of the order parameters and their variation along the chain are the same as in bilayers of (C16:0,C18:1)PC (Seelig and Seelig 1980). Thus the presence of membrane proteins has no significant effect on the extent of motion of the lipid fatty acyl chains of the bulk of the lipids, on the NMR time-scale.

6.4.1 Is there a Special Role for Lipids Preferring a Non-Bilayer Phase?

A number of experiments have addressed the question of whether or not the presence of lipids favouring the hexagonal H_{II} phase is required for proper membrane function. For example, the microorganism *Acholeplasma laidlawii* contains six amphiphilic lipids, three uncharged and three anionic; the major uncharged lipids are monoglucosyldiacylglycerol (MGlcDG) and diglucosyldiacylglycerol (DGlcDG), and the anionic lipid is phosphatidylglycerol. Of these, MGlcDG favours non-lamellar phases (cubic and hexagonal H_{II}), particularly when the fatty acyl chains are unsaturated, whereas DGlcDG favours the lamellar phase (Lindblom et al. 1986). Under a variety of growth conditions (medium composition, temperature) the ratio of MGlcDG/DGlcDG in the membranes of *A. laidlawii* is maintained such that the cell lipids are in the liquid crystalline phase (Rilfors et al. 1984; Lindblom et al. 1986). The question then arises why a non-bilayer favouring lipid such as MGlcDG is there in the first place. One possibility is that it is simply less costly for a cell to synthesize MGlcDG than DGlcDG, and that MGlcDG will do as well in the membrane as DGlcDG, as long as the level of MGlcDG does not become so high that the stability of the lipid bilayer becomes compromised. It is also possible that curvature stress arising from the presence of MGlcDG is required in some way for proper function of the membrane; this could be because of effects on the functions of membrane proteins or because processes such as cell division were affected by bulk properties of the membrane. The strongest evidence for a special role for non-bilayer favouring lipids in *A. laidlawii* is probably the fact that the membranes also contain small amounts of lipids with three acyl chains, monoacylmonoglucosyldiacylglycerol and monacyldiglucosyldiacylglycerol, the former of which has a very strong tendency to form cubic phases (Lindblom et al. 1993; Andersson et al. 1996), although even here it has to be considered that it is less costly to make monoacylmonoglucosyldiacylglycerol than any other of the lipid species, since monoacylmonoglucosyldiacylglycerol contains three fatty acyl chains per lipid headgroup.

Similarly, the fact that most bacteria contain phosphatidylethanolamine as the zwitterionic lipid rather than phosphatidylcholine may simply reflect the simpler structure and smaller cost of phosphatidylethanolamine than phosphatidylcholine. The *E. coli* inner membrane contains about 70% phosphatidylethanolamine. Mutant strains unable to synthesize phosphatidylethanolamine replace phosphatidylethanolamine with cardiolipin and phosphatidylglycerol (Rietveld et al. 1993). Cardiolipin, in the absence of divalent metal ions, adopts a bilayer structure but, in the presence of divalent metal ions, and depending on the degree of fatty acyl chain unsaturation, can adopt a hexagonal H_{II} phase structure (Rietveld et al. 1993). Unlike the wild-type strain, the mutant strain displays an obligate requirement for high concentrations of divalent metal ions (Rietveld et al. 1993). Although this could indicate a requirement for non-bilayer favouring lipids it could also simply reflect a requirement to reduce the high membrane surface potential introduced by the negatively charged lipids (Rietveld et al. 1993; Wikstrom et al. 2004). A specific role for phosphatidylethanolamine is suggested by experiments showing that phosphatidylethanolamine is required for proper folding of the lactose permease, LacY; in the absence of phosphatidylethanolamine, insertion of LacY into the inner membrane results in the normally cytosolic N-terminal half of the protein being exposed to the periplasm (Bogdanov et al. 1996, 1999). Correct insertion of LacY requires the presence of a phospholipid with an amine group, such as phosphatidylethanolamine or phosphatidylserine, in a bilayer structure (Bogdanov et al. 1999). However, incorporation of the *A. laidlawii* lipid MGlcDG into *E. coli* membranes lacking phosphatidylethanolamine was also found to result in partial recovery of LacY function, suggesting either that a non-bilayer favouring lipid was required for proper insertion of LacY or that phosphatidylethanolamine and MGlcDG interacted similarly with the machinery involved in LacY insertion (Wikstrom et al. 2004).

Although phosphatidylethanolamine is the most common of the zwitterionic lipids in bacteria, phosphatidylcholines are found in some bacteria, mostly in the rhizobial and rhodobacterial groups, the presence of phosphatidylcholine being related to specific characteristics of the bacteria (Sohlenkamp et al. 2003). Phosphatidylcholines can be synthesized from phosphatidylethanolamine by three methylations with S-adenosylmethionine as the methyl donor or by a novel pathway in which choline is condensed directly with CDP-diacylglycerol to form phosphatidylcholine in a single step (Sohlenkamp et al. 2003). Bacteria of the rhizobial class could require phosphatidylcholine to interact well with their hosts. For example, the presence of phosphatidylcholines in the membranes of many of the bacteria colonizing the respiratory tract or other epithelia could allow the bacteria to mimic the membranes of their hosts, allowing them to avoid host defence mechanisms (Goldfine 1984). The existence of a direct pathway for the synthesis of phosphatidylcholines from choline allows choline to be utilized from the animal hosts, which contain considerable amounts of choline in their body fluids (Goldfine 1984). Rhodobacteria such as *Rhodobacter sphaeorodies* are unusual in containing an extensive intracellular membrane system, involved in photosynthesis. The membrane contains ca. 25% of its lipid as phosphatidylcholine, the lipid composition also being unusual in that over 75% of the fatty acyl chains are monounsaturated (Goldfine 1984). It has been suggested that the membrane

could contain phosphatidylcholine rather than just phosphatidylethanolamine and phosphatidylglycerol in order to maintain a stable bilayer structure with such unsaturated lipids (Goldfine 1984). Mutants of *R. sphaeorodies* unable to synthesize phosphatidylcholines show normal growth under normal laboratory conditions, showing that the presence of phosphatidylcholine is not essential for function (Arondel et al. 1993).

Another example concerns the thylakoid membrane, the internal photosynthetic membrane of higher plant chloroplasts. About 50% of the lipid in these membranes is monogalactosyldiacylglycerol (MGalDG), about 30% is digalactosyldiacylglycerol (DGalDG) and about 10% is phosphatidylglycerol (PG) (Harwood and Russell 1984). As well as having unusual headgroups, MGalDG and DGalDG are unusual in containing two highly unsaturated fatty acyl chains (linoleic acid); most natural lipids contain one saturated and one unsaturated chain. The presence of the two unsaturated chains in MGalDG give this lipid a conical shape so that it prefers a hexagonal H_{II} phase; MGalDG with two saturated chains prefers a bilayer phase (Sen et al. 1981). DGalDG with its larger headgroup adopts a bilayer phase with either saturated or unsaturated chains (Sen et al. 1981).

Thylakoids are arranged as stacks or grana, photosystem II being concentrated in the stacked membranes (Hankamer et al. 1997). Light-harvesting complex II (LHC-II) is important in the stacking process (McDonnel and Staehelin 1980). When LHC-II, purified with its native lipid, is reconstituted into bilayers of phosphatidylcholine, vesicles are formed which aggregate in the presence of divalent cations with formation of extensive membrane stacks. The LHC-II molecules are found to be clustered at the adhering membrane regions (McDonnel and Staehelin 1980). However, LHC-II only causes stacking in the presence of MGalDG; stacking is not observed with DGalDG (Simidjiev et al. 1998, 2000). It is not known for certain how the presence of MGalDG leads to membrane stacking. One possibility is that the presence of non-bilayer forming lipids is important; an alternative possibility is that what is important is the ability of the lipid headgroup to take part in hydrogen bonding with water molecules or with adjacent lipid headgroups. The uncharged galactose headgroup of MGalDG is difficult to hydrate; rather than hydrogen bonding to water, it is expected that strong hydrogen bonds will be formed between adjacent galactose headgroups. This has been demonstrated in studies of monolayers of MGalDG, where stronger interactions are observed between MGalDG molecules than between phosphatidylcholines with comparable degrees of chain unsaturation (Bishop et al. 1980). It is possible that it is this hydrogen bonding potential that leads to the formation of stacked membranes in the presence of MGalDG. The LHC-II protein only extends about 5 Å above the surface of the membrane on the outer (stromal) surface (Kuhlbrandt et al. 1994). When interactions between LHC-II molecules bring about membrane stacking, the surfaces of the stacked membranes will therefore be brought very close together. Hydrogen bonds could then form between MGalDG headgroups in the two surfaces, leading to a strengthening of the interaction between the two surfaces. A potential problem is, however, that strong interactions could also occur between galactose headgroups in the plane of the membrane. This type of interaction is indeed seen in monolayers of MGalDG containing saturated fatty acyl chains, where strong interactions between adjacent headgroups lead to the

formation of highly condensed, solid-like monolayers (Sen et al. 1981). A way to prevent lateral headgroup interactions would be to keep the headgroups well apart. Having two polyunsaturated fatty acyl chains per lipid molecule would achieve this; the bulky chains, by keeping the headgroups apart, will prevent the formation of lateral hydrogen bonds between the headgroups. The headgroups will then be poised to form transverse hydrogen bonding between two apposed membrane surfaces. The larger DGalDG headgroup would prevent close apposition of the membranes.

6.5 Summary

The conclusion appears to be that most, if not all, of the effects of phospholipids on the function of membrane proteins can be explained, at least in principle, in microscopic rather than macroscopic terms. This makes sense from a biological perspective. A biological membrane is a multicomponent system, containing a wide variety of different intrinsic and extrinsic membrane proteins, each with their own particular role to play in the cell. These proteins need to be able to work independently; a membrane system in which every protein affected the function of every other protein would be impossibly difficult to control. If membrane protein function depends only on the interactions of that particular membrane protein with the lipids, or proteins, in its immediate vicinity, then the proteins will function independently, as required. On the other hand, if membrane protein function was affected by macroscopic properties of the whole membrane such as viscosity, pressure, or curvature stress, then the function of all the membrane proteins would be interdependent, leading to chaos. This can be illustrated by assuming membrane curvature stress, a thermodynamic property of the whole membrane, is important, affecting the binding of intrinsic membrane proteins and the conformational state of intrinsic membrane protein (Sect. 6.3.3 and Fig. 6.12). The result would then be, for example, that binding of an extrinsic membrane protein to a membrane would affect the conformational state for the intrinsic membrane proteins in the membrane, and thus affect their function, in uncontrolled ways. This is clearly not allowable if the membrane is to be a functionally stable and predictable system, as it must be. It seems therefore that the biologically important interactions in membranes will be microscopic rather than macroscopic. Of course, an important corollary is then that intrinsic membrane proteins must have a design such that they are not affected by any changes in the macroscopic properties of a membrane that could occur physiologically.

References

Allinger NL, Yuh YH, Lii JH (1989) Molecular mechanics. The MM3 force field for hydrocarbons. J Amer Chem Soc 111:8551–8566

Andersson AS, Rilfors L, Bergqvist M, Persson S, Lindblom G (1996) New aspects on membrane lipid regulation in Acholeplasma laidlawii A and phase equilibria of monoacyldiglucosyldiacylglycerol. Biochemistry 35:11119–11130

Andree HA, Reutelingsperger CPM, Hauptmann R, Hemker HC, Hermens WT, Willems GM (1990) Binding of vascular anticoagulant alpha (VAC alpha) to planar phospholipid bilayers. J Biol Chem 265:4923–4928

Applegate KR, Glomset JA (1986) Computer-based modelling of the conformation and packing properties of docosahexaenoic acid. J Lipid Res 27:658–680

Armen RS, Uitto OD, Feller SE (1998) Phospholipid component volumes: Determination and application to bilayer structure calculations. Biophys J 75:734–744

Arnis S, Fahmy K, Hofmann KP, Sakmar TP (1994) A conserved carboxylic acid group mediates light-dependent proton uptake and signaling by rhodopsin. J Biol Chem 269:23879–23881

Arondel V, Benning C, Somerville CR (1993) Isolation and functional expression in Escherichia coli of a gene encoding phosphatidylethanolamine methyltransferase (EC 2.1.1.17) from Rhodobacter sphaeroides. J Biol Chem 268:16002–16008

Attard GS, Templer RH, Smith WS, Hunt AN, Jackowski S (2000) Modulation of CTP:phosphocholine cytidylyltransferase by membrane curvature elastic stress. Proc Nat Acad Sci USA 97:9032–9036

Bishop DG, Kenrick JR, Bayston JH, MacPherson AS, Johns SR (1980) Monolayer properties of chloroplast lipids. Biochim Biophys Acta 602:248–259

Blackwood RA, Ernst JD (1990) Characterization of calcium-dependent phospholipid binding, vesicle aggregation, and membrane fusion by annexins. Biochem J 266:195–200

Bloom M, Evans E, Mouritsen OG (1991) Physical properties of the fluid lipid-bilayer component of cell mermbranes: a perspective. Quart Rev Biophys 24:293–397

Bogdanov M, Sun J, Kaback HR, Dowhan W (1996) A phospholipid acts as a chaperone in assembly of a membrane transport protein. J Biol Chem 271:11615–11618

Bogdanov M, Umeda M, Dowhan W (1999) Phospholipid-assisted refolding of an integral membrane protein – Minimum structural features for phosphatidylethanolamine to act as a molecular chaperone. J Biol Chem 274:12339–12345

Boni LT, Hui SW (1983) Polymorphic phase behaviour of dilinoleoylphosphatidylethanolamine and palmitoyloleoylphosphatidylcholine mixtures. Structural changes between hexagonal, cubic and bilayer phases. Biochim Biophys Acta 731:177–185

Borle F, Seelig J (1983) Hydration of Escherichia coli lipids. Deuterium T1 relaxation time stuides of phosphatidyglycerol, phosphatidylethanolamine and phosphatidylcholine. Biochim Biophys Acta 735:131–136

Botelho AV, Gibson NJ, Thurmond RL, Wand Y, Brown MF (2002) Conformational energetics of rhodopsin modulated by nonlamellar-forming lipids. Biochemistry 41:6354–6368

Brown MF (1994) Modulation of rhodopsin function by properties of the membrane bilayer. Chem Phys Lipids 73:159–180

Brown MF (1997) Influence of nonlamellar-forming lipids on rhodopsin. Curr Top Memb 44:285–356

Buldt G, Wohlgemuth R (1981) The headgroup conformation of phospholipids in membranes. J Membr Biol 58:81–100

Campos B, Mo YD, Mealy TR, Li CW, Swairjo MA, Balch C, Head JF, Retzinger G, Dedman JR, Seaton BA (1998) Mutational and crystallographic analyses of interfacial residues in an-

nexin V suggest direct interactions with phospholipid membrane components. Biochemistry 37:8004–8010

Cantor RS (1997) Lateral pressures in cell membranes: a mechanism for modulation of protein function. J Phys Chem B 101:1723–1725

Cevc G, Watts A, Marsh D (1981) Titration of the phase transition of phosphatidylserine bilayer membranes. Effects of pH, surface electrostatics, ion binding, and head-group hydration. Biochemistry 20:4955–4965

Cronan JE (2003) Bacterial membrane lipids: Where do we stand? Annu Rev Microbiol 57:203–224

Cullis PR, de Kruijff B (1979) Lipid polymorphism and the functional roles of lipids in biological membranes. Biochim Biophys Acta 559:399–420

Damodaran KV, Merz KM (1994) A comparison of DMPC- and DLPE-based lipid bilayers. Biophys J 66:1076–1087

de Kruijff B, Cullis PR, Verkleij AJ, Hope MJ, Van Echteld CJA, Taraschi TF, Van Hoogevest P, Killian JA, Rietveld A, Van der Steen ATM (1985) Modulation of lipid polymorphism by lipid-protein interactions. In: Watts A, De Pont JJHHM (eds) Progress in Protein–Lipid Interactions. Elsevier, Amsterdam, pp 89–142

de Vries AH, Mark AE, Marrink SJ (2004) The binary mixing behavior of phospholipids in a bialyer: a molecular dynamics study. J Phys Chem B 108:2454–2463

Demel RA, Paltauf F, Hauser H (1987) Monolayer characteristics and thermal behavior of natural and synthetic phosphatidylserines. Biochemistry 26:8659–8665

Dorfler HD, Miethe P (1990) Phase diagrams of pseudo-binary phospholipid systems. II. Selected calorimetric studies on the influence of branching on the mixing properties of phosphatidylcholines. Chem Phys Lipids 54:61–66

East JM, Jones OT, Simmonds AC, Lee AG (1984) Membrane fluidity is not an important physiological regulator of the (Ca^{2+} –Mg^{2+})-dependent ATPase of sarcoplasmic reticulum. J Biol Chem 259:8070–8071

East JM, Melville D, Lee AG (1985) Exchange rates and numbers of annular lipids for the calcium and magnesium ion dependent adenosinetriphosphatase. Biochemistry 24:2615–2623

Eldho NV, Feller SE, TristramNagle S, Polozov IV, Gawrisch K (2003) Polyunsaturated docosahexaenoic vs docosapentaenoic acid – differences in lipid matrix properties from the loss of one double bond. J Am Chem Soc 125:6409–6421

Elmore DE, Dougherty DA (2001) Molecular dynamics simulations of wild-type and mutant forms of the Mycobacterium tuberculosis MscL channel. Biophys J 81:1345–1359

Elmore DE, Dougherty DA (2003) Investigating lipid composition effects on the mechanosensitive channel of large conductance (MscL) using molecular dynamics simulations. Biophys J 85:1512–1524

Evans E, Hochmuth RM (1978) Mechanical properties of membranes. Curr Top Membr Transp 10:1–64

Evans E, Needham D (1987) Physical properties of surfactant bilayer membranes; thermal transitions, elasticity, rigidity, cohesion, and colloidal interactions. J Phys Chem 91:4219–4228

Fattal DR, Ben-Shaul A (1993) A molecular model for lipid–protein interaction in membranes: the role of hydrophobic mismatch. Biophys J 65:1795–1809

Feller SE, Gawrisch K, MacKerell AD (2002) Polyunsaturated fatty acids in lipid bilayers: intrinsic and environmental contributions to their unique physical properties. J Am Chem Soc 124:318–326

Feller SE, Gawrisch K, Woolf TB (2003) Rhodopsin exhibits a preference for solvation by polyunsaturated docosohexaenoic acid. J Amer Chem Soc 125:4434–4435

Fenske DB, Jarrell HC, Guo Y, Hui SW (1990) Effect of unsaturated phosphatidylethanolamine on the chain order profile of bilayers at the onset of the hexagonal phase transition. A 2H NMR study. Biochemistry 29:11222–11229

Froud RJ, East JM, Rooney EK, Lee AG (1986) Binding of long-chain alkyl derivatives to lipid bilayers and to (Ca^{2+}–Mg^{2+})-ATPase. Biochemistry 25:7535–7544

Galdiero S, Gouaux E (2004) High resolution crystallographic studies of alpha-hemolysin-phospholipid complexes define heptamer-lipid head group interactions: Implication for understanding protein–lipid interactions. Protein Sci 13:1503–1511

Goldfine H (1984) Bacterial membranes and lipid packing theory. J Lipid Res 25:1501–1507

Gruner SM (1985) Intrinsic curvature hypothesis for biomembrane lipid composition: A role for nonbilayer lipids. Proc Natl Acad Sci 82:3665–3669

Gullingsrud J, Schulten K (2004) Lipid bilayer pressure profiles and mechanosensitive channel gating. Biophysical J 86:3496–3509

Hamill OP, Martinac B (2001) Molecular basis of mechanotransduction in living cells. Physiol Rev 81:685–740

Hankamer B, Barber J, Boekema EJ (1997) Structure and membrane organization of photosystem II in green plants. Annu Rev Plant Physiol 48:641–671

Harlos K, Eibl H, Pascher I, Sundell S (1984) Conformation and packing properties of phosphatidic acid: the crystal structure of monosodium dimyristoylphosphatidate. Chem Phys Lipids 34:115–126

Harroun TA, Heller WT, Weiss TM, Yang L, Huang HW (1999) Experimental evidence for hydrophobic matching and membrane-mediated interactions in lipid bilayers containing gramicidin. Biophys J 76:937–945

Harwood JL, Russell NJ (1984) Lipids in plants and microbes, George Allen & Unwin, London

Heller H, Schaefer M, Schulten K (1993) Molecular dynamics simulation of a bilayer of 200 lipids in the gel and in the liquid-crystal phases. J Phys Chem 97:8343–8360

Holte LL, Peter SA, Sinnwell TM, Gawrisch K (1995) ^{2}H nuclear magnetic resonance order parameter profiles suggest a change of molecular shape for phosphatidylcholines containing a polyunsaturated acyl chain. Biophys J 68:2396–2403

Hsieh CH, Wu WG (1997) Structure and dynamics of primary hydration shell of phosphatidylcholine bilayers at subzero temperatures. Biophys J 71:3278–3287

Huang P, Perez JJ, Loew GH (1994) Molecular dynamics simulations of phospholipid bilayers. J Biomolec Struct Dynamics 5:927–956

Hyvonen MT, Rantala TT, Ala-Korpela M (1997) Structure and dynamic properties of diunsaturated 1- palmitoyl-2- linoleoyl-sn-glycero-3-phosphatidylcholine lipid bilayer from molecular dynamics simulation. Biophys J 73:2907–2923

Jang H, Crozier PS, Stevens MJ, Woolf TB (2004) How environment supports a state: molecular dynamics simulations of two states in bacteriorhodopsin suggest lipid and water compensation. Biophys J 87:129–145

Johnston DS, Chapman D (1988) A calorimetric study of the thermotropic behaviour of mixtures of brain cerebrosides with other brain lipids. Biochim Biophys Acta 939:603–614

Knoll W, Ibel K, Sackmann E (1981) Small-angle neutron diffraction scattering studies of lipid phase diagrams by the contrast variation method. Biochemistry 20:6379–6383

Knoll W, Schmidt G, Sackmann E (1983) Critical demixing in fluid bilayers of phospholipid mixtures: a neutron diffraction study. J Chem Phys 79:3439–3442

Kuhlbrandt W, Wang DN, Fujiyoshi Y (1994) Atomic model of plant light-harvesting complex by electron crystallography. Nature 367:614–621

Lafleur M, Cullis PR, Bloom M (1990) Modulation of the orientational order profile of the lipid acyl chain in the Lα phase. Eur Biophys J 19:55–62

Laroche G, Dufourc EJ, Pezolet M, Dufourcq J (1990) Coupled changes between lipid order and polypeptide conformation at the membrane surface. A ^{2}H NMR and Raman study of polylysine-phosphatidic acid systems. Biochemistry 29:6460–6465

Lee AG (1977) Lipid phase transitions and phase diagrams. II. Mixtures involving lipids. Biochim Biophys Acta 472:285–344

Lee AG (2003) Lipid–protein interactions in biological membranes: a structural perspective. Biochim Biophys Acta 1612:1–40

Lee AG (2004) How lipids affect the activities of integral membrane proteins. Biochim Biophys Acta 1666:62–87

Lewis BA, Engelman DM (1983) Lipid bilayer thickness varies linearly with acyl chain length in fluid phosphatidylcholine vesicles. J Mol Biol 166:211–217

Li S, Lin HN, Wang ZQ, Huang C (1994) Identification and characterization of kink motifs in 1-palmitoyl-2-oleoyl-phosphatidylcholines: a molecular mechanics study. Biophys J 66:2005–2018

Lindahl E, Edholm O (2000) Spatial and energetic-entropic decomposition of surface tension in lipid bilayers from molecular dynamics simulations. J Chem Phys 113:3882–3893

Lindblom G, Brentel I, Sjolund M, Wikander G, Wieslander A (1986) Phase equilibria of membrane lipids from Acholeplasma laidlawii: Importance of a single lipid forming nonlamellar phases. Biochemistry 25:7502–7510

Lindblom G, Hauksson JB, Rilfors L, Bergenstahl B, Wieslander A, Eriksson PO (1993) Membrane lipid regulation in Acholeplasma laidlawii grown with saturated fatty acids. J Biol Chem 268:16198–16207

Litman BJ, Mitchell DC (1996) Rhodopsin structure and function. In: Lee AG (ed) Biomembranes. Volume 2A. Rhodopsin and G-protein linked receptors. JAI Press, Greenwich, Connecticut, pp 1–32

Lohner K (1996) Is the high propensity of ethanolamine plasmalogens to form non-lamellar lipid structures manifested in the properties of biomembranes? Chem Phys Lipids 81:167–184

Lopez Cascales JJ, Garcia de la Torre J, Marrink SJ, Berendsen HJC (1996) Molecular dynamics simulation of a charged biological membrane. J Chem Phys 104:2713–2720

Lundbaek JA, Andersen OS (1999) Spring constants for channel-induced lipid bilayer deformations estimates using gramicidin channels. Biophys J 76:889–895

Lundbaek JA, Birn P, Hansen AJ, Sogaard R, Nielsen C, Girshman J, Bruno MJ, Tape SE, Egebjerg J, Greathouse DV, Mattice GL, Koeppe RE, Andersen OS (2004) Regulation of sodium channel function by bilayer elasticity: the importance of hydrophobic coupling. Effects of micelle-forming amphiphiles and cholesterol. J Gen Physiol 123:599–621

Marrink SJ, Berendsen HJC (1994) Simulation of water transport through a lipid membrane. J Phys Chem 98:4155–4168

Marsh D (1996) Lateral pressure in membranes. Biochim Biophys Acta 1286:183–223

Marsh D, Pali T (2004) The protein–lipid interface: perspectives from magnetic resonance and crystal structures. Biochim Biophys Acta 1666:118–141

McCabe MA, Griffith GL, Ehringer WD, Stillwell W, Wassall SR (1994) 2H NMR studies of isomeric ω3 and ω6 polyunsaturated phospholipid membranes. Biochemistry 33:7203–7210

McDonnel A, Staehelin LA (1980) Adhesion between liposomes mediated by the chlorophyll a/b light-harvesting complex isolated from chloroplast membranes. J Cell Biol 84:40–56
McIntosh TJ, Simon SA (1986) Area per molecule and distribution of water in fully hydrated dilauroylphosphatidylethanolamine bilayers. Biochemistry 25:4948–4952
Mouritsen OG, Bloom M (1984) Mattress model of lipid–protein interactions in membranes. Biophys J 46:141–153
Murzyn K, Rog T, Jezierski G, Takaoka Y, Pasenkiewicz-Gierula M (2001) Effects of phospholipid unsaturation on the membrane/water interface: A molecular simulation study. Biophys J 81:170–183
Nagle JF, Wiener MC (1988) Structure of fully hydrated bilayer dispersions. Biochim Biophys Acta 942:1–10
Nagle JF, Tristram-Nagle S (2000) Structure of lipid bilayers. Biochim Biophys Acta 1469:159–195
Nielsen C, Andersen OS (2000) Inclusion-induced bilayer deformations: Effects of monolayer equilibrium curvature. Biophys J 79:2583–2604
Nielsen C, Goulian M, Andersen OS (1998) Energetics of inclusion-induced bilayer deformations. Biophys J 74:1966–1983
Nogi T, Fathir I, Kobayashi M, Nozawa T, Miki K (2000) Crystal structures of photosynthetic reaction center and high-potential iron–sulfur protein from Thermochromatium tepidum: Thermostability and electron transfer. Proc Nat Acad Sci 97:13561–13566
O'Keeffe AH, East JM, Lee AG (2000) Selectivity in lipid binding to the bacterial outer membrane protein OmpF. Biophys J 79:2066–2074
Olson R, Nariya H, Yokota K, Kamio Y, Gouaux E (1999) Crystal structure of Staphylococcal LukF delineates conformational changes accompanying formation of a transmembrane channel. Nature Struct Biology 6:134–140
Paltauf F (1994) Ether lipids in biomembranes. Chem Phys Lipids 74:101–139
Pascher I, Lundmark M, Nyholm PG, Sundell J (1992) Crystal structures of membrane lipids. Biochim Biophys Acta 1113:339–373
Pasenkiewicz-Gierula M, Takaoka Y, Miyagawa H, Kitamura K, Kusumi A (1999) Charge pairing of headgroups in phosphatidylcholine membranes: A molecular dynamics simulation study. Biophys J 76:1228–1240
Pearson RH, Pascher I (1979) The molecular structure of lecithin dihydrate. Nature 281:499–501
Periole X, Ceruso MA, Mehler EL (2004) Acid–base equilibria in rhodopsin: Dependence of the protonation state of Glu134 on its environment. Biochemistry 43:6858–6864
Perly B, Smith ICP, Jarrell HC (1985) Effects of the replacement of a double bond by a cyclopropane ring in phosphatidylethanolamines: a deuterium NMR study of phase transitions and molecular organization. Biochemistry 24:1055–1063
Petrache HI, Feller SE, Nagle JF (1997) Determination of component volumes of lipid bilayers from simulations. Biophys J 70:2237–2242
Petrache HI, Tristram-Nagle S, Gawrisch K, Harries D, Parsegian VA, Nagle JF (2004) Structure and fluctuations of charged phosphatidylserine bilayers in the absence of salt. Biophysical J 86:1574–1586
Poastor RW, Venable RM, Karplus M, Szabo A (1988) A simulation based model of NMR T1 relaxation in lipid bilayer vesicles. J Chem Phys 89:1128–1140
Pott T, Maillet JC, Dufourc EJ (1995) Effects of pH and cholesterol on DMPA membranes: a solid state ^{2}H- and ^{31}P-NMR study. Biophys J 69:1897–1908

Powl AM, East JM, Lee AG (2003) Lipid–protein interactions studied by introduction of a tryptophan residue: the mechanosensitive channel MscL. Biochemistry 42:14306–14317

Powl AM, East JM, Lee AG (2005) Heterogeneity in the binding of lipid molecules to the surface of a membrane protein: hot spots on the surface of the mechanosensitive channel of large conductance MscL. Biochemistry 44:5873–5883

Rand RP, Fuller N, Parsegian VA, Rau DC (1988) Variation in hydration forces between neutral phospholipid bilayers: evidence for hydration attraction. Biochemistry 27:7711–7722

Raynal P, Pollard HB (1994) Annexins: the problem of assessing the biological role for a gene family of multifunctional calcium- and phospholipid-binding proteins. Biochim Biophys Acta 1197:63–93

Rich MR (1993) Conformational analysis of arachidonic and related fatty acids using molecular dynamics simulations. Biochim Biophys Acta 1178:87–96

Rietveld AG, Killian JA, Dowham W, de Kruijff B (1993) Polymorphic regulation of membrane phospholipid composition in Escherichia coli. J Biol Chem 268:12427–12433

Rilfors L, Wieslander A, Lindblom G, Christiansson A (1984) Lipid bilayer stability in biological membranes In: Kates M, Manson LA (eds) Membrane fluidity. Biomembranes Vol. 12. Plenum Press, New York, pp 205–245

Sachs F, Morris CE (1998) Mechanosensitive ion channels in nonspecialized cells. Rev Physiol Biochem Pharmacol 132:1–78

Sackmann E (1995) Physical basis of self-organization and function of membranes: physics of vesicles In: Lipowsky R, Sackmann E (eds) Handbook of Biological Physics. Vol. 1. Structure and Dynamics of Membranes. Elsevier, Amsterdam, pp 213–304

Sanson A, Monck MA, Neumann JM (1995) 2D ^{1}H-NMR conformational study of phosphatidylserine diluted in perdeuterated dodecylphosphocholine micelles. Evidence for a pH-induced conformational transition. Biochemistry 34:5938–5944

Scherer PG, Seelig J (1987) Structure and dynamics of the phosphatidylcholine and the phosphatidylethanolamine head group in L-M fibroblasts as studied by deuterium nuclear magnetic resonance. EMBO J 6:2915–2922

Schlaepfer DD, Mehlman T, Burgess WH, Haigler HT (1987) Structural and functional characterization of endonexin II, a calcium- and phospholipid-binding protein. Proc Natl Acad Sci USA 84:6078–6082

Seddon JM (1990) Structure of the inverted hexagonal (H_{II}) phase, and non-lamellar phase transitions of lipids. Biochim Biophys Acta 1031:1–69

Seelig A, Seelig J (1975) Bilayers of dipalmitoyl-3-sn-phosphatidylcholine: Conformational differences between the fatty acyl chains. Biochim Biophys Acta 406:1–5

Seelig J, Seelig A (1980) Lipid conformation in model membranes. Quart Rev Biophys 13:19–61

Seelig J, Macdonald PM, Scherer PG (1987) Phospholipid head groups as sensors of electric charge in membranes. Biochemistry 26:7535–7541

Sen A, Williams WP, Quinn PJ (1981) The structure and thermotropic properties of pure 1,2-diacylgalacosylglycerols in aqueous systems. Biochim Biophys Acta 663:380–389

Shimshick EJ, McConnell HM (1973) Lateral phase separation in phospholipid membranes. Biochemistry 12:2351–2360

Shipley GG, Green JP, Nichols BN (1973) The phase behaviour of monogalactosyl, digalactosyl, and sulphoquinosyl diglycerides. Biochim Biophys Acta 311:531–544

Simidjiev I, Barzda V, Mustardy L, Garab G (1998) Role of thylakoid lipids in the structural flexibility of lamellar aggregates of the isolated light-harvesting chlorophyll a/b complex of photosystem II. Biochemistry 37:4169–4173

Simidjiev I, Stoylova S, Amenitsch H, Javorfi T, Mustardy L, Laggner P, Holzenburg A, Garab G (2000) Self-assembly of large, ordered lamellae from non-bilayer lipids and integral membrane proteins in vitro. Proc Natl Acad Sci 97:1473–1476

Small DM (1986) The physical chemistry of lipids. Handbook of lipid research, Vol. 4. Plenum Press, New York

Sohlenkamp C, Lopez-Lara IM, Geiger O (2003) Biosynthesis of phosphtaidylcholine in bacteria. Prog Lipid Res 42:115–162

Sperotto MM, Mouritsen OG (1988) Dependence of lipid membrane phase transition temperature on the mismatch of protein and lipid hydrophobic thickness. Eur Biophys J 16:1–10

Stouch TR, Alper HE, Bassolino-Klimas D (1994) Supercomputing studies of biomembranes. Supercomputer Appl High Perf Computing 8:6–23

Swairjo MA, Concha NO, Kaetzel MA, Dedman JR, Seaton BA (1995) Ca^{2+}-bridging mechanism and phospholipid head group recognition in the membrane-binding protein annexin V. Nature Struct Biology 2:968–974

Volke F, Eisenblatter S, Galle J, Klose G (1994) Dynamic properties of water at phosphatidylcholine lipid bilayer surfaces as seen by deuterium and pulsed field gradient proton NMR. Chem Phys Lipids 70:121–131

Warren GB, Toon PA, Birdsall NJM, Lee AG, Metcalfe JC (1974) Reconstitution of a calcium pump using defined membrane constituents. Proc Natl Acad Sci 71:622–626

Watanabe M, Tomita T, Yasuda T (1987) Membrane-damaging action of staphylococcal α-toxin on phospholipid-cholesterol liposomes. Biochim Biophys Acta 898:257–265

White SH, Ladokhin AS, Jayasinghe S, Hristova K (2001) How membranes shape protein structure. J Biol Chem 276:32395–32398

White SH, Wiener MC (1995) Determination of the structure of fluid lipid bilayer membranes. In: Disalvo EA, Simon SA (eds) Permeability and stability of lipid bilayers. CRC Press, Boca Raton, pp 1–19

Wiener MC, King GI, White SH (1991) Structure of a fluid dioleoylphosphatidylcholne bilayer determined by joint refinement of X-ray and neutron diffraction data. I. Scaling of neutron data and the distribution of double bonds and water. Biophys J 60:568–576

Wiener MC, White SH (1992) Structure of a fluid dioleoylphosphatidylcholne bilayer determined by joint refinement of X-ray and neutron diffraction data. III. Complete structure. Biophys J 61:434–447

Wikstrom M, Xie J, Bogdanov M, Mileykovskaya E, Heacock P, Wieslander A, Dowhan W (2004) Monoglucosyldiacylglycerol, a foreign lipid, can substitute for phosphatidylethanolamine in essential membrane-associated functions in Escherichia coli. J Biol Chem 279:10484–10493

Williamson IM, Alvis SJ, East JM, Lee AG (2002) Interactions of phospholipids with the potassium channel KcsA. Biophys J 83:2026–2038

Yeagle PL (1978) Phospholipid headgroup behavior in biological assemblies. Acc Chem Res 11:321–327

Zaccai G, Buldt G, Seelig A, Seelig J (1979) Neutron diffraction studies on phosphatidylcholine model membranes. J Mol Biol 134:693–706

Zhou F, Schulten K (1995) Molecular dynamics study of a membrane–water interface. J Phys Chem 99:2194–2207

Peptide–Lipid Interaction: Shedding Light into the Mode of Action and Cell Specificity of Antimicrobial Peptides

Yechiel Shai

7.1 Introduction

Endogenous peptide antibiotics are known as evolutionarily old components of innate immunity. They were found initially in invertebrates (Agerberth et al.1995), but later on also in vertebrates, including humans (Agerberth et al.1995; Gudmundsson et al. 1996). This secondary, chemical immune system provides organisms with a repertoire of small peptides that are promptly synthesized upon induction, and act against invasion (for both offensive and defensive purposes) by occasional and obligate pathogens (Agerberth et al.1995; Hancock and Diamond 2000; Nicolas and Mor 1995; Saberwal and Nagaraj 1994; Zasloff 2002; Hoffmann and Reichhart 2002). These peptides are a group within water/membrane soluble proteins and peptide toxins used in the defense and offense systems of all organisms. They include peptides that vary significantly in their length, secondary structure, tertiary structure, and the presence or absence of disulfide bridges. Their size also varies significantly and includes ~9–100 amino acids (aa) (mostly common L-aa), but very short synthetic antimicrobial peptides (AMPs) (6 aa) were also reported (Jing et al. 2003). Most antimicrobial peptides are characterized by several properties including: (1) high percentage of hydrophobic amino acids (>50%), (2) a net positive charge, and (3) the potential to form an amphipatic structure in membranes, in the form of an α-helix, β-sheet or any other structure (Boman 1995; Dimarcq et al. 1998; Breukink et al. 1999; Shai 1999; Tossi et al. 2000; Brotz and Sahl 2000). The updated list of native AMPs contains more than 800 sequences, and several thousands of de novo designed antimicrobial peptides (the reader is referred to http://www.bbcm.univ.trieste.it/~tossi/search.htm for an updated list).

Because bacterial resistance to conventional antibiotics has become a major problem worldwide due to their extensive use, the development of new families of antibiotics that can overcome resistance has become an important task. In fact, strains of bacteria that are resistant to all available antibiotics already exist (Wong et al. 2000; Bonomo, R. A. 2000). AMPs vary in their spectrum of activity and they can be classified into several groups:

1. Peptides that are highly toxic to microorganisms but are not active, or have low toxicity toward normal mammalian cells. This group includes peptides that are selective to different types of bacteria, e.g. cecropins isolated from the cecropia moth, which are active mainly on Gram-positive bacteria (Steiner et al. 1981). Others are active on both Gram-positive and Gram-negative bacteria, e.g.

Springer Series in Biophysics
C.R. Mateo et al. (Ed.)
Protein-Lipid Interactions

magainins (Zasloff 1987) and dermaseptins (Mor et al.1991), both isolated from the skin of frogs; cathelicidins (Zanetti et al. 2002; Lehrer and Ganz 2002) and many others. This family also includes peptides that are active toward bacteria and fungi or active solely on fungi and not on other targets (Landon et al. 1997).

2. Peptides that are toxic to microorganisms and mammalian cells, such as the bee venom melittin (Habermann and Jentsch 1967), the *Moses sole* fish venom pardaxin (Shai et al. 1988; Oren and Shai 1996), and to some extent the human cecropin-like LL-37 (the first amphipatic α-helical peptide isolated from human), and other cathelicidins (Johansson et al. 1998; Oren et al. 1999) and defensins (Lehrer et al. 1993). The reader is referred to the many studies in the field for more examples.

Understanding the mode of action of AMPs and the parameters involved in their target cell specificity have been the subject of intense studies in recent years. Importantly, potential toxicity makes it of great importance to know the underlying properties of AMPs that control selectivity to a specific target (Hancock and Rozek 2002). In contrast to available antibiotics, most AMPs cause physical damage to the microorganism by disrupting and increasing the permeability of its cytoplasmic membrane, damage that is hard to fix (Hancock and Diamond 2000; Nicolas and Mor 1995; Boman 1991; Zasloff 1992; Lehrer and Ganz 1999; Hoffmann et al. 1999; Guder et al. 2000). Further support for the difficulties encountered by bacteria to become resistant to AMPs is the fact that AMPs are ancient components of all species of life, and their induction pathways in all organisms, including insects and plants, are conserved, and yet they are active for millions of years. Since the killing mechanism of AMPs is different from that of the available antibiotic, to which bacteria become resistant, AMPs are considered as attractive substitute and/or additional drugs to conventional antibiotics. Note, however, that bacteria can develop resistance to some AMP (which will be discussed later on). The long list of natural AMPs isolated so far, as well as the synthetic peptides, makes it hard to review most of them. Therefore, this chapter will focus on only a few representative peptides.

7.2 The Target of Most Antimicrobial Peptides

Mode-of-action studies have revealed that most AMPs use the microorganisms' cytoplasmic membrane as their final and lethal target. Note, however, that several studies have pointed out that they have other targets inside the cell as well (Bowdish et al. 2004; Davidson et al. 2004). Lehrer et al. (1989) were the first to demonstrate a membrane permeabilization mechanism in intact bacteria. They showed that human neutrophil peptide defensin [HNP]-mediated bactericidal activity against *E. coli* is associated with sequential permeabilization of the outer and inner membranes, and that inner membrane permeabilization appears to be the lethal event. For this study they utilized the ability of the normally impermeable substrate o-nitrophenyl galactoside (ONPG) to be hydrolyzed by a cytoplasmic enzyme L-galactosidase as a test of increased permeability. Since the main constituents of these membranes are phospholipids, many studies were conduct-

ed on the interaction of AMPs with model phospholipid membranes (Shai 1999; Matsuzaki 1999; Wieprecht et al. 2000; Bechinger 1999; Wu et al. 1999). Note, however, that the peptides need to traverse first the outer wall of the cell before they can reach the cytoplasmic membrane. The importance of this barrier in determining the mode of action of AMPs will be elaborated later on. The following paragraphs will focus on several questions including: (1) What are the binding sites for antimicrobial peptides? (2) What is the molecular mechanism by which AMPs recognize and increase the permeability of phospholipid membranes? (3) Is there a direct correlation between the activity of AMPs on model membranes mimicking the membranes of different microorganisms, and their corresponding biological function on these organisms? (4) Is there a need for a specific peptide sequence and structure to gain potent antimicrobial activity?

(1) *The cell membrane as a non-specific receptor.* A non-receptor-mediated mode of action of AMPs was proposed because enantiomers of AMPs (composed solely of D-aa) preserved the same biological function of their all L-amino acid parental native peptides. Examples include melittin (a non-cell-selective α-helical lytic peptide), cecropin (a non-hemolytic α-helical peptide active mainly on Gram-positive bacteria), magainin (a non-hemolytic α-helical peptide active on both Gram-positive and Gram-negative bacteria) androctonin (a non-hemolytic β-sheeted peptide containing cysteine) and others (Wade et al. 1990; Bessalle et al. 1990; Merrifield, et al. 1995; Hetru et al. 2000). Very interestingly, it was also shown that diastereomers (containing both L- and D-aa) of non-cell-selective lytic peptides preserved their antimicrobial activity, but lost their lytic activity toward mammalian cells. This has been shown with diastereomers of pardaxin, melittin, and *de novo* designed lytic peptides composed of leucine and lysins (Oren and Shai 1996; Shai and Oren 1996; Oren et al. 1997; Hong et al. 1999; Kondejewski et al. 1999; Avrahami et al. 2001). The structure of the diastereomers is different from that of their parental peptides composed solely of L-amino acid peptides, and therefore the same receptor should not recognize both the all-L-aa and the diastereomeric forms. Note, however, that if the recognition is within the membrane milieu such interaction is possible, since it has been shown that recognition within the membrane milieu is chirality independent (Gerber et al. 2004a, b, 2005; Sal-Man et al. 2004; Gerber and Shai 2002). Other studies further demonstrated the advantages of incorporating D-aa into membrane-active and AMPs (Jelokhani-Niaraki et al. 2000; Fernandez-Lopez et al. 2001).

These studies suggest that AMPs have a general and common target. This target is believed to be the bacterial cell wall and the cytoplasmic membrane, both of which are negatively charged (Brock 1974), compared with the zwitterionic mammalian membranes (Verkleij et al. 1973), as will be discussed in the following paragraphs. The net positive charge allows preferential binding to the negatively charged constituents of the bacterial wall (reviewed in Shai 1999; Tossi et al. 2000; Wu et al. 1999; Matsuzaki et al. 1998; Oren and Shai 1998; and Bulet et al. 1999).

(2) *AMPs that bind to specific receptors.* A few peptides use receptors for their interaction with the bacteria cell wall. Peptides belonging to this group are produced mainly by bacterial, they are active at nanomolar concentrations, and have a narrow spectrum of activity. They contain two regions: a receptor-binding domain and a membrane-binding domain. The receptor increases the peptides af-

finity to the membrane, and as a consequence they reach a high concentration of membrane-bound peptide which induces an increase in membrane permeability. The first identified peptide within this group was nisin Z, which uses the membrane-anchored cell-wall precursor lipid II as a receptor (Breukink et al. 1999). Nisin combines the high affinity for lipid II with pore-forming ability. It is not clear, however, how the pore-forming domain permeates the target membrane. It has also been shown that lipid II is not only the receptor for nisin but an intrinsic component of the pore formed by nisin, and that the stoichiometry between nisin and lipid II is either 1:1 or 1:2 (Breukink et al. 2003; Hsu et al. 2004; Hasper et al. 2004). Furthermore, Wiedemann et al. (2004) performed single-channel experiments in the absence of lipid II and found that a constant voltage of 100 mV had to be applied in order to obtain a strong current. However, when the membrane was doped with 1 mol% lipid II, only 5 mV was sufficient to produce regular patterns of membrane conductance, corresponding to an average pore diameter of 2–2.5 nm. Bacteriocins are another group of AMPs with a receptor-mediated activity. They are composed of 37–44 amino acids, ribosomally synthesized by lactic acid bacteria (Marugg et al. 1992; Fleury et al. 1996). These peptides show potent activity toward a narrow spectrum of Gram-positive food spoilage and pathogenic bacteria, e.g. *Listeria*. They display no toxicity toward humans or other eukaryotes (Ennahar et al. 2000). An enantiomer of leuA, a member of this family, composed of only D-aa, was completely inactive against bacteria, thereby demonstrating that a chiral interaction is required at the target-cell surface for bacteriocin to display its effects (Yan et al. 2000). Removal of the receptor-binding domain in members of this group resulted in a loss of bacteria-specific selectivity. The resultant analogs became active toward other bacteria at a micromolar range.

Most of the AMPs reported so fare do not use receptors for their function. Therefore, the following paragraphs will focus on a non-receptor-mediated killing mechanism of AMPs.

7.3 How do AMPs Select Their Target Cell?

Data from many reports revealed no correlation between the specific biological function of AMPs, and their sequence or structure. Some kill specifically bacteria and others are active also against eukaryotic cells. These intriguing properties led to a fundamental question: what are the parameters that are involved in their activities toward a particular target? These parameters were found to be dependent on the properties of both the peptide and the target cell.

7.3.1 The Role of the Membrane and Peptide Properties in the Biological Function

The majority of AMPs share two properties: they are highly cationic and they are composed of approximately 50% hydrophobic amino acids (reviewed in Sab-

erwal and Nagaraj 1994; Shai 1999; Tossi et al. 2000; Bulet et al.1999; Kobayashi et al. 2000; Hwang and Vogel 1998; Andreu and Rivas 1998). However, there are exceptions, such as temporins, 13 amino acid AMPs isolated from the skin of frogs, which contain only one positively charged amino acid (Simmaco et al. 1996; Mangoni et al. 2004). Regarding the compositions of the membranes of the target cells, there are several major differences between the phospholipids of the cytoplasmic membranes, as well as between the compositions of the outer wall/layer of various target cells. The outer surface of Gram-negative bacteria contains lipopolysaccarides (LPS), and that of Gram-positive bacteria contains acidic polysaccharides (teichoic acids), conferring a net negative charge to the surface of both Gram-positive and Gram-negative bacteria (Brock 1974). Furthermore, the phospholipids of the inner membrane of Gram-negative bacteria and the single membrane of Gram-positive bacteria are negatively charged and composed predominantly of phosphatidyl glycerol (PG) and phosphatidylethanol amine (PE). In addition, Gram-negative bacteria have a thinner cell-wall peptidoglycan layer compared with Gram-positive bacteria. In contrast to bacteria, the distribution of phospholipids in normal mammalian cells is asymmetric; the outer leaflet is composed predominantly of zwitterionic phosphatydilcholine (PC), cholesterol and sphingomyelin, whereas the inner leaflet is composed of negatively charged phosphatydilserine (PS) (Verkleij et al. 1973). However, they also contain a large number of highly negatively charged sialic acid-containing carbohydrate moieties in the form of glycoproteins and glycosphingolipids, which form the glycocalix layer. Similarly, the outer surface of fungi is composed of PC and ergosterol. It should be noted also that the outer surface of many cancer cells is slightly more negatively charged compared with normal cells because (1) they are slightly enriched with PS in their outer surface compared with normal cells, and (2) they are enriched with O-glycosylated mucines, high molecular weight glycoproteins comprising a backbone protein, to which oligosaccharides are attached via the hydroxylic groups of serine or threonine (Cappelli et al. 1999). This might explain why some AMPs efficiently lyse both bacteria and cancer cells (Ohsaki et al. 1992; Baker et al. 1993; Papo et al. 2003; Papo and Shai 2003; Papo et al. 2004).

7.3.2 Peptide Sequence and Organization in Solution and Membranes

The biological function of AMPs does not depend on their specific structure. In addition, in some cases more than 60% of the amino acids were substituted in a particular AMP without affecting its biological function, while in others, minor changes in their primary sequence markedly affected their spectrum of activity. These topics and others are elaborated in the following paragraphs.

7.3.2.1 Peptide Hydrophobicity and Charge

The distribution of the positive charges along the peptide backbone have an effect on the biological function of AMPs. AMPs with their positively charged amino acids, spread along the peptidic chain, act better toward bacteria compared with mammalian cells. Examples include magainin (Matsuzaki 1998), cecropins (Steiner et al. 1981; Gazit et al. 1994; Bechinger 1997), dermaseptins (Mor et al. 1991; Pouny et al. 1992), and others (Tossi et al. 2000; Andreu and Rivas 1998). In contrast, AMPs that are not cell-selective have either a low number of positive charges, or alternatively, most of their positively charged amino acids are segregated at the termini of the peptides. Examples include melittin (Blondelle and Houghten 1991; Sharon et al. 1999), pardaxin analogs (Oren and Shai 1996), indolicidin (Selsted et al. 1992), and bombinins (Mignogna et al. 1993). However, there are exceptions that include highly potent antifungal AMPs that do not have their positively charged amino acids segregated at the peptide termini. The list includes defensines (Hoffmann and Reichhart 2002), dermaseptins (Strahilevitz et al. 1994; Ghosh et al. 1997), cathelicidines (Zanetti et al. 1997), the human-like cecropin, LL-37 (Johansson et al. 1998; Oren et al. 1999), tachystatin (Osaki et al. 1999), bovine lactoferricin (Vogel et al. 2002), and others. Note that peptides which are active against fungi are in most cases also more hemolytic. This is because the predominant component of the outer leaflet of the membranes of both mammalian and fungal cells is zwitterionic (predominantly PC phospholipids), although those of fungi are slightly more acidic due to the presence of PI. However, a few native positively charged AMPs and lipopeptides are sensitive to this mild difference in lipid composition, and therefore act on fungi at concentrations which do not lyse mammalian cells. The list includes dermaseptin, LL-37 and de novo designed short (12-mer) fatty-acid-conjugated diasteriomeric peptides (Avrahami and Shai 2003, 2004). Loss of cell specificity can also result if the peptide hydrophobicity is increased, concomitant with a reduction in the number of positively charged amino acids (Oren et al. 1997; Hong et al. 1999).

7.3.2.2 The Role of the Amphipatic Structure and its Stability

Most studies were carried out with L-amino acid peptides possessing amphipathic α-helix or β-sheet structures, which are known to be important for biological activities. In contrast, studies which compared the effect of significantly altering the sequence of an amphipathic α-helical peptide (15 aa long) and its diastereomer (composed of both L- and D-aa) did not support the need for a preferred structure or sequence (Papo et al. 2002, Papo and Shai 2004). Table 7.1 lists the sequences of the all-L-amino acid peptides and their D,L-amino acid diastereomers. These peptides were investigated regarding their structure, function, and interaction with model membranes and intact bacteria. Sequence alteration included changing the positions of the D-aa, shuffling between the amino acids, scrambling, as well segregating the hydrophobic and positively charged amino

Table 7.1. Designations, sequences, retention times, and percentage of enzymatic degradation of *de* novo designed all-L-amino acid cationic peptides and their diastereomers, in which the sequences were drastically altered while keeping the same amino acid composition

Peptide designation	Sequence[a] retention	RP-HPLC of enzymatic time (min)	Percentage degradation[b]
L-aa peptides			
Amphipathic-1L	L K L L K K L L K K L L K L L-NH_2	24.23	100
Scrambled-4L	K L K L L K L L K L L K L L K-NH_2	24.41	100
Segregated-5L	K K K L L L L L L L L L K K K-NH_2	23.30	100
Diastereomers			
Amphipathic-1D	L K **L** L K K L **L** **K** K L L **K** L L-NH_2	22.95	58
Amphipathic-2D	L L **K** K L L K **L** **L** L K L **L** K K-NH_2	23.12	100
Amphipathic-3D	L L **K** L L K K **L** **L** K K L **L** K L-NH_2	21.31	100
Scrambled-4D	K L **K** L L K L **L** **K** L L K L **K** L K-NH_2	23.02	26
Segregated-5D	K K **K** L L L L **L** **L** L L L **K** K K-NH_2	25.05	0
Segregated-6D	L L **L** L L **K** K **K** **K** K K L **L** L L-NH_2	26.98	100

[a] Underlined and bold amino acids are D-enantiomers. All the peptides are amidated in their C-terminus.

[b] Peptides were treated for 2 h with trypsin or proteinase-K.

acids. Interestingly, the effect of sequence alteration on biological function was similar for the L-amino acid peptides and the diastereomers, despite some differences in their structure in the membrane as revealed by ATR-FTIR spectroscopy. However, whereas the all-L-amino acid peptides were highly hemolytic, had low solubility, lost their activity in serum, and were fully cleaved by trypsin and proteinase-K, the diastereomers were non-hemolytic and maintained full activity in serum. Furthermore, sequence alteration allowed making the diastereomers fully, partially, or totally protected from degradation by the enzymes, which should be an advantage for future design of such peptides for therapeutic purposes (Papo et al. 2002).

Regarding AMPs with a stable amphipatic structure, they can expose their hydrophobic face to the hydrophobic constituents of the target cell membrane. This should permit strong interactions with the cell membrane, driven by hydrophobic interactions rather than by electrostatic interactions. As a consequence, they are

non-cell-selective. The bee venom melittin serves as a good example. It adopts ~80% α-helical structure when bound to phospholipid membranes. A diastereomeric analog of melittin was synthesized by substituting four L-aa along the peptide with their D-aa enantiomers. This diastereomer bound strongly and destabilized only negatively charged phospholipid vesicles, in contrast to native melittin, which bound strongly also zwitterionic phospholipids. As a result, this diastereomer was not active against erythrocytes, but preserved activity toward bacteria (Oren and Shai 1996). The structure of the diastereomer was determined by NMR in water, as well as in three different membrane-mimicking environments, 40% 2,2,2-trifluoroethanol (TFE)/water, methanol, and dodecylphosphocholine /phosphatidylglycerol (DPC/DMPG) micelles (Sharon et al. 1999) (Fig. 7.1). The NMR data revealed a stable amphipatic α-helix only in the C-terminal region of the diastereomer in membrane-like environments. In solution, native melittin forms tetramers which stabilize its α-helix (Terwilliger and Eisenberg 1982). However, the diastereomer is completely unstructured and exists as monomers in solution. This structural alteration affects the free energy of binding and insertion into membranes. The free energy cost of inserting unfolded peptides into both negatively charged and zwitterionic phospholipids membranes include the hydrophobic interactions between the non-polar amino acids and the phospholipid hydrocarbon layer, and the cost of partitioning the polar amino acids and the peptide bond (CONH) into a non-polar environment (Wimley and White 1996). Electrostatic interactions play an important role in the initial binding of the diastereomer to negatively charged membranes (Papo and Shai 2003). When bound to these membranes, the positive charges of the diastereomer are partially neutralized by the negative charges of the phospholipid headgroups, thus reducing the energy cost of adsorbing the peptide into the membrane. Subsequently, it allows the hydrophobic forces to manifest themselves following the formation of a stable α-helical structure in the C-terminal of the peptide. This drives the peptide further into the interface, leading to membrane lysis. This does not occur with zwitterionic phospholipids, and therefore, the diastereomer binds these membranes 100–1000-fold less than native melittin (Papo and Shai 2003; Ladokhin and White 1999).

Interestingly, even though the structure of a diastereomer is not preserved it can form a kind of amphipatic structure. An NMR study was conducted to determine the structure of an amphipathic α-helical peptide KLLLKWLLKLLK-NH_2 (K_4L_7W) and its diastereomer KL**LL**KWL**L**K**L**LK-NH_2 (D-$L^{3,4,8,10}K_4L_7W$) (where bold and underlined letters indicate D-aa) in hydrophobic environments (Oren et al. 2002). The structures in DPC micelles of all L-aa K_4L_7W and D-$L^{3,4,8,10}K_4L_7W$ shown in Figs. 7.1(B) left side and 3(B) right side, respectively, display the relative positions of the two central lysine residues (Lys-5 and Lys-9) and adjacent leucines (Leu-4 and Leu-8). Interestingly, the α-helix was clearly observed for K_4L_7W in the DPC micelles, and less defined, although somewhat helical structure was observed for D-$L^{3,4,8,10}K_4L_7W$. Importantly, the positions of the leucine and lysine side-chains illustrate the amphipathic organization of the peptides. The relative side-chain orientations depicted in Fig. 7.1(b) clearly reveal segregation between charged (lysine side-chains) and hydrophobic (leucine side-chains) interfaces within the membrane-associated peptides.

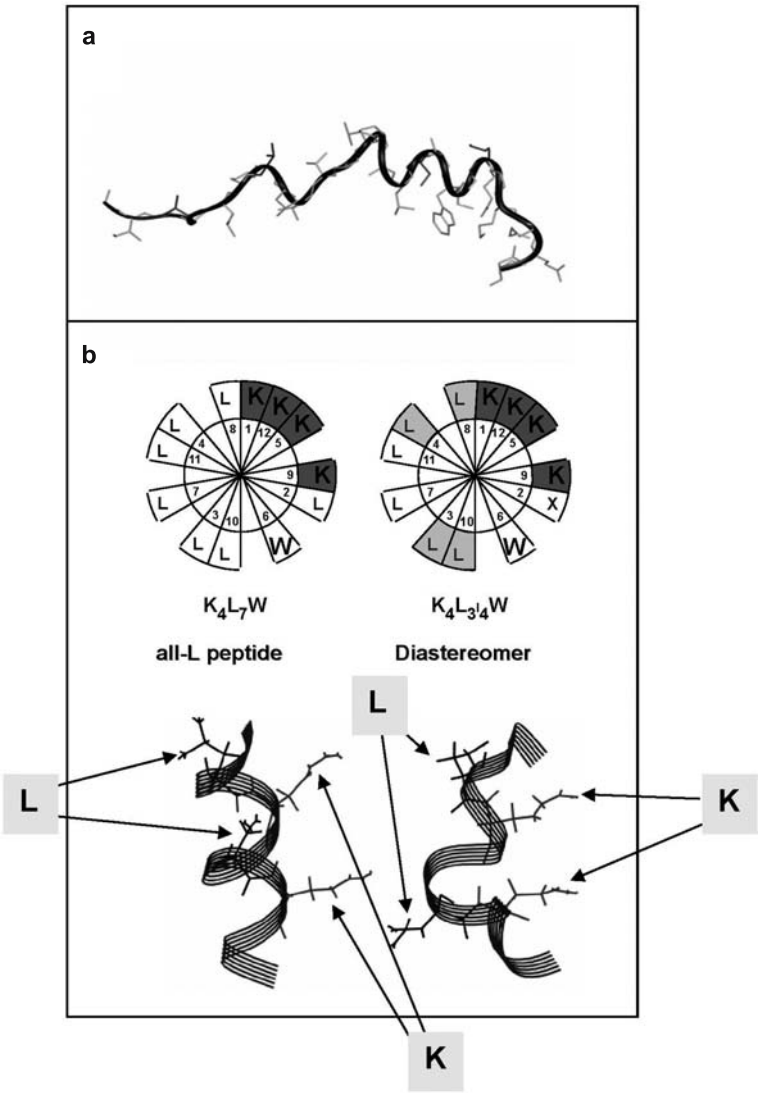

Fig. 7.1. (a) The NMR structure of [D]-$V^{5,8},I^{17},K^{21}$-melittin in DPC/DMPG micelles (Sharon et al. 1999). **(b)** Wheel structure and calculated average structures of diastereomeric peptides composed of Lys and Leu, showing the orientation of residues Leu-4, Leu-8, Lys-5 and Lys-9 in DPC micelles (Oren et al. 2002)

7.3.2.3 The Role of Peptide Self-Association in Solution and/or in Membranes

Self-association of AMPs is an important parameter which affects their selectivity toward different cells. Self-association is driven either by the peptidic chain, or by the attachment of extrinsic hydrophobic groups such as fatty acids, resulting in the formation of α-helical bundles that could initiate strong hydrophobic binding to zwitterionic membranes (Oren et al. 1999; Strahilevitz et al. 1994; Ghosh et al. 1997). The role of self-association of AMPs in their selective binding to target cells is elaborated in the following paragraphs.

(1) *AMP self-association driven by amino-acid interaction*. The effect of peptide self-association on the function of AMPs has been demonstrated in several studied.
   (a) Dermaseptin and its native mutants, isolated from the skin of the *Phyllomedusa* frog (Mor et al. 1994), were shown to have different cell specificities. Mode-of-action studies demonstrated that those which are non-cell-selective oligomerize in the membrane and bind and permeate both zwitterionic and negatively charged membranes (Strahilevitz et al. 1994; Kustanovich et al. 2002). Assembly was driven either by the hydrophobic N-terminal of one mutant or by the additional negative charge (Asp at the fifth position) in another mutant. In another study, dermaseptin S3 (DS3) was shown to be toxic only toward the intraerythrocytic parasite, while another mutant, dermaseptin S4 (DS4), was toxic to both the parasite and the host erythrocyte (Ghosh et al. 1997). Studies with fluorescently labeled peptides revealed that DS4 forms larger aggregates in aqueous solution compared with DS3.
   (b) The role of peptide oligomerization in selective lytic activity was addressed also with the human cecropin-like LL-37, which is cytotoxic to both bacteria and normal eukaryotic cells. In contrast, its N-terminal truncated form, FF-33, preserved the antimicrobial activity of the parental LL-37 but was devoid of hemolytic activity. Using fluorescently labeled peptides, it was found that LL-37, but not FF-33 exists in equilibrium between monomers and oligomers in solution at very low concentrations (Oren et al. 1999).
   (c) A series of amphipatic all-L-amino acid peptides and their diastereomers were de novo synthesized. The template for the sequence was $KX_3KWX_2KX_2K$ where X = Gly, Ala, Val, Ile, or Leu (Avrahami et al. 2001). The data revealed that most of the L-amino acid peptides oligomerized and adopted distinct structures (random coil, α-helix or β sheet) in solution and in a membrane mimetic environment. Among this group, only the Leu-containing peptide was active on both bacteria and human erythrocytes, while its diastereomer, which did not oligomerize in solution, was active only on bacteria. The large size of these oligomers probably prevented them from penetration into the bacterial phospholipid membrane, and therefore, their all L-amino acid parental peptides were practically inactive (Avrahami et al. 2001).

(2) *AMP self-association driven by the conjugation of fatty acids*. The attachment of fatty acids has been shown to control hydrophobicity and self-assembly of monomeric AMPs, without altering the properties of the peptidic chain. In a first study magainin was used (Avrahami and Shai 2002). When aliphatic acids with different lengths were attached to its N-terminal they affected its organization in solution. The attachment of heptanoic, undecanoic, and palmitic acids resulted in lipopeptides with three distinct structures and oligomeric states in solution, at their minimal inhibitory concentration (MIC): (a) the attachment of heptanoic acid resulted in a monomeric, unordered structure; (b) the attachment of undecanoic acid yielded concentration-dependent oligomers of α-helices; and (c) the attachment of palmitic acid yielded concentration-independent α-helical monomers, a novel lipopeptide structure, which is resistant to proteolytic digestion. A cartoon illustrating possible organizations of these three lipopeptides is shown in Fig. 7.2. As expected, the increase in hydrophobicity and the oligomeric state of magainin analogs increased its activity toward mammalian cells. Similar results were obtained with fatty acid-conjugated de-novo synthesized 12-mer diastereomeric AMPs (Avrahami and Shai 2003).

In another study conjugation of fatty acids to non-membrane active peptides endowed them with antimicrobial activities (Avrahami and Shai 2003, 2004). A new group of lipopeptides with potent antifungal or both antibacterial and antifungal activities was developed by conjugation of palmitic acid to short positively charged peptides, which are devoid of biological activity. The parental peptides also did not have the threshold hydrophobicity required for

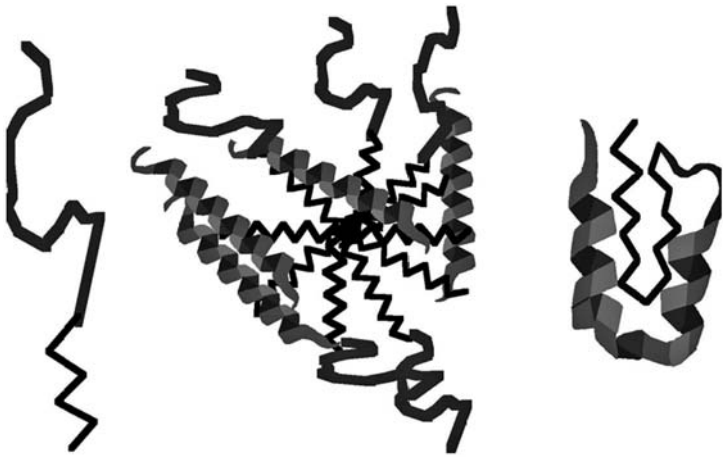

Fig. 7.2. A cartoon illustrating possible organizations of three lipophilic magainin analogs in solution. *Thick lines* and *helices* represent the peptides and *thin lines* represent the fatty acid moieties (modified from Avrahami and Shai 2002)

membrane binding and permeation. Specifically, a group of diastereomeric peptides with a general sequence K_4X_7W (X designates one of the following aliphatic amino acids: Gly, Ala, Val, or Leu) were palmitoylated at their N-terminus. Most importantly, palmitoylated K_4G_7W and K_4A_7W gained potent antibacterial and antifungal activity with low hemolytic activity, despite the fact that both parental peptides were completely devoid of any activity toward microorganisms and model phospholipid membranes. In contrast, palmitoylated K_4L_7W lost the potent antibacterial activity of the parental peptide but preserved antifungal activity albeit with different selectivities. Interestingly, both K_4V_7W and its palmitoylated analog were inactive toward bacteria, and only the palmitoylated peptides was highly potent toward yeast. Both the Leu and Val derived lipopeptides were also endowed with hemolytic activity. Mode-of-action studies suggested that this group of lipopeptides act by increasing the permeability of the cell membrane, and that differences in their potencies and target specificities are the result of differences in their oligomeric state and ability to dissociate and insert through the cell wall into the cytoplasmic membrane.

(3) *Cyclization of linear lytic peptides decreases assembly and increases selectivity towards bacteria*. Cyclization of linear amphipatic α-helical peptides reduced the extent of their α-helical structure, and as a consequence reduced their oligomeric state, which in turn affected their biological function. Examples include the following. Cyclic forms of magainin 2 and melittin were synthesized by incorporation of cysteins at both the N- and C-termini of the peptides (Avrahami and Shai 2002). Cyclization of magainin markedly reduced its cytolytic activity toward both erythrocytes and bacteria. In contrast with magainin, cyclization of melittin analog significantly reduced its hemolytic activity but preserved or increased activity toward bacteria. The reduction in hemolytic activity of both peptides upon cyclization was correlated with a reduction in their binding and the ability to increase the permeability of PC/cholesterol membranes, the major component of the outer leaflet of red blood cells. Most importantly, at similar molar ratios of bound peptide:lipid, both linear and cyclic magainin analogs showed similar membrane permeation activity with both zwitterionic and negatively charged phospholipid membranes, indicating that the linearity of this peptides is not required for membrane binding and permeation. However, the finding that cyclic magainin is much less active than linear magainin in the killing of bacteria, points to the role of linearity in reaching the bacterial inner phospholipid membrane.

7.4 Mode of Action of AMPs

The studies described above indicated the cell membrane as the major target of AMPs. However, internal targets were proposed for some of them (Hancock and Diamond 2000; Hancock and Rozek 2002; Wu et al. 1999). To interact and insert into the target membrane, AMPs undergo conformational changes from

water-soluble to membrane-soluble form, but the details of the actual membrane permeation pathways for most AMPs are still not clear. Although several models were proposed in recent years, the majority of them suggest that the membrane permeation process takes place via two consecutive steps: (1) peptides bind onto the surface of the membrane until a local threshold concentration has been reached, and (2) peptides permeate the membrane (Zasloff 2002; Shai 1999; Tossi et al. 2000; Hancock and Rozek 2002).

7.4.1 The Barrel-Stave Model

The barrel–stave model was first proposed to describe the formation of transmembrane channels/pores by bundles of amphipatic α-helical peptides (Ehrenstein and Lecar 1977; Sansom 1993, 1998). Peptides which act via this mechanism are inserted into the membrane such that their hydrophobic surfaces interact with the lipid core of the membrane and their hydrophilic surfaces point inward producing an aqueous pore (Fig. 7.3). Amphipatic α-helical lytic peptides which act on a specific or several types of cells including bacteria, fungi and mammalian cells, were among the first to be discovered, and therefore used as models for mode-of-action studies. It has been suggested that following binding, linear amphipatic α-helical peptides would form transmembrane pores, presumably via a barrel–stave mechanism (Ehrenstein and Lecar 1977) (Fig. 7.3). The experimental evidence for this model was predominantly the ability of many of these peptides to induce single channels in planar lipid membranes (Christensen et al. 1988; Westerhoff et al. 1989; Duclohier et al. 1989; Matsuzaki et al. 1991). Peptides that act via the barrel–stave mechanism need to insert into the hydrophobic lipidic core of the membrane, and therefore their interaction with the target membrane is governed predominantly by hydrophobic interactions. The following steps are involved in the barrel–stave mechanism: (1) the peptides bind onto the surface of the membrane and self-associate; (2) the bundle inserts into the membrane to

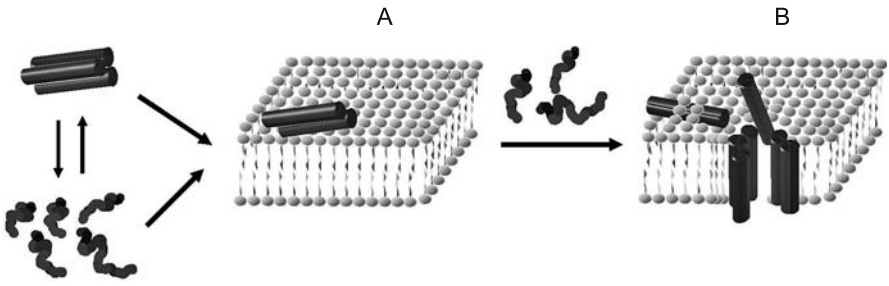

Fig. 7.3. A cartoon illustrating the formation of channels/pores via the barrel–stave model. Peptides reach the membrane either as monomers or oligomers and assemble on the surface of the membrane (step **A**). In the next step they insert into the lipid core of the membrane following recruitment of additional monomers (step **B**)

form a transmembrane pore; (3) the pore increases due to the recurrent of more monomers; (4) a minimal length of ~22 aa is required for a peptide to transverse the lipid bilayers if it adopts an α-helical structure, or ~8 aa if the peptide adopts a β-sheeted structure. Studies have shown that only a few lytic amphipatic peptides act via the barrel–stave mechanism. All of these peptides bind to membranes via hydrophobic interactions and are usually very toxic to all types of cells including bacteria, mammalian cells and fungi. Examples include alamethicin (Sansom 1993; Rizzo et al. 1987), melittin (DeGrado et al. 1982; Vogel et al. 1983; Dempsey and Butler 1992; Ladokhin and White 2001), pardaxin (Shai et al. 1990; Rapaport and Shai 1991, 1992), and the helix α5 of δ-endotoxin (Gazit and Shai 1993; Gazit et al. 1994).

7.4.2 The Carpet Model

The barrel–stave mechanism was found to be used by the non-cell-selective AMPs but not by those peptides that are selectively active on bacteria (Strahilevitz et al. 1994; Shai et al. 1990; Rapaport and Shai 1991, 1992; Gazit et al. 1994; Pouny and Shai 1992; Shai 1994). Detailed mode-of-action studies suggested an alternative model, termed the carpet model or a detergent-like model (Pouny and Shai 1992; Gazit et al. 1995a, b).

Figure 7.4 depicts the four steps proposed to be involved in the carpet mechanism:

(1) The peptides bind, in a monomeric or oligomeric form, onto the surface of the negatively charged target membrane and cover it in a carpet-like manner.
(2) The peptides reorient themselves such that their hydrophobic face is toward the lipids and the hydrophilic face toward the phospholipid head groups.
(3) The peptides reach a threshold concentration.
(4) The peptides permeate/disintegrate the membrane by disrupting the bilayer curvature.

According to the carpet model, peptides are in contact with the phospholipid head group throughout the entire process of membrane permeation. An early step before the collapse of the membrane packing may include the formation of transient holes in the membrane. Such holes were described in the torodial model for pore formation or in the two-state model, in which the lipid bends back on itself like the inside of a torus (Matsuzaki et al. 1995; Ludtke et al. 1996; Heller et al. 1998; Huang 2000). Major differences between the carpet and barrel–stave models are: (1) the carpet model does not require recognition between membrane-bound peptide monomers; (2) in the carpet model peptides do not insert into the hydrophobic core of the membrane; and (3) the carpet model does not require a specific peptide structure. Based on the above, a major advantage of the carpet mechanism is that many peptides can fall within the criteria required, which indeed explains why thousands of peptides have antimicrobial activity regardless of their length, sequence and secondary structure.

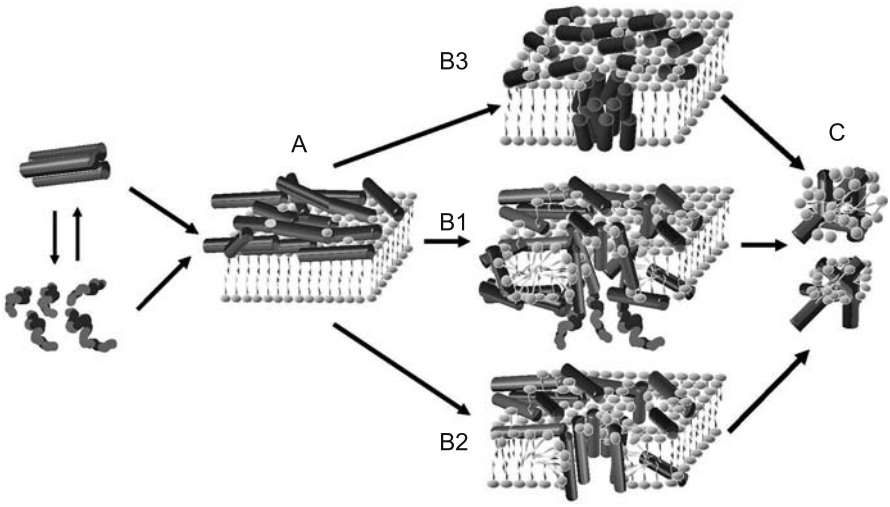

Fig. 7.4. A cartoon illustrating the carpet model suggested for membrane permeation. The peptides reach the membrane as monomers or oligomers, followed by binding to the surface of the membrane with their hydrophobic surfaces facing the membrane and their hydrophilic surfaces facing the solvent (step **A**). After a threshold concentration of peptide monomers has been reached, the peptides permeate the membrane. This can be achieved in different ways, e.g. a detergent-like effect via the formation of non-organized transient pores (step **B1**), formation of organized transient or permanent toroidal pores (step **B2**) or hydrophobic pore/channel aggregates **(B3**) when the peptide is very hydrophobic. The final stage in all cases may be membrane disintegration (step **C**)

The carpet mechanism described the mode of action of many other AMPs, such as dermaseptin natural analogues (Strahilevitz et al. 1994; Ghosh et al. 1997; La Rocca et al. 1999), cecropins (Gazit et al. 1994, 1995a, 1996), the human AMP LL-37 (Oren et al. 1999), caerin 1.1 (Wong et al. 1997), trichogin GA IV (Monaco et al. 1999), androctonin (Hetru et al. 2000), diastereomers of lytic peptides (Shai and Oren 1996; Oren et al. 1997, 1999; Fernandez-Lopez et al. 2001; Sharon et al. 1999; Oren and Shai 2000), Kassinatuerin-1 (Mattute et al. 2000), melittin in anionic lipids (Ladokhin and White 2001; Steinem et al. 2000), mastoparan X (Whiles et al. 2001), and apomyoglobin 56-131 peptide (Mak et al. 2001) (also reviewed in Zasloff 2002; Tossi et al. 2000; Bechinger 1999; Lohner and Prenner 1999; Epand and Vogel 1999; Dathe and Wieprecht 1999; Sitaram and Nagaraj 1999; Mor 2000). Note, however, that the carpet model is not characteristic only of AMPs, because short lytic peptides which are highly hydrophobic and are toxic to erythrocytes and fungi also act via the carpet mechanism (Oren et al. 1997, 1999; Kustanovich et al. 2002).

In support of the membrane disintegration step, studies on the morphology of bacteria after treatment with AMPs that act via the carpet mechanism demonstrated the breakage of the bacterial membrane (Oren and Shai 1996, 2000; Shai and Oren 1996; Oren et al. 1997, 1999). Figure 7.5 shows an example of electron

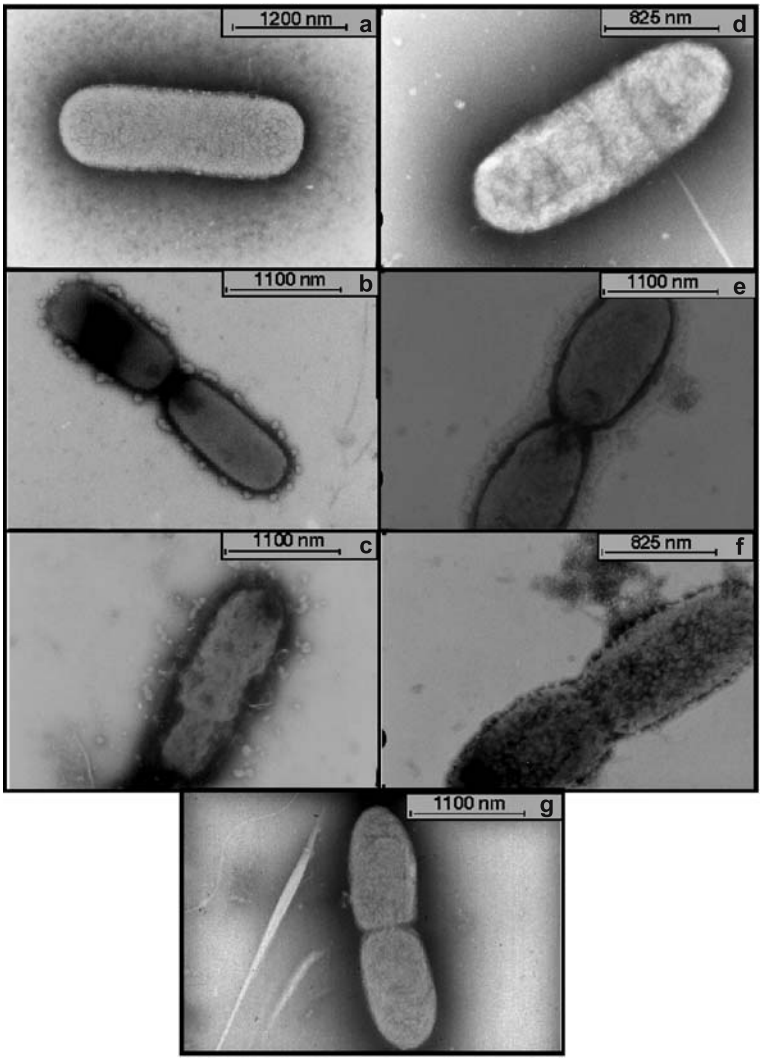

Fig. 7.5. Electron micrographs of negatively stained *E. coli* D21 and *P. aeruginosa* untreated and treated with the diastereomers shown in Table 7.1 at 60% MIC and at their MIC. **(a)** untreated; **(b)** after treatment of *E. coli* with Amphipathic-1D (60% of MIC); **(c)** *E.coli* after treatment with Amphipathic-1D (at MIC); **(d)** untreated *P. aeruginosa*; **(e)** after treatment of *P. aeruginosa* with Amphipathic-1D (60% of MIC); **(f)** *P. aeruginosa* treated with Amphipathic-1D (at MIC); **(g)** *P. aeruginosa* treated with Segregated-5D at the same concentration as indicated in **(e)**

micrographs of negatively stained bacteria untreated and treated with diastereomeric peptides listed in Table 7.1.

7.5 Summary

AMPs are integral components of the innate immunity system which serve to kill various cells, including bacteria, fungi and mammalian cells. They do not require a specific sequence or structure but rather an appropriate balance between hydrophobicity and a net positive charge. However, their cell specificity depends on parameters such as the level of hydrophobicity and the aggregation state of the molecule in solution and membranes. These parameters also affect the mode of action of the peptides. The finding that there are thousands of AMPs with variable lengths and sequences and that they are active at similar micromolar concentrations, suggests a general carpet mechanism for their mode of action. Overall the carpet model was successful because it allowed developing a novel family of diastereomeric antibacterial peptides. The unique properties of this family, such as controlled enzymatic degradation, stability in serum and in whole blood, make them promising candidates for systemic treatment of infectious diseases and cancer. Indeed recent studies demonstrated this ability (Papo and Shai 2003; Papo et al. 2004; Braunstein et al. 2004). Finally, although many studies suggest that the lethal event is the damage of the bacterial membrane, some studies point to a multihit mechanism in which the peptide binds to targets in the cytoplasmic region of the bacteria (Hancock and Rozek 2002).

Acknowledgements. The studies described in this chapter were supported by the Israel Science Foundation, The Prostate Cancer Foundation (former CapCure), the Israel Cancer Association and the Israel Cancer Research Foundation.

References

Agerberth B, Gunne H, Odeberg J, Kogner P, Boman HG, Gudmundsson GH (1995) FALL-39: a putative human peptide antibiotic, is cysteine-free and expressed in bone marrow and testis. Proc Natl Acad Sci USA 92:195–199

Andreu D, Rivas L (1998) Animal antimicrobial peptides: an overview. Biopolymers 47:415–433

Avrahami D, Shai Y (2002) Conjugation of a magainin analogue with lipophilic acids controls hydrophobicity, solution assembly, and cell selectivity. Biochemistry 41:2254–2263

Avrahami D, Shai Y (2003) Bestowing antifungal and antibacterial activities by lipophilic acid conjugation to D,L-amino acid-containing antimicrobial peptides: a plausible mode of action. Biochemistry 42:14946–14956

Avrahami D, Shai Y (2004) A new group of antifungal and antibacterial lipopeptides derived from non-membrane active peptides conjugated to palmitic acid. J Biol Chem 279:12277–12285

Avrahami D, Oren Z, Shai Y (2001) Effect of multiple aliphatic amino acids substitutions on the structure, function, and mode of action of diastereomeric membrane active peptides. Biochemistry 40:12591–12603

Baker MA, Maloy WL, Zasloff M, Jacob LS (1993) Anticancer efficacy of Magainin2 and analogue peptides. Cancer Res 53:3052–3057

Bechinger B (1997) Structure and functions of channel-forming peptides: magainins, cecropins, melittin and alamethicin. J Membr Biol 156:197–211

Bechinger B (1999) The structure, dynamics and orientation of antimicrobial peptides in membranes by multidimensional solid-state NMR spectroscopy. Biochim Biophys Acta 1462:157–183

Bessalle R, Kapitkovsky A, Gorea A, Shalit I, Fridkin M (1990) All- D-magainin: chirality, antimicrobial activity and proteolytic resistance. FEBS Lett 274:151–155

Blondelle SE, Houghten RA (1991) Hemolytic and antimicrobial activities of the twenty-four individual omission analogues of melittin. Biochemistry 30:4671–4678

Boman HG (1991) Antibacterial peptides: key components needed in immunity. Cell 65:205–207

Boman HG (1995) Peptide antibiotics and their role in innate immunity. Annu Rev Immun 13:61–92

Bonomo RA (2000) Multiple antibiotic-resistant bacteria in long-term-care facilities: an emerging problem in the practice of infectious diseases. Clin Infect Dis 31:1414–1422

Bowdish DM, Davidson DJ, Speert DP, Hancock RE (2004) The human cationic peptide LL-37 induces activation of the extracellular signal-regulated kinase and p38 kinase pathways in primary human monocytes. J Immunol 172:3758–3765

Braunstein A, Papo N, Shai Y (2004) In vitro activity and potency of an intravenously injected antimicrobial peptide and its DL amino acid analog in mice infected with bacteria. Antimicrob Agents Chemother 48:3127–3129

Breukink E, van Heusden HE, Vollmerhaus PJ, Swiezewska E, Brunner L, Walker S, Heck AJ, de Kruijff B (2003) Lipid II is an intrinsic component of the pore induced by nisin in bacterial membranes. J Biol Chem 278:19898–19903

Breukink E, Wiedemann I, van Kraaij C, Kuipers OP, Sahl H, de Kruijff B (1999) Use of the cell wall precursor lipid II by a pore-forming peptide antibiotic. Science 286:2361–2364

Brock T D (1974) Biology of microorganisms, 2nd edn. Prentice-Hall, Englewood Cliffs

Brotz H, Sahl HG (2000) New insights into the mechanism of action of lantibiotics-diverse biological effects by binding to the same molecular target. J Antimicrob Chemother 46:1–6

Bulet P, Hetru C, Dimarcq JL, Hoffmann D (1999) Antimicrobial peptides in insects; structure and function. Dev Comp Immunol 23:329–344

Cappelli G, Paladini S, D'Agata A (1999) Tumor markers in the diagnosis of pancreatic cancer. Tumori 85:S19–21

Christensen B, Fink J, Merrifield RB, Mauzerall D (1988) Channel-forming properties of cecropins and related model compounds incorporated into planar lipid membranes. Proc Natl Acad Sci USA 85:5072–5076

Dathe M, Wieprecht T (1999) Structural features of helical antimicrobial peptides: their potential to modulate activity on model membranes and biological cells. Biochim Biophys Acta 1462:71–87

Davidson DJ, Currie AJ, Reid GS, Bowdish DM, MacDonald KL, Ma RC, Hancock RE, Speert DP (2004) The cationic antimicrobial peptide LL-37 modulates dendritic cell differentiation and dendritic cell-induced T cell polarization. J Immunol 172:1146–1156

DeGrado WF, Musso GF, Lieber M, Kaiser ET, Kezdy FJ (1982) Kinetics and mechanism of hemolysis induced by melittin and by a synthetic m elittin analogue. Biophys J 37:329–338

Dempsey CE, Butler GS (1992) Helical structure and orientation of melittin in dispersed phospholipid membranes from amide exchange analysis in situ. Biochemistry 31:11973–11977

Dimarcq JL, Bulet P, Hetru C, Hoffmann J (1998) Cysteine-rich antimicrobial peptides in invertebrates. Biopolymers 47:465–477

Duclohier H, Molle G, Spach G (1989) Antimicrobial peptide magainin I from Xenopus skin forms anion-permeable channels in planar lipid bilayers. Biophys J 56:1017–1021

Ehrenstein G, Lecar H (1977) Electrically gated ionic channels in lipid bilayers. Q Rev Biophys 10:1–34

Ennahar S, Sashihara T, Sonomoto K, Ishizaki A (2000) Class IIa bacteriocins: biosynthesis, structure and activity. FEMS Microbiol Rev 24:85–106

Epand RM, Vogel HJ (1999) Diversity of antimicrobial peptides and their mechanisms of action. Biochim Biophys Acta 1462:11–28

Fernandez-Lopez S, Kim HS, Choi EC, Delgado M, Granja JR, Khasanov A, Kraehenbuehl K, Long G, Weinberger DA, Wilcoxen KM, Ghadiri MR (2001) Antibacterial agents based on the cyclic D,L-alpha-peptide architecture. Nature 412:452–455

Fleury Y, Dayem MA, Montagne JJ, Chaboisseau E, Le Caer JP, Nicolas P, Delfour A (1996) Covalent structure, synthesis, and structure–function studies of mesentericin Y 105(37), a defensive peptide from gram-positive bacteria Leuconostoc mesenteroides. J Biol Chem 271:14421–14429

Gazit E, Shai Y (1993) Structural and functional characterization of the α-5 segment of Bacillus thuringiensis δ-endotoxin. Biochemistry 32:3429–3436

Gazit E, Bach D, Kerr ID, Sansom MS, Chejanovsky N, Shai Y (1994) The alpha-5 segment of Bacillus thuringiensis delta-endotoxin: in vitro activity, ion channel formation and molecular modelling. Biochem J 304:895–902

Gazit E, Boman A, Boman HG, Shai Y (1995a) mechanism of interaction of the mammalian antibacterial peptide cecropin P1 with phospholipid vesicles. Biochemistry 34:11479–11488

Gazit E, Boman A, Boman HG, Shai Y (1995b) Interaction of the mammalian antibacterial peptide cecropin P1 with phospholipid vesicles. Biochemistry 34:11479–11488

Gazit E, Lee WJ, Brey PT, Shai Y (1994) Mode of action of the antibacterial cecropin B2: a spectrofluorometric study. Biochemistry 33:10681–10692

Gazit E, Miller IR, Biggin PC, Sansom MSP, Shai Y (1996) Structure and orientation of the mammalian antibacterial peptide cecropin P1 within phospholipid membranes. J Mol Biol 258:860–870

Gerber D, Shai Y (2002) Chirality-independent protein–protein recognition between transmembrane domains in vivo. J Mol Biol 322:491–495

Gerber D, Pritsker M, Gunther-Ausborn S, Johnson B, Blumenthal R, Shai Y (2004b) Inhibition of HIV-1 envelope glycoprotein-mediated cell fusion by a DL-amino acid-containing fusion peptide: possible recognition of the fusion complex. J Biol Chem 279:48224–48230

Gerber D, Quintana F, Bloch I, Cohen I, Shai Y (2005) A D-enantiomer peptide of the TCR? Transmembrane domain inhibits T-cell activation in vitro and in vivo. FASEB J 19:1190–1192

Gerber D, Sal-Man N, Shai Y (2004a) Structural adaptation of the glycophorin A transmembrane homodimer to d-amino acid modifications. J Mol Biol 339:243–250

Ghosh JK, Shaool D, Guillaud P, Ciceron L, Mazier D, Kustanovich I, Shai Y, Mor A (1997) Selective cytotoxicity of dermaseptin S3 toward intraerythrocytic Plasmodium falciparum and the underlying molecular basis. J Biol Chem 272:31609–31616

Guder A, Wiedemann I, Sahl HG (2000) Posttranslationally modified bacteriocins – the lantibiotics. Biopolymers 55:62–73

Gudmundsson GH, Agerberth B, Odeberg J, Bergman T, Olsson B, Salcedo R (1996) The human gene FALL39 and processing of the cathelin precursor to the antibacterial peptide LL-37 in granulocytes. Eur J Biochem 238:325–332

Habermann E, Jentsch J (1967) Hoppe Seyler's Z. Physiol Chem 348:37–50

Hancock RE, Diamond G (2000) The role of cationic antimicrobial peptides in innate host defences. Trends Microbiol 8:402–410

Hancock RE, Rozek A (2002) Role of membranes in the activities of antimicrobial cationic peptides. FEMS Microbiol Lett 206:143–149

Hasper HE, de Kruijff B, Breukink E (2004) Assembly and stability of nisin-lipid II pores. Biochemistry 43:11567–11575

Heller WT, Waring AJ, Lehrer RI, Huang HW (1998) Multiple states of beta-sheet peptide protegrin in lipid bilayers. Biochemistry 37:17331–17338

Hetru C, Letellier L, Oren Z, Hoffmann JA, Shai Y (2000) Androctonin, a hydrophilic disulphide-bridged non-haemolytic anti-microbial peptide: a plausible mode of action. Biochem J 345:653–664

Hoffmann JA, Reichhart JM (2002) Drosophila innate immunity: an evolutionary perspective. Nat Immunol 3:121–126

Hoffmann JA, Kafatos FC, Janeway CA, Ezekowitz RA (1999) Phylogenetic perspectives in innate immunity. Science 284:1313–1318

Hong J, Oren Z, Shai Y (1999) The structure and organization of hemolytic and nonhemolytic diastereomers of antimicrobial peptides in membranes. Biochemistry 38:16963–16973

Hong SY, Oh JE, Lee KH (1999) Effect of D-amino acid substitution on the stability, the secondary structure, and the activity of membrane-active peptide. Biochem Pharmacol 58:1775–1780

Hsu ST, Breukink E, Tischenko E, Lutters MA, de Kruijff B, Kaptein R, Bonvin AM, van Nuland NA (2004) The nisin-lipid II complex reveals a pyrophosphate cage that provides a blueprint for novel antibiotics. Nat Struct Mol Biol 11:963–967

Huang HW (2000) Action of antimicrobial peptides: two-state model. Biochemistry 39:8347–8352

Hwang PM, Vogel HJ (1998) Structure–function relationships of antimicrobial peptides. Biochem Cell Biol 76:235–246

Jelokhani-Niaraki M, Kondejewski LH, Farmer SW, Hancock RE, Kay CM, Hodges RS (2000) Diastereoisomeric analogues of gramicidin S: structure, biologicalactivity and interaction with lipid bilayers. Biochem J 349:747–755

Jing W, Hunter HN, Hagel J, Vogel HJ (2003) The structure of the antimicrobial peptide Ac-RRWWRF-NH2 bound to micelles and its interactions with phospholipid bilayers. J Pept Res 61:219–229

Johansson J, Gudmundsson GH, Rottenberg ME, Berndt KD, Agerberth B (1998) Conformation-dependent antibacterial activity of the naturally occuring human peptide LL-37. J Biol Chem 273:3718–3724

Kobayashi S, Takeshima K, Park CB, Kim SC, Matsuzaki K (2000) Interactions of the novel antimicrobial peptide buforin 2 with lipid bilayers: proline as a translocation promoting factor. Biochemistry 39:8648–8654

Kondejewski LH, Jelokhani-Niaraki M, Farmer SW, Lix B, Kay CM, Sykes BD, Hancock RE, Hodges RS (1999) Dissociation of antimicrobial and hemolytic activities in cyclic peptide diastereomers by systematic alterations in amphipathicity. J Biol Chem 274:13181–13192

Kustanovich I, Shalev DE, Mikhlin M, Gaidukov L, Mor A (2002) Structural requirements for potent versus selective cytotoxicity for antimicrobial dermaseptin S4 derivatives. J Biol Chem 277:16941–16951

La Rocca P, Biggin PC, Tieleman DP, Sansom MS (1999) Simulation studies of the interaction of antimicrobial peptides and lipid bilayers. Biochim Biophys Acta 1462:185–200

Ladokhin AS, White SH (1999) Folding of amphiphatic alpha-helices on membranes:energetics of helix formation by melittin. J Mol Biol 285:1363–1369

Ladokhin AS, White SH (2001) , Detergent-like' permeabilization of anionic lipid vesicles by melittin. Biochim Biophys Acta 1514:253–260

Landon C, Sodano P, Hetru C, Hoffmann J, Ptak M (1997) Solution structure of drosomycin, the first inducible antifungal protein from insects. Protein Sci 6:1878–1884

Lehrer RI, Ganz T (1999) Antimicrobial peptides in mammalian and insect host defence. Curr Opin Immunol 11:23–27

Lehrer RI, Ganz T (2002) Cathelicidins: a family of endogenous antimicrobial peptides. Curr Opin Hematol 9:18–22

Lehrer RI, Barton A, Daher KA, Harwig SS, Ganz T, Selsted ME (1989) Interaction of human defensins with Escherichia coli Mechanism of bactericidal activity. J Clin Invest 84:553–561

Lehrer RI, Lichtenstein AK, Ganz T (1993) Defensins-antimicrobial and cytotoxic peptides of mammalian cells. Annu Rev Immun 11:105–128

Lohner K, Prenner EJ (1999) Differential scanning calorimetry and X-ray diffraction studies of the specificity of the interaction of antimicrobial peptides with membrane-mimetic systems. Biochim Biophys Acta 1462:141–156

Ludtke SJ, He K, Heller WT, Harroun TA, Yang L, Huang HW (1996) Membrane pores induced by magainin. Biochemistry 35:13723–13728

Mak P, Szewczyk A, Mickowska B, Kicinska A, Dubin A (2001) Effect of antimicrobial apomyoglobin 56-131 peptide on liposomes and planar lipid bilayer membrane. Int J Antimicrob Agents 17:137–142

Mangoni ML, Papo N, Barra D, Simmaco M, Bozzi A, Di Giulio A, Rinaldi AC (2004) Effects of the antimicrobial peptide temporin L on cell morphology, membrane permeability and viability of Escherichia coli. Biochem J 380:859–865

Marugg JD, Gonzalez CF, Kunka BS, Ledeboer AM, Pucci MJ, Toonen MY, Walker SA, Zoetmulder LC, Vandenbergh PA (1992) Cloning, expression, and nucleotide sequence of genes involved in production of pediocin PA-1, and bacteriocin from Pediococcus acidilactici PAC10. Appl Environ Microbiol 58:2360–2367

Matsuzaki K (1998) Magainins as paradigm for the mode of action of pore forming polypeptides. Biochim Biophys Acta 1376:391–400

Matsuzaki K (1999) Why and how are peptide–lipid interactions utilized for self-defense? Magainins and tachyplesins as archetypes. Biochim Biophys Acta 1462:1–10

Matsuzaki K, Harada M, Funakoshi S, Fujii N, Miyajima K (1991) Physicochemical determinants for the interactions of magainins 1 and 2 with acidic lipid bilayers. Biochim Biophys Acta 1063:162–170

Matsuzaki K, Murase O, Miyajima K (1995) Kinetics of pore formation by an antimicrobial peptide, magainin 2:in phospholipid bilayers. Biochemistry 34:12553–12559

Matsuzaki K, Sugishita K, Ishibe N, Ueha M, Nakata S, Miyajima K, Epand RM (1998) Relationship of membrane curvature to the formation of pores by magainin 2. Biochemistry 37:11856–11863

Mattute B, Knoop FC, Conlon JM (2000) Kassinatuerin-1: a peptide with broad-spectrum antimicrobial activity isolated from the skin of the hyperoliid frog Kassina senegalensis. Biochem Biophys Res Commun 268:433–436

Merrifield RB, Juvvadi P, Andreu D, Ubach J, Boman A, Boman HG (1995) Retro and retroenantio analogs of cecropin–melittin hybrids. Proc Natl Acad Sci USA 92:3449–3453

Mignogna G, Simmaco M, Kreil G, Barra, D (1993) Antibacterial and haemolytic peptides containing D-alloisoleucine from the skin of Bombina variegata. Embo J 12:4829–4832

Monaco V, Formaggio F, Crisma M, Toniolo C, Hanson P, Millhauser GL (1999) Orientation and immersion depth of a helical lipopeptaibol in membranes using TOAC as an ESR probe. Biopolymers 50:239–253

Mor A (2000) Peptide-based antibiotics: A potential answer to raging antimicrobial resistance. Drug Dev Res 50:440–447

Mor A, Hani K, Nicolas P (1994) The vertebrate peptide antibiotics dermaseptins have overlapping structural features but target specific microorganisms. J Biol Chem 269:31635–31641

Mor A, Nguyen VH, Delfour A, Migliore-Samour D, Nicolas P (1991) Isolation, amino acid sequence, and synthesis of dermaseptin, a novel antimicrobial peptide of amphibian skin. Biochemistry 30:8824–8830

Nicolas P, Mor A (1995) Peptides as weapons against microorganisms in the chemical defense system of vertebrates. Annu Rev Microbiol 49:277–304

Ohsaki Y, Gazdar AF, Chen HC, Johnson BE (1992) Antitumor activity of magainin analogues against human lung cancer cell lines. Cancer Res 52:3534–3538

Oren Z, Shai Y (1996) A class of highly potent antibacterial peptides derived from pardaxin, a pore-forming peptide isolated from Moses sole fish Pardachirus marmoratus. Eur J Biochem 237:303–310

Oren Z, Shai Y (1996) Selective lysis of bacteria but not mammalian cells by diastereomers of melittin: structure–function study. Biochemistry 36:1826–1835

Oren Z, Shai Y (1998) Mode of action of linear amphipathic alpha-helical antimicrobial peptides. Biopolymers 47:451–463

Oren Z, Shai Y (2000) Cyclization of a cytolytic amphipathic alpha-helical peptide and its diastereomer: effect on structure, interaction with model membranes, and biological function. Biochemistry 39:6103–6114

Oren Z, Hong J, Shai Y (1997) A repertoire of novel antibacterial diastereomeric peptides with selective cytolytic activity. J Biol Chem 272:14643–14649

Oren Z, Hong J, Shai Y (1999) A comparative study on the structure and function of a cytolytic alpha-helical peptide and its antimicrobial beta-sheet diastereomer. Eur J Biochem 259:360–369

Oren Z, Lerman JC, Gudmundsson GH, Agerberth B, Shai Y (1999) Structure and organization of the human antimicrobial peptide LL-37 in phospholipid membranes: relevance to the molecular basis for its non-cell selective activity. Biochem J 341:501–513

Oren Z, Ramesh J, Avrahami D, Suryaprakash N, Shai Y, Jelinek R (2002) Structures and mode of membrane interaction of a short α-helical lytic peptide and its diastereomer determined by NMR FTIR, and fluorescence spectroscopy. Eur J Biochem 269:3869–3880

Osaki T, Omotezako M, Nagayama R, Hirata M, Iwanaga S, Kasahara J, Hattori J, Ito I, Sugiyama H, Kawabata S (1999) Horseshoe crab hemocyte-derived antimicrobial polypeptides, tachystatins, with sequence similarity to spider neurotoxins. J Biol Chem 274:26172–26178

Papo N, Oren Z, Pag U, Sahl HG, Shai Y (2002) The Consequence of Sequence Alteration of an Amphipathic α-Helical Antimicrobial Peptide and Its Diastereomers. J Biol Chem. 277:33913-33921.

Papo N, Shai Y (2004) Effect of Drastic Sequence Alteration and d-Amino Acid Incorporation on the Membrane Binding Behavior of Lytic Peptides. Biochemistry 43:6393-6403.

Papo N, Shai Y (2003) Exploring peptide membrane interaction using surface plasmon resonance: differentiation between pore formation versus membrane disruption by lytic peptides. Biochemistry 42:458–466

Papo N, Shai Y (2003) New lytic peptides based on the D,L-amphipathic helix motif preferentially kill tumor cells compared to normal cells. Biochemistry 42:9346–9354

Papo N, Braunstein A, Eshhar Z, Shai Y (2004) Suppression of human prostate tumor growth in mice by a cytolytic D- L-amino Acid Peptide: membrane lysis, increased necrosis, and inhibition of prostate-specific antigen secretion. Cancer Res 64:5779–5786

Papo N, Shahar M, Eisenbach L, Shai Y (2003) A novel lytic peptide composed of DL-amino acids selectively kills cancer cells in culture and in mice. J Biol Chem 278:21018–21023

Pouny Y, Shai Y (1992) Interaction of D-amino acid incorporated analogues of pardaxin with membranes. Biochemistry 31:9482–9490

Pouny Y, Rapaport D, Mor A, Nicolas P, Shai Y (1992) Interaction of antimicrobial dermaseptin and its fluorescently labeled analogues with phospholipid membranes. Biochemistry 31:12416–12423

Rapaport D, Shai Y (1991) Interaction of fluorescently labeled pardaxin and its analogues with lipid bilayers. J Biol Chem 266:23769–23775

Rapaport D, Shai Y (1992) Aggregation and organization of pardaxin in phospholipid membranes A fluorescence energy transfer study. J Biol Chem 267:6502–6509

Rizzo V, Stankowski S, Schwarz G (1987) Alamethicin incorporation in lipid bilayers: a thermodynamic study. Biochemistry 26:2751–2759

Saberwal G, Nagaraj R (1994) Cell-lytic and antibacterial peptides that act by perturbing the barrier function of membranes: facets of their conformational features, structure–function correlations and membrane-perturbing abilities. Biochim Biophys Acta 1197:109–131

Sal-Man N, Gerber D, Shai Y (2004) Hetero-assembly between all-l- and all-d-amino acid transmembrane domains: forces involved and implication for inactivation of membrane proteins. J Mol Biol 344:855–864

Sansom MS (1993) Alamethicin and related peptaibols – model ion channels. Eur Biophys J 22:105–124

Sansom MS (1998) Models and simulations of ion channels and related membrane proteins. Curr Opin Struct Biol 8:237–244

Selsted ME, Novotny MJ, Morris WL, Tang YQ, Smith W, Cullor JS (1992) Indolicidin, a novel bactericidal tridecapeptide amide from neutrophils. J Biol Chem 267:4292–4295

Shai Y, Oren Z (1996) Diastereoisomers of cytolysins, a novel class of potent antibacterial peptides. J Biol Chem 271:7305–7308

Shai Y (1994) Pardaxin: channel formation by a shark repellant peptide from fish. Toxicology 87:109–129

Shai Y (1999) Mechanism of the binding, insertion and destabilization of phospholipid bilayer membranes by alpha-helical antimicrobial and cell non-selective membrane-lytic peptides. Biochim Biophys Acta 1462:55–70

Shai Y, Bach D, Yanovsky A (1990) Channel formation properties of synthetic pardaxin and analogues. J Biol Chem 265:20202–20209

Shai Y, Fox J, Caratsch C, Shih YL, Edwards C, Lazarovici P (1988) Sequencing and synthesis of pardaxin, a polypeptide from the Red Sea Moses sole with ionophore activity. FEBS Lett 242:161–166

Sharon M, Oren Z, Shai Y, Anglister J (1999) 2 D-NMR and ATR-FTIR study of the structure of a cell-selective diastereomer of melittin and its orientation in phospholipids. Biochemistry 38:15305–15316

Simmaco M, Mignogna G, Canofeni S, Miele R, Mangoni ML, Barra D (1996) Temporins, antimicrobial peptides from the European red frog Rana temporaria. Eur J Biochem 242:788–792

Sitaram N, Nagaraj R (1999) Interaction of antimicrobial peptides with biological and model membranes: structural and charge requirements for activity. Biochim Biophys Acta 1462:29–54

Steinem C, Galla H, Janshoff A (2000) Interaction of melittin with solid supported membranes. Phys Chem Chem Phys 2:4580–4585

Steiner H, Hultmark D, Engstrom A, Bennich H, Boman HG (1981) Sequence and specificity of two antibacterial proteins involved in insect immunity. Nature 292:246–248

Strahilevitz J, Mor A, Nicolas P, Shai Y (1994) Spectrum of antimicrobial activity and assembly of dermaseptin-b and its precursor form in phospholipid membranes. Biochemistry 33:10951–10960

Terwilliger TC, Eisenberg D (1982) The structure of melittin. J Biol Chem 257:6016–6022

Tossi A, Sandri L, Giangaspero A (2000) Amphipathic, alpha-helical antimicrobial peptides. Biopolym 55:4–30

Verkleij AJ, Zwaal RF, Roelofsen B, Comfurius P, Kastelijn D, Deenen LV (1973) The asymmetric distribution of phospholipids in the human red cell m embrane A combined study using phospholipases and freeze-etch electron microscopy. Biochim Biophys Acta 323:178–193

Vogel HJ, Schibli DJ, Jing W, Lohmeier-Vogel EM, Epand RF, Epand RM (2002) Towards a structure–function analysis of bovine lactoferricin and related tryptophan- and arginine-containing peptides. Biochem Cell Biol 80:49–63

Vogel H, Jahnig F, Hoffmann V, Stumpel J (1983) The orientation of melittin in lipid membranes A polarized infrared spectroscopy study. Biochim Biophys Acta 733:201–209

Wade D, Boman A, Wahlin B, Drain CM, Andreu D, Boman HG, Merrifield RB (1990) All-D amino acid-containing channel-forming antibiotic peptides. Proc Natl Acad Sci USA 87:4761–4765

Westerhoff HV, Juretic D, Hendler RW, Zasloff M (1989) Magainins and the disruption of membrane-linked free-energy transduction. Proc Natl Acad Sci USA 86:6597–6601

Whiles JA, Brasseur R, Glover KJ, Melacini G, Komives EA, Vold RR (2001) Orientation and effects of mastoparan X on phospholipid bicelles. Biophys J 80:280–293

Wiedemann I, Benz R, Sahl HG (2004) Lipid II-mediated pore formation by the peptide antibiotic nisin: a black lipid membrane study. J Bacteriol 186:3259–61

Wieprecht T, Apostolov O, Beyermann M, Seelig J (2000) Membrane binding and pore formation of the antibacterial peptide PGLa: thermodynamic and mechanistic aspects. Biochemistry 39:442–452

Wimley WC, White S H (1996) Expermentally determined hydrophobicity scale for proteins at membrane interfaces. Nature Struct Biol 3:842–848

Wong AH, Wenzel RP, Edmond MB (2000) Epidemiology of bacteriuria caused by vancomycin-resistant enterococci – a retrospective study. Am J Infect Control 28:277–281

Wong H, Bowie JH, Carver JA (1997) The solution structure and activity of caerin 11: an antimicrobial peptide from the Australian green tree frog Litoria splendida. Eur J Biochem 247:545–557

Wu M, Maier E, Benz R, Hancock RE (1999) Mechanism of interaction of different classes of cationic antimicrobial peptides with planar bilayers and with the cytoplasmic membrane of Escherichia coli. Biochemistry 38:7235–7242

Yan LZ, Gibbs AC, Stiles ME, Wishart DS, Vederas JC (2000) Analogues of bacteriocins, antimicrobial specificity and interactions of leucocin A with its enantiomer, carnobacteriocin B2, and truncated derivatives. J Med Chem 43:4579–4581

Zanetti M, Gennaro R, Romeo D (1997) The cathelicidin family of antimicrobial peptide precursors: a component of the oxygen-independent defense mechanisms of neutrophils. Ann NY Acad Sci 832:147–162

Zanetti M, Gennaro R, Skerlavaj B, Tomasinsig L, Circo R (2002) Cathelicidin peptides as candidates for a novel class of antimicrobials. Curr Pharm Des 8:779–793

Zasloff M (1987) Magainins, a class of antimicrobial peptides from Xenopus skin: isolation, characterization of two active forms, and partial c DNA sequence of a precursor. Proc Natl Acad Sci USA 84:5449–5453

Zasloff M (1992) Antibiotic peptides as mediators of innate immunity. Curr Opin Immunol 4:3–7

Zasloff M (2002) Antimicrobial peptides of multicellular organisms. Nature 415:389–395

Structural and Functional Modulation of Ion Channels by Specific Lipids: from Model Systems to Cell Membranes

Asia M. Fernández, José A. Poveda, José A. Encinar, Andrés Morales and José M. González-Ros

8.1 Introduction

Biological membranes provide specialized permeability barriers for cells and cell organelles, in which the interplay of lipids and membrane proteins facilitates a wide range of key biochemical processes. These include respiration, photosynthesis, protein and solute transport, signal transduction, and motility. The interactions between membrane proteins and the lipid bilayer have to allow for structural protein rearrangements while keeping the sealed nature of the membrane. This is especially important because many membrane proteins undergo conformational changes that take place in or affect the transmembrane regions which are essential for their activity. The mobile and flexible lipid molecules are excellent candidates for maintaining this sealing function as they can adhere to the surface of integral membrane proteins and adjust to a changing environment.

A large number of biochemical and biophysical studies have demonstrated the importance of protein–lipid interactions in the assembly, stability, and function of membrane proteins (Lee 2003). Indeed, intrinsic membrane proteins, including ion channels, often show an absolute requirement for lipid. In the study of such requirements, different aspects of membrane protein–lipid interactions have to be considered. First, the lipid bilayer provides the matrix in which membrane proteins are partially or fully embedded. However, the bilayer is not a passive homogeneous medium; in fact, partitioning of certain proteins is enhanced by specific interactions with lipids. This sometimes leads to the formation of microdomains or "lipid rafts", which are proposed to have a role in signal transduction, membrane transport, and protein sorting, and might serve as mobile platforms for the clustering and organization of bilayer constituents, including ion channels (Brown and London 1997; Simons and Toomre 2000; Shogomori and Brown 2003). Second, spin-label EPR experiments show that a first shell of motionally restricted lipids surrounds the transmembrane segments of proteins (Marsh and Horvath 1998). Lipid specificity has been demonstrated as well in numerous biochemical studies, which showed that certain phospholipids are essential for the activity of several membrane proteins (Dowhan 1997; Lee 2004; Tillman and Cascio 2003). Finally, tightly bound lipids have been detected in the X-ray crystal structure of several membrane proteins and have been included in the model and refined with the protein (see references in Lee 2003). In most cases, these structurally resolved lipids are co-purified with the membrane proteins, and crystallized as protein–lipid complexes. The existence of such high-affinity lipid binding sites

Springer Series in Biophysics
C.R. Mateo et al. (Ed.)
Protein-Lipid Interactions

on the protein has provoked discussion and stimulated research to elucidate their possible functions (Pebay-Peyroula and Rosenbusch 2001).

The aim of this chapter is to examine how the nature and properties of the bilayer affect ion channel structure and function. As examples, we have focused on specific K^+ ion channels and on the nicotinic acetylcholine receptor (nAChR), two classes of ion channels representative of voltage-gated and ligand-gated ionic channel (LGIC) families, respectively, and whose structure and function have been documented during the past decade (Doyle et al. 1998; Unwin 2003). The responsiveness of these ion channels to changes in the lipid environment illustrates how ion channels, and perhaps many other membrane proteins, may be regulated via cellular control of membrane composition.

8.2 Importance of Lipid–Protein Interactions in Ion Channel Modulation

Ion channels are at the centre of many complex physiological processes such as the control of the beating rate in the heart or the generation of electrical signals in the brain. Ion channels involved in these processes possess two basic characteristics. The first is that they are selective, either for a range of ions (e.g. the nAChR channel, which is cation-selective) or for specific ions (e.g. K^+ channels). Second, the channels have the ability to control movement of these ions, that is, to open or close the ion conduction pathway, a process known as channel gating.

Ion channels accomplish their function of ion permeation after being inserted into the lipid bilayer of the membrane. The process of insertion is poorly understood and most likely rather heterogeneous. Once the ion channel is placed into the lipid membrane, it is believed that the protein assumes an energetic minimum, leading to a stable structure. However, molecular insights into the functioning of ion channels indicate that the processes of ligand-binding (Karlin 2002) and voltage sensing (Starace and Bezanilla 2004) are able to modify such structures.

Ion channels are generally multi-subunit complexes, with the ion conduction pathway formed as an aqueous pore at the interface between the subunits. The movement of transmembrane segments is crucial in controlling the diameter of the ion pathway and, as a consequence, determines whether the channel is in either the closed or in the open state. So far, three possible alternatives have been entertained to explain movement of the transmembrane helices during channel gating based on the recently determined structures of mechanosensitive (Chang et al. 1998), ligand-gated (Unwin 2003) and voltage-gated channels (Kuo et al. 2003). All of them move transmembrane segments away from the central ion conduction pathway which results in the displacement of a hydrophobic gate from the ion conduction pathway, allowing ion movement through the channel. The channels would achieve this by moving the transmembrane helices as rigid bodies using three major types of motion: helix tilting as in MscL (Sukharev et al. 2001), rotation as in the nAChR (Miyazawa et al. 2003), or bending as in Kv1.1 (Doyle 2004). In all cases there are large movements that require a certain degree of flexibility and may cause modifications at the protein–lipid interface. Thus, it

is possible that changes in the lipid composition may affect channel function by stabilizing distinct functional states.

Reconstitution experiments have established that specific lipids or particular combinations of lipids are often necessary for ion channels to exhibit their native properties (Lee 2004). These preferences may reflect the optimization of protein structure by the specific lipid environment in which the protein is found, but may also be related to the folding of the nascent protein and its oligomerization, to its targeting to a given membrane microdomain, or to a lipid-mediated regulation of the protein function.

Although several important questions regarding the molecular details of such lipid modulation remain open, emerging data indicate that protein–lipid interactions should be considered as a new explanation for ion channel function modulation that might even result in possible therapeutical interest.

8.3 Hypothetical Nature of Lipid–Protein Interactions

Despite the extensive information obtained on the functional and structural dependence of several ionic channels on its surrounding lipids (Lee 2004; Palsdottir and Hunte 2004), several aspects of the modulation exerted by the different lipid classes on the membrane proteins still remain unclear. Various hypotheses have been implicated in the modulation of ion channels function by lipids: (1) modification of physical properties of the bilayer, such as fluidity, membrane curvature, and/or lateral pressure (Cantor 1997; de Kruijff 1997; van den Brink-van der Laan 2004); (2) direct effects, exerted through binding to specific sites on transmembrane portions of the protein (Fong and McNamee 1987; Jones and McNamee 1988; Blanton and Wang 1990; Fernández et al. 1993; Fernández-Ballester et al. 1994; Powl 2005), in some cases acting like allosteric modulators; and (3) promotion of lateral segregation of specific lipids and formation of lipid domains (Martens et al. 2000; Brown and London 2000). One possibility does not preclude others; the affinity of a protein for specific lipids may either stabilize certain protein conformations, induce domain formation or serve to target the protein to specific membrane domains with different biophysical properties.

In the case of modulation of ion channel structure or function by changes in physical properties of the bilayer, it is known that the effect of packing different lipid species with each other and with proteins results in mechanical pressures in the biological membrane, the redistribution of pressures being related to changes in bilayer thickness, curvature stress or hydrophobic matching. Such biophysical phenomena have been suggested as a possible mechanism to explain the influence of bilayer properties on ion channel structure and function. The lateral pressure profile may influence protein conformation directly, by mechanical pressure at the lipid–protein interface or indirectly by changes in other membrane parameters. An example of an ion channel unambiguously influenced by this mechanism is the mechanosensitive channel (Perozo et al. 2002).

On the other hand, biological membranes contain a wide variety of lipid species with different fatty acyl chains so that the lateral diffusion of lipid molecules

within the plane of the membrane will result in local fluctuation of membrane thickness. The hydrophobic thickness of the lipid bilayer is expected to match well the region of any protein embedded in the bilayer, because of the high cost of exposing either fatty acyl chains or hydrophobic amino acids to water. Any mismatch between the hydrophobic thicknesses of the lipid bilayer and the protein would be expected to lead to distortion of the lipid bilayer, or the protein, or both, to minimize the mismatch. The activity of a number of membrane proteins is sensitive to the thickness of the lipid bilayer, with the optimal thickness usually corresponding to that of the bilayer of dioleoylphosphatidylcholine (Lee 1998).

A second alternative mechanism to explain modulation ion channel structure and function by lipids may be through a direct interaction. In this respect, a large variety of biochemical and biophysical studies have demonstrated the existence of a direct lipid–protein interaction. These studies include fluorescence spectroscopy, electron paramagnetic resonance spectroscopy, photoaffinity labelling, X-ray crystallography and electron microscopy (EM).

The first clue about how lipid molecules might interact with an intrinsic membrane protein came from electron spin resonance (ESR) studies using phospholipid molecules with nitroxide spin labels attached to selected positions in the fatty acyl chains. These studies show the presence of a subpopulation of highly immobilized spin labels, not found in protein-free membranes (Marsh and Horvath 1998; Marsh 2004). The ESR approach can be used to estimate the number of lipid molecules bound to the surface of a membrane protein. In a series of studies, Marsh and Horvath (1998) showed that the number of bound lipid molecules fits reasonably well to the expected circumference of the trans-membrane region of the protein. The close relationship between the number of lipid molecules estimated to surround a membrane protein and the diameter of the protein supports the presence of a distinct annular shell of lipid molecules around that protein.

Fluorescence quenching studies show binding of specific phospholipids with different affinities to some ion channels. These lipids, often bound between transmembrane α-helices either within a protein or at protein–protein interfaces in multi-subunit proteins, have been referred to as non-annular lipids (Marsh et. al 1982). For example, the KcsA channel requires the presence of some anionic lipids for its function, and fluorescence quenching studies show the presence of two classes of lipid binding sites on KcsA. At one of them (non-annular sites) anionic phospholipids bind more strongly than phosphatidylcholine (PC), whereas at the other (annular sites) PC and anionic phospholipids bind with equal affinity. (Williamson et al. 2002).

The high-resolution structure of membrane proteins obtained by X-ray or EM sometimes show tightly bound lipids, thus providing a new insight into protein–lipid interactions. However only a small number of lipid molecules have been resolved from the structures of membrane proteins by high-resolution X-ray or EM. Since only highly ordered lipid molecules are seen in these structures, such lipid molecules should not correspond to the bulk of lipid molecules surrounding the protein. Furthermore, annular lipids will normally be too disordered to appear in high-resolution structures. Therefore, most of the lipid molecules resolved in high-resolution crystal structures of membrane proteins are likely to be non-annular lipids. Their strong binding to the protein leads to immobilization

of, at least, part of the lipid molecule so that they appear in the high-resolution structure. In both X-ray diffraction and EM studies, the lipid headgroups are disordered but many fatty acyl chains are well resolved, mostly bound in distinct grooves on the surface of the protein. Phosphatidylglycerol (PG) is a typical non-annular lipid molecule bound between transmembrane α-helices at monomer–monomer interfaces in the homotetrameric potassium channel KcsA. Again the headgroups of the lipid molecules are not resolved, and the lipids have therefore been modelled as diacylglycerol (Zhou et al. 2001). KcsA requires the presence of PG or some other anionic phospholipid to function and it has been suggested that the presence of the anionic lipid cofactor could be important in the gating process (Valiyaveetil et al. 2002; Heginbotham et al. 1998).

The third hypothetical mechanism by which lipids can modulate the function and/or structure of ion channels is the formation of lipid domains. These dynamic structures, generally termed lipid rafts, are rich in tightly packed sphingolipids and cholesterol (Harder et al. 1997) and are believed to exist in a different phase state to that of the surrounding phospholipids (Brown and London 1997). The first report of ion channels localized in lipid microdomains described the targeting of Shaker-like K^+ channels to lipid rafts (Martens et al. 2000). Biochemical isolation of rafts shows that the $K_V2.1$ channel is associated with rafts in transfected fibroblasts and rat brain. Depletion of membrane cholesterol using cyclodextrin, an agent known to perturb raft organization (Brown and London 2000), causes a dramatic hyperpolarizing shift in the steady-state inactivation properties of the $K_V2.1$ channel, whereas other K_V channels in the same cell type, such as $K_V4.2$ channels, are unaffected. Therefore, at least for some channel proteins, there is a functional consequence of their association to lipid rafts. Additional reports suggest that other types of ion channels, including both voltage- and LGIC, are also associated with lipid rafts. For example, Ca^{2+}-activated K^+ channels are sorted to lipid rafts on the apical membrane of Madin–Darby canine kidney cells (Bravo-Zehnder et al. 2000). The neural α7 nAChR, a protein which is well-known to have a preference for certain lipids, was recently shown to target lipid rafts in the somatic spines of ciliary neurons (Bruses et al. 2001). The muscle like nAChR had been shown to produces lateral phase separation of the mono-anionic phosphoryl form of the phosphatidic acid (PA) probe, causing the formation of specific PA-rich lipid domains that become segregated from the bulk lipids (Poveda et al. 2002). Although it appears that several ion channels might be localized to these raft domains, several questions regarding the mechanism and function of ion channel–raft association need to be addressed.

It is clear that while the role that membrane lipids play in membrane structure and function is beginning to be understood, there is still a gap in our knowledge of the complexity of the specific interactions. Since a detailed understanding of the lipid–protein interactions in the membrane requires knowledge of the dynamic phenomena involved, it appears that complementary methods, including static, like crystallographic analyses, and dynamic, like functional assays of reconstituted proteins, should be considered to achieve a better comprehension of this interaction.

8.4 Influence of Lipids on nAChR Function

LGICs are membrane proteins that transiently open a pore through the lipid membrane in response to neurotransmitter binding. The nAChR is one of the best-understood members of this family, principally due to two factors that have aided in its characterization: (1) the rich source of nAChR present in the electric organ of some fishes (*T. marmorata, T. californica and E. electricus*) and (2) the presence of neurotoxins in snake venoms that bind specifically to the nAChR providing the means for assaying receptor binding and for affinity purification.

nAChRs are heteropentamers comprised of four different but highly homologous subunits designated as α, β, γ, and δ (Fig. 8.1; for reviews see the references in Karlin 2002). Each subunit contains an extracellular N-terminal domain (which includes the ACh (acetylcholine) binding sites), four hydrophobic transmembrane (TM) domains (M1–M4), and a small extracellular C-terminal domain. Several studies have provided convincing evidence that the TM2 domain segments from each subunit cluster around a central axis to form the ion channel pore, whereas TM1 TM3 and TM4 domains are in close proximity or exposed to the lipid interface (Miyazawa et al. 2003; Barrantes 2003).

These receptors are implicated in the propagation of electrical signals between the cells at the neural and neuromuscular synapse. Upon activation by agonist, nAChRs transiently open a cationic channel responsible for the initiation of post-

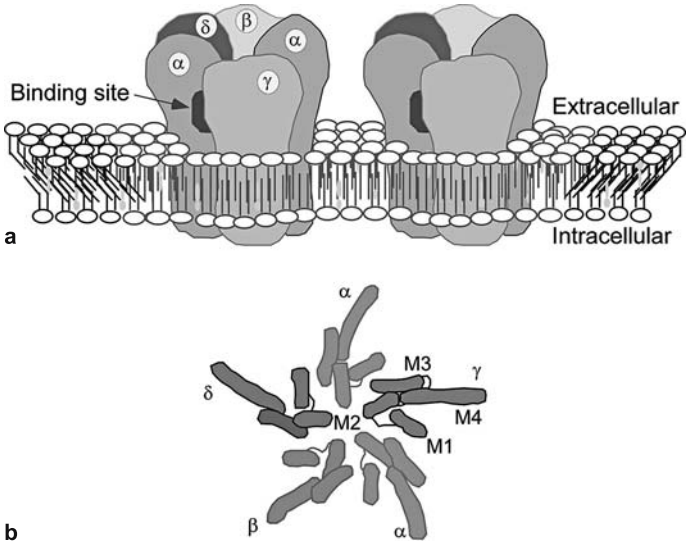

Fig. 8.1. (**a**) Schematic representation of the quaternary structure showing the arrangement of the AChR subunits in reconstituted vesicles. (**b**) Cross-sectional slab through the pentamer at the middle of the membrane showing the four transmembrane segments (M1–M4) of each subunit. Based on Unwin (2003)

synaptic membrane depolarization. In the continued presence of agonist, the nAChR become refractory to the stimulus and the ionic current declines. This process, called desensitization, occurs because the fully liganded receptor eventually adopt a stable, high-affinity conformation that is not permeable to ions.

Extensive biochemical studies have demonstrated that the ability of the nAChR to support ion channel function requires the presence of specific lipids. In 1978 Epstein and Racker opened the way for more detailed studies of the influence of the lipid environment on the nAChR by measuring in a reproducible manner integrated flux responses specifically induced by cholinergic agonist in reconstituted systems. Since then, many experiments reconstituting nAChRs into artificial liposomes of defined composition have shown that the presence of certain lipids in the reconstituted samples, namely cholesterol and acidic phospholipids, are important in preserving the ability of this protein to exhibit an optimal cation channel activity (Gonzalez-Ros et al. 1980; Criado et al. 1984; Fong and McNamee 1986; Jones et al. 1988; Sunshine and McNamee 1992; Fernández et al. 1993). Such lipid effects on nAChR function are also known to be fully reversible. For instance, McNamee's group used the re-reconstitution approach (reconstituting the protein twice, first in a lipid matrix that does not allow nAChR function, then in whole asolectin lipids) to demonstrate that an apparently "inactive" nAChR regains its function upon a second reconstitution into an appropriate lipid matrix (Jones et al. 1988). Rapid-kinetics stopped-flow studies have demonstrated that the presence of PA in the reconstituted membranes maintains an optimal nAChR cation channel activity. On the other hand, reconstitution into cholesterol/zwitterionic phospholipids, in the absence of anionic phospholipids, causes a loss in nAChR function (authors' submitted manuscript; Fig. 8.2). The lack of ion channel activity in samples containing PC as the only phospholipid present has been reported previously, using several different chemical species of synthetic PCs (Fong and McNamee 1986; Ochoa et al. 1989; Sunshine and McNamee 1992) or egg yolk PC (Fernández et al. 1993). It seems that this lipid stabilizes the nAChR in a non-responsive, desensitized state. Also, the need of cholesterol and negatively charged

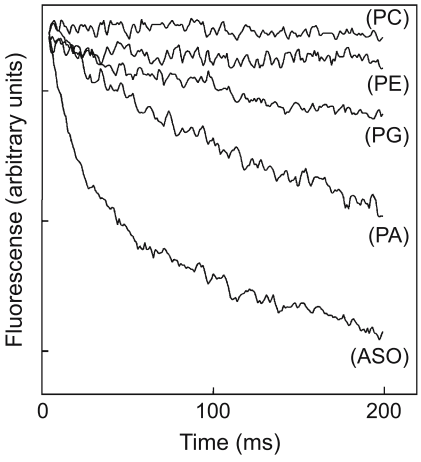

Fig. 8.2. Representative stopped-flow traces corresponding to the rapid collisional quenching of the fluorescence on 1,3,6,8-pyrene tetrasulfonate entrapped into reconstituted nAcChR vesicles by externally added Tl^+. The figure shows Tl^+ influx responses to 500 μM carbamylcholine exhibited by reconstituted nAcChR vesicles made from different lipid mixtures

phospholipids, particularly PA, to retain nAChR function upon reconstitution has been widely documented (Criado et al. 1984; Fong and McNamee 1986; Jones et al. 1988; Sunshine and McNamee 1992; Fernández et al. 1993). Similarly, preliminary data using the approach of transplanting the nAChR from reconstituted vesicles to the plasma membrane of live *Xenopus* oocytes (Morales et al. 1995; see below), show that microinjecting samples reconstituted in whole asolectin lipids (fully active samples) or in just egg phosphatitylcholine (inactive samples) produce comparable agonist-induced nAChR ion currents upon incorporation of the protein into the host cell membrane (manuscript in preparation).

These effects of specific lipids in nAChR function may be exerted through binding to specific sites of the protein or by modification of the physical properties of the bilayer. Previous results have demonstrated that membrane lipids interact differentially with nAChR. For example, sterol, PA and fatty acid spin labels have a relatively high affinity for nAChR compared with other spin labelled phospholipids (Ellena et al. 1983).

Additionally, several lines of evidence indicate a separate binding site for neutral lipids, namely non-annular sites. McNamee´s group used the ability of brominated lipids to partially quench the intrinsic or modified fluorescence of the nAChR to monitor contacts with the surrounding lipid in reconstituted membranes. They found that quenching of PC was independent of and additive with that due to brominated cholesterol derivatives (Jones and McNamee 1988). These results argue strongly for independent binding sites for cholesterol and phospholipids.

Although cholesterol may affect the nAChR directly, it definitely has profound effects on the structure of the membrane environment, most notably in changes of membrane order or fluidity. In earlier studies both the agonist affinity and ion flux seemed to require an optimal fluidity (Fong and McNamee 1986). However, subsequent studies showed that while the ion flux activity of the nAChR was strongly influenced by lipid composition (Fernández-Ballester et al. 1994), there was no correlation with membrane fluidity as measured by steady state anisotropy of membrane probes (Shunshine and McNamee 1994). Measurements of membrane fluidity showed that cholesterol further ordered membranes containing PC and PA, but other sterols, like androstanol, did not; however, both neutral lipids supported similar ion fluxes. Thus neutral lipids do not exert their effect on the nAChR by changing bulk membrane order. Nevertheless, effects on bulk membrane order are sometimes different from those at the protein–lipid interface and it is possible that protein promotes the lateral segregation of specific lipids that allows an optimal packing density (daCostaet al. 2002; Poveda et al. 2002).

Careful delipidation experiments showed that a lipid/protein mole ratio approximately below 45 caused irreversible inactivation of the nAChR, consistent with the requirement of an annular shell of lipids around the periphery of the hydrophobic region (Jones et al. 1998). This requirement for a lipid annulus of 40–50 lipid molecules is supported by a variety of spectroscopic techniques establishing the presence of a lipid phase associated with the protein that differs from the bulk bilayer lipids in terms of molecular motion (Antollini et al. 1996). It is also in good agreement with theoretical predictions, which suggests the presence of a inner shell annulus of approximately 42–51 lipid molecules (Barrantes 1993).

The nature of the molecular species making up this dynamic annulus has not been wholly ascertained, although it seems obvious that both neutral and negatively charged lipids must play a role. It becomes clear that the nAChR annular lipids are important for its correct functional activity, but the precise mechanism by which these annular lipids affect the nAChR is not yet known.

8.5 nAChR Modulation by other Lipophilic Compounds

As indicated above, some of the lipids surrounding the nAChR play an important role in determining its functional activity. Besides, many other hydrophobic molecules, with astonishingly different molecular structures, modulate the nAChR function, including:

(1) Free fatty acids (Andreasen and McNamee 1980; Villar et al. 1988);
(2) Steroid hormones, both glucocorticoids (Bouzat and Barrantes 1996; Nurowska and Ruzzier 1996) and sex hormones (Valera et al. 1992);
(3) Local anaesthetics (Katz and Miledi 1975; Gentry and Lukas 2001);
(4) Some cholinesterase inhibitors, such as tacrine (Cantí et al. 1998) or 1,5-bis (4-allyldimethylammoniumphenyl)pentan-3-one dibromide (BW284c51) (Olivera et al. 2005); and
(5) Other lipophilic compounds such as alcohols and general anaesthetics (Liu et al. 1994).

Most of these hydrophobic molecules act as non-competitive blockers (NCB) on the nAChRs. The similar inhibitory effect mediated by such a broad range of lipophilic compounds can be explained assuming that the nAChRs function as an allosteric protein (Changeux 1990; Hogg et al. 2003). This assumption postulates that the protein can exist in different states (closed, open and desensitized, each characterized by its affinity for the agonist, or other ligands, and its conductance) and undergoes spontaneous conformational transitions. At rest, the equilibrium between these conformational states is in favour of the closed state, but when the agonist is bound, the equilibrium shifts towards the active or desensitized states. The binding of molecules at specific regulatory sites (different of the agonist-binding site) may shift the isomerization equilibrium towards one of the possible states (Galzi et al. 1996). Nevertheless, the detailed mechanism by which such heterogeneous group of hydrophobic compounds affects nAChR activity remains largely unknown.

Two main different locations in the nAChR have been proposed for the interaction with NCBs: (1) a high-affinity site, located at, or close to, the lumen of the ion channel; and (2) several (up to 30) low-affinity sites located at the annular interface receptor–lipid bilayer. The high-affinity site is thought to be at or close to the ion channel pore since photoaffinity labelling experiments using either [^{3}H] chlorpromazine ([^{3}H]CPZ) (Revah et al. 1990) or [^{125}I] 3-trifluoromethyl-3-(-m-iodophenyl)diazirine ([^{125}I]TID) (White and Cohen 1992) label several residues

within the M2 sequence of each subunit, which corresponds to the lining wall of the ion pore. Different experimental approaches further reinforced this view:

(1) Site-directed mutagenesis of the M2 residues in neuronal α7 nAChR affected the apparent affinity of the nAChR for NCB, although it also modified the affinity for agonists and competitive antagonists and the desensitization rate (Revah et al. 1991); and
(2) Membrane current recordings of nAChR activity, either in the presence of local anaesthetics (Neher and Steinbach 1978) or TID (Forman 1999), indicate that these compounds cause an open channel block, likely due to their affinity for a site within the open ion channel.

The low-affinity sites located at the receptor–lipid interface bind a heterogeneous group of hydrophobic molecules, such as fatty acids, sterols, steroids, alcohols and general anaesthetics. The binding sites for these compounds may be located in the middle (M1, M3) and/or outer (M4) transmembrane domains of the nAChR (Barrantes 2003). Although these segments do not form part of the ion conduction pathway, in contrast to the M2, they are lipid-exposed and can modulate the receptor function (Arias 1998; Barrantes 2003). As a rule, all NCB acting on these sites cause similar functional effects: they reduce the channel mean open time (τ_{on}), but without changing the maximal agonist binding. Furthermore, some of them enhance desensitization. Remarkably, comparable changes in gating kinetics are observed when lipid-exposed residues in the M4 domain of the nAChR are mutated (Bouzat et al. 1998).

As for $GABA_A$ and glycine receptors, members of the same superfamily of LGIC, nAChRs seem to have specific binding sites for alcohols and anaesthetics, located in water-filled cavities between the inner (M2) and the outer (M4) set of helices (Miyazawa et al. 2003; Chiara et al. 2003). In the case of steroids, it is known that all of them affect nAChR channel kinetics in a similar way, but the magnitudes of their effects are inversely related to their lipophilicity (Garbus et al. 2001). This suggests that their effect is not exerted through a simple perturbation of the lipid bilayer properties but through the binding to a site located at superficial regions of the nAChR-lipid interface, i.e. close to the phospholipid polar head region. In addition, it should be mentioned that when progesterone (Ke and Lukas 1996) or corticosterone (Nurowska and Ruzzier 1996) are bound to bovine serum albumin, forming a cell-impermeant complex, they retain their modulating actions on the nAChR. Therefore, these steroids should be acting on an extracellularly accessible site of the nAChR. Although almost all steroids tested to date on nAChR have an inhibitory action (negative allosteric effect) on nAChR, potentiating effects of 17β-estradiol on rat (Paradiso et al. 2000) and human (Paradiso et al. 2001; Curtis et al. 2002) neuronal α4β2 nAChRs have been recently reported. The potentiating effect is mediated at a site in the C-terminal tail of the α4 subunit (Paradiso et al. 2001; Curtis et al. 2002), being therefore markedly different to that involved in the steroid inhibiting action. Finally, it should be mentioned that there is no competition between the inhibitory actions of steroids (hydrocortisone) and local anaesthetics (QX-222), as would be expected from their different acting sites on the nAChR (Bouzat and Barrantes 1996).

In summary, besides the nAChR dependence on specific lipids, such as PA or cholesterol, for its correct function, there are many other lipophilic compounds, including endogenous molecules, acting on specific loci of this protein. This allows a multifactorial and extremely complex modulation of the nAChR function.

8.6 Influence of Lipids on nAChR Structure

Structural knowledge of nAChR and other LGIC has been greatly hindered by the absence of a crystal structure. The most informative structure is from electron micrographs of the tightly packed arrays of nAChR in tubular membranes isolated from the electric organ of *Torpedo* electric rays (Toyoshima and Unwin 1988; Unwin 1995; Miyazawa et al. 2003). These studies indicate that the transmembrane segments (M1–M4) are basically α helices, although M1 seems to have a distorted helical structure, probably due to the presence of a proline residue. These data have been confirmed through NMR and other spectroscopic studies of the peptides corresponding to the different transmembrane segments of the protein or with biochemical approaches such as photolabelling, protein modification and site-directed mutagenesis of the entire protein (Karlin et al. 1986; Akabas et al. 1994; Blanton and Cohen 1994; Blanton et al. 1998; Corbin et al. 1998; Lugovskoy et al. 1998; Opella et al. 1999; Pashkov et al. 1999; Williamson et al. 2004; Barrantes et al. 2000; Tamamizu et al. 2000; Cruz-Martin et al. 2001; Guzman et al. 2003; Ortiz-Acevedo et al. 2004; Santiago et al. 2004). Finally, site-directed mutagenesis and NMR experiments proposed that M3 contains a mixture of α helix and 3_{10}-helix (Lugovskoy et al. 1998; Guzman et al. 2003). The secondary structure of the entire protein has also been studied through spectroscopic techniques such as Raman, FT-IR or CD. The calculated α-helix content ranges from 20 to 43%, β sheet content from 29 to 48%, and non-ordered structure from 20 to 28% (Moore et al. 1974; Mielke and Wallace 1988; Yager et al. 1984; Fong and McNamee 1987; Butler and McNamee 1993; Methot et al. 1994; Castresana et al. 1992). On the other hand, theoretical predictions estimate 44% α-helix and 27% β-sheet (Finer-Moore and Stroud 1984). The lack of concordance of these data is probably due to the low sensitivity of CD to detect beta structures, the diversity of the FT-IR quantification methods, and finally to the different conditions used to reconstitute the protein.

As stated in the previous section, lipid surrounding nAChR modulates protein function, possibly through changes in the general properties of the membrane or by direct binding to the protein. This modulation should be caused by some effect on the protein conformation, probably acting on one or several of the transmembrane domains that are in direct contact with lipids (M1, M3 and M4). In fact, site-directed mutagenesis studies report many examples of residues located at the lipid–protein interface whose mutation to tryptophan dramatically affects protein function (Tamamizu et al. 2000; Guzman et al. 2003; Ortiz-Acevedo et al. 2004; Santiago et al. 2004). In order to detect the possible structural changes associated with lipid nAChR modulation, different spectroscopic studies have been done, mainly through analysis of the FT-IR amide I' band. Lipid membranes

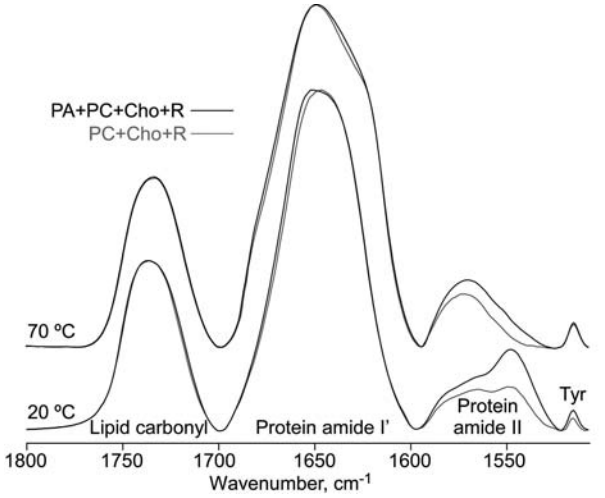

Fig. 8.3 Infrared spectra (1800–1505 cm^{-1}) of nAChR reconstituted in different lipid vesicles at 20 and 70°C. Spectra show lipid carbonyl, amide I′, amide II and tyrosine bands

where nAChR is fully functional, typically those containing PA and cholesterol, are those where the protein presents a higher α-helical content relative to non-ordered structure, whereas nAChR in lipid membranes where it is less active, such as those with only zwitterionic phospholipids, shows a larger non-ordered structure concomitant with a decrease in the α-helix. Meanwhile, the β-sheet content remains basically unchanged (Fig. 8.3).

These FT-IR experiments were done after submitting the samples to a D_2O for H_2O exchange. This process can be followed through the FT-IR amide II band, which diminishes with the H–D exchange, and depends on the accessibility of the different amino acids to the solvent, so it reports information about the tertiary protein structure (Hvidt and Nielsen 1966; Pershina and Hvidt 1974). Once the equilibrium for the H–D exchange is reached, the remaining amide II band was quantified, showing that those samples with a larger remaining amide II, that is, with the lower H to D exchange, are precisely those with less non-ordered structure. Furthermore, if those samples are constantly heated this amide II band disappears, showing a sigmoidal behaviour. From these curves, it is possible to calculate a temperature (T_m) for the collapse of the tertiary structure. Again it is observed that samples with a higher content of ordered secondary structure are those with a higher T_m. These results support nAChR structure data calculations from amide I' analysis, since those samples with more ordered secondary structure, typically α-helical, are those more resistant to H–D exchange (authors' submitted manuscript). The mechanism by which anionic lipids, especially PA, stabilize the α-helix structure of nAChR is not clear, although some authors have pointed to an interaction between the dipole from the α-helical structure of nAChR and the PA phosphates (Hol et al. 1978; Sali et al. 1988). In addition, some work has been done with model peptides that also detect stabilization of α-helical structure by anionic phospholipids (Liu and Deber 1997). However, other authors have reported an increment in β-sheet content upon addition of anionic

phospholipids (Butler and McNamee 1993; Fong and McNamee 1987), although these studies were done in a region of the infrared spectrum where bands are rather weak and its assignment to secondary structure is not clear. It has also been reported that cholesterol favours an increment in α-helical structure (Fernandez-Ballester et al. 1994; Fong and McNamee 1987; Butler and McNamee 1993) and even the β sheet (Fernandez-Ballester et al. 1994). To explain this result it has been postulated that the rigid sterol ring, oriented parallel to the receptor axis, may localize in between helices at the lipid–protein interface, causing their stabilization (Fong and McNamee 1987).

Among the different regions conforming to the nAChR overall structure, the M1 transmembrane segment may be a good candidate to be modulated by lipids (Williamson et al. 2004; dePlanque et al. 2004). NMR studies of this transmembrane segment reconstituted in lipids show that some portions adopt an α-helical conformation but that the presence of a proline located in the middle of the segment significantly disrupts the α-helical structure. In fact, a proline and about four surrounding residues typically form a kink in the transmembrane stretch with an angle that can vary between 5º and 60º, and these hinge regions are thought to play a key role in membrane proteins because of their expected inherent flexibility (Cordes et al. 2002; Arshava et al. 2002). Furthermore, conformational studies as a function of the lipid environment suggest that the degree of helicity in this region strongly depends on the lipid environment, and that M1 orders DMPC acyl chains and interact more favourably with cholesterol containing PC bilayers, mimicking several aspects of the effect of the entire nAChR on model membranes (de Planque et al. 200). This flexibility could be maintained in the entire protein as transmembrane segments in nAChR are loosely packed, and M1, M3 and M4 are largely separated by water-filled cavities from the inner ring of M2 helices (Miyazawa et al. 2003). These results, together with the observed M1 labelling from both hydrophobic and hydrophilic probes (Blanton and Cohen 1994; Karlin et al. 1986), and the close proximity between M1 and M2, suggest that the conformational flexibility around the proline in the M1-transmembrane may be important for the modulation of channel gating by the lipid environment and by other molecules which partition into the lipid bilayer, such as general anaesthetics.

Opposite to these results are those using ATR spectroscopy (Ryan et al. 1996; Baenziger et al. 2000). These authors find very faint variations in the amide I' band for nAChR reconstituted in different lipid vesicles, only detectable after band deconvolution. They propose that these little variations are caused by the different rate of H–D exchange for the different samples, due to subtle variations in the protein dynamics that do not involve changes in the secondary structure. These variations may be those causing the lipid modulation on nAChR function. This could explain the small differences they find in the amide I' band, but not the large differences referred to above, as there is evidence showing that large variations in H–D exchange do not cause significant changes in the quantification of secondary structure motifs from the amide I' band (authors' submitted manuscript). One reason to explain why these authors do not detect large variations in the amide I' band could be the fact that nAChR-containing samples are submitted to a drying cycle accompanied by a long period of rehydration (up to three days) before doing the FT-IR experiments. The consequences of this process have not

been tested, since no functional experiments were done after these treatments. It is possible then, that nAChR is in a desensitized-like state, independently of the lipids where it is reconstituted. In the same sense, cholesterol has been proposed to modulate nAChR function without varying protein structure. To do so, it would localize in the spaces between different nAChR subunits facilitating the sliding between them, so making possible the conformational changes necessaries for channel function (Corbin et al. 1998).

nAChR, like other ligand-gated ion channels, after binding of the corresponding agonist, suffers a conformational change in transmembrane segments, probably a rotational movement, destabilizing the hydrophobic girdle that forms the channel gate and thus allowing ions to pass through the pore. The mechanisms and pathway to transform the energy of ligand binding at the extracytoplasmic domain of the protein into the movements of the M2 segments are largely unknown. Electrostatic and hydrophobic interactions have been proposed between the M2–M3 loop and other loops in the agonist-binding domain as being responsible for this transmission (Kash et al. 2003; Miyazawa et al. 2003). The action of phospholipids to modulate nAChR function should interfere with either the transmission between ligand-binding domain towards transmembrane segments or the subsequent transmembrane movement. Possibility to do that is causing the protein to enter into a non-active conformation, through changes in the secondary and/or tertiary nAChR structure. Considering the above results, zwitterionic lipids may stabilize a conformation with less ordered α-helical content that would impede some of the steps that allow the protein function. By contrast, anionic lipids and cholesterol would stabilize a more compact conformation able to transmit movements of the binding domain towards the transmembrane domain.

8.7 PA–nAChR Interaction

As stated above, nAChR binds preferentially anionic lipids, which are positive modulators of its function. Among them, PA seems to interact in a special fashion with this protein. In vitro studies with nAChR reconstituted in lipid vesicles of controlled composition show that PA is among those phopholipids that bind the protein with a higher affinity, and it is the most effective lipid in preserving nAChR function (Jones and McNamee 1988; Marsh and Barrantes 1978; Ellena et al. 1983; Esmann and Marsh 1985; Dreger et al. 1997), possibly through a stabilization of the resting versus the desensitized state of the protein (da Costa et al. 2002). On the other hand, as if a bidirectional coupling takes place, nAChR in a PA-containing membrane leads to a dramatic increase in both the lateral packing densities and the gel-to-liquid-crystal phase-transition temperatures of the reconstituted lipid bilayers (da Costa et al. 2002; Wenz and Barrantes 2005). This strong interaction leads to the segregation of a PA-enriched domain from a complex mixture of lipids at determined lipid-to-protein ratios (Fig. 8.4; Poveda et al. 2002; Wenz and Barrantes 2005). However, nAChR has no detectable effect on the lateral distribution of lipids when PA is substituted by other zwitterionic or anionic phospholipids such as PC, PG or phosphatidylserine (PS) (Poveda et

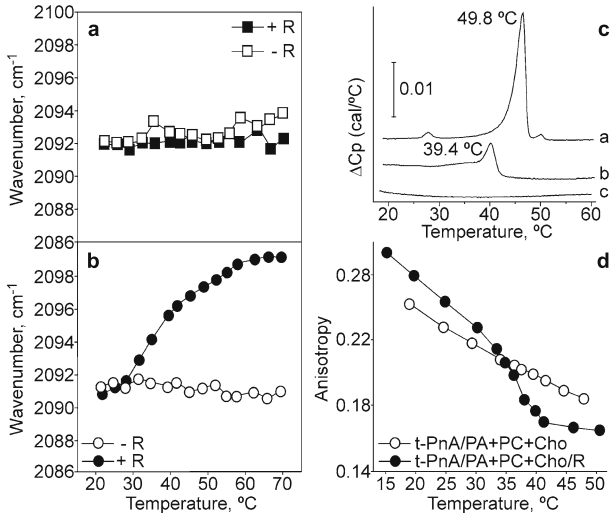

Fig. 8.4. (**a, b**) Representative temperature dependence of the infrared CD_2 symmetric stretching vibration from perdeuterated phospholipids contained in reconstituted vesicles. Vesicles were prepared by detergent dialysis, in the absence (*open symbols*) or in the presence (*filled symbols*) of nAChR protein, from identical amounts of lipid mixtures containing 25 mol% of cholesterol, 50 mol% of egg PC and 25 mol% of either d-DMPC (panel **a**) or d-DMPA (panel **b**). Protein-containing samples were prepared at a protein-to-phospholipid molar ratio of 1:3500. CaF_2 windows were used in the spectrometer cell. (**c**) Differential scanning calorimetry studies on the effect of nAChR on lipid organization in reconstituted vesicles. The scans correspond to: pure DMPA (a), 25 mol% of cholesterol, 50 mol% of egg PC and 25 mol% of DMPA with (b) or without (c) nAChR. (**d**) Fluorescence anisotropy of the transparinaric acid (t-PnA) probe incorporated into vesicles composed by 25 mol% of cholesterol, 50 mol% of egg PC and 25 mol% of either DMPA in the absence (*open symbols*) or in the presence (*filled symbols*) of nAChR protein

al. 2002; da Costa el al. 2004), although the segregation of a saturated PC from an unsaturated PC by the action of nAChR has recently been reported (Wenz and Barrantes 2005). In this case the authors suggest that the maintenance of this domain is predominantly due to lipid–lipid interactions opposite to that with PA, more stable and mainly maintained by protein–lipid interactions. The PA domain has been detected either through fluorescence, or FT-IR and DSC techniques, the latter sensitive to macroscopic events, indicating that macrodomains should be formed. In addition, from resonance energy transfer experiments it has been shown that these domains are located next to the protein (Poveda et al. 2002).

Membrane phospholipids, including those interacting with membrane proteins, diffuse very fast, around 10^8 cm^2 s^{-1} (Ellena et al. 1983; East et al. 1985), so the ability of nAChR to change the lipid lateral distribution segregating PA around it will dramatically enhance its interaction with this phospholipid, hence explaining the strong modulating effect of PA on nAChR.

There are several publications describing the segregation of lipid domains by peptides or extrinsic proteins but only one for a membrane protein, rhodopsin (Polozova and Litman 2000). This kind of domain, whose organization is directed by a transmembrane protein, seems opposite to that of the so-called "rafts" (Simons and Ikonen 1997), where it is postulated that the physical properties of lipids are responsible for the segregation. However, a "clustering" model has been proposed that could be valid for the nAChR–PA interaction. In it, the action of certain proteins could cluster little initial rafts dispersed in the membrane (Harder et al. 1998). On the other hand, there are some examples dealing with a special selectivity of certain proteins for PA, such as that of the vesicular-stomatitis virus envelope-proteins (Luan el al. 1995). In spite of the low PA concentration in host membranes, these proteins interact specifically with PA giving cause for PA domains, which is an essential event for new viral particles to be formed. Moreover, PA domains have been proposed as scavengers of other essential biological anionic phospholipids such as PIP_2 (Denisov et al. 1998), so the domain formation could configure an important regulation site in the membrane. PS is another anionic phospholipid present at high levels in membranes from the *Torpedo* electric organ (Gonzalez-Ros et al. 1982), so it could be a good candidate to enter the PA domain as reported in the stomatitis virus, where PS is only segregated when PA is present (Luan et al. 1995).

The fact that PA is the main component of the nAChR segregated domain (Poveda et al. 2002) opens a new possibility to regulate nAChR activity by activation of phospholipase D, as reported previously in other systems (Exton 1990; Billah and Anthes 1990). In addition, the activity of this enzyme can be regulated through the agonist binding to receptors coupled to G-proteins. In this way, addition of phospholipase D to nAChR-enriched vesicles results in an increase in protein function (Bhushan and McNamee 1993). Finally, PA levels can be increased by phosphorilation by diacylglycerol kinase of diacylglycerols resulting from phospholipase C hydrolysis of phosphatidylinositol.

Another important question about the segregation of the PA domain is related to the determinants in the protein and in PA responsible of this strong interaction that finally leads to domain segregation. Calorimetric studies and other experiments using proteases point to the transmembrane segments as the main structure responsible for domain segregation (Poveda et al. 2002). It has been proposed that some positive charged amino acid present at the end of the nAChR transmembrane helices, such as Arg-429 or His-408 at the M4, could be responsible for the stronger binding to anionic phospholipids, although there are no definite results (Blanton and Wang 1990, 1991; Blanton and Cohen 1992). On the other hand, the exact determinants in the PA molecule that could explain its strong interaction with nAChR are also unknown and only general properties of this phospholipid have been pointed out, such as its negative charge, its very small headgroup or its high capacity to form hydrogen bonds (Baenziger et al. 1999). Evidently, the negative charge is not the only factor, as salt screening or pH titration does not destabilize the domain. Moreover, other anionic lipids are not segregated by nAChR. At this point it is important to stress that PA has a higher pK_a when the protein is present, so its anionic charge is diminished (Poveda et al. 2002). This could facilitate the formation of the PA domains since a lower repul-

sion and an enhanced attraction through hydrogen bonds between PA molecules would occur (Garidel et al. 1997), decreasing the electrostatic contribution to the free energy of the system (Denisov et al. 1998) so as to overcome the entropic effect that favours the homogeneous mixing of lipid components.

8.8 From Model In vitro Systems to Cell Membranes: the *Xenopus* Oocyte as a Cell Model for the Study of Lipid–Protein Interactions

Most of the studies dealing with the functional and structural dependence of nAChR on its surrounding lipids have been carried out on model membrane systems to avoid the complexity of the cell membrane and to prevent the changes that a single variable can make in the whole system. Though these model systems are useful, providing a reductionism approach, we must develop novel methods allowing the study of the lipid–protein interaction in native cell membranes in order to confirm the results obtained in artificial systems.

One of the putative cell models for these studies is the *Xenopus* oocyte. These cells have been widely used for the biophysical characterization of many ion channels, neurotransmitter receptors and transporters, thanks to their ease of use, amenability for electrophysiological recordings and their capability to translate efficiently and faithfully exogenous mRNAs (Miledi et al. 1989; Soreq and Seidman 1992; Miller and Zhou 2000). Though *Xenopus* oocytes are capable of making a large number of post-translational modifications of the proteins coded by exogenous mRNA (such as acetylation, glycosylation or phosphorylation), and to assemble oligomeric receptor/channel complexes, they cannot always match the processing carried out by the cells that natively express them. Almost certainly, this is the reason for the failed or altered function of some foreign proteins expressed in oocytes. So, for instance, *Torpedo* nAChRs expressed in oocytes display an altered pattern of glycosylation (Buller and White 1990) and neuronal nAChRs do not exhibit the properties of native receptors, likely because oocytes fail to assemble their different subunits correctly (Sivilotti et al. 1997). Besides, there are specific lipid requirements of membrane proteins, which might constitutes a handicap for heterologous expression in a functional form (Opekarová and Tanner 2003). To overcome this handicap, nAChRs, and other membrane proteins, have been functionally transplanted to the *Xenopus* oocyte membrane by intracellular injection of plasma membranes (Marsal et al. 1995; Aleu et al. 1997; Sanna et al. 1998; Miledi et al. 2002; Palma et al. 2003; Miledi et al. 2004) or proteoliposomes bearing the purified protein (Morales et al. 1995; Le Cahérec et al. 1996; Ivorra et al. 2002).

Oocyte injection of proteoliposomes bearing a purified protein, instead of fragments of cellular membranes, has several advantages:

(i) It allows the study of single molecular entities.
(ii) The transplanted protein does not need to be one of the most abundant in the cellular membrane, although the presence of a large amount of protein simplifies its purification.
(iii) It permits to study the influence that the lipid composition of the reconstitution matrix has on the functional properties of the transplanted protein.

This last point has special relevance, since many proteins are, and need to be, surrounded by specific lipids to develop their full functional activity (see above). Therefore, microtransplantation of purified proteins into the *Xenopus* oocyte membrane arises as an excellent way to unravel lipid–protein interactions, since it allows the insertion of proteins with specific lipids bound to them. Moreover, using this approach it is possible not only to change the ratio of different phospholipids surrounding the protein, to determine their functional relevance, but also the length of the acyl chains, to induce local changes in bilayer thickness and elasticity that might also be important for the protein activity (Martinac and Hamill 2002; Lundbaek et al. 2004).

Furthermore, an additional advantage of using *Xenopus* oocytes as the cell model for functional and biophysical studies of heterologous proteins is that their membrane lipid composition is well known (Caldironi et al. 1996; Stith et al. 2000) and can be, at least partially, customized. For instance, the cholesterol content in the oocyte membrane can be easily modified, inducing not only changes in bilayer stiffness but also in the functional activity of different proteins, including nAChRs (see above). The normal cholesterol/phospholipid (C/P) molar ratio in the *Xenopus* oocyte membrane (about 0.5) can be almost duplicated by incubating the cells in a solution containing cholesterol-enriched liposomes, whereas a significant decrease in this ratio is obtained by incubating them with methyl-β-cyclodextrin (Santiago et al. 2001). Likewise, the content of other specific lipid molecules can be modify either by oocyte incubation with lipid-defined liposomes or by activating specific pathways of lipid metabolism. It should be noticed that some lipids are charged molecules and hence certain changes in the lipid composition around some proteins, mainly ion channels, might affect their function by an electrostatic mechanism. So, it is well known that the ion channel biophysical properties can be modulated by fixed charges present in the protein itself or by charged molecules in its surroundings, specially phospholipids. This is because a charged surface in the neighbourhood of the ion channel influences the concentration of ions at the channel mouth and consequently its conductance (Latorre et al. 1992; Anzai et al. 1994).

Interestingly, the PA modulation of nAChR observed on in vitro systems has been corroborated in vivo using the *Xenopus* oocyte model (Morales et al. in preparation; Fig. 8.5). In these experiments, purified nAChRs reconstituted in either PA:PC:Chol (25:50:25 molar ratio), PC:Chol (75:25 molar ratio), or soybean lipids, are injected in oocytes, where they are efficiently inserted in the plasma membrane. Then, the functional activity, and properties, of the transplanted nAChRs are assessed using the voltage clamp technique. The amplitude of the acetylcholine (ACh)-elicited currents in the injected oocytes depended on the reconstitu-

tion matrix used. The ACh-current was higher when the nAChR was reconstituted in PA than when it was reconstituted either in soybean or PC lipids, which were very similar each other (see Fig. 8.5). This effect was not due to the different fusion efficiency of the different proteoliposomes to the oocyte membrane. It is worth noting that when nAChRs are reconstituted with those lipid mixtures in vitro, the activity is higher for soybean lipids than for the PA-mixture while no activity is found in PC:Chol mixtures. The fact that in the cell membrane the nAChR in PC:Chol reversibly recovers its function suggests that the system is sufficiently dynamic to allow the injected lipid around nAChR to be exchanged for the own oocyte membrane lipids. On the other hand, when reconstituted nAChR in PA is injected into oocytes, larger Ah currents were elicited suggesting that nAChR binds PA tightly, impeding its free exchange with other bulk membrane lipids and leading to the formation of a PA-rich domain segregated around the protein. The permanent interaction with PA, a positive modulator, would result in enhanced protein activity. An interesting observation that supports this hypothesis is the fact that, as nAChR is purified from the *Torpedo* electric organ, the PA content of the lipids which accompanies the protein is progressively increased from 0.5–1.6% up to 2.2–2.9% (Gonzalez-Ros et al. 1982).

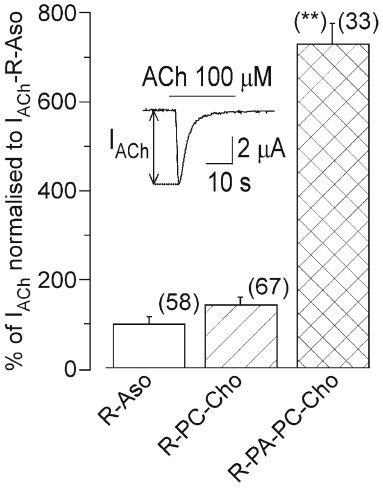

Fig. 8.5. Bar diagram showing the amplitude of the peak ACh (100 μM) currents (I_{ACh}) elicited in oocytes previously injected with nAChRs reconstituted in asolectin (R-Aso, *open bar*), a mixture of PC (75%) and cholesterol (25%, R-PC+Cho, hatched bar) or a mixture of PA (25%), PC (50%), and cholesterol (25%, R-PA+PC+Cho, *crossed bar*). Values were normalized to the amplitude of the currents obtained in the R-Aso group. The inset shows a representative record of the I_{ACh} recorded in the R-Aso group. The *arrow* indicates the measurement of I_{Ach} and the *bar* indicates the ACh application time. In all experiments the membrane potential was held at –60 mV. The number of observations is given in brackets. *Asterisks* indicate significant differences with the R-Aso group ($p < 0.01$)

Many more studies are needed on in vivo models to fully understand the functional modulation of membrane proteins by their surrounding lipids, but undoubtedly these are the first steps in this direction.

References

Akabas MH, Kaufmann C, Archdeacon P, Karlin A (1994) Identification of acetylcholine receptor channel-lining residues in the entire M2 segment of the alpha subunit. Neuron 13:919–927

Aleu J, Ivorra I, Lejarreta M, González-Ros JM, Morales A, Ferragut JA (1997) Functional incorporation of P-glycoprotein into Xenopus oocyte plasma membrane fails to elicit a swelling-evoked conductance. Biochem Biophys Res Com 237:407–412

Andreasen TJ, McNamee MG (1980) Inhibition of ion permeability control properties of acetylcholine receptor from Torpedo californica by long-chain fatty acids. Biochemistry 19:4719–4726

Antollini SS, Soto MA, Bonini de Romanelli I, Gutierrez-Merino C, Sotomayor P, Barrantes FJ (1996) Physical state of bulk and protein-associated lipid in nicotinic acetylcholine receptor-rich membrane studied by laurdan generalized polarization and fluorescence energy transfer. Biophys J 70(3):1275–84

Anzai K, Takano C, Tanaka K, Kirino Y (1994) Asymmetrical lipid charge changes the subconducting state of the potassium channel from sarcoplasmic reticulum. Biochem Biophys Res Com 199:1081–1087

Arias HR (1998) Noncompetitive inhibition of nicotinic acetylcholine receptors by endogenous molecules. J Neurosci Res 52:369–379

Arshava B, Taran I, Xie H, Becker JM, Naider F (2002) High resolution NMR analysis of the seven transmembrane domains of a heptahelical receptor in organic-aqueous medium. Biopolymers 64:161–76

Baenziger JE, Chew JP (1997) Desensitization of the nicotinic acetylcholine receptor mainly involves a structural change in solvent-accessible regions of the polypeptide backbone. Biochemistry 36:3617–3624

Baenziger JE, Darsaut TE, Morris ML (1999) Internal dynamics of the nicotinic acetylcholine receptor in reconstituted membranes. Biochemistry 38:4905–11

Baezinger JE, Morris ML, Darsaut TE (2000) Effect of membrane lipid composition on the conformational equilibria of the nicotinic acetylcholine receptor. J Biol Chem 275:777–784

Barrantes FJ (1993) The lipid annulus of the nicotinic acetylcholine receptor as a locus of structural–functional interactions. In: Walts A (ed) Protein–lipid interactions. Elsevier, Amsterdam, pp 231–256

Barrantes FJ (2003) Modulation of nicotinic acetylcholine receptor function through the outer and middle rings of transmembrane domains. Curr Opin Drug Discov Develop 6:620–632

Barrantes FJ, Antollini SS, Blanton MP, Prieto M (2000) Topography of nicotinic acetylcholine receptor membrane-embedded domains. J Biol Chem 275:37333–37339

Bhushan A, McNamee MG (1993) Correlation of phospholipid structure with functional effects on the nicotinic acetylcholine receptor. A modulatory role for phosphatidic acid. Biophys J 64:716–723

Billah MM, Anthes JC (1990) The regulation and cellular functions of phosphatidylcholine hydrolysis. Biochem J 269:281–291

Blanton MP, Wang HH (1991) Localization of regions of the Torpedo californica nicotinic acetylcholine receptor labeled with an aryl azide derivative of phosphatidylserine. Biochim Biophys Acta 5:1067:1–8

Blanton MP, Cohen JB (1994) Identifying the lipid–protein interface of the Torpedo nicotinic acetylcholine receptor: secondary structure implications. Biochemistry 33:2859–2872

Blanton MP, McCardy EA, Huggins A, Parikh D (1998) Probing the structure of the nicotinic acetylcholine receptor with the hydrophobic photoreactive probes [125I]TID-BE and [125I]TIDPC/16. Biochemistry 37:14545–4555

Blanton MP, Cohen JB (1992) Mapping the lipid-exposed regions in the Torpedo californica nicotinic acetylcholine receptor. Biochemistry 31:3738–3750

Blanton MP, Wang HH (1990) Photoaffinity labeling of the Torpedo californica nicotinic acetylcholine receptor with an aryl azide derivative of phosphatidylserine Biochemistry 29:1186–1194

Bouzat C, Barrantes FJ (1996) Modulation of muscle nicotinic aceylcholine receptors by the glucocorticoid hydrocortisone: possible allosteric mechanism of channel blockade. J Biol Chem 271:25835–25841

Bouzat C, Roccamo AM, Garbus I, Barrantes FJ (1998) Mutations at lipid-exposed residues of the acetylcholine receptor affect its gating kinetics. Molec Pharmacol 54:146–153

Brown DA, London E (1997) Structure of detergent-resistant membrane domains: does phase separation occur in biological membranes? Biochem Biophys Res Commun 240:1–7

Brown DA, London E (1998) Functions of lipid rafts in biological membranes. Ann Rev Cell Dev Biol 14:111–136

Brown DA, London E (2000) Structure and function of sphingolipid- and cholesterol-rich membrane rafts. J Biol Chem 275:17221–17224

Bruses JL, Chauvet N, Rutishauser U (2001) Membrane lipid rafts are necessary for the maintenance of the (alpha)7 nicotinic acetylcholine receptor in somatic spines of ciliary neurons. J Neurosci 21:504–512

Buller AL, White M (1990) Altered patterns of N-linked glycosylation of the Torpedo acetylcholine receptor expressed in Xenopus oocytes. J Membrane Biol 115:179–189

Butler DH, McNamee MG (1993) FTIR analysis of nicotinic acetylcholine receptor secondary structure in reconstituted membranes. Biochim Biophys Acta 1150:17–24

Caldironi HA, ALonso TS (1996) Lipidic characterization of full-grown amphibian oocytes and their plasma membrane-enriched fractions. Lipids 31:651–656

Canti C, Bodas E, Marsal J, Solsona C (1998) Tacrine and physostigmine block nicotinic receptors in Xenopus oocytes injected with Torpedo electroplaque membranes. Eur J Pharmacol 363:197–202

Cantor, RS (1997) Lateral pressures in cell membranes: a mechanism for modulation of protein function. J Phys Chem 101:1323–1325

Castresana J, Fernandez-Ballester G, Fernandez AM, Laynez JL, Arrondo JL, Ferragut JA, JM Gonzalez-Ros (1992) Protein structural effects of agonist binding to the nicotinic acetylcholine receptor. FEBS Lett 314:171–175

Chang G, Spencer RH, Lee AT, Barclay MT, Rees DC (1998) Structure of the MscL homolog from Mycobacterium tuberculosis: a gated mechanosensitive ion channel. Science 282:2220–2226

Changeux JP (1990) The nicotinic acetylcholine receptor: an allosteric protein prototype of ligand-gated ion channels. Trends Pharmacol Sci 11:485–492

Chiara DC, Dangott LJ, Eckenhoff RG, Cohen JB (2003) Idendtification of nicotinic aceylcholine receptor amino acids photolabeled by the volatile anesthetic halothane. Biochemistry 42:13457–13467

Corbin J, Methot N, Wang HH, Baenziger JE, Blanton MP (1998) Secondary structure analysis of individual transmembrane segments of the nicotinic acetylcholine receptor by circular dichroism and Fourier transform infrared spectroscopy. J Biol Chem 273:771–7

Corbin J, Wang HH, Blanton MP (1998) Identifying the cholesterol binding domain in the nicotinic acetylcholine receptor with [125I]azido-cholesterol. Biochim Biophys Acta 1414:65–74

Cordes FS, Bright JN, Sansom MS (2002) Proline-induced distortions of transmembrane helices. J Mol Biol 323:951–960

Criado, M, Eib H, Barrantes FJ (1984) Functional properties of the acetylcholine receptor incorporated in model lipid membranes Differential effects of chain length and head group of phospholipids on receptor affinity states and receptor-mediated ion translocation. J Biol Chem 259:9188–9198

Cruz-Martin A, Mercado JL, Rojas LV, McNamee MG, Lasalde-Dominicci JA (2001) Tryptophan substitutions at lipid-exposed positions of the gamma M3 transmembrane domain increase the macroscopic ionic current response of the Torpedo californica nicotinic acetylcholine receptor. J Membr Biol 183:61–70

Curtis L, Buisson B, Bertrand S, Bertrand D (2002) Potentiation of human 4 2 neuronal nicotinic acetylcholine receptor by estradiol. Molec Pharmacol 61:127–135

daCosta CJ, Ogrel AA, McCardy EA, Blanton MP, Baenziger JE (2002) Lipid–protein interactions at the nicotinic acetylcholine receptor A functional coupling between nicotinic receptors and phosphatidic acid-containing lipid bilayers. J Biol Chem 277:201–208

daCosta CJ, Wagg ID, McKay ME, Baenziger JE (2004) Phosphatidic acid and phosphatidylserine have distinct structural and functional interactions with the nicotinic acetylcholine receptor. J Biol Chem 279:14967–14974

de Kruijff B (1997) Lipid polymorphism and biomembrane function. Curr Opin Chem Biol 1:564–9

de Planque MR, Bonev BB, Demmers JA, Greathouse DV, Koeppe RE 2nd, Separovic F, Watts A, Killian JA (2003) Interfacial anchor properties of tryptophan residues in transmembrane peptides can dominate over hydrophobic matching effects in peptide–lipid interactions. Biochemistry 42:5341–5348

de Planque MR, Goormaghtigh E, Greathouse DV, Koeppe RE 2nd, Kruijtzer JA, Liskamp RM, de Kruijff B, Killian JA (2001) Sensitivity of single membrane-spanning alpha-helical peptides to hydrophobic mismatch with a lipid bilayer: effects on backbone structure, orientation, and extent of membrane incorporation. Biochemistry 40:5000–5010

Denisov G, Wanaski S, Luan P, Glaser M, McLaughlin S (1998) Binding of basic peptides to membranes produces lateral domains enriched in the acidic lipids phosphatidylserine and phosphatidylinositol 4,5-bisphosphate: an electrostatic model and experimental results. Biophys J 74:731–744

Dowhan W (1997) Molecular basis for membrane phospholipid diversity: why are there so many lipids? Annu Rev Biochem 66:199–232

Doyle DA (2004) Structural changes during ion channel gating. Trends Neurosci (6):298–302

Doyle DA, Morais Cabral J, Pfuetzner RA, Kuo A, Gulbis JM, Cohen SL, Chait BT, MacKinnon R (1998) The structure of the potassium channel: molecular basis of K+ conduction and selectivity. Science 280:69–77

Dreger M, Krauss M, Herrmann A, Hucho F (1997) Interactions of the nicotinic acetylcholine receptor transmembrane segments with the lipid bilayer in native receptor-rich membranes. Biochemistry 36:839–847

East JM, Melville D, Lee AG (1985) Exchange rates and numbers of annular lipids for the calcium and magnesium ion dependent adenosinetriphosphatase. Biochemistry 24:2615–2623

Ellena JF, Blazing MA, McNamee MG (1983) Lipid–protein interactions in reconstituted membranes containing acetylcholine receptor. Biochemistry 22:5523–3555

Esmann M, Marsh D (1985) Spin-label studies on the origin of the specificity of lipid–protein interactions in Na+,K+-ATPase membranes from Squalus acanthias. Biochemistry 24:3572–3578

Exton JH (1990) Signalling through phosphatidylcholine breakdown. J Biol Chem 265:1–4

Fernandez AM, Fernandez-Ballester G, Ferragut JA, Gonzalez-Ros JM (1993) Labeling of the nicotinic acetylcholine receptor by a photoactivatable steroid probe: effects of cholesterol and cholinergic ligands. Biochim Biophys Acta 1149:135–144

Fernandez-Ballester G, Castresana J, Fernandez AM, Arrondo JL, Ferragut JA, Gonzalez-Ros JM (1994) A role for cholesterol as a structural effector of the nicotinic acetylcholine receptor. Biochemistry33:4065–4071

Finer-Moore J, Strooud RM (1984) Amphipathic analysis and possible formation of the ion channel in an acetylcholine receptor. Proc Natl Acad Sci USA 81:155–9

Fong TM, McNamee MG (1986) Correlation between acetylcholine receptor function and structural properties of membranes. Biochemistry 25:830–40

Fong TM, McNamee MG (1987) Stabilization of acetylcholine receptor secondary structure by cholesterol and negatively charged phospholipids in membranes. Biochemistry 26:3871–80

Forman SA (1999) A hydrophobic photolabel inhibits nicotinic acetylcholine receptors via open-channel block following a slow step. Biochemistry 38:14559–14564

Galzi JL, Edelstein SJ, Changeux JP (1996) The multiple phenotypes of allosteric receptor mutants. Proc Natl Acad Sci USA 93:1853–1858

Garbus I, Bouzat C, Barrantes FJ (2001) Steroids differentially inhibit the nicotinic aceylcholine receptor. Neuro Report 12:227–231

Garidel P, Johann C, Blume A (1997) Nonideal mixing and phase separation in phosphatidylcholine-phosphatidic acid mixtures as a function of acyl chain length and pH. Biophys J 72:2196–2210

Gentry CL, Lukas R (2001) Local anesthetics noncompetitively inhibit function of four distinct nicotinic acetylcholine receptor subtypes. J Pharmacol Exp Ther 299:1038–1048

Gonzalez-Ros JM, Llanillo M, Paraschos A, Martinez-Carrion M (1982) Lipid environment of acetylcholine receptor from Torpedo californica. Biochemistry 21:3467–74

Gonzalez-Ros JM, Paraschos A, Martinez-Carrion M (1980) Reconstitution of functional membrane-bound acetylcholine receptor from isolated Torpedo californica receptor protein and electroplax lipids. Proc Natl Acad Sci USA 198077:1796–1800

Guzman GR, Santiago J, Ricardo A, Marti-Arbona R, Rojas LV, Lasalde-Dominicci JA (2003) Tryptophan scanning mutagenesis in the alphaM3 transmembrane domain of the Torpedo californica acetylcholine receptor: functional and structural implications. Biochemistry 42:12243–50

Harder T, Scheiffele P, Verkade P, Simons K (1998) Lipid domain structure of the plasma membrane revealed by patching of membrane components. J Cell Biol 141:929–942

Harder T, Simons K (1997) Caveolae, DIGs, and the dynamics of sphingolipid-cholesterol microdomains. Curr Opin Cell Biol 9:534–542

Heginbotham L, Kolmakova-Partensky L, Miller C (1998) Functional reconstitution of a prokaryotic K+ channel. J Gen Physiol 111:741–749

Hogg RC, Raggenbass M, Bertand D (2003) Nicotinic acetylcholine receptors: from structure to brain function. Rev Physiol Biochem Pharmacol 147:1–46

Hol WG, van Duijnen PT, Berendsen HJ (1978) The alpha-helix dipole and the properties of proteins. Nature 273:443–446

Hvidt A, Nielsen SO (1966) Hydrogen exchange in proteins. Adv Protein Chem 21:287–386

Ivorra I, Fernandez A, Gal B, Aleu J, Gonzalez-Ros JM, Ferragut JA, Morales A (2002) Protein orientation affects the efficiency of functional protein transplantation into the Xenopus oocyte membrane. J Membrane Biol 185:117–127

Jones OT, Eubanks JH, Earnest JP, McNamee MG (1988) A minimum number of lipids are required to support the functional properties of the nicotinic acetylcholine receptor. Biochemistry 27:3733–3742

Jones OT, McNamee MG (1988) Annular and nonannular binding sites for cholesterol associated with the nicotinic acetylcholine receptor. Biochemistry 27:2364–2374

Karlin A (2002) Emerging structure of the nicotinic acetylcholine receptor. Nat Rev Neurosci 3:102–114

Karlin A, Cox RN, Dipaola M, Holtzman E, Kao PN, Lobel P, Wang L, Yodh N (1986) Functional domains of the nicotinic acetylcholine receptor. Ann NY Acad Sci 463:53–69

Kash TL, Jenkins A, Kelley JC, Trudell JR, Harrison NL (2003) Coupling of agonist binding to channel gating in the GABA(A) receptor. Nature 421:272–5

Katz B, Miledi R (1975) The effect of procaine on the action of acetylcholine at the neuromuscular junction. J Physiol 249:269–284

Ke L, Lukas RJ (1996) Effects of steroid exposure on ligand binding and functional activities of diverse nicotinic acetylcholine receptor subtypes. J Neurochem 67:1100–1112

Kuo A, Gulbis JM, Antcliff JF, Rahman T, Lowe ED, Zimmer J, Cuthbertson J, Ashcroft FM, Ezaki T, Doyle DA (2003) Crystal structure of the potassium channel KirBac11 in the closed state. Science 300:1922–1926

Latorre R, Labarca P, Naranjo D (1992) Surface charge effects on ion conduction in ion channels. Methods Enzymol 207:471–501

Le Cahèrec F, Bron P, Verbavatz JM, Garret A, Morel G, Cavalier A, Bonnec G, Thomas D, Gouranton J, Hubert JF (1996) Incorporation of proteins into (Xenopus) oocytes by proteoliposome microinjection: functional characterization of a novel aquaporin. J Cell Sci 109:1285–1295

Lee AG (1998) How lipids interact with an intrinsic membrane protein: the case of the calcium pump. Biochim Biophys Acta 1376:381–90

Lee AG (2003) Lipid–protein interactions in biological membranes: a structural perspective. Biochim Biophys Acta 1612:1–40

Lee AG (2004) How lipids affect the activities of integral membrane proteins. Biochim Biophys Acta 3:1666:62–87

Liu LP, Deber CM (1997) Anionic phospholipids modulate peptide insertion into membranes. Biochemistry 36(18):5476–5482

Liu Y, Dilger JP, Vidal AM (1994) Effects of alcohols and volatile anaesthetics on the activation of nicotinic acetylcholine receptor channels. Mol Pharmacol 45:1235–1241

Luan P, Yang L, Glaser M (1995) Formation of membrane domains created during the budding of vesicular stomatitis virus. A model for selective lipid and protein sorting in biological membranes. Biochemistry 34:9874–83

Lugovskoy AA, Maslennikov IV, Utkin YN, Tsetlin VI, Cohen JB, Arseniev AS (1998) Spatial structure of the M3 transmembrane segment of the nicotinic acetylcholine receptor alpha subunit. Eur J Biochem 255:455–461

Lundbaek JA, Birn P, Hansen AJ, Søgaard R, Nielsen C, Girshman J, Bruno MJ, Tape SE, Egebjerg J, Greathouse DV, Mattice GL, Koeppe II RE, Andersen OS (2004) Regulation of sodium channel function by bilayer elasticity: the importance of hydrophobic coupling. Effects of micelle-forming amphiphiles and cholesterol. J Gen Physiol 121:599–621

MacKinnon R (2003) Potassium channels. FEBS Lett 555:62–65

Marheineke K, Grunewald S, Christie W, Reilander H (1998) Lipid composition of Spodoptera frugiperda (Sf9) and Trichoplusia ni (Tn) insect cells used for baculovirus infection. FEBS Lett 441:49–52

Marsal J, Tigy G, Miledi R (1995) Incorporation of acetylcholine receptors and Cl-channels in Xenopus oocytes injected with Torpedo electroplaque membranes. Proc Natl Acad Sci USA 92:5224–5228

Marsh D, Barrantes FJ (1978) Immobilized lipid in acetylcholine receptor-rich membranes from Torpedo marmorata Proc Natl Acad Sci USA 73:4329–4333

Marsh D, Horvath LI (1998) Structure, dynamics and composition of the lipid–protein interface perspectives from spin-labelling. Biochim Biophys Acta 1376:267–296

Marsh D, Pali T (2004) The protein–lipid interface: perspectives from magnetic resonance and crystal structures. Biochim Biophys Acta 1666:118–41

Marsh D, Pellkofer R, Hoffmann-Bleihauer P, Sandhoff K (1982) Incorporation of lipids into cellular membranes – a spin-label assay. Anal Biochem 122:206–12

Marsh D, Watts A, Barrantes FJ (1981) Phospholipid chain immobilization and steroid rotational immobilization in acetylcholine receptor-rich membranes from Torpedo marmorata. Biochim Biophys Acta 645:97–101

Martens JR, Kwak YG, Tamkun MM (1999) Modulation of Kv channel alpha/beta subunit interactions. Trends Cardiovasc Med 8:253–258

Martens JR, Navarro-Polanco R, Coppock EA, Nishiyama A, Parshley L, Grobaski TD, Tamkum MM (2000) Differential targeting of shaker-like potassium channels to lipid rafts. J Biol Chem 275:7443–7446

Martinac B, Hamill OP (2002) Gramicidin A channels switch between stretch activation and stretch inactivation depending on bilayer thickness. Proc Natl Acad Sci USA 99:4308–4312

Maxfield FR (2002) Plasma membrana microdomains. Curr Opin Cell Biol 14:483–487

Methot N, McCarthy MP, Baenziger JE (1994) Secondary structure of the nicotinic acetylcholine receptor: implications for structural models of a ligand-gated ion channel. Biochemistry 33:7709–7717

Mielke DL, Wallace BA (1988) Secondary structural analyses of the nicotinic acetylcholine receptor as a test of molecular models. J Biol Chem 263(7):3177–3182

Miledi R, Dueñas Z, Martinez-Torres A, Kawas CH, Eusebi F (2004) Microtransplantation of functional receptors and channels from the Alzheimer's brain to frog oocytes. Proc Natl Acad Sci USA 101:1760–1763

Miledi R, Eusebi F, Martínez-Torres A, Palma E, Trettel F (2002) Expression of functional neurotransmitter receptors in Xenopus oocytes after injection of human brain membranes. Proc Natl Acad Sci USA 99:13238–13242

Miledi R, Parker I, Sumikawa K (1989) Transplanting receptors from brains into oocytes. In: Fidia Research Foundation Neuroscience Award Lectures 3, pp 57–90, Raven Press, New York

Miller AJ, Zhou JJ (2000) Xenopus oocytes as an expression system for plant transporters. Biochim Biophys Acta 1465:343–358

Miyazawa A, Fujiyoshi Y, Unwin N (2003) Structure and gating mechanism of the acetylcholine receptor pore. Nature 423:949–955

Moore WM, Holliday LA, Puett D, Brady RN (1974) On the conformation of the acetylcholine receptor protein from Torpedo nobiliana. FEBS Lett 45:145–149

Morales A, Aleu J, Ivorra I, Ferragut JA, González-Ros JM, Miledi R (1995) Incorporation of reconstituted acetylcholine receptors from Torpedo into the Xenopus oocyte membrane. Proc Natl Acad Sci USA 92:8468–8472

Neher E, Steinbach H (1978) Local anaesthetics transiently block currents through single acetylcholine-receptor channels. J Physiol 277:153–176

Nurowska E, Ruzzier F (1996) Corticosterone modifies the murine muscle acetylcholine receptor channel kinetics. Neuro Report 8:77–80

Ochoa EL, A Chattopadhyay, MG McNamee (1989) Desensitization of the nicotinic acetylcholine receptor: molecular mechanisms and effect of modulators. Cell Mol Neurobiol 9:141–178

Oliver D, Lien CC, Soom M, Baukrowitz T, Jonas P, Fakler B (2004) Functional conversion between A-type and delayed rectifier K+ channels by membrane lipids. Science 304:265–270

Olivera S, Ivorra I, Morales A (2005) The acetylcholinesterase inhibitor BW284c51 is a potent blocker of Torpedo nicotinic AchRs incorporated into the Xenopus oocyte membrane. Br J Pharmacol (in press)

Opekarová M, Tanner W (2003) Specific lipid requirements of membrane proteins – a putative bottleneck in heterologous expression. Biochim Biophys Acta 1610:11–22

Opella SJ, Marassi FM, Gesell JJ, Valente AP, Kim Y, Oblatt-Montal M, Montal M (1999) Structures of the M2 channel-lining segments from nicotinic acetylcholine and NMDA receptors by NMR spectroscopy. Nat Struct Biol 4:374–379

Ortiz-Acevedo A, Melendez M, Asseo AM, Biaggi N, Rojas LV, Lasalde-Dominicci JA (2004) Tryptophan scanning mutagenesis of the gammaM4 transmembrane domain of the acetylcholine receptor from Torpedo californica. J Biol Chem 279:42250–42257

Paas Y, Cartaud J, Recouvreur M, Grailhe R, Dufresne V, Pebay-Peyroula E, Landau EM, Changeux JP (2003) Electron microscopic evidence for nucleation and growth of 3D acetylcholine receptor microcrystals in structured lipid–detergent matrices. Proc Natl Acad Sci USA 100:11309–11314

Palma E, Trettel F, Fucile S, Renzi M, MIledi R, Eusebi F (2003) Microtransplantation of membranes from cultured cells to Xenopus oocytes: A method to study neurotransmitter receptors embedded in native lipids. Proc Natl Acad Sci USA 100:2896–2900

Palsdottir H, Hunte C (2004) Lipids in membrane protein structures. Biochim Biophys Acta 1666:2–18

Paradiso K, Sabey K, Evers AS, Zormski CF, Covey DF, Steinbach JH (2000) Steroid inhibition of rat neuronal nicotinic 4 2 receptors experessed in HEK 293 cells. Mol Pharmacol 58:341–351

Paradiso K, Zhang J, Steinbach JH (2001) The C terminus of the human nicotinic 4 2 receptor forms a binding site required for potentiation by an estrogenic steroid. J Neurosci 21:6561–6568

Pashkov VS, Maslennikov IV, Tchikin LD, Efremov RG, Ivanov VT, Arseniev AS (1999) Spatial structure of the M2 transmembrane segment of the nicotinic acetylcholine receptor alpha-subunit. FEBS Lett 45:117–121

Pebay-Peyroula E, Rosenbusch JP (2001) High-resolution structures and dynamics of membrane protein–lipid complexes: a critique. Curr Opin Struct Biol 11:427–432

Perozo E, Cortes DM, Somporspisut P, Kloda A, Martinac B (2002) Open channel structure of MscL and gating mechanism of mechanosensitive channels. Nature 418:942–948

Pershina L, Hvidt A (1974) A study by the hydrogen-exchange method of the complex formed between the basic pancreatic trypsin inhibitor and trypsin. Eur J Biochem 48:339–344

Polozova A, Litman BJ (2000) Cholesterol dependent recruitment of di22:6-PC by a G protein-coupled receptor into lateral domains. Biophys J 79:2632–4263

Poveda JA, Encinar JA, Fernandez AM, Mateo CR, Ferragut JA, Gonzalez-Ros JM (2002) Segregation of phosphatidic acid-rich domains in reconstituted acetylcholine receptor membranes. Biochemistry 41:12253–12262

Powl AM, East JM, Lee AG (2005) Heterogeneity in the binding of lipid molecules to the surface of a membrane protein: hot spots for anionic lipids on the mechanosensitive channel of large conductance MscL and effects on conformation. Biochemistry 44:5873–5883

Revah F, Bertrand D, Galzi JL, Devillers-Thiery A, Mulle C, Hussy N, Bertrands S, Ballivet M, Changeux JP (1991) Mutations in the channel domain alter desensitization of a neuronal nicotinic receptor. Nature 353:846–849

Revah F, Galzi JL, Giraudat J, Haumont PY, Lederer F, Changeux JP (1990) The noncompetitive blocker [3H]chlorpromazine labels three amino acids of the acetylcholine receptor gamma subunit: implications for the alpha-helical organization of regions MII and for the structure of the ion channel. Proc Natl Acad Sci USA 87:4675–4679

Sackmann E (1984) Physical basis for trigger processes and membrane structures. In: Chapman D (ed) Biological membranes, Vol. 5, Academic Press, London, pp 105–143

Sali D, Bycroft M, Fersht AR (1988) Stabilization of protein structure by interaction of alpha-helix dipole with a charged side chain. Nature 335:740–743

Sanna E, Motzo C, Usala M, Pau D, Cagetti E, Biggio G (1998) Functional changes in rat nigral GABAA receptors induced by degeneration of the striatonigral GABAergic pathway: an electrophysiological study of receptors incorporated into Xenopus oocytes. J Neurochem 70:2539–2544

Sansom MS , Shrivastava IH, Bright JN, Tate J, Capener CE, Biggin PC (2002) Potassium channels: structures, models, simulations. Biochim Biophys Acta 1565(2):294–307

Santiago J, Guzmán GR, Rojas LV, Marti R, Asmar-Rovira GA, Santana LF, McNamee M, Lasalde-Dominicci JA (2001) Probing the effects of membrane cholesterol in the Torpedo californica acetylcholine receptor and the novel lipid-exposed mutation C418W in Xenopus oocytes. J Biol Chem 276:46523–46532

Santiago J, Guzman GR, Torruellas K, Rojas LV, Lasalde-Dominicci JA (2004) Tryptophan scanning mutagenesis in the TM3 domain of the Torpedo californica acetylcholine receptor beta subunit reveals an alpha-helical structure. Biochemistry 43:10064–70

Schlegel A, Volonte D, Engelman JA, Galbiati F, Mehta P, Zhang XL, Scherer PE, Lisanti MP (1998) Crowded little caves: structure and function of caveolae. Cell Signal 10:457–463

Shogomori H, Brown DA (2003) Use of detergents to study membrane rafts: the good, the bad, and the ugly. J Biol Chem 384:1259–1263

Simmonds AC, East JM, Jones OT, Rooney EK, McWhirter J, Lee AG (1982) Annular and non-annular binding sites on the (Ca2++Mg2+)-ATPase. Biochim Biophys Acta 693 398–406

Simons K, Ikonen E (1997) Functional rafts in cell membranes. Nature 387:569–572

Simons K, Toomre D (2000) Lipid rafts and signal transduction. Nat Rev Mol Cell Biol 1:31–39

Singer S, Nicolson GL (1972) The fluid mosaic model of cell membranes. Science 172:720–730

Sivilotti LG, Mcneil DK, Lewis TM, Nassar MA, Schoepfer R, Colquhoun D (1997) Recombinant nicotinic receptors, expressed in Xenopus oocytes, do not resemble native rat sympathetic ganglion receptors in single-channel behaviour. J Physiol 500:123–138

Soreq H, Seidman S (1992) Xenopus oocyte microinjection: from gene to protein. Meth Enzymol 207:225–265

Starace DM, Bezanilla F (2004) A proton pore in a potassium channel voltage sensor reveals a focused electric field. Nature 427:548–553

Stith BJ, Hall J, Ayres P, Waggoner L, Moore JD, Shaw WA (2000) Quantification of major classes of Xenopus phospholipids by high performance liquid chromatography with evaporative light scattering detection. J Lipid Res 41:1448–1454

Sukharev S, Betanzos M, Chiang CS, Guy HR (2001) The gating mechanism of the large mechanosensitive channel MscL. Nature 409:720–724

Sunshine C, McNamee MG (1992) Lipid modulation of nicotinic acetylcholine receptor function: the role of neutral and negatively charged lipids. Biochim Biophys Acta 1108:240–246

Sunshine C, McNamee MG (1994) Lipid modulation of nicotinic acetylcholine receptor function: the role of membrane lipid composition and fluidity. Biochim Biophys Acta 1191:59–64

Tamamizu S, Guzman GR, Santiago J, Rojas LV, McNamee MG, Lasalde-Dominicci JA (2000) Functional effects of periodic tryptophan substitutions in the alpha M4 transmembrane domain of the Torpedo californica nicotinic acetylcholine receptor. Biochemistry 39:4666–73

Tillman TS, Cascio M (2003) Effects of membrane lipids on ion channel structure and function. Cell Biochem Biophys 38:161–190

Toyoshima C, Unwin N (1998) Ion channel of acetylcholine receptor reconstructed from images of postsynaptic membranes. Nature 336:247–250

Turnheim K, Gruber J, Cristoph W, Ruiz Gutierrez V (1999) Membrane phospholipids composition affects function of potassium channels from rabit colon epithelium. Am Phys Soc 277:83–90

Unwin N (1993) Nicotinic acetylcholine receptor at 9 Å resolution. J Mol Biol 229:1101–1124

Unwin N (1995) Acetylcholine receptor channel imaged in the open state. Nature 373:37–43

Unwin N (2003) Structure and action of the nicotinic acetylcholine receptor explored by electron microscopy. FEBS Lett 555:91–95

Valera S, Ballivet M, Bertrand D (1992) Progesterone modulates a neuronal nicotinic acetylcholine receptor. Proc Natl Acad Sci USA 89:9949–9953

Valiyaveetil FI, Zhou Y, Mackinnon R (2002) Lipids in the structure, folding and function of the KcsA K+ channel. Biochemistry 41:10771–10777

van den Brink-van der Laan E, Killian JA, de Kruijff B (2004) Nonbilayer lipids affect peripheral and integral membrane proteins via changes in the lateral pressure profile. Biochim Biophys Acta 1666:275–288

Villar MT, Artigues A, Ferragut JA, Gonzalez-Ros JM (1988) Phospholipase A2 hydrolysis of membrane phospholipids causes structural alteration of the nicotinic acetylcholine receptor. Biochim Biophys Acta 938:35–43

Wenz JJ, Barrantes FJ (2005) Nicotinic acetylcholine receptor induces lateral segregation of phosphatidic acid and phosphatidylcholine in reconstituted membranes. Biochemistry 44(1):398–410

White BH, Cohen JB (1992) Agonist-induced changes in the structure of the acetylcholine receptor M2 regions revealed by photoincorporation of an uncharged nicotinic non-competitive antagonist. J Biol Chem 267:15770–15783

Williamson IM, Alvis SM, East JM, Lee AG (2002) Interactions of phospholipids with the potassium channel KcsA. Biophys J 83:2026–2038

Williamson PT, Meier BH, Watts A (2004) Structural and functional studies of the nicotinic acetylcholine receptor by solid-state NMR. Eur Biophys J 33(3):247–54

Wu L, Bauer CS, Zhen XG, Xie C, Yang J (2002) Dual regulation of voltage-gated calcium channels by PtdIns(4,5)P2. Nature 419:947–952

Yager P, Chang EL, Williams RW, Dalziel AW (1984) The secondary structure of acetylcholine receptor reconstituted in a single lipid component as determined by Raman spectroscopy. Biophys J 45:26–28

Zhang H, Karlin A (1997) Identification of acetylcholine receptor channel-lining residues in the M1 segment of the beta-subunit. Biochemistry 36:15856–15864

Zhou Y, Morals-Cabral JH, Kaufman A, Mackinnon R (2001) Chemistry of ion coordination and hydration revealed by a K+ channel-Fab complex at 2.0 Å resolution. Nature 414:43–48

Subject Index